# Réseaux époxy-amine hétérogènes à partir de dispersions de microparticules polymères réticulées

Marie-Laure Michon

N° d'ordre: 2014ISAL0018 Année 2014

Thèse

# Heterogeneous epoxy-amine networks from the dispersion of cross-linked polymer microparticles

*Présentée devant*
**L'institut national des sciences appliquées de Lyon**

*Pour obtenir*
**Le grade de docteur**

*École doctorale* : Matériaux de Lyon
*Spécialité :* Matériaux Polymères et Composites

*Par*
**Michon Marie-Laure**
Ingénieur CPE Lyon

Soutenue le 14 février 2014 devant la Commission d'examen

*Jury*

| | |
|---|---|
| M. Duskova-Smrckova | Researcher, IMC, Prague, République Tchèque |
| M. Dumon | Professeur, LCPO, ENSCBP Bordeaux |
| T. McKenna | Directeur de recherche CNRS, C2P2, CPE Lyon |
| J. Galy | Directrice de recherche CNRS, IMP@INSA, INSA de Lyon |
| J-F. Gérard | Professeur, IMP@INSA, INSA de Lyon |
| T. Dikic | Dow Chemical, Terneuzen, Pays-Bas |
| T. Verbrugge | Dow Chemical, Terneuzen, Pays-Bas |

# INSA Direction de la Recherche - Ecoles Doctorales – Quinquennal 2011-2015

| SIGLE | ECOLE DOCTORALE | NOM ET COORDONNEES DU RESPONSABLE |
|---|---|---|
| CHIMIE | **CHIMIE DE LYON**<br>**http://www.edchimie-lyon.fr**<br><br>Sec :Renée EL MELHEM<br>Bat Blaise Pascal<br>3e etage<br>Insa : R. GOURDON | M. Jean Marc LANCELIN<br>Université de Lyon – Collège Doctoral<br>Bât ESCPE<br>43 bd du 11 novembre 1918<br>69622 VILLEURBANNE Cedex<br>Tél : 04.72.43 13 95<br>directeur@edchimie-lyon.fr |
| E.E.A. | **ELECTRONIQUE, ELECTROTECHNIQUE, AUTOMATIQUE**<br>**http://edeea.ec-lyon.fr**<br><br>Secrétariat : M.C. HAVGOUDOUKIAN<br>eea@ec-lyon.fr | M. Gérard SCORLETTI<br>Ecole Centrale de Lyon<br>36 avenue Guy de Collongue<br>69134 ECULLY<br>Tél : 04.72.18 60.97 Fax : 04 78 43 37 17<br>Gerard.scorletti@ec-lyon.fr |
| E2M2 | **EVOLUTION, ECOSYSTEME, MICROBIOLOGIE, MODELISATION**<br>**http://e2m2.universite-lyon.fr**<br><br>Insa : H. CHARLES | Mme Gudrun BORNETTE<br>CNRS UMR 5023 LEHNA<br>Université Claude Bernard Lyon 1<br>Bât Forel<br>43 bd du 11 novembre 1918<br>69622 VILLEURBANNE Cédex<br>Tél : 06.07.53.89.13<br>e2m2@ univ-lyon1.fr |
| EDISS | **INTERDISCIPLINAIRE SCIENCES-SANTE**<br>**http://www.ediss-lyon.fr**<br><br>Sec :<br>Insa : M. LAGARDE | Mme Emmanuelle CANET-SOULAS<br>INSERM U1060, CarMeN lab, Univ. Lyon 1<br>Bâtiment IMBL<br>11 avenue Jean Capelle INSA de Lyon<br>696621 Villeurbanne<br>Tél : 04.72.68.49.09 Fax :04 72 68 49 16<br>Emmanuelle.canet@univ-lyon1.fr |
| INFOMATHS | **INFORMATIQUE ET MATHEMATIQUES**<br>**http://infomaths.univ-lyon1.fr**<br><br>Sec :Renée EL MELHEM<br>Bat Blaise Pascal<br>3e etage<br>infomaths@univ-lyon1.fr | Mme Sylvie CALABRETTO<br>LIRIS – INSA de Lyon<br>Bat Blaise Pascal<br>7 avenue Jean Capelle<br>69622 VILLEURBANNE Cedex<br>Tél : 04.72. 43. 80. 46 Fax 04 72 43 16 87<br>Sylvie.calabretto@insa-lyon.fr |
| Matériaux | **MATERIAUX DE LYON**<br>**http://ed34.universite-lyon.fr**<br><br>Secrétariat : M. LABOUNE<br>PM : 71.70 –Fax : 87.12<br>Bat. Saint Exupéry<br>Ed.materiaux@insa-lyon.fr | M. Jean-Yves BUFFIERE<br>INSA de Lyon<br>MATEIS<br>Bâtiment Saint Exupéry<br>7 avenue Jean Capelle<br>69621 VILLEURBANNE Cedex<br>Tél : 04.72.43 83 18 Fax 04 72 43 85 28<br>Jean-yves.buffiere@insa-lyon.fr |
| MEGA | **MECANIQUE, ENERGETIQUE, GENIE CIVIL, ACOUSTIQUE**<br>**http://mega.universite-lyon.fr**<br><br>Secrétariat : M. LABOUNE<br>PM : 71.70 –Fax : 87.12<br>Bat. Saint Exupéry<br>mega@insa-lyon.fr | M. Philippe BOISSE<br>INSA de Lyon<br>Laboratoire LAMCOS<br>Bâtiment Jacquard<br>25 bis avenue Jean Capelle<br>69621 VILLEURBANNE Cedex<br>Tél :04.72 .43.71.70 Fax : 04 72 43 72 37<br>Philippe.boisse@insa-lyon.fr |
| ScSo | **ScSo***<br>**http://recherche.univ-lyon2.fr/scso/**<br><br>Sec : Viviane POLSINELLI<br>Brigitte DUBOIS<br>Insa : J.Y. TOUSSAINT | M. OBADIA Lionel<br>Université Lyon 2<br>86 rue Pasteur<br>69365 LYON Cedex 07<br>Tél : 04.78.77.23.86 Fax : 04.37.28.04.48<br>Lionel.Obadia@univ-lyon2.fr |

*ScSo : Histoire, Géographie, Aménagement, Urbanisme, Archéologie, Science politique, Sociologie, Anthropologie

**ACKNOWLEGMENT**

I would like to express my sincere gratitude to my supervisors Dr. Jocelyne Galy and Prof. Jean-François Gérard. It was a pleasure working with you in the lab every day, sharing results (the successful ones as well as the unexpected ones), and discussing the thesis at great lengths. Thank you for your advice, your continued support and your trust over these past three years.

I would also like to thank all the members of the Jury - Dr. Miroslava Duskova-Smrckova, Prof. Michel Dumon and Dr. Timothy McKenna - to have accepted to report on my research study, but also for your encouragements and insightful comments. Thank you to Dr. Tamara Dikic and Tom Verbrugge from the Dow Chemical Company, for taking a chance on me with this research topic, supporting me from the start and collaborating with me during three years. I do not forget their colleagues: Brian Dickie and Sylvie Vervoort for their help with the DSC and rheology experiments.

For their help and insightful discussions (scientific or not), thank you to all the members of the IMP lab: Mallou and Isabelle, Raphael, Gilbert and Guilhem, the lunch team at the CNRS restaurant, the people sharing lunch in the "salle à café" and my "co-bureaux" of my two different offices (Vincent, Jean-Marc, Ismail, Nicolas D, Ali, Marco, Loic, Cédric, Julien, Marion T, Damien, Arthur). Thank you for your help, the laughs and more difficult moments we've shared!

Without forgetting the others students / engineers I have met during these 3 years, "ma jumelle" Marianne, Suzanne and Hélène, Elie, Ludovic, Sylvain, Yann, Nicolas L., Nora, Noellie, Camille, Florianne, Marie C., Maxime, Séphane, Alexia, Marie V, Johanna, Gino, Thibault, Florent, Gabriela, Miren, Marion C., Aymeric F. & G…some of you already know we became friends and that the story will not stop today!

Of course thanks to all my friends from Lyon, Avignon and further away (Marie, Micha, Laura, Marion, Else, Milena, Céline, Marie-Claire, Fanny, Anne-Catherine, Lea, Aurélia, Julie, Odile, the wcs team, and to my family. Now for you " me voilà le seul Docteur de la famille qui ne pourra même pas nous soigner!!" Thanks to my sister Pauline who is "repairing me" so often, and of course also to M-No, JC, Jeanette, Georges, Denise, Agnes, Jean-Jacques, Myriam, Gérard, Maud, Hugo, Nicolas, Auguste, Guilhem, Cyril, Sabrina, Chloe, Anne-Sophie…You were always there when I needed…

Merci, Gramaci

## CONTENTS

# GENERAL INTRODUCTION

Thermosetting polymers are very attractive materials due to their many useful properties such as high strength, good dimensional stability at elevated temperatures, very low creep, solvent and water resistance [1]. However, the design of thermosetting polymers is always limited by transformations of the material during the polymerization. Indeed, during the processing of thermosetting polymers, large changes in the rheological behavior occur. Thermosetting polymers are formed by the crosslinking of polyfunctional systems which involves several reaction stages.

The crucial phenomenon during crosslinking is gelation. It characterizes the processability of the system and network formation as it corresponds to the irreversible point when viscosity becomes infinite.

The second major phenomenon during thermoset crosslinking is vitrification, due to the rise of Tg by the formation of the network which comes close to the curing temperature and leads to the decrease in motion of the segments of the network. Diffusion control becomes operative, which can stop the reaction at incomplete conversion. The final structure of the material can be severely affected, resulting in poor mechanical properties and material instability.

Improvement in the properties of thermosetting matrices is often of great interest for composites and also many other applications. As a consequence, fillers, additives and second phases are used to provide new properties for the final materials; for example improved fracture toughness, conductivity and reduced flammability.

Many studies have reported the interest in the addition of thermoplastic polymers, inorganic particles, and fibers into thermosetting matrices to alter the network architecture, optimize and diversify the performances of the materials. However, few studies have been performed on the addition of cross-linked polymer microparticles.

The present study focuses on epoxy thermosetting networks filled with cross-linked epoxy microparticles. These particles are used as modifiers of heterogeneity, as they are pre-cross-linked thermoset entities. A preliminary study [2] showed how to easily synthesize cross-linked epoxy microparticles by precipitation polymerization. The same concept is considered and applied in this

project. It has been financially supported by The Dow Chemical Company (Dow), Terneuzen, The Netherlands.

The main challenges are:
- Develop and better understand the process of precipitation polymerization applied to form cross-linked microparticles
- Synthesize the particle as reactive fillers to provide a better compatibility with the epoxy matrix
- Identify and quantify the reactive functionalities
- Understand the particle behavior in epoxy-amine mixtures
- Investigate the influence of the microparticles on the filled networks generated.

This manuscript is divided into four chapters.
*Chapter 1* is an overview of the main characteristics of the buildup of epoxy networks and their solid state properties. The discussion is based on what was reported previously in the literature regarding CPM synthesis and their addition in epoxy-amine systems. The principle of precipitation polymerization used to form polymer microparticles is described. Previous particles synthesized by this route are reported as well as their use in epoxy formulations.

The 3 others chapters present the results obtained during this 3 year project.

*Chapter 2* reports the CPM synthesis as well as their solid state properties. The protocol used and monitoring of the reaction is described. Then, the properties of the particles in term of size, glass transition temperature, and presence of residual solvents are presented. The influence of the synthesis parameters are investigated as the polymerization time, the stoichiometric ratio of amino hydrogen on epoxy groups and the monomer chemical structure, with regard to the final properties of the CPMs. Special efforts were made to form amino functionalized particles with the aim of having reactive functionalities towards epoxy systems.

*Chapter 3* focuses on the methods used to highlight the presence of amino groups in the CPM structure and how to quantify them. A review of the techniques described in the literature to quantify primary and secondary amines on solid supports is first reported. A preliminary calculation of the theoretical amount of residual amino groups on the CPMs has been realized. It is based on the stoichiometric ratio used to synthesize the CPMs and by taking the surface thickness into account. Then, several techniques were used to show the amine functionality on the CPMs as well as their accessibility and reactivity towards epoxy systems. Quantification of the concentration

of residual primary and secondary amino groups per gram of CPM was carried out and compared to the theoretical calculation.

*Chapter 4* is dedicated to the properties of the CPM-filled epoxy network obtained from the dispersion of the CPMs. Results are reported according to the dispersion process used: in epoxy, in epoxy with the aid of solvent or in the hardener. Influence of the addition of the CPMs in epoxy-amine formulation is investigated on the kinetics of the network formation, the morphology and dynamic solid state properties of the final materials, and is reported in this last chapter.

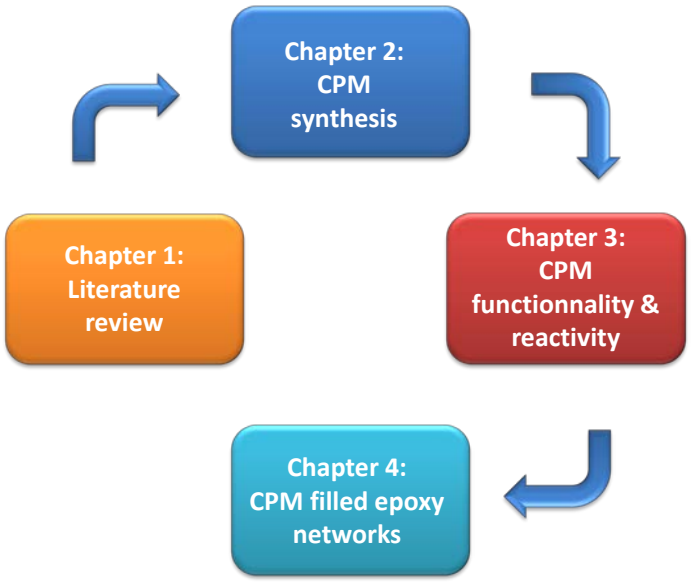


***Figure 1: Structure of the manuscript***

# I LITERATURE REVIEW

## 1 Background on epoxy networks

Epoxy polymers are primarily part of the family of thermosetting polymers that also includes phenolic polymers, urea-formaldehyde resins, unsaturated polyester, and polyurethanes etc. [3,4] Their main applications are in composites, coatings, electronics, sport goods, automobile, aircraft and so on.

Epoxy networks are synthesized using an epoxy prepolymer referring to a molecule bearing an oxirane ring. Its general structure is given in Figure 2. The main epoxy prepolymer used in 75% of the applications [5] is the diglycidyl ether of bisphenol A (DGEBA) synthesized from the reaction of the bisphenol A and the epichlorohydrin as shown in Figure 3.

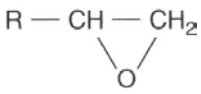


***Figure 2: Chemical structure of the oxirane ring***

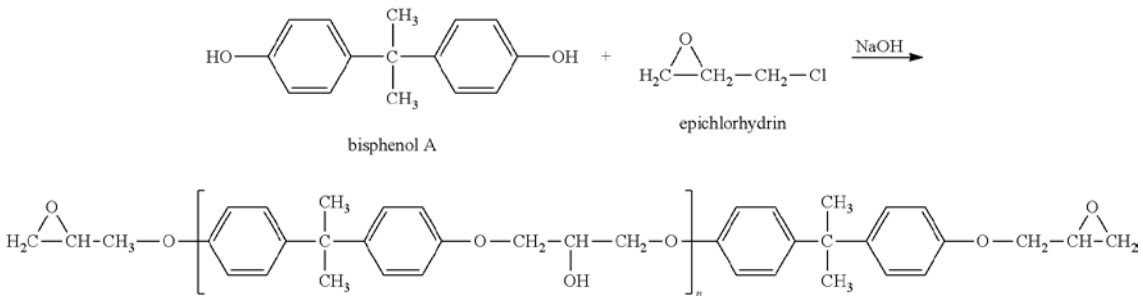


***Figure 3: DGEBA synthesis from bisphenol A and epichlorhydrin***

Thermosetting epoxy polymers are formed by infusible 3D networks, which are obtained by the use of a comonomer-denoted cross-linker, hardeners or a curing agent. Due to the ring strain of the epoxy functionality, the use of a wide variety of curing agents is possible. Among many possibilities, amines and anhydrides are the most commonly used. This bibliographic study is focused only on diepoxy-diamine networks.

### 1.1 Reminders on epoxy-amine chemistry

The reaction mechanism is a step-growth polymerization referred to as polyaddition between the epoxy groups from the prepolymer and the amines from the cross-linker. A scheme of the non-catalytic reaction scheme between isophorone diamine, IPD (a classical curing agent), and an epoxy

prepolymer is reported in Figure 4. Each primary amine can react twice, and each epoxy group reacts once creating a 3D network. A primary amine opens the oxirane ring and forms a secondary amine and a hydroxyl. Then, a second reaction from the secondary amine with another oxirane leads to a tertiary amine. The reactivity of the amine increases with its nucleophilic character: aliphatic > cycloaliphatic > aromatic. The etherification reaction, from the hydroxyl groups formed with the oxirane, is considered negligible, i.e., only present for reactions at very high temperatures with epoxy-rich systems [6–7]. Another mechanism that can also be presented is the autocatalytic reaction scheme. The catalytic effect comes from the hydroxyl groups due to the opening of the oxirane ring (see mechanism in the literature [8]).

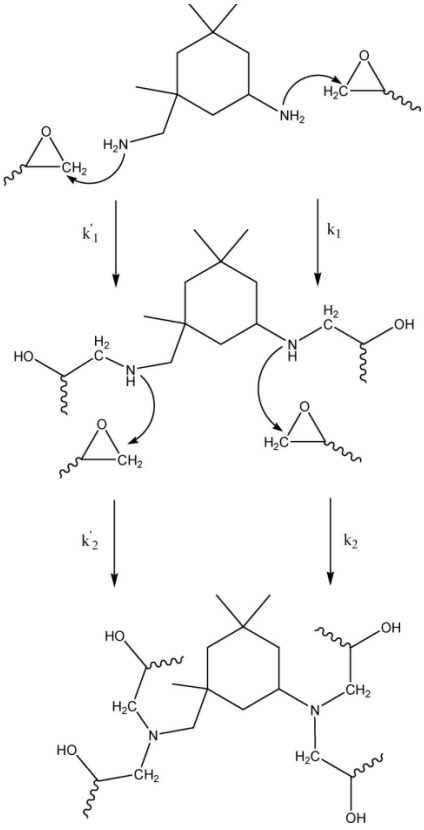


***Figure 4: Epoxy-amine non-catalytic reaction mechanism creating a 3D irreversible network [8]***

## 1.2 Transitions during network buildup

### *1.2.1 Gelation*

Epoxy-amine networks, as well as all thermosetting materials, are characterized during their buildup by a gelation phenomenon. This involves an abrupt change of behavior of the blend and corresponds to the buildup of a giant 3D macromolecule. So, all the boundaries of the system are connected. The final shape of the material is reached. At the gel point, with the conversion of

reactive groups defined by x, x = $x_{gel}$; the zero shear viscosity[1] increases dramatically to become infinite. There is the buildup of the elastic response. An insoluble fraction appears, which increases as the conversion increases (Figure 5). Conversion is not stopped by this phenomenon, it goes on increasing. At that point, the weight-average molar mass, $M_w$, becomes infinite contrary to the number-average molar mass, $M_n$, which continues to increase.

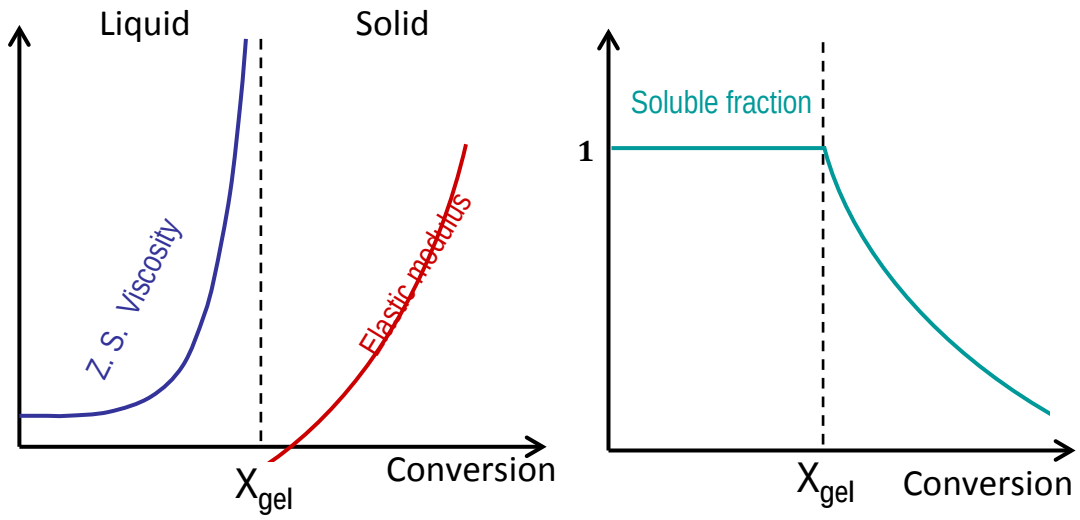


***Figure 5: Evolution of physical properties at the critical transition of gelation – zero shear (Z.S.) viscosity, elastic modulus, and soluble fraction as a function of conversion of epoxy or amino groups. [3]***

This phenomenon of polymerization leading to the network buildup is homogeneous for a polyaddition polymerization. It is not the same behavior for radical-free polymerization. The schematic formation of the epoxy-amine (diepoxy + diamine) network before gelation and its completion after the gelation is given in Figure 6. Before gelation, epoxy and amine molecules react homogeneously to create soluble oligomers. After gelation there is still a soluble fraction that will be included little by little in the network to finally reach a maximum conversion of 1.

***<u>Conversion at the gel point</u>***

Flory and Stockmayer were the first to establish a relationship to calculate the extent of the reaction at the gel point in non-linear polymers [9,10, 11]. This was based on a statistical model and for an ideal network with the following assumptions:

1: Functional groups are equally reactive.

2: The reactivity of the functional groups is independent of the size or the structure of the molecule (or the network) in which they are taking part.

3: Intramolecular reactions are negligible.

[1] Zero shear viscosity is the apparent viscosity in the limit of zero shear rate.

For an $RA_{fA}$ + $R'B_{fB}$ polymerization system, with A and B two different monomers and f their functionality, the Flory-Stockmayer theory of gelation corresponds to:

$$(f_A-1)x_A.\ (f_B-1)x_B = 1 \qquad \textit{Equation 1}$$

with $x_A$, the conversion of the functional groups A,

$x_B$, the conversion of the functional groups B,

for an epoxy-amine system $RA_4$ + $R'B_2$, Equation 1 becomes:

$$(4-1)\ x_A.\ (2-1)\ x_B = 1$$

$$3x_A.x_B = 1 \qquad \textit{Equation 2}$$

with the stoichiometric ratio amino hydrogen to epoxy: r=a/e = 1, $x_A = x_B = x_{gel}$

$$x_{gel} = (1/3)^{1/2} = 0.577 \qquad \textit{Equation 3}$$

In excess of amine, r=a/e>1, $x_B = r.\ x_A$

$$x_{B,gel} = (r/3)^{1/2} \qquad \textit{Equation 4}$$

In excess of epoxy, r=a/e<1, $x_a = 1/r\ .\ x_B$

$$x_{A,gel} = (1/3r)^{1/2} \qquad \textit{Equation 5}$$

As a consequence, the gelation phenomenon in epoxy systems occurs at a specific conversion. This conversion is constant regardless of temperature but is affected by the stoichiometric ratio r=a/e. The dependence of the conversion at gelation of the limiting reactant is reported as a function of the stoichiometric ratio (Figure 7) [3].

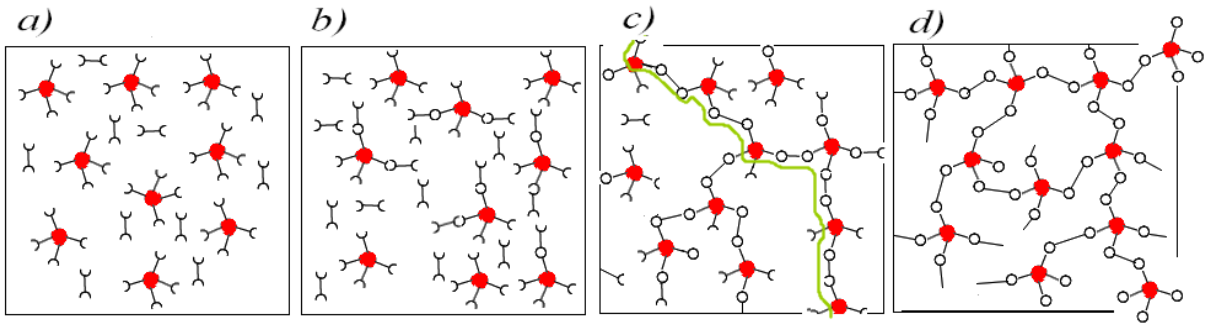


***Figure 6: Network buildup for a diepoxy – diamine system – r=a/e=1*– a) epoxy prepolymer and hardener, b) formation of oligomers, c) gel point, d) 3D cross-linked network**

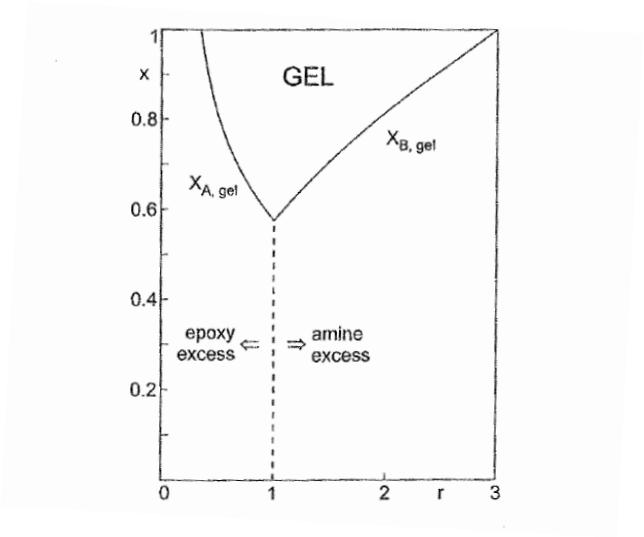


***Figure 7: Variation of the gelation conversion of the limiting reactant as a function of the stoichiometric ratio r = a/e [3].***

However, results from this model can slightly differ from experimental data. Delayed gelation can occur due to intramolecular reactions, which were disregarded. Moreover, the unequal reactivity of the functional groups can also lead to delayed or early gelation [12].

***Experimental determination of the gelation time***

Several methods are used to determine gel times [13].

The first one is based on the ***formation of an insoluble network***. Indeed, here the principle is to visually observe the appearance of the first insoluble fraction in an appropriate solvent of the polymer. For epoxy-amine networks, tetrahydrofuran, THF is commonly used. Gel time is determined when the first fraction of insoluble polymer is observed. It corresponds to the point when Mw dramatically increases (measured by size exclusion chromatography, Mw, Mn = f(t)).

Also, **the viscosity** can be a parameter to measure the gel time as the viscosity diverges close to the gel point. The time to reach a certain arbitrarily chosen value of viscosity ($10^4$, $10^5$…) is taken as the gel point. This criterion cannot be considered universal but can be considered empirical.

***Rheology measurements*** are widely used to determine the gel point of a cross-linking polymer cured isothermally between parallel plates. However, different criteria are used. The most precise is to use the time corresponding to the crossover of the damping factor, tan δ (tan δ = G''/G'), for several frequencies that correspond to the Winter and Chambon criterion [14]. Indeed, at the crossover of all the curves, gel point is independent of the frequency of the dynamic experiment [15]: the storage and loss modulus can be described by a power law as a function of the pulsation:

G' (ω) ∝ G" (ω) ∝ ω. So, at the gelation, the damping factor tan δ = G" /G' is independent on the frequency and:

$\delta_{gel} = \pi . \Delta/2$ where Δ is the relaxation exponent that can be predicted by Rouse's percolation theory.

Figure 8 shows the measure of the gel point in multifrequency mode by Matejka [16] during the cross-linking of a DGEBA-D400 (polyetheramine) system. The gel point is taken at the crossover of the tan δ.

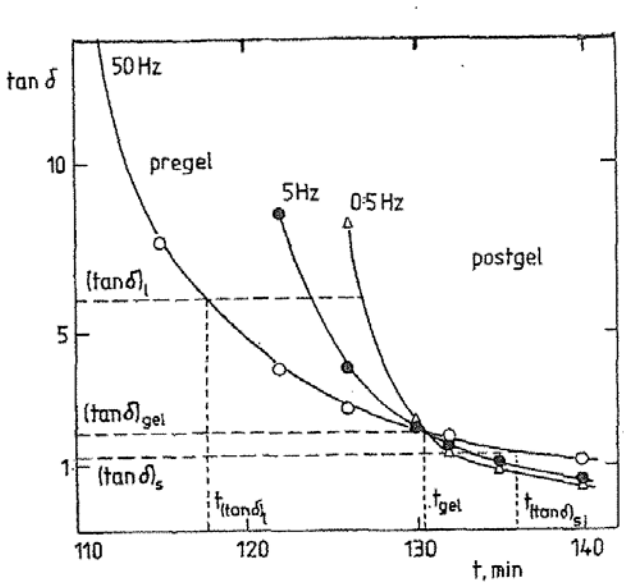


***Figure 8: Dynamic mechanical measurements for DGEBA-D400–Determination of the gel point at the crossover of the tan δ for several frequencies: 50, 5, 0.5 Hz; a/e=1, T=70°C***

### *1.2.2 Vitrification*

Vitrification corresponds to the change from a liquid or a rubber (if gelation has already occurred) into an ungelled or gelled glass, respectively. A reduction of the molecular mobility of the macromolecular chains is observed as the glass transition temperature of the polymer reaches the temperature of reaction. As a consequence, relaxation times increase, substantially slowing down the reaction kinetics. Moreover, a small increase of functional group conversion also produces an increase in relaxation time, which rapidly leads to the end of the reaction. Thus, close to the vitrification, the kinetics are affected by the local viscosity, which is function of the extent of the reaction and temperature. Polymerization can be restarted by increasing the temperature (post-curing step).

Gelation and vitrification of thermosetting polymers are often represented in a transformation diagram. Enns and Gillham [17] were the first to suggest the use of a ***Time-Temperature-Transformation (TTT)*** cure diagram. To plot this diagram for an epoxy-amine system, the times required to reach gelation, $t_{gel}$, and vitrification during isothermal curing were measured. Gillham

generalized his diagram for thermosetting polymers [18]. The schematic diagram obtained is given in Figure 9.

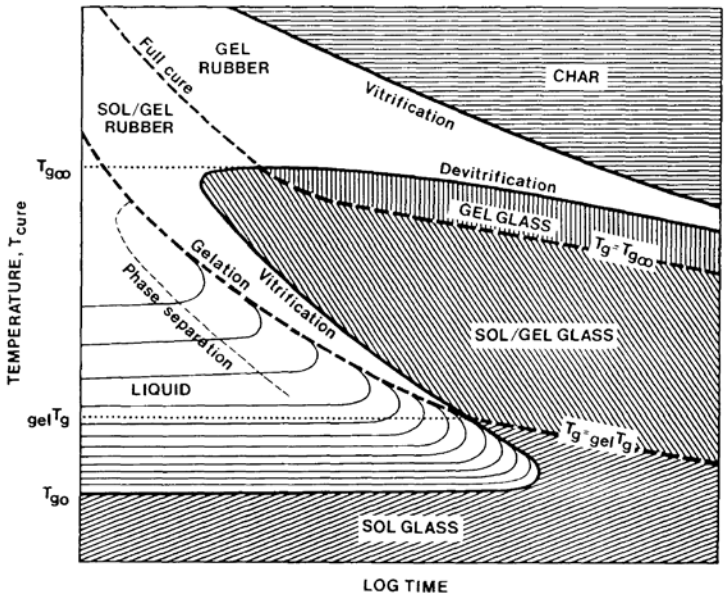


***Figure 9: Time-Temperature-Transformation (TTT) isothermal cure diagram for a thermosetting system [18]***

In a TTT diagram, only trajectories at a constant temperature have a physical meaning. Three values of glass transition temperatures can be noticed: $Tg_0$ for the uncured monomer mix, $_{gel}Tg$ for which gelation and vitrification occur at the same time and $Tg_\infty$ for the fully cured network. This diagram shows four possible behaviors of the material depending on the curing temperature ($T_{cure}$).

1. Below $Tg_0$, almost no reaction occurs; the reactive functions are immobilized in the glassy state.
2. If $Tg_0 < T_{cure} < {}_{gel}Tg$, the reaction starts, but the material is vitrified before being gelled. The material remains processable by an increase in temperature. The cross-linking is a diffusion-controlled process. At $T_{cure} = {}_{gel}Tg$, vitrification and gelation take place at the same time.
3. For $_{gel}Tg < T_{cure} < Tg_\infty$, once the reaction starts, gelation occurs before vitrification.
4. With $T_{cure} > Tg_\infty$, the reaction leads to the gelation but not to vitrification. The cross-linking can proceed to completion. The network remains in its rubbery state.

At high temperature the char region is noted, which corresponds to the thermal degradation for an exposure that is too long at a too high temperature.

Several teams measured gel and vitrification time ($t_{gel}$ and $t_{vit}$ respectively) to establish the TTT diagram of their system, as has been done for triglycidyl ether of tris(hydroxyphenyl)methane-diaminodiphenylsulfone (DDS) (Figure 10) [19].

The TTT diagram can be plotted measuring $t_{gel}$ and $t_{vit}$, but the following equation can also be integrated, with *r(x, $T_{cure}$)*, the polymerization rate, depending on the conversion and the curing temperature.

$$t = \int_0^x \frac{dx}{r(x, T_{cure})}$$

Replacing t with $t_{gel}$, $t_{vit}$ and x with $x_{gel}$ and $x_{vit}$, the following equations were obtained:

$$t_{gel} = \int_0^{x_{gel}} \frac{dx}{r(x, T_{cure})} \qquad \textit{Equation 6}$$

$$t_{vit} = \int_0^{x_{vit}} \frac{dx}{r(x, T_{cure})}$$

Knowing the conversion and r, the gelation and vitrification times can be calculated.

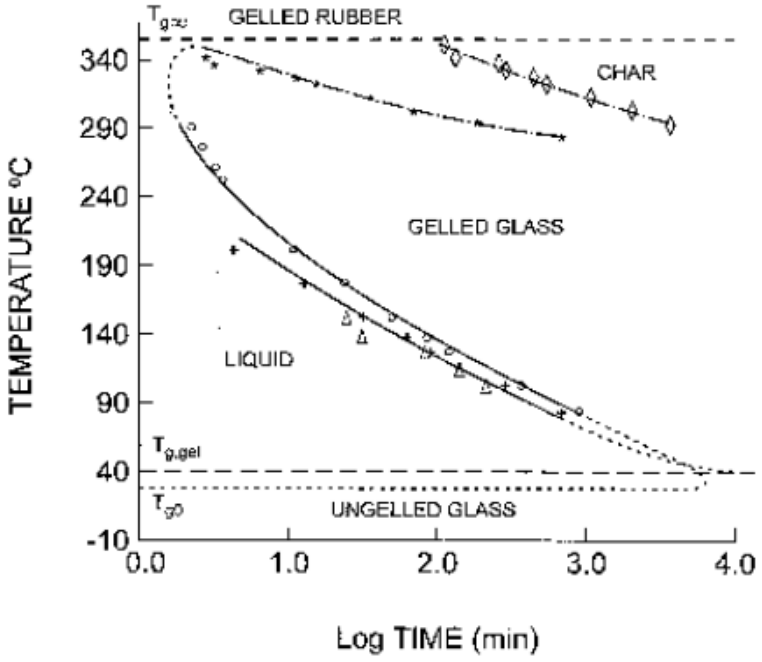


***Figure 10: TTT diagram for a triglycidyl ether of tris(hydroxyphenyl)methane-DDS system [19]***

Another type of diagram to represent the transitions and transformations of the material is the ***Conversion-temperature-transformation (CTT) diagram***. It also represents the gelation, vitrification and degradation curves. A general representation of this diagram for thermoset materials is given in Figure 11. It can only be used when conversion at gelation is independent of temperature and when there is a unique relationship between Tg and conversion.

Here also, four primary domains exists that lead to maximum or incomplete conversion. Under $Tg_0$, material becomes glassy without gelation phenomenon with a low conversion. At the specific temperature of $Tg_{gel}$, gelation and vitrification occurs, leading to a gelled glass with a conversion of $x_{gel.}$ To reach a conversion of 1, $T_{cure}$ has to be higher than $Tg_\infty$; otherwise the conversion is limited by the vitrification phenomenon. However, curing at high temperature usually leads to a high polymerization rate and high exothermicity of the reaction, which is difficult to dissipate. This means that at high temperature, maintaining isothermal conditions is almost impossible. This is why usual curing conditions consist of a first isothermal step at an intermediate temperature, between $Tg_\infty$ and $Tg_{gel}$, to dissipate the generated heat. Then, several or at least one more isothermal step is necessary at Tcure > $Tg_\infty$ to complete the reaction until complete conversion.

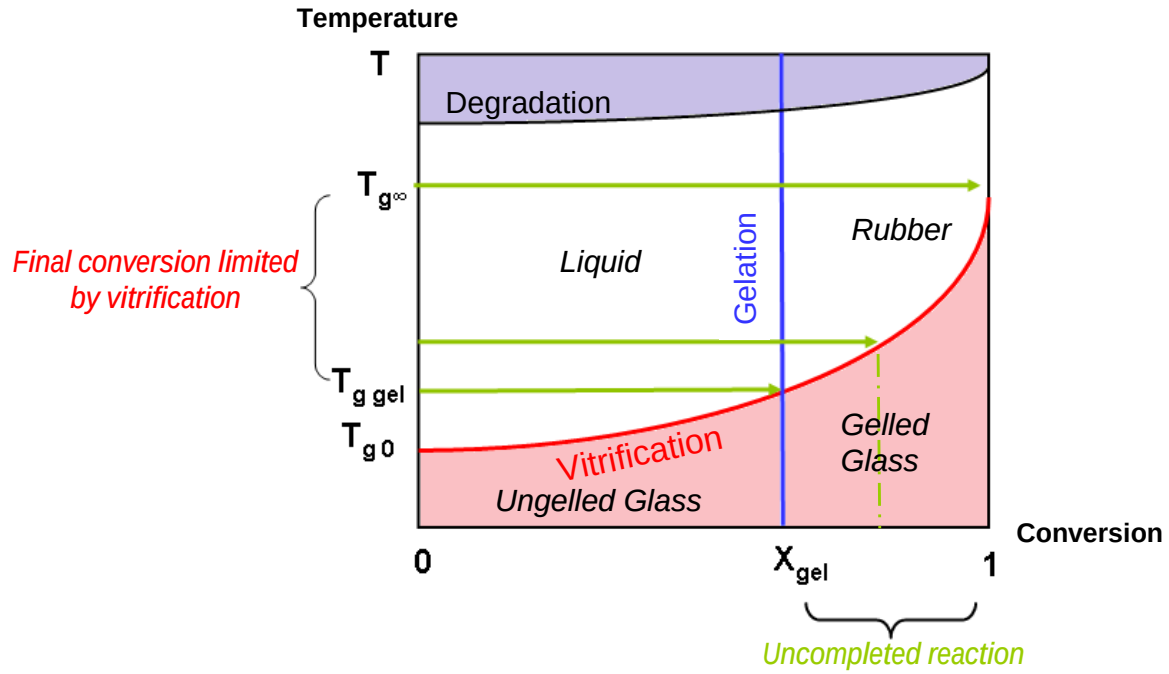


***Figure 11: Conversion-temperature-transformation (CTT) diagram with gelation, vitrification, and degradation curves***

As discussed previously, curing thermoset at temperatures below the glass transition temperature of the fully cured material brings the problem of vitrification of the system during polymerization and stops the reaction at partial conversion.

This effect of vitrification on the conversion, glass transition temperature, fracture toughness and tensile properties is clearly illustrated by Marks and Snelgrove [20]. They studied five formulations representative of the most commonly used epoxy resin and amine hardeners. The epoxy resin was DGEBA DER332, the hardeners were ethylenediamine (EDA), diethylenetriamine (DETA), isophoronediamine (IPDA), m-xylylenediamine (mXDA) and diaminodiphenylsuphone (DDS). Networks were obtained after 2 hours of curing at different isothermal temperatures. Their Tg and

conversions were obtained by DSC. The variation of conversion is plotted as a function of the isothermal curing temperature in Figure 12. There is an evident link between conversion and curing temperature.

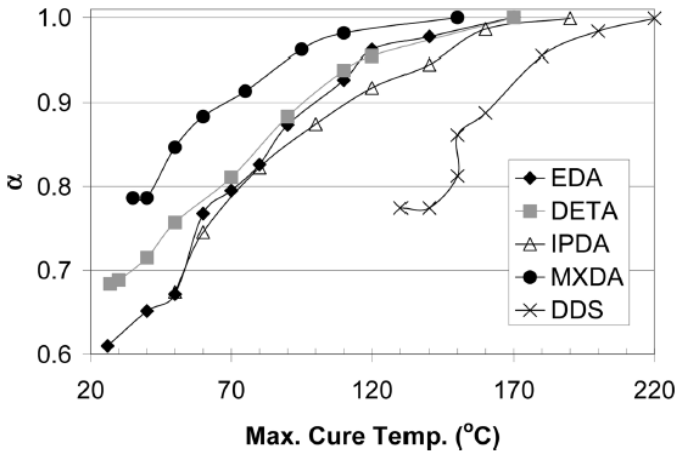


***Figure 12: Conversion versus maximum cure temperature for DER 332-amine thermosets (isothermal curing for 2h) [20]***

The influences of the curing temperature on Tα (temperature at the peak maximum of tan δ) and on G' in the particular case of DGEBA-DDS systems are shown in Figure 13 and Figure 14, respectively. The Tα reached was only slightly above the curing temperature. For example, curing 2 hours at 180°C gave a Tα close to 190°C, while Tα was equal to 235°C after full curing.

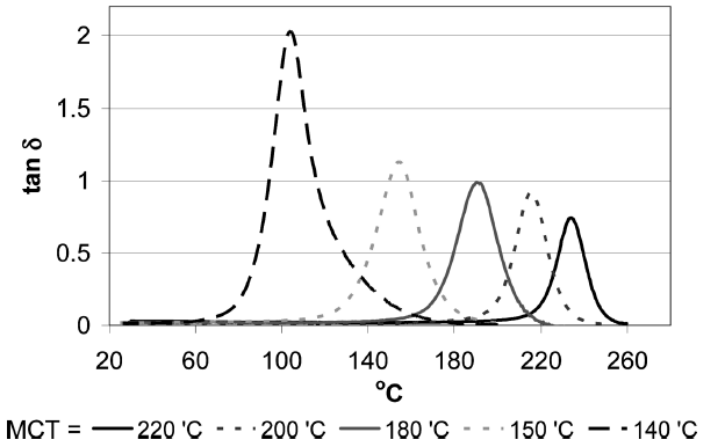


***Figure 13: Peak tan δ obtained by DMA for DER 332-DDS thermoset samples isothermally cured different maximum temperatures (MCT) [20]***

The rubbery storage moduli were increased when the curing temperature was increased. (Figure 14).

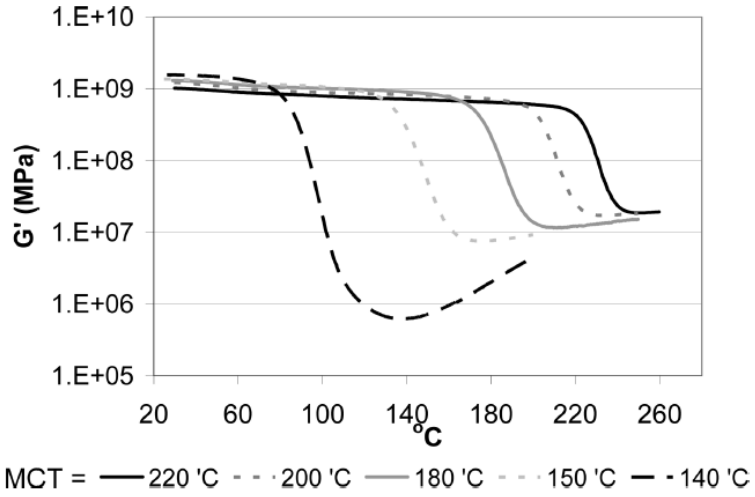


***Figure 14: G' obtained by DMA for DER 332-DDS thermosets samples isothermally cured at different maximum temperatures (MCT) [20]***

The authors also followed the evolution of tensile modulus and toughness. The tensile modulus showed a decrease with an increase of conversion in all of the epoxy systems studied. The trend is not as clear regarding the fracture toughness, $K_{IC}$. In some cases, for relatively flexible amines, the maximum of $K_{IC}$ is at 90 % conversion. Aromatic diamines such as DDS give brittle networks, with low $K_{IC}$, which show a moderate increase with an increase in conversion.

Obtaining high-Tg polymers by curing the monomers at low temperatures would be interesting for many practical applications. In the glassy state, the reaction is very slow, and structure evolution is stopped. Poor mechanical properties and material instability are obtained. Despite this fact, low-temperature curing often results in a material of high glass transition temperature significantly exceeding the cure temperature. This effect could be attributed to the exothermicity of the reaction, which leads to a higher temperature than the target one, especially in bulk samples.
Indeed, this is what was highlighted by Kroutilova et al. [21] in their study of curing at sub-glass transition temperature. They could obtain a difference between Tg and $T_{cure}$ of 70°C (Table 1). They explained that in slowly reacting systems, heat generation is slow compared to its dissipation. In contrast, in a fast-reacting system, heat generation is quicker than its dissipation and the temperature of the reaction medium increases. Therefore, Tg of the final material increases. The effect of the sample volume was also thought to be responsible for weak dissipation of heat and leads to same effect of Tg increase. However, they also showed it was possible to obtain a fully cured material with a curing temperature 10°C below the maximum Tg, despite the absence of an exothermal temperature rise.

***Table 1: Glass transition temperatures obtained for epoxy-amines samples cured at three different temperatures [21]- Epoxy 513: low-molecular weight epoxyacrylate resin – Epoxy 521: low-molecular weight epoxy resin modified with a reactive solvent based on aliphatic glycidyl ether – Epoxy 531: low-molecular weight epoxy resin modified with a reactive solvent based on aliphatic diglycidyl ether - DETA: diethylenetriamine***

| System | $T_c$ (°C) | $T_\alpha$ (°C) |
|---|---|---|
| Epoxy 513–DETA | 150[a] | 30 |
| | 20 | 30 |
| | 8 | 20 |
| Epoxy 521–DETA | 150[a] | 72 |
| | 20 | 51 |
| | 8 | 29 |
| Epoxy 531–DETA | 150[a] | 95 |
| | 20 | 87 |
| | 8 | 40 |

Thickness $d$ of the cured samples was 9 mm.
[a] $d$ = 1.5 mm.

In 2001, Bowman and coworkers [22] investigated the factors that could dictate the relationship between Tg and $T_{cure}$. They studied the cross-linking of three model systems with different degrees of heterogeneities (expressed by the width of Tg), triethylene glycol dimethacrylate (TEGDMA), diethylene glycol dimethacrylate (DEGDMA) (more heterogeneous), and styrene-divinyl-benzene copolymer (St-co-DVB) (more homogeneous). It was found that the differences between Tg and $T_{cure}$ were significantly greater for the more heterogeneous system with the difference measured to be as large as 100°C (Figure 15). They showed that using a monomer that forms a heterogeneous polymer allows one to obtain a high-Tg material even if it has been cured at ambient conditions. However, this was demonstrated for free radical polymerization, which is a completely different process from the epoxy-amine polymerization process.

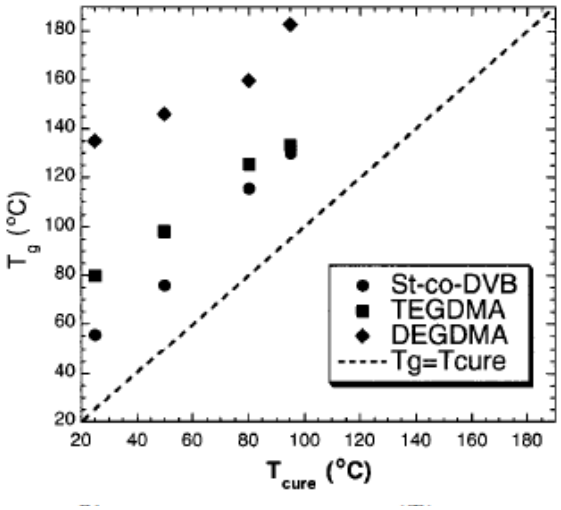


***Figure 15: Glass transition temperatures St-co-DVB, TEGDM, DEGDMA systems, versus the cure temperature [22]***

***Prediction of Tg knowing the conversion***

The glass transition temperature can be estimated for a given conversion, x, using the modified Di Benedetto equation [23]:

$$\frac{Tg - Tg_0}{Tg_\infty - Tg_0} = \frac{\lambda x}{1-(1-\lambda)x} \qquad \textit{Equation 7}$$

$$\textit{with} \qquad \lambda = \frac{\Delta Cp_\infty}{\Delta Cp_0} \qquad \textit{Equation 8}$$

$\Delta Cp_0$ is the change in heat capacity at the glass transition of the initial monomer blend and $\Delta Cp_\infty$ of the fully cross-linked network measured by DSC, as well as the $Tg_0$ and $Tg_\infty$.

The comparison between experimental data and results obtained with the modified Di Benedetto equation was reported for a DGEBA-DETDA (diethyltoluene diamine) system [24]. Authors used the DSC to measure the conversion of partially cured samples of their system by integration of the enthalpy peak, as well as to obtain the corresponding Tg of the networks cured for different times. The plot of the Tg measured versus the conversion is given in Figure 16. Di Benedetto's model was added to the experimental values and fit the conversion of reactive groups of DGEBA-DETDA very well.

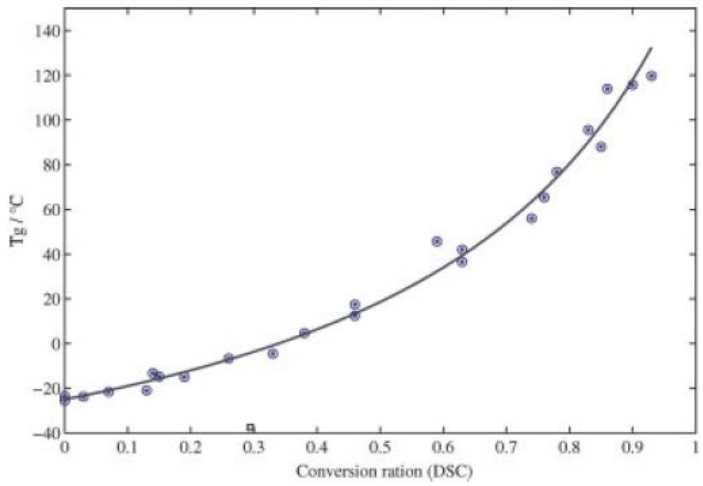


***Figure 16: Glass transition as a function of the DSC conversion ratio for a DGEBA-DETDA network. Experimental results (o) and Di Benedetto fit (–) [24]***

### *1.2.3 Influence of the stoichiometric ratio*

The variation of the stoichiometric ratio r= a/e has a strong influence on the kinetics of the reaction and on the final solid-state properties (thermomechanical properties, aging, etc.). A summary of the trends observed in the literature with the variation of a/e are reported in the following section.

***Influence on the kinetic of the reaction***

In their work, Wu and co-authors [28] investigated the effect of the stoichiometric ratio, r, on the polymerization rate. They observed and explained the increase of the polymerization rate with the amount of amine for their epoxy-amine system based on DGEBA-TETA (triethylenetetramine).

The following semi-empirical equation [25] based on kinetic model of epoxy-amine reaction catalyzed by the hydroxyl generated by the reaction or by initial hydroxyl or impurities, was used to explain the phenomenon:

$$\frac{dx}{dt} = (k_1 + k_2 x^m)(1-x)^a (r-x)^b \qquad \textit{Equation 9}$$

where $k_1$ and $k_2$ are constants proportional to the rate constants

r =a/e: stoichiometric ratio

a and b are semi-empirical coefficient

During the initial stage, x=0, Equation 9 is simplified to:

$$\frac{dx}{dt} = k_1 r^b \qquad \textit{Equation 10}$$

Therefore, the rate of reaction, dx/dt, increases with the stoichiometric ratio r and so the amine content.

Karayannidou [26] studied the kinetics of the reaction of DGEBA-IPD at 70°C using IR spectroscopy to measure the epoxy conversion (Figure 17). An increase in the reaction rate was observed for an increased amount of amine (a/e>1), as well as an increase in the conversion reached.

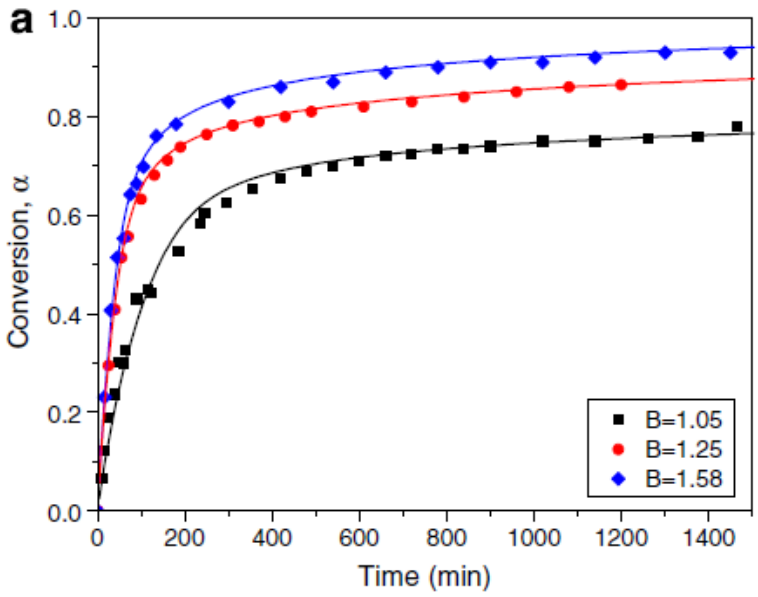


***Figure 17: Conversion of epoxy groups versus time for DGEBA-IPD cross-linked at 70°C, for different stoichiometric ratio (B=r) [26]***

***<u>Influence on gelation</u>***

The influence of the stoichiometric ratio on the *conversion at gelation* was already discussed in section 1.2.1 and reported in Figure 7 for the limiting reactant. Conversion of epoxy groups and amino groups at gelation for an epoxy-amine system (epoxy functionality = 2 and amine functionality = 4) depends on r=a/e as $x_{epoxy,gel} = (r/3)^{1/2}$ and $x_{-NH,gel} = (1/3r)^{1/2}$[3].

At gelation:

- In excess of amine: r=a/e>1, the conversion of epoxy groups is increased, whereas the conversion of amino groups is decreased as the amine amount increases;
- In excess of epoxy: r=a/e<1, the conversion of amino groups is increased, whereas the conversion of epoxy groups is decreased as epoxy amount increased.

*Gelation time* depends on the temperature, reaction mechanism, and composition of the system as well as the functionality of precursors. The evolution of gelation time as a function of the stoichiometry is not discussed as much in the literature.

Serrano and Harran [27] did a rheological study of an epoxy system composed of TGDDM (tetraglycidyl diamino diphenyl methane), which is a tetrafunctional epoxy, and DDS (diaminodiphenylsulfone). The time to gelation and vitrification as a function of the stoichiometric ratio are reported in Figure 18.

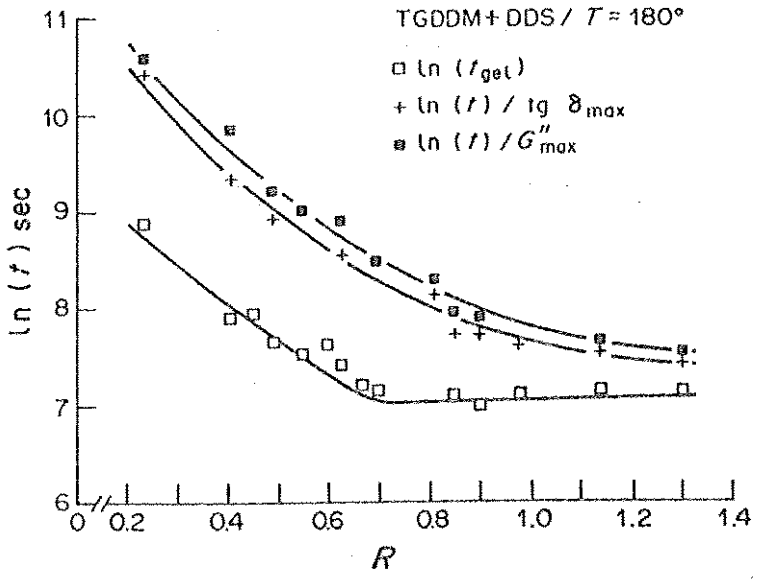


***Figure 18: time of gelation and vitrification***

The gelation time is the longest for a large excess of epoxy (a/e = 0.2), and then it becomes constant above a/e = 0.7. The time to vitrification shows a constant decrease from a/e = 0.2 to a/e = 1.3. Matejka [16] observed that the gelation time was the shortest for a/e = 1. His study was done on a DGEBA–D400 (polyetheramine) system.

Experimental data provided in Figure 17 can be used to determine gelation time from the theoretical gelation conversion of this DGEBA-IPD system, given by: $x_{epoxy,gel} = (r/3)^{1/2}$

At the gel point, for r = 1.05, $x_{gel} = (1.05/3)^{1/2} = 0.59$

r = 1.58, $x_{gel} = (1.58/3)^{1/2} = 0.73$

According to the conversion curves plotted, gel times at the stoichiometric ratio of 1.05 and 1.58 should be close to:

r = 1.05, $t_{gel} \approx 200$ min

r = 1.58, $t_{gel} \approx 100$ min

For a/e>1, i.e., in amine excess, the gelation time decreases with an increase of the stoichiometric ratio. No data were provided for epoxy excess.

Different behaviors were observed in the literature regarding the variation of gelation time as a function of the stoichiometric ratio: the chemical structure of the prepolymer and hardener may impact the results if the reaction mechanism is modified—for example, if etherification reaction or cyclisation occurred.

***Influence on the glass transition temperature***

The glass transition temperature, Tg, is an important piece of data for a thermosetting material as it corresponds to the softening of the network. This key property is directly linked to the structure of the network. Changing the initial stoichiometric ratio induces some modification in structure and in dominating reactions. In excess of amine, as reported by Wu [28], the reaction between the primary and the epoxy group dominates the cross-linking, and the etherification can be ignored. In the case of excess of epoxy, once primary and secondary amines are consumed, the etherification reaction can occur. The different kinetics of cross-linking lead to different architectures and cross-link densities of the resulting networks.

The different structures of epoxy-amine networks are discussed in the next paragraphs according to the three main possibilities of stoichiometric ratios: a/e=1, a/e>1, or a/e<1, for an ideal network formed only by epoxy-amine comonomers addition and without the occurrence of etherification reactions.

***At the stoichiometry a/e = 1:*** there is no defect in the network, meaning that all epoxy groups and amino hydrogens reacted together. The cross-linked density reached its maximum. This structure corresponds to the maximum Tg possible for given amine and epoxy comonomers.

***In excess of amine a/e > 1:*** chains between cross-linking points will be longer with mainly unreacted secondary amino groups. Therefore the cross-linked density compared to a network at the stoichiometry, i.e., (a/e=1) is diminished. Tg is below the one of the stoichiometric network.

***In excess of epoxy a/e < 1:*** pendant epoxy groups are present. The maximum cross-linked density cannot be reached. This network has a better macromolecular mobility. As a consequence, Tg of the corresponding network is lower than the one synthesized from a/e=1.

Therefore, the global shape of the curves of Tg as a function of the stoichiometric ratio shows a maximum for a/e = 1. It has been verified on many epoxy-amine systems [29]. An example is given by Chrysanthos [4] for three epoxy–amine networks: DGEBA, $DGEDAS_n$ oligomers of diglycidyl ether of isosorbide, and $DGEDAS_0$, pure monomers of diglycidyl ether of isosorbide cured with IPD (Figure 19).

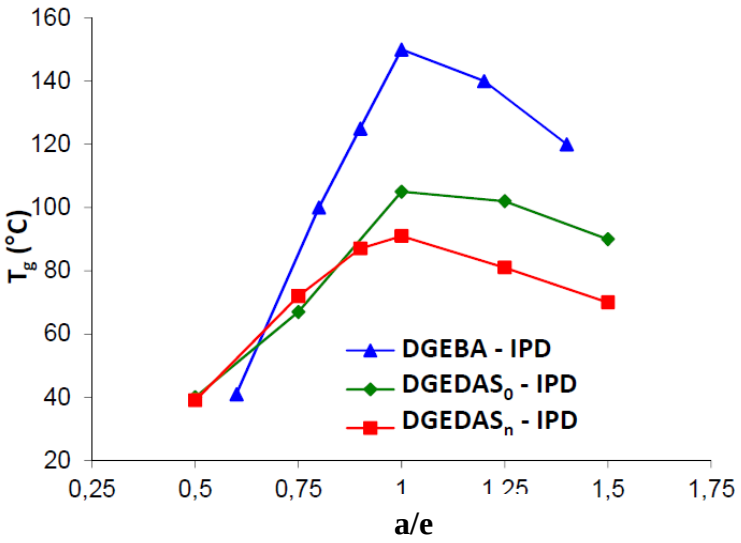


***Figure 19: Glass transition temperature versus a/e for networks based on DGEBA, DGEDAS$_n$ oligomers of diglycidyl ether of isosorbide, and DGEDAS$_0$, pure monomer of diglycidyl ether of isosorbide from in combination with IPD [4]***

### 1.3 Topological homogeneity of the network

Inhomogeneities described in the literature for polymer networks are ascribed to permanent fluctuations of cross-link density and composition, with sizes ranging from 10 nm to 200 nm [3]. The presence of such heterogeneities has long been recognized in polymer networks formed by free radical chain-wise polymerization. However, this cannot be generalized to all thermosets.

Regarding epoxy networks, the subject is still a controversial matter. Indeed, the interpretation of experimental data is often disturbing; for example, some authors used atomic force microscopy (AFM) [30] to show the existence of a two-phase structure, while other observations of a DGEBA-IPD-fractured surface show the homogeneity of the network as reported in Figure 20.

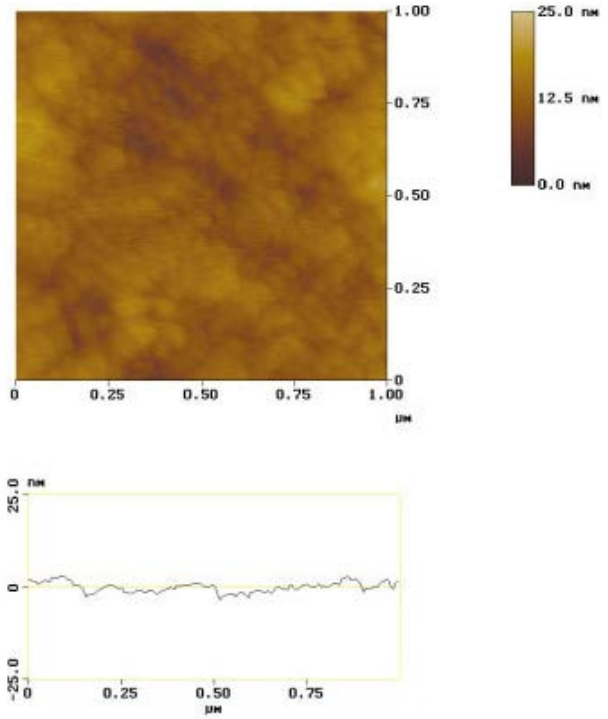


***Figure 20: Tapping mode AFM on DGEBA-IPD fractured surface: height images and height profiles***

This subject was discussed in depth by Dusek [31]. Even if historically some electron microscopy studies tended to say the contrary [32], small angle neutron scattering (SANS) [34] proved the homogeneity of epoxy-amine networks. Moreover, the fact that thermal and thermo-mechanical analyses give only one main glass transition with a well-defined relaxation peak also confirm this result. Another strong argument that supports the view of homogeneous epoxy networks is the good agreement between experimental values of conversion at the gel point and evolution of $M_w$, with the theoretical values alculated with the assumptions of an ideal and homogeneous (mean-field model).

However, even nowadays the debate is not closed. Recently, Sahagun and Morgan [33] reported a study on the influence of cure temperature on the network-building cross-linking reactions in a DGEBA-DDS system, and the subsequent effect on the homogeneity of the epoxy network. Cross-linked nodules were observed by AFM, with a size depending on the cure temperature. It was explained by the fact that temperature influences the ratio of the production rate of linear molecular segments compared to cross-linked or branched segments in the structure that form during the pre-gelation stage.

Dusek mentioned in his article [31] that inhomogeneous networks produced by step polymerization can be obtained if three different monomers are used (chemically induced inhomogeneities), or if there is a decrease of the solubility of reaction products (thermodynamic

driving force) also commented on by Wu [34]. An example is the case of the DGEBA and D2000 system. He also reported that inhomogeneities can result from the competition between two reaction mechanisms; for example, epoxy-amine reactions (step polymerization) and epoxy homopolymerization (chain polymerization) in DGEBA-dicyandiamide-catalyzed systems. In the general case, such inhomogeneities are induced by fast chemical reactions and are difficult to control. For this reason precursors of different architectures have been developed—among them cross-linked polymer microparticles.

## 1.4 CPM-filled epoxy networks

Cross-linked polymer microparticles can be used for many applications in epoxy network. They are suitable as organic fillers, pigments, matting agents, and reinforcing agents, and are important components of paint formulations, coatings, molding compositions, and adhesives [35].

Hönel et al. described in their patent [36] the use of cross-linked epoxy microparticles with an average particle size close to 5 μm and a Tg of at least 30°C as fillers and/or as partial substitutes of white pigments in aqueous paint preparations. The corresponding paints showed increased spreading power, less tendency for sedimentation and reduced crater formation.

With a similar protocol, Geisler [35] reported how to synthesize cross-linked polymer microparticles containing epoxide groups primarily via homopolymerization in presence of a Lewis base to avoid the tendency of the CPM to become yellow when they are heated to high temperatures.

Jansen et al. [37] prepared thermoset rubbery aliphatic epoxy particles and applied them as toughening modifiers for glassy epoxy networks. The advantage of these irreversibly preformed particles is the control of the size, shape and concentration of the toughening agent as compared to the use of a standard carboxy-terminated butadiene acrylonitrile (CTBN). These particles are prepared by curing droplets of an aliphatic epoxy (DGEPPO, diglycidylether of polypropyleneoxide) in an aqueous medium with polyetheramine (Jeffamine D230) to form DGEPPO particles. Two methods were used to disperse the particles in the DGEBA monomer: either an ultra-turax or a solvent (toluene). The curing agent was either piperidine or DETDA (an aromatic diamine). The first method yielded the formation of agglomerates, while with the solvent method aggregation was prevented, as it can be seen in Figure 21. The authors compared the fracture toughness, $K_{Ic}$, obtained for different modified networks (Table 2). $K_{Ic}$ was clearly improved for the two networks with the lowest Tgs (those cured with Epikure DX-6510, a cycloaliphatic amine, or piperidine). The authors concluded that preformed rubbery epoxy particles were promising toughening agents.

Another application reported by the same team is the use of aromatic-based particles as tracers in flow visualization of polymer melt.

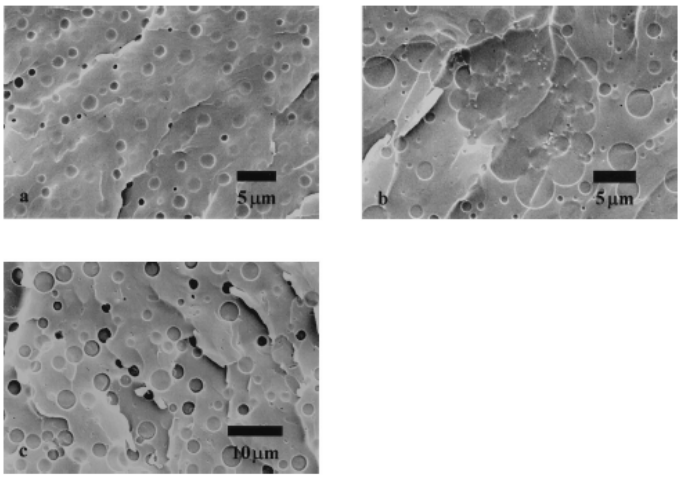


***Figure 21: SEM images of rubber dispersion for three different systems: (a) CTBN modified system, (b) dried rubbery particles directly dispersed in the epoxy resin, (c) rubbery epoxy particles dispersed in epoxy via the phase transfer route using toluene [37]***

***Table 2: Fracture toughness and Tg for different epoxy systems [37]***

| Epoxy resin | Curing agent | Rubber (15 wt%) | $K_{Ic}$ | $T_g$°C |
|---|---|---|---|---|
| Epikote 828 | DETDA | — | 0.51 ± 0.03 | 190 |
| | | CTBN | 0.67 ± 0.03 | 176 |
| | | DEGPPO-particles | 0.69 ± 0.02 | 185 |
| Epikote 862 | EpikureDX-6510 | — | 0.83 ± 0.02 | 133 |
| | | CTBN | 1.52 ± 0.07 | 130 |
| | | DGEPPO-particles | 1.47 ± 0.04 | 132 |
| Epikote 828 | Piperidine | — | 0.74 ± 0.08 | 96 |
| | | CTBN | 2.16 ± 0.05 | 92 |
| | | DGEPPO-particles | 1.71 ± 0.03 | 93 |

A similar approach was developed in a study by Imanaka [38], who investigated the crack-growth behavior of epoxy adhesives modified with cross-linked rubber particles called DCS, and CTBN, under mode I loading. Stress-strain curves of the matrix, the adhesive-modified formulation and of the matrix with YED111 (a reactive diluent), which was used to improve the deformability of the matrix, are reported (Figure 22). It was observed that the brittle behavior of the matrix was changed into a ductile behavior for both type of modification: with the cross-linked particles and with CTBN, and exactly in the same way. This study showed that cross-linked particles can be used to replace CTBN in some applications.

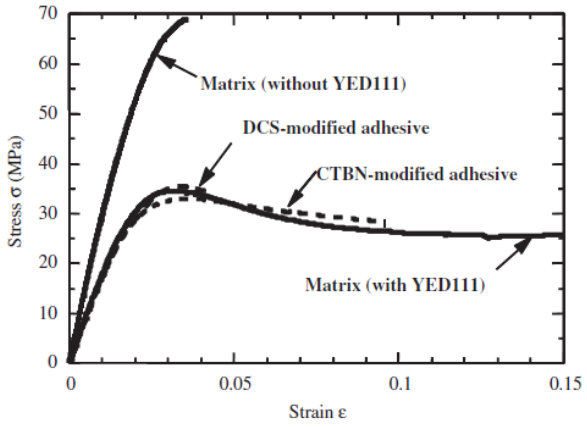


***Figure 22: (a) Stress-Strain curves of the modified and unmodified matrix [38]***

In the study of Valette [39], (Meth)acrylic CPMs were functionalized with hydroxyl groups in order to act as chain transfer agents with respect to the cationic photopolymerization of epoxy. As a consequence, reactive CPMs reacted with the epoxy network after the transfer reaction and re-initiation. Since the cationic epoxy network is glassy, rubbery CPMs have been used to improve the coating flexibility. Adding hydrophobic particles was also expected to reduce the water absorption of photopolymerized films. This is what is shown in Figure 23, where water absorption was plotted for three different epoxy systems. It was always measured at about 2% of water absorption whatever the ratio [e]/[OH]. The authors concluded that the presence of the CPMs strongly reduced the hydrophilic behavior of the epoxy network. They attributed this very specific behavior to the densely cross-linked structure of the CPM, which prevents the water molecules from penetrating into the network.

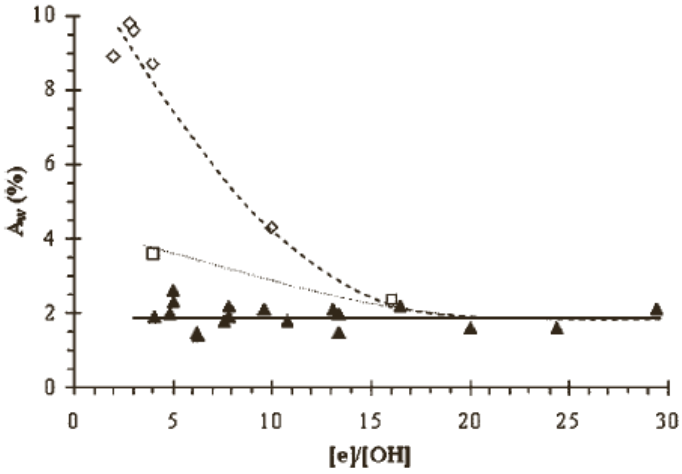


***Figure 23: Water absorption $A_w$, as a function of [e]/[OH] where [e] is the epoxy concentration for various transfer agents: ◊ TMP (trimethylol propane), □ HB5 (hyperbranched polyester polyol), ▲ CPM [39]***

Carfagna and coworkers used epoxy cross-linked microparticles synthesized by precipitation polymerization as active fillers for epoxy networks in order to modify the thermomechanical and rheological properties of epoxy systems.

In their first study [40], they investigated how to change the viscosity of epoxy resin by inclusion of reactive cross-linked microparticles. 10 and 20 wt% of DGEBA-DAT microparticles synthesized in excess of amino groups were added in DGEBA-DDS blends. The plot of the viscosity versus the temperature showed that the temperature value for the minimum viscosity decreases with increasing percentages of microparticles (Figure 24). The authors concluded that a higher reactivity of the system was due to the presence of the particles with amino groups, and they deduced that gel times decrease as the amount of microspheres rises. They commented on the attractive use of these particles as rheology control modifiers for fiber-reinforced composites and adhesives. It was also observed that the addition of these CPMs led to an increase of Tg. This was attributed to an increase in the cross-link density due to the presence of microparticles. Concerning the $G_c$ and $K_c$ values, only a very slight increase was observed. The authors concluded that the use of these particles could be an advantage in applications where thermal resistance is the priority and toughness is not a critical issue.

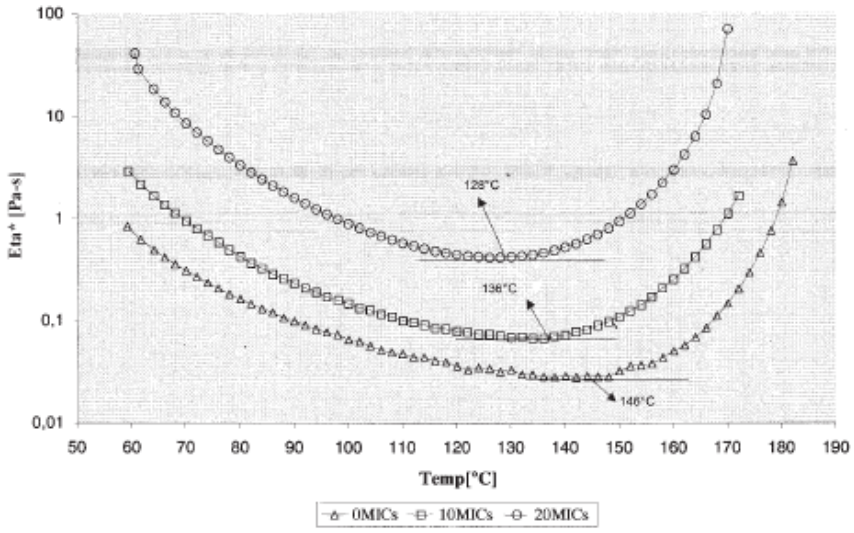


***Figure 24: Viscosity versus temperature curves for 0wt%, 10wt%, and 20wt% of microparticles added in DGEBA-DDS systems–heating rate 2°C.min$^{-1}$ [40]***

In a second study [41], epoxy cross-linked microparticles were added to epoxy-amine systems of the same chemical composition i.e. DGEBA-DAT. Calorimetric experiments were carried. The measure of a higher enthalpy of reaction for the system filled with the particles enabled the authors to conclude that unreacted groups of the particles can react both with themselves and with the epoxide groups from the matrix. Dynamic mechanical analysis showed that the presence of the

particles does not affect the Tg of the cured epoxy-amine system. Gel times were arbitrary recorded when the viscosity was about $10^4$ Pa.s (Table 3). The authors concluded that the inclusion of 5 and 10 pphr microparticles did not affect the gel time of the system, whereas adding a higher amount like 20 pphr resulted in the observation of a significant decrease in the gel time.

No enhancement of the toughness of the epoxy network was observed as a consequence of the strong adhesion between the matrix and the microparticles.

***Table 3: Gel times ($\eta^*=10^4$ Pa.s)–140°C–(MS=microparticles) [41]***

| System | Gel time (s) |
|---|---|
| Der 332/DAT | 1418 |
| Der 332/DAT/5 pphr MS | 1448 |
| Der 332/DAT/10 pphr MS | 1419 |
| Der 332/DAT/20 pphr MS | 888 |

***Figure 25: Complex viscosity versus time for the DER 332-DAT neat network and also with the addition of 5, 10, 20 pphr of CPMs, cured at 140°C***

Finally, a third study was carried out [42] on the effect of DGEBA-DAT and DGEBF-DETDA (diethyltoluenediamine) microparticles added in DGEBA-DDS system. Here also they observed a decrease of the temperature at the minimum viscosity with the addition of the particles and concluded that a higher reactivity of the system with an increase of the microparticle amount occurred. They attributed this effect to the presence of amino groups on the shell of the particles that can react with the epoxy groups in addition to those of the curing agent. They also gave data for the gel times whose method of determination was not well explained.

***Table 4: Gel times at various temperatures for filled (10, 20 wt%) and neat epoxy-amine systems–Mic = microparticles in DGEBA-DDS system[42]***

| | $t_{gel}$ (min) | | | | |
|---|---|---|---|---|---|
| $T$ (°C) | 0%Mic | 10%Mic1 | 20%Mic1 | 10%Mic2 | 20%Mic2 |
| 120 | 153.00 | 130.15 | 110.52 | 143.80 | 135.26 |
| 130 | 97.96 | 80.78 | 69.13 | 89.86 | 80.02 |
| 140 | 55.58 | 53.14 | 45.03 | 54.85 | 47.00 |
| 150 | 38.60 | 34.10 | 28.17 | 34.06 | 27.96 |

DMTA as well were investigated on the filled epoxy-amine system and showed an increase of Tg in the presence of the particles. This effect was attributed to the increase of cross-link density due to the microparticles, which behave as multifunctional sites and the reduction of free volumes of epoxy network by the expansion of the microparticles upon heating.

***Conclusions:***

The applications of epoxy-based CPMs reported in the literature were as flow modifiers and toughening agent in epoxy networks. Main conclusions that can be drawn are the following:

- In general an increase of the initial viscosity of the CPM-filled epoxy formulation was observed.
- Regarding gelation, contrasted results were published: with a given type of CPM, a significant decrease in the gel time was observed, while with the others, at least 20 wt% of CPMs was needed to see a slight influence.
- An increase in the final glass transition temperature of the filled networks may be observed in some cases.
- No enhancement of toughness was observed if glassy or rubbery CPMs were added to a high Tg matrix, while on the contrary, rubbery particles added into a medium Tg matrix lead to higher toughness. Good adhesion at the interface did favor the crack propagation and prevent the CPMs to act as crack stoppers.

This last property, toughness of some CPM, was exploited in some patents to develop aqueous paints. Such particles seem interesting to synthesize to be dispersed in epoxy-amine formulations and to further investigate their influence and behavior during the cross-linking. Before presenting our experimental results with the use of CPMs, all the microparticles already synthesized by precipitation polymerization by other teams will be reported in the next section, as well as the route to obtain them.

## 2 Technologies to synthesize polymer microparticles

Micron-sized monodispersed polymer particles are used in a wide variety of applications and at the interface of many domains as presented in Figure 26 [43]. Their main industrial applications can be divided into three large categories: components of binders for organic coatings, carriers of dyes or pharmaceutical and chemical compounds, and fillers or materials for reinforced plastics [44]. Nevertheless, they are not limited to these domains, and also have very useful properties for ink toners, instrument calibration standards, column-packing materials for chromatography, spacers for liquid crystal displays, and in electronics for instance. As a consequence, because of the commercial and scientific interest in microparticles for many applications, research into their preparation has been active for the past four decades.

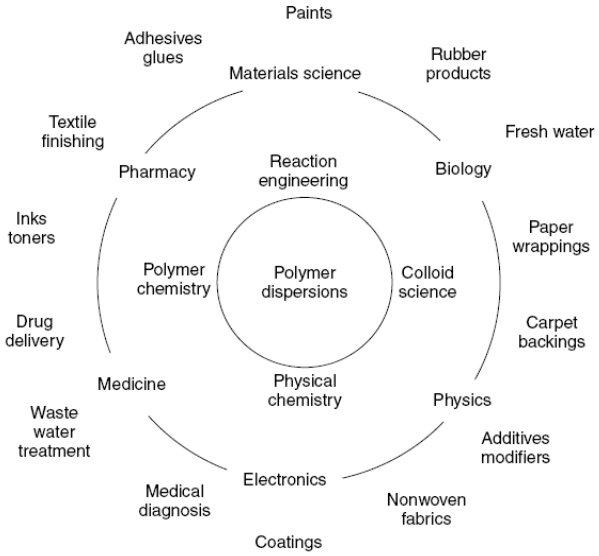


***Figure 26: Important application fields of polymer microparticles produced by polymerization in dispersed media [43]***

### 2.1 Overview of synthesis techniques

Polymer particles can be synthesized via several techniques including emulsion, dispersion, suspension and precipitation polymerization. Micron-sized monodispersed particles were usually difficult to produce because this size is in-between the diameter range of particles produced by conventional emulsion polymerization (0.06–0.7 μm) in a batch process and suspension polymerization (10–1000 μm) [45,46]. We will comment in a short summary on the emulsion, dispersion, and suspension polymerization and will give more details about precipitation polymerization, which is the method used in the framework of this project.

Particle size ranges traditionally given by the different techniques are summarized in Figure 27.

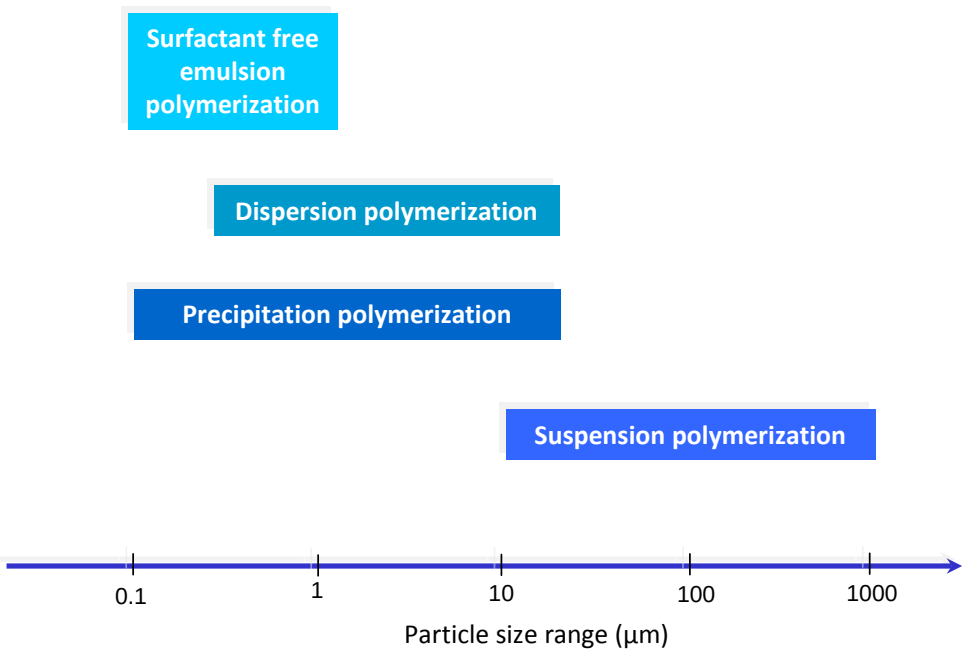


***Figure 27: Particle size range of synthesis techniques to form micron-sized particles***

***Dispersion precipitation***

The dispersion polymerization [45, 47, 48] produce particles whose diameter is about 0.15 to 15 µm, often with excellent monodispersity. The polymerization occurs in the presence of a suitable polymeric stabilizer. The solvent selected is a good solvent for both the monomer and the steric polymer stabilizer, but a non-solvent for the polymer being formed. Therefore, dispersion polymerization involves a homogeneous solution of monomer(s) with initiators and dispersant, in which sterically stabilized polymer particles are formed by the precipitation of the resulting polymers. Most studies on dispersion polymerization involve vinyl monomers such as styrene [49], (meth)acrylate [50], and their copolymers combined with stabilizers such as polyvinylpyrrolidone (PVP) in polar media, usually alcohols. A good alternative to the use of stabilizers is the use of reactive functional co-monomers. They participate in the polymerization process and become covalently attached to the polymer chain. They can easily help to incorporate functional groups into microparticle structure [51–52]. Moreover, another interesting method is the seeded polymerization technique utilizing a two-step swelling process [53–54]. After the synthesis of microparticles by dispersion polymerization, monomers are adsorbed by the polymer particles, which are then polymerized in a second step once they are separated from the medium.

***Suspension polymerization***

Suspension polymerization [55] is one of the major heterogeneous polymerization techniques used to produce polymer particles on an industrial scale [56]. The suspension polymerization technology was developed in the early 1900s in Germany in the quest for synthetic rubber [57–58]. It was later adopted in the synthesis of other polymers and the first polymer particles were commercially available in the 1930s. Suspension polymerization is distinguished from other heterogeneous techniques (emulsion, dispersion, and precipitation polymerization) in that an oil phase containing monomer and initiator is dispersed in a continuous phase (usually water), with the polymerization taking place within the oil droplets [46], [59].

This produces polymer particles that can be from about 10 μm up to several millimeters in diameter. Commercially important polymers produced by suspension polymerization today include PVC, PS, and PMMA.

A major advantage of suspension polymerization over homogeneous polymerization techniques such as bulk or solution polymerization includes the facilitated removal of heat evolved during the polymerization. This is important in order to ensure stable product properties and a safe process. The high heat capacity of water, combined with the large surface area of the organic droplets, provides excellent heat transfer from the organic droplets to the water phase.

***Emulsion polymerization***

Conventional emulsion polymerization traditionally leads to submicron size particles (0.05–0.2 μm) [46] more often considered nanoparticles rather than microparticles. One technique to obtain micron-sized particles is to use the surfactant-free emulsion polymerization method. Thus using with route, particles about 1μm can be synthesized. The polymerization is carried out in the same way as in emulsion polymerization but without adding any surfactant. In the absence of surfactants, limited flocculation of particles greatly reduces their number per unit volume and increases particle size [60,61,62].

## 2.2 Precipitation polymerization

In our study, we focused on the synthesis of micron-sized particles by precipitation polymerization, which is a very convenient method to avoid the use of surfactants or stabilizers and also mechanical stirring during reaction. Precipitation polymerization allows flexible control over important physicochemical properties of microparticles, such as size distribution, surface charge, chemical composition and microstructure [63]. This paragraph will focus on cross-linked polymer microparticles (CPMs) also called microgels.

### *2.2.1 Principle of the reaction-induced phase separation (RIPS) phenomenon*

Phase separation phenomenon is driven by thermodynamics, from changes in the free energy of the polymer solution called the mix [64]:

$$\Delta G_m = \Delta H_m - T\Delta S_m \qquad \textit{Equation 11}$$

where $G_m$ is the Gibbs free energy of the mix, $H_m$ is the enthalpy associated with the energetic level of the mix, T, the temperature in Kelvin and $S_m$, the entropy related to the randomness of the mix.
The Flory-Huggins' solution theory is a mathematical model for the thermodynamics of polymer solutions, which takes into account the great dissimilarity in molecular sizes in adapting the usual expression for the entropy of mixing increments associated with mixing process [65].

$$\frac{\Delta G_m}{k_B T} = (1-\phi)\ln(1-\phi) + \frac{\phi}{n}\ln\phi + X\phi(1-\phi) \qquad \textit{Equation 12}$$

where: $k_B$ is the Boltzmann's constant

$\phi$ : volume fraction of polymer

$(1-\phi)$: volume fraction of solvent

n: number of monomer units in oligomers

X : interaction parameter of the polymer/solvent

With:

$$X \equiv \frac{U_0}{k_B T} \qquad \textit{Equation 13}$$

$U_0$: dispersing energy

T: absolute temperature

In Equation 12, the first two terms decrease during the polymerization. Consequently, the third term becomes predominant and shows the importance of the interaction parameter X, of the polymer/solvent to control the RIPS phenomenon. Also consequently, the critical step to employ this method is to determine the appropriate solvent, specific for each monomer/polymer combination to obtain a phase separation once the polymer starts to grow.
The ternary phase diagram of the phase separation phenomenon is given in Figure 28. It shows that only the right proportion of monomer/solvent leads to phase separation, which can be critical to find.

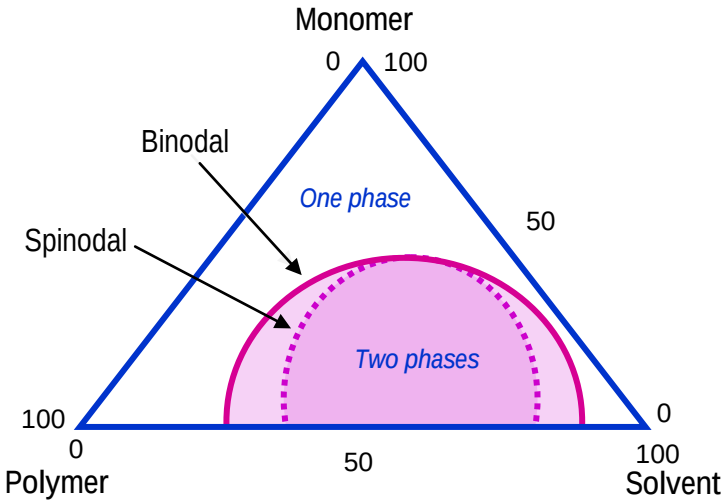


***Figure 28: Ternary polymer-monomer-solvent phase diagram***

Monomers and an initiator if needed, are dissolved in the solvent to give a perfectly homogeneous solution. The solvent chosen to dissolve the monomers is a poor solvent of the polymer formed. The solvent is then also called the precipitant. Induced by polymerization, the solubility parameter of the growing polymer is modified, leading to 3 types of different morphologies, as visible in Figure 29. The first possibility is the formation of microparticles precipitating as an insoluble polymer. The opposite morphology is also possible and concerns the formation of microporous networks with solvent cavities, which must be removed to obtain a porous solid. Porous materials have received much attention in recent years, but thermosetting porous materials have been rarely used [66,67]. The last morphology is to produce bicontinuous phases.

Several works were found in the literature reporting how to synthesize microparticles by precipitation polymerization and are presented in the next two paragraphs classified according to their polymerization process: the free radical polymerization and polyaddition polymerization.

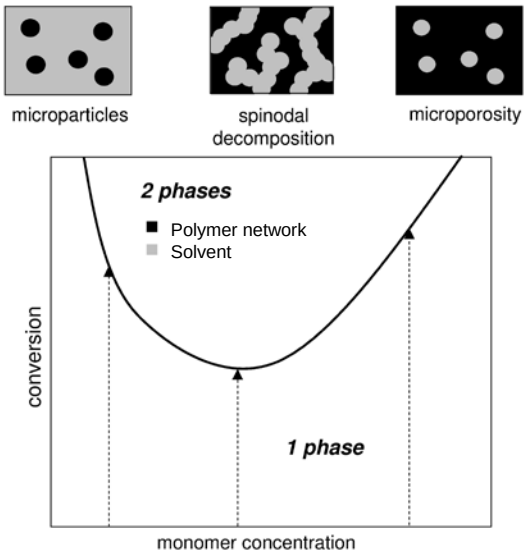


***Figure 29: Phase diagram of the 3 possible morphologies obtained by RIPS for a polymer solvent blend [2]***

### *2.2.2 Synthesis of CPMs via free radical polymerization*

Precipitation polymerization was used for the first time by Chibante [68] in 1986 for the synthesis of cross-linked poly(N-isopropylacrylamide) (PNIPAM) microparticles in aqueous media. Potassium persulfate was used as initiator. The reaction took place at 70°C. TEM micrograph of the uncleaned particles obtained is reported in Figure 30. These PNIPAM particles had a specific behavior. They exhibited a temperature-sensitive phase transition in water [69] leading to different diameter size depending on the temperature. At low temperatures, the particles had a diameter about 1 μm, whereas at higher temperatures, they contracted by a factor of 10 in volume.

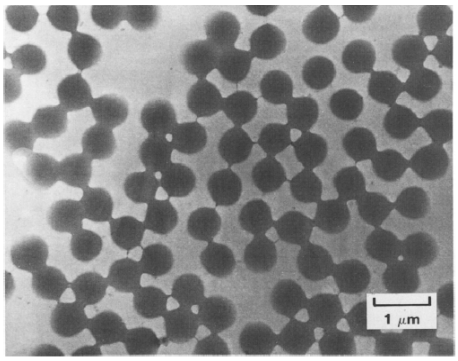


***Figure 30: TEM observation of uncleaned PNIPAM latex obtained by precipitation polymerization [68]***

Other chemistries have since been applied with the same method to synthesize microgels [70]. Free radical polymerization is one of the most famous polymerization routes to make microparticles from styrene [71], acrylate [72], methyl methacrylate [73, 74, 48], methacrylic acid [75], or divinylbenzene (DVB) [76], as shown in Figure 31. These specific particles were synthesized by the

copolymerization of divinylbenzene and methylstyrene with AIBN as initiator. The authors made a morphology map based on the DVB level and solvent composition (percentage of methyl ethyl ketone, MEK and heptane). This map indicated that poly(DVB-x) micro-spheres were formed as an intermediate morphology between microgels, macrogels, and coagulum. The solvent composition strongly affects the polymerization of DVB-x by controlling the dimensions of the polymer coil as it is formed. Neat MEK, a good solvent for styrenic polymers, leads to a typical solution type polymerization with or without cross-linking. Neat heptane, on the other hand, leads to classical precipitation polymerization. In mixtures of MEK and heptane there is a transition from solution polymerization to precipitation polymerization.

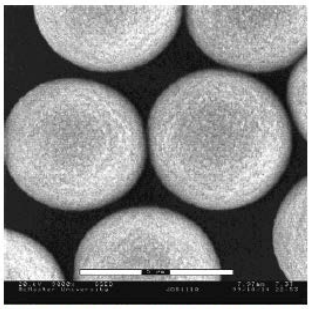

***Figure 31: SEM images of DVB microparticles synthesized in monomer concentration of 4 wt% in a mix of 80:20 MEK:Heptane – scale bar: 5 µm [76]***

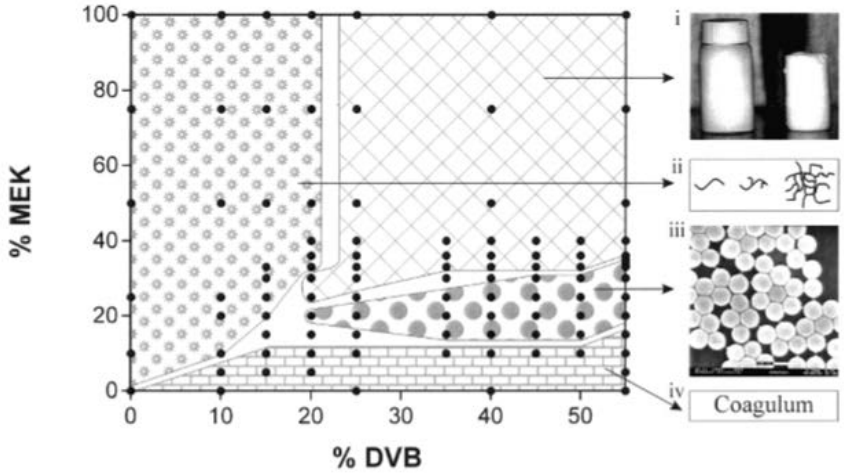


***Figure 32: Morphology map for divinylbenzene/methylstyrene polymerization in MEK:heptane– Morphologies are shown after 24 h of polymerization at 70°C. (i)= space-filling macrogel, (ii)=soluble polymer, which includes linear, branched, and microgel structures, (iii):microparticles, (iv):coagulum [76]***

### *2.2.3 Synthesis of CPM via polyaddition polymerization*

Works published on the synthesis of microparticles by precipitation polymerization via polyaddition are fewer compared to the synthesis via free radical polymerization. Most of these published works concern particles synthesized from the epoxy chemistry.

Hseih and Woo [77] were the first to show in 1996 the possibility of obtaining epoxy microparticles via phase separation in organic solvent. Indeed, in their work, polymethylmethacrylate,PMMA, was used as a solvent in a DGEBA/DDS/PMMA system, which was homogeneous before the cross-linking. PMMA concentration was adjusted to obtain different particle morphologies. Large epoxy particles were obtained with diameters between 10 and 60 µm. They were extracted from the PMMA by dissolution in methylene chloride. Tg of the particles was measured by DSC and varied from 135 to 165°C depending on the reaction temperature. The SEM image of the particle obtained is shown in Figure 33.

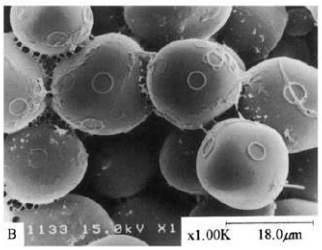


***Figure 33: SEM image of DGEBA/DDS microparticles synthesized in PMMA (100/30/20) after etching with methylene chloride, 2-h reaction at 177°C [77]***

In 2000, Hibino [78] synthesized epoxy-amine particles by polymerization of epoxy, in a stationary system using polyether as organic media. Several cross-linkers were used, such as methylenedianiline (MDA), ethyelediamine(EDA), and isophorone diamine (IPD) leading to particle Tg at 70°C and 120°C. The particles were obtained after 10 h of reaction at 25°C and 100°C, respectively. Particles diameter were observed of sizes between 3 and 8 µm, depending on the synthesis conditions. SEM image of the particles synthesized with MDA are shown in Figure 34.

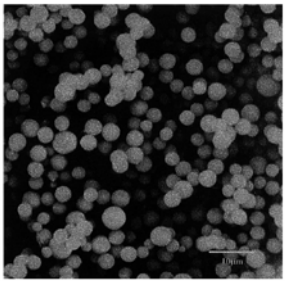

***Figure 34: SEM image of epoxy microparticles obtained in polyether, 10 h at 100°C – scale bar: 10 µm [78]***

Then, an Italian team published three papers on the synthesis of micron-sized epoxy particles with the aim to use them as fillers in epoxy-amine-based networks [40,41,42] as already discussed in section 1.4 of this chapter. Particles were obtained as products of the reaction between a bisphenol F or A epoxy resin (DGEBF or DGEBA) and an aromatic amine hardener (DAT) in polypropylene glycol (PPG). The particle formation occurred under constant temperature without any stirring. These microgels were synthesized in excess of reactive amino groups to keep some on the outer surface of the particle. An example of the particles obtained from DGEBA and DAT, after 15 h at 130°C in PPG 1000, are shown in Figure 35.

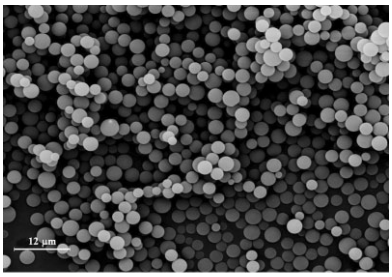


***Figure 35: Microparticles obtained from DGEBA and DAT (diamine toluene)dissolved in PPG1000, polymerized for 15 h at 130°C – scale bar: 12 µm***

Traina et al. [2] also synthesized similar epoxy-based particles and deeply investigated the influence of the synthesis parameters (monomer concentration, stoichiometry, and reaction temperature) on the morphology, Tg of the particles, and effective stoichiometry. The glass transition temperatures of the particles was found to vary between 130 and 160°C using an aromatic diamine (DAT) and between 116 and 141°C using a cycloaliphatic diamine (IPD). It was also found that the effective stoichiometry of the particles was different from the initial stoichiometry in the feed solution.

Tsujioka and coworkers [65] also synthesized similar epoxy particles from DGEBA and diglycidyl ether of hydrogenated bisphenol A, DGEHBA, with Bis(4-aminocyclohexyl)methane, BACM, and polyaminoamide (PAA) in several types of polyethylene glycols. Mapping of the different morphologies obtained was done varying the reaction temperature and the stoichiometric ratio (γ=a/e) from 90 to 120°C and 0.8 to 1.3, respectively. Microparticles, bicontinuous structures, and porous monoliths were observed, depending on the synthesis conditions (Figure 36).

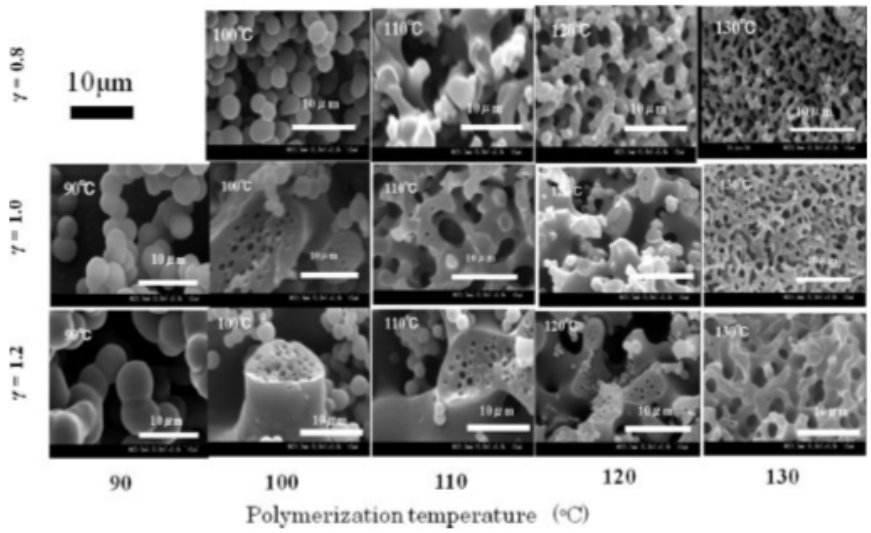


***Figure 36: SEM micrographs of DGEBA/BACM system polymerized in PEG200, monomer concentration: 0.285 wt%, Temperature: 90–130°c, a/e=γ=0.8-1.2***

Recently, Yu et al. [79] prepared cross-linked epoxy microspheres via reaction-induced phase separation, RIPS, using caprolactone as solvent. These particles were used as precursors for accessing macroporous silica materials via pyrolysis at elevated temperatures. Particles were first functionalized to bear 2-bromopropionyl groups, which were then used as initiators to obtain poly(glycidylmethacrylate)-grafted microspheres. In a third step, these particles were reacted with 3-aminopropyltrimethoxylsilane (APTMS) to obtain the epoxy microspheres with a high amount of trimethoxysilane groups. In the last step, sol-gel reactions were conducted between the particles and tetraethoxysilane to obtain organic/inorganic glassy solids.

From the data presented so far, it appears that epoxy microspheres can be synthesized quite easily via precipitation polymerization if the experimental conditions and especially the chosen solvent are well suited. One of the main advantages of this technique is to avoid the use of a surfactant, which is always difficult to eliminate.

To our knowledge, the epoxy-based CPMs were only characterized by their diameter obtained by electron microscopy and their glass transition temperature obtained by DSC. In particular the real functionality of these CPMs has never been measured despite it was considered as a key point. Only assumptions and not quantitative analysis were made. These assumptions were based on the fact that if amino groups were present in excess in the unreacted formulation, then CPMs should bear amino groups on their surface. The presence of these amino groups was expected in order to react

with epoxy groups as CPMs were introduced in epoxy-amine formulation and to establish covalent bonds at the interface.

## 2.3 Conclusions

This literature survey highlighted, on one hand, the potential interest in synthesizing epoxy-based CPM and applying them in some specific applications. On the other hand, it also shows the lack of understanding of the relationship between the structure, the functionality of CPM, the chemorheological behavior of the dispersion, and the final properties of the CPM-filled networks. This is what is presented in the following chapters where a special effort was made to quantify the surface amine of the particles and understand how the particles behave in epoxy formulation and their influence on the final materials.

# II SYNTHESIS AND CHARACTERIZATION OF EPOXY-BASED CROSS-LINKED POLYMER MICROPARTICLES (CPMS) VIA PRECIPITATION POLYMERIZATION

## 1 Introduction

The aim of this chapter is to describe the synthesis of epoxy-based cross-linked microparticles and to report relationships between synthesis parameters and CPM properties.

CPMs were chosen among several techniques (see chapter 1) to be synthesized by a precipitation polymerization via the reaction-induced phase separation (RIPS). This technique, which does not employ any surfactant, is of great interest for generating micron-size particles and avoiding surface pollution of the particles, but is based on a phenomenon which occurs only in specific conditions of temperature, monomer concentration, reaction time and nature of solvent [40, 41, 42, 77, 78, 80]. Indeed, the solvent needs to have a good affinity with the monomers and a poor affinity with the resulting polymer, which therefore precipitates during the reaction. A previous study was carried out to determine the right combination of epoxy-amine/solvent [2]. Thus, perfectly spherical microparticles were synthesized utilizing polypropylene glycol (PPG) as the solvent which can also be denoted the precipitant.

A similar protocol was employed in our study to form particles. These cross-linked epoxy microparticles, CPMs, can be used as fillers in an epoxy-amine matrix. According to this objective, these microparticles need to be reactive fillers in order to form covalent bonds with the matrix. As a consequence, they were synthesized with an initial excess of amino hydrogen to conserve residual amino groups in the structure at the end of their synthesis.

Reference parameters were established as standards and led to the precipitation of reference CPMs (CPM ref). Their synthesis and properties are reported in the first part of the chapter. Then, the influence of the synthesis parameters, i.e. the stoichiometric ratio, the reaction time and chemical structure of monomers on the final properties of the CPMs, is reported in the second part of the chapter.

# 2 Experimental

## 2.1 Materials

The CPMs were prepared by the reaction of a low molar mass epoxy resin with an amine hardener. The epoxy resin was a diglycidyl ether of bisphenol A (DGEBA) (DER™331; DER is a trademark of the Dow Chemical Company) with an epoxy equivalent weight of 182-192 $g.eq^{-1}$. The curing agent, isophorone diamine (IPD), was a cycloaliphatic amine with a hydrogen equivalent weight of 42.5 $g.eq^{-1}$; this was purchased from Sigma Aldrich. Polypropylene glycol (PPG) with an average molar mass of 1,000 $g.mol^{-1}$ and dodecane were both purchased from Sigma Aldrich. PPG and dodecane were mixed at 90:10 wt ratio and this mixture is hereafter referred to as a solvent. A higher molar mass epoxy pre-polymer, DER™662E, with an average epoxy equivalent of 610 $g.mol^{-1}$ as well as another hardener, an aliphatic amine, Jeffamine D230 (manufactured by Huntsman) were also utilized. All products were used as received. Their structures are reported in Table 5.

***Table 5: Monomers and solvent used to synthesize CPMs***

| EPOXY | AMINE | SOLVENT | |
|---|---|---|---|
| DER 331 | IPD | PPG | Dodecane |
| 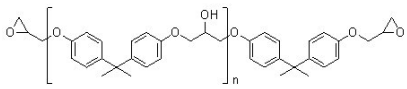 | 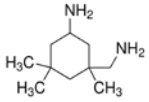 | 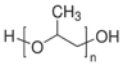 | 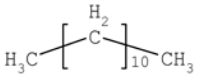 |
| Mw = 374 $g.mol^{-1}$ | Mw = 170 $g.mol^{-1}$ | Mw = 1000 $g.mol^{-1}$ | Mw = 170 $g.mol^{-1}$ |

| EPOXY | AMINE |
|---|---|
| DER 662E | D230 |
| 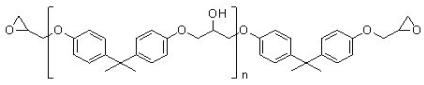 | 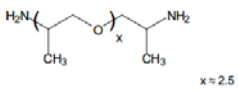 |
| Mw = 1220 $g.mol^{-1}$ | Mw = 230 $g.mol^{-1}$ |

## 2.2 Synthesis protocol

DGEBA and IPD were dissolved separately in the solvent at 40°C for 20 min in order to obtain homogeneous solutions. Then, the two solutions were mixed and placed in the pre-heated oven at 100°C to allow the reaction between epoxy and amine to proceed. The reaction mixture was not stirred during the polymerization. A white precipitate was formed in the course of the reaction which was further isolated by filtration and subsequent washing with solvents: 3 times with acetone, 3 times with THF and one more time with acetone. Finally, the powder was dried under vacuum at 60°C for at least 48 h. Agglomerates of dry particles were obtained. CPMs with different stoichiometric ratios (a/e = amino hydrogen / epoxy) were prepared, from a/e = 0.9 to a/e = 1.5, in

order to generate different residual amine concentrations. CPMs were collected after 24 h of polymerization at 100°C.

The conditions corresponding to the synthesis of the reference CPMs (CPM ref) were as follows: a stoichiometric ratio a/e = 1.35, monomer concentration of 10 wt%, PPG + dodecane (weight ratio: 90/10), reaction temperature of 100°C and reaction time of 24 h. These are reported in Table 6.

***Table 6: Synthesis parameters for CPM ref***

| a/e | Monomer concentration (wt%) | Solvent PPG:dodecane | Temperature (°C) | Time (h) |
|---|---|---|---|---|
| 1.35 | 10 | 90:10 | 100 | 24 |

## 2.3 Characterization techniques

***Cloud point measurement***

During the CPM synthesis, the light transmittance through the solution was monitored using a home–made instrument. Once the reaction had started, the initial homogenous transparent solution of monomers and solvent reached the critical conversion, which induced the phase separation phenomenon. The time to obtain a cloudy solution was measured and called time to phase separation: $t_{ph.s}$, or cloud point (CP).

***Size exclusion chromatography (SEC)***

SEC was used to separate and calculate the content of DGEBA in the solution during the CPM formation. Calibration of the DGEBA response was previously realized using 5 solutions of different DGEBA concentrations. The elution solvent used was tetrahydrofuran (THF) and the flow rate was 1mL/min. Three columns (Waters ultrastyragel HR0.5, HR1 and HR2) were used for the separation. The detection was done using a refractive index detector Shimadzu RID 10A. Injection volume was 100 µL.

***Thermogravimetric analysis (TGA)***

The measurements were performed with a Q500 from TA Instrument. Samples of about 10 mg were heated at a rate of 10°C/min within the temperature interval of 25°C to 550°C, under a nitrogen atmosphere.

***Thermogravimetric analysis –Fourier transform Infrared (TGA-FTIR)***

TGA was performed on a Q50 from TA Instrument from room temperature to 600°C at 10°C/min under a nitrogen atmosphere. Then gases released from the TGA were analyzed by infrared with a Nicolet Nexus equipped with a globar (CSi) source, a KBr/Ge beam splitter and an MCT/A detector cooled down with nitrogen. All spectra were collected with a resolution of 4 $cm^{-1}$, 16 scans per spectrum. The infrared cell was heated at 240°C.

***Differential scanning calorimetry (DSC)***

The dried CPM powders were analyzed by DSC in order to obtain the glass transition temperature: Tg, measured at the inflection point. DSC measurements were performed with Q20 (TA) calorimeters. The recording program was as follows:

1- First heating ramp (10°C/min) from -10°C up to 220°C.
2- Cooling stage down to 0°C (50°C/min).
3- Second heating ramp from 10°C up to 200°C.

All of the tests were conducted under nitrogen in open Aluminum pans. The data were analyzed using the software TA Universal Analysis.

***Near-Infrared spectroscopy (NIR)***

The NIR spectra, in the range of 4,000–12,000 $cm^{-1}$, were obtained in transmission mode with an FT-NIR spectrometer Bruker (Billerica, MA) Equinox 55, equipped with a tungsten halogen source, a quartz beam splitter, and an InGaAs detector. All spectra were collected with a resolution of 4 $cm^{-1}$, 32 scans per spectrum. NIR was used for the characterization of neat CPMs. Pure particle pellets with a thickness of about 0.5 mm were realized and their spectra were acquired at room temperature. This method was used to identify the residual amino or epoxy groups in the CPMs. Integration under the absorption band for the epoxy conversion was given by the software OPUS from Bruker. Typical bands observed for the epoxy-amine reaction were those corresponding to the disappearance of the oxirane ring at 4530 $cm^{-1}$ and 6071 $cm^{-1}$.

***Scanning electron microscopy (SEM)***

SEM was carried out to study the morphology of particles and to evaluate their diameter size and size distribution. CPMs were observed with a Philips XL20. The CPM powder was placed on a metal stub covered with a conductive graphite adhesive and then gold coated by sputtering. Micrographs were collected at several magnifications by applying a voltage of 15-20 kV. Open source software, Image J, was employed to extract the average particle diameter.

# 3 Results and discussion

## 3.1 Synthesis and characterization of the reference CPMs

### *3.1.1 Monitoring of the CPM synthesis*

***Visual observations and solubility parameters***

The solution of reactants, DER 331, IPD, PPG+dodecane (marked as t = 0 min) was homogeneous. The solution became hazy during the course of the reaction at 100°C, once the phase separation induced by the epoxy-amine reaction had started. Photos representative of the evolution of the reaction blend from a transparent solution to the white dispersion are presented in Figure 37. The filtration of the solution gave a white powder composed of CPMs, as shown in the picture on the right. The successive reactions between epoxy and amine induced a progressive change in the interaction parameters between the solvent and the growing epoxy-amine network through an increase of its solubility parameter [81].

Solubility parameters (van Krevelen contribution group method) [82] of the components used are given in Table 7. The solubility parameter of the PPG-dodecane mixture was calculated with the following law:

$$\delta_{mix} = \delta_1.\varphi_1 + \delta_2.\varphi_2 \qquad \textit{Equation 14}$$

with δ: solubility parameter (MPa ½)

φ: volume fraction

1: solvent 1

2: solvent 2

Dodecane, which has a very low solubility parameter ($\delta_{dod}$ = 16.2 MPa ½) compared to PPG ($\delta_{PPG}$ = 18.9 MPa ½), was added as a non-solvent to achieve an earlier phase separation. As expected, with the addition of 10 wt% of dodecane, the value of the solvent mix was decreased to $\delta_{mix}$ = 18.5 MPa ½. The solubility parameters of the epoxy-amine blend before the reaction and for a cross-linked network were calculated by Mezzenga [83]. It is worth noting that the solubility parameter of the network formed was significantly increased compared to the unreacted mixture. Therefore, the gap between the solubility parameter of the solvent mix and that of the polymer formed was also increased leading to the phase separation phenomenon.

*Table 7: Solubility parameters from Van Krevelen additive group method*

| Product | PPG | Dodecane | PPG/dodecane 90:10 (wt%) | DGEBA/IPD *before reaction* | DGEBA-IPD *after reaction[83]* |
|---|---|---|---|---|---|
| δ (MPa ½) | 18.9 | 16.2 | 18.5 | 18 | 20.6 |

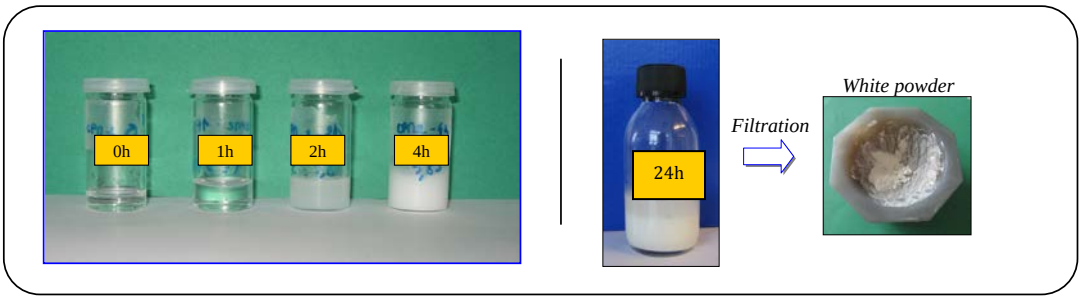


*Figure 37: CPM solutions at different stages of the reaction @ 100°C: from 0 h to 24 h - CPMs obtained after filtration*

## ***Cloud point measurement***

The reaction was followed by measuring light transmittance through the sample. Cloud point (CP) corresponds to the time of reaction when the solution became opaque and light detected through the solution was severely decreasing. Indeed, the presence of microparticles with dimensions comparable to the wavelength of light induced scattering. The light transmittance signal monitored through the solution during the CPM formation at 100°C is given in Figure 38. CP was taken just after the severe decrease of light transmittance, as explained graphically hereafter. According to this method, the CP of the CPM ref was measured after 1h47 of the reaction at 100°C.

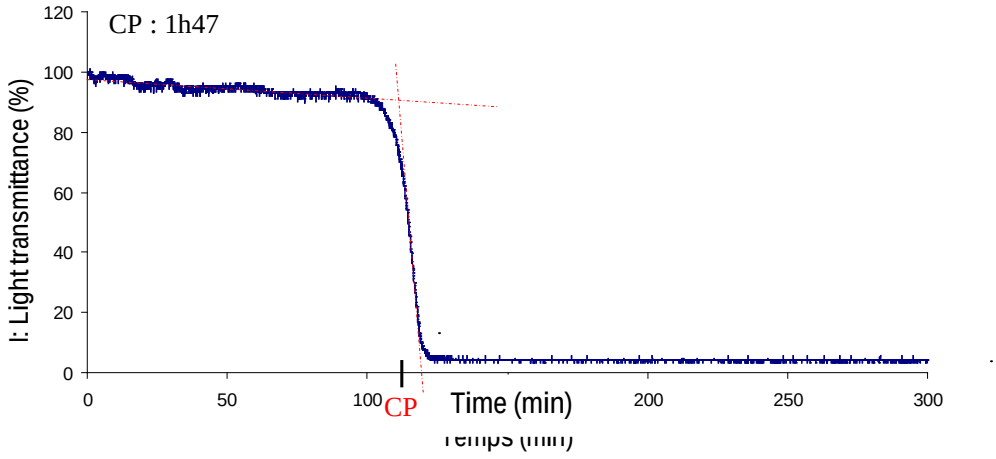


*Figure 38: Cloud point (CP) measurement – Percentage of light transmittance through the solution during the CPM formation at 100°C*

The phase separation for the reference system was also monitored by microdielectrometry. The results are reported in appendix.

***Epoxy conversion during CPM formation monitored by SEC***

The conversion of the epoxy groups was calculated by monitoring the residual DGEBA concentration in the supernatant. Previously, each component (PPG, DGEBA, dodecane) was injected separately into the size exclusion chromatography (SEC) to determine whether separation between different components could be detected (Figure 39). The elution volumes for PPG, DGEBA (n=0) and dodecane were 21.3, 25.7 and 26.7 mL, respectively. IPD did not give any exploitable signal. The SEC signal was calibrated with different concentrations of DGEBA to give a linear response between the concentration of DGEBA solutions and the area under the refractive index (RI) peak detected (see Figure 40).

Hence, the supernatant was analyzed after different reaction times and filtration of the CPMs. The decrease in the DGEBA peak (retention volume: 25.7 mL) due to its reaction with the hardener is shown in Figure 41. By the integration of this peak, the remaining concentration of DGEBA was calculated. Then, the conversion of DGEBA was calculated according to Equation 15 and [84], and plotted as the function of the reaction time. This is reported in Figure 42.

The conversion of the DGEBA monomer, X, is given by:

$$X = 1 - A_t/A_0 \qquad \textit{Equation 15}$$

where $A_0$ and $A_t$ are the area of the DGEBA signal (25.7 mL) at t=0 and t=reaction time, respectively.

After 24h of reaction at 100°C, 12% of DGEBA remained in the supernatant, which means that 88% of the DGEBA molecules had been converted into the CPM. CP measured at 1h47 of reaction corresponded to the conversion of approximately 47% of DGEBA. After 4h of reaction, there was a decrease in the rate of the reaction. At this stage, 75% of the DGEBA molecules were included in the CPM structure.

One should pay attention to the fact that, a DGEBA molecule bears 2 epoxy groups. Only one group can have reacted to consider the molecule incorporated into the CPM structure. We are interested in the value of the conversion of epoxy functions, x. A relationship has been established between X and x, which is based on the following assumptions [84]:

- Each DGEBA molecule has 2 epoxy functions, and all epoxy functions have the same reactivity.
- An epoxy molecule remains in the medium if simultaneously two epoxy functions (from the same molecule) have not reacted
- The probability of finding an unreacted epoxy function is: p = 1-x

- The probability of finding an unreacted epoxy molecule is: P = 1-X

It is expressed by: $P = p^2 \rightarrow (1-X) = (1-x)^2$ Equation 16

$$x = 1-(A_t / A_0)^{1/2}$$

From such a calculation, the cloud point (CP = 1h 47) corresponded to an epoxy function conversion close to 30%, as calculated from the SEC signal. After 24 h, about 70% of epoxy functions had already reacted (Figure 43).

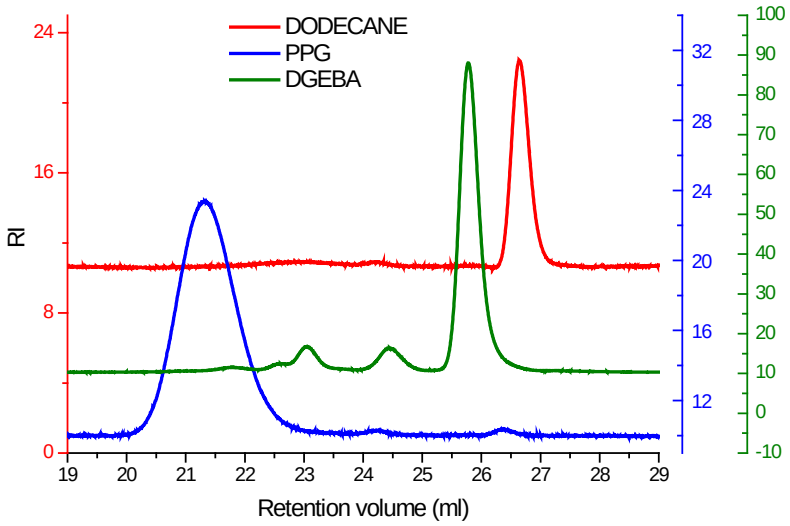


***Figure 39: Chromatograms of dodecane, PPG and DGEBA. [C]=3mg/mL***

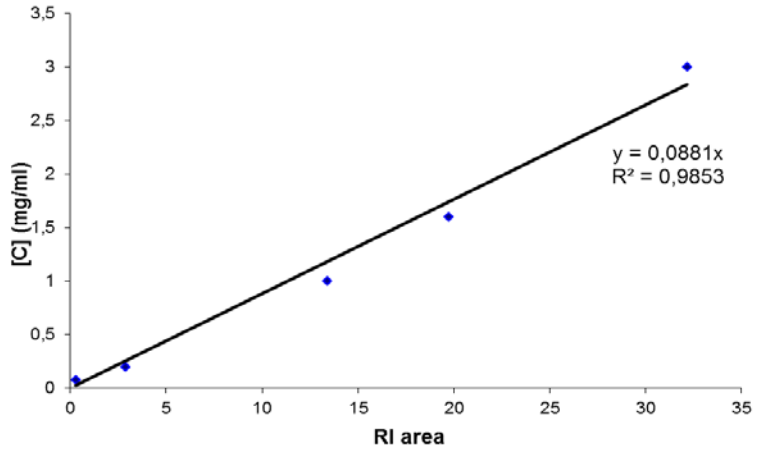


Figure 40: Calibration curve of the DGEBA response by SEC: Concentration versus RI area

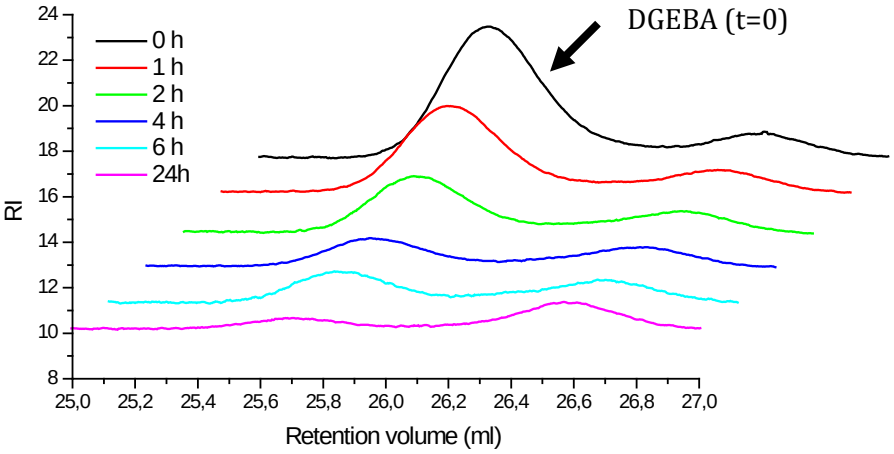


Figure 41: Decrease of DGEBA response as a function of the reaction time for CPM ref synthesis (waterfall representation)

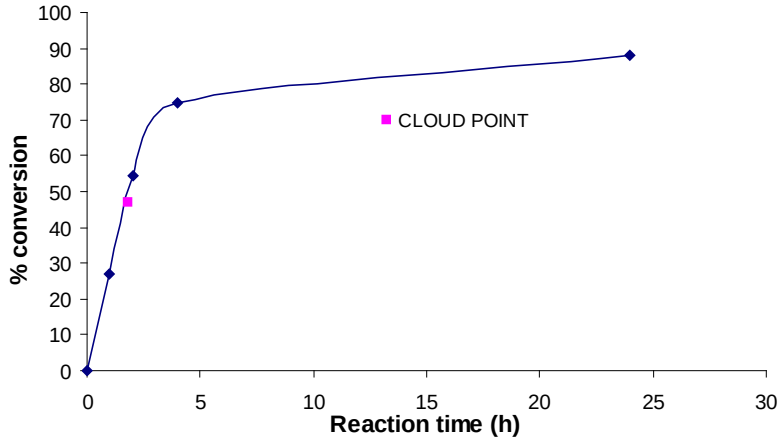


***Figure 42: DGEBA conversion in the supernatant of the CPM ref solution***

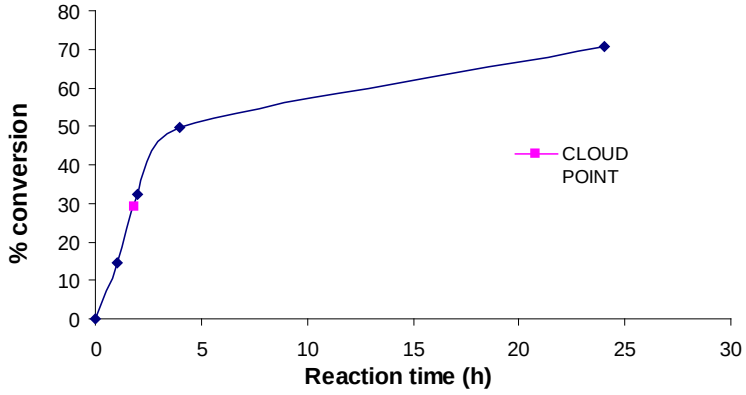


***Figure 43: Epoxy functions conversion in the supernatant of CPM ref solution***

### *3.1.2 Characterization of the CPMs*

Once the particles were obtained, the morphology, composition and thermal properties of the CPMs were investigated using different techniques.

***Morphology***

The morphology, particle size and distribution of the filtered, washed and dried CPMs were investigated by scanning electron microscopy, SEM. As observed in Figure 44, particles have a spherical shape and very narrow diameter dispersity. Their average diameter was 4.5 µm.

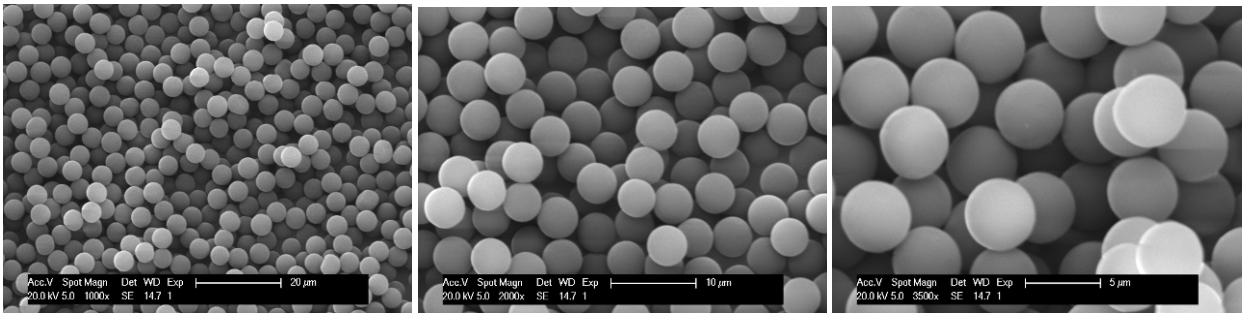


Figure 44: SEM images of CPM ref. (a/e = 1.35, 100°C, [monomers]=10%, solvent 90:10 (PPG: dodecane), 24 h of polymerization); scale bar: 20 µm, 10 & 5 µm respectively

***Analysis of the content of residual solvent***

TGA was performed to evaluate the presence of residual solvent, PPG, dodecane, THF or acetone, in CPMs after particle washing and drying. As shown in Figure 45, a mass loss was observed below 130°C, which could correspond to some residual solvent adsorbed in the particle. This amount of residual impurities represented less than 2 wt% of the total mass of the CPM retrieved, which was in the acceptable range. To confirm the presence of only residual solvent, TGA-FTIR was also performed. Water, THF and potentially also dodecane and acetone release was observed, but no PPG release was seen (spectrum given in appendix). It was important to check that PPG was not adsorbed on the CPM because its presence could modify the reactivity of the CPMs. The impurities detected were the residual inert solvents used to synthesize or wash the CPMs.

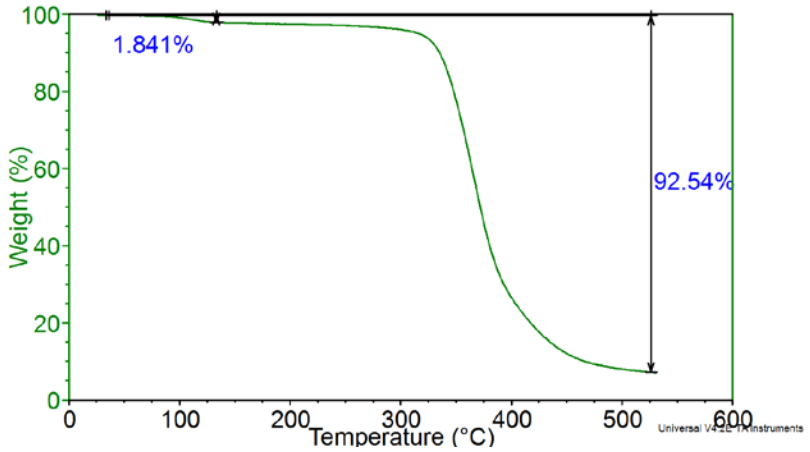


***Figure 45: Thermogram of CPM ref (a/e = 1.35, 100°C, [monomers] = 10%, PPG:dodecane (90:10), 24h of polymerization), after filtration, washing and drying (heating: 10°C.min$^{-1}$).***

***<u>Thermal properties and structure composition from DSC</u>***

DSC was performed on the CPMs to evaluate their glass transition temperature. Two heating ramps were realized. The first one gave the "actual" state of the particles (after washing and drying) related to $Tg_1$ and the second provided the maximum Tg which can be obtained, denoted $Tg_2$. If there is a difference between these two Tgs, this means that either the residual solvent had plasticized the CPMs or a post-curing occurred during the first heating ramp. As observed in Figure 46, $Tg_1$ = 112°C was slightly lower than $Tg_2$ = 121°C. No change in the shape of DSC signals, significant for solvent evaporation, or post-curing reactions were observed. Therefore, the Tg increase highlights the influence of one or both simultaneous phenomena. The following conclusions were made: the plasticizing effect of solvents has a minor effect and the majority of epoxy groups in CPMs were converted due to the long reaction time (24 h).

Moreover, assuming all epoxy groups - which were in defect in the feed - are converted after the first heating ramp, $Tg_2$ is related to the a/e ratio of the CPM. Indeed, for a fully cross-linked epoxy-amine network, Tg is dependent on the a/e [85]. As a consequence, a series of DGEBA-IPD networks were synthesized with an a/e ranging from 0.7 to 1.5, and fully cross-linked in an oven 2 h at 80°C followed by 2 h at 180°C. The Tg measured by DSC was plotted as a function of the a/e ratio (Figure 47). As already known [85], the maximum Tg corresponds to the highest cross-link density which is obtained for a/e = 1, if only epoxy-amine reactions occur. Indeed, an excess of epoxy groups or amino groups lead to dangling chains or chain extension, respectively, in the network and therefore to a decrease of the Tg. This experimental curve was then used as a master curve to determine the real a/e ratio of particles from their Tg.

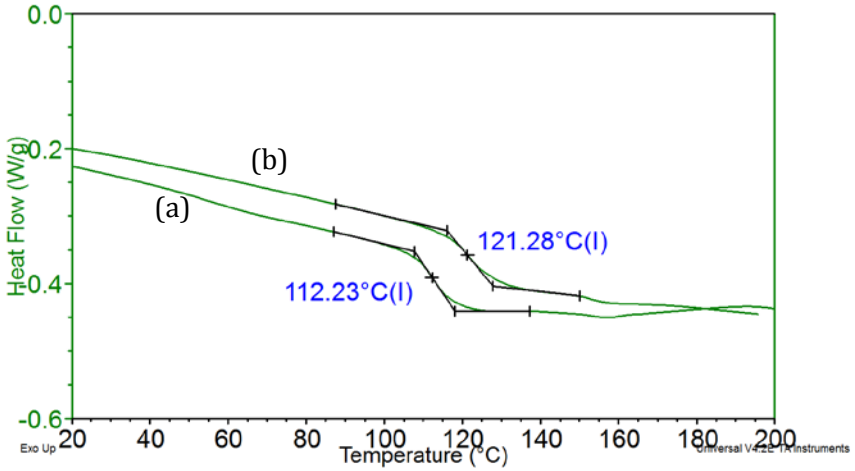


***Figure 46: DSC thermogram (a/e = 1.35, 100°C, [monomers] = 10% in PPG: dodecane (90:10), 24 h of polymerization) – Two successive heating ramps (a) & (b) respectively – (heating ramp: 10°C.min$^{-1}$)***

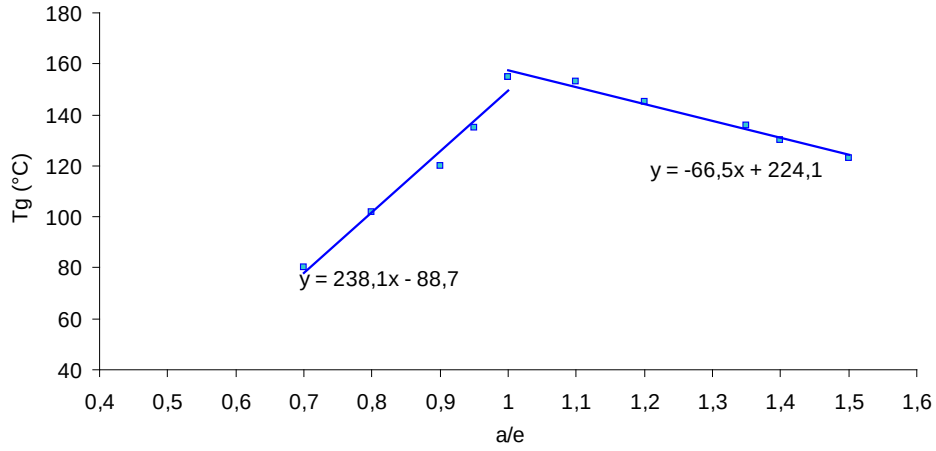


***Figure 47: Glass transition temperature (Tg) as a function of stoichiometric ratio (amino hydrogen/epoxy) of the DGEBA-IPD network***

Utilizing the curve of the Tg as a function of the stoichiometric ratio for CPM ref, $Tg_2$ = 121°C corresponds to a/e=1.55, i.e. superior to the initial stoichiometric ratio a/e $_{t=0}$ introduced in the feed, equal to 1.35 (Table 8). Such a result was already observed in previous works by Traina [2]. Moreover, it was shown by SEC that 12% of DGEBA remained in the supernatant after 24 h of synthesis of the CPM ref. Not all epoxy groups were incorporated into the CPM structure.

***Table 8: Glass transition temperatures, $Tg_{1\&2}$, initial and final stoichiometry of CPM ref***

| | $Tg_1$ (°C) | $Tg_2$ (°C) | a/e $_{t=0}$ (feed) | a/e $_{t=24h}$ (experimental) |
|---|---|---|---|---|
| CPM ref | 112 | 121 | 1.35 | 1.55 |

***Composition by elemental analysis (EA)***

Another way to determine the real stoichiometry of CPM ref is to identify their elemental composition (N, C, H, and O) and to compare it to the theoretical one. There is no difference in the mass of each element for an epoxy-amine mix before the reaction and an epoxy-amine cross-linked network. The epoxy-amine reaction does not release side products; there is conservation of the weight percentage of each element. Reference CPMs were analyzed by elemental analysis, the results of which are given in Table 9.

Theoretical values were calculated, taking into account the chemical structure of monomers (DGEBA and IPD) and their mass ratio in the initial reaction mixture. The calculation was done for the ratios of 1.35 and 1.5 as we experimentally measured an increased stoichiometric ratio close to 1.55 for the CPM ref. The presence of 0.5-2% of residual solvent adsorbed by the CPM was not included in the elemental analysis calculations. A sample of epoxy-amine network synthesized in bulk at the stoichiometry was also sent for elemental analysis as comparison with the theory for a/e=1. The results show that values for the network synthesized at a/e=1 differs from the theoretical calculation above all for the carbon and the oxygen percentage. The composition of CPM ref also does not fit the theoretical composition for a CPM a/e=1.35 and a CPM a/e=1.5. The weight percentage of the nitrogen atom (N) is directly related to the quantity of IPD. For the CPM ref, a percentage of Nitrogen, $\%N_{\text{CPM ref}}$ = 4.06, between 3.89 and 4.21 was measured, which were the values for the ratio a/e=1.35 and a/e=1.5, respectively. The percentage of oxygen was higher than expected, possibly due to the presence of THF, which also bears an atom of oxygen or just the usual gap given by this method as also observed for the network synthesized at stoichiometry.

Finally, it is difficult to conclude the exact stoichiometry of CPM ref from the results of elemental analysis. The use of $Tg_2$ seems to be more appropriate.

***Table 9: Elemental analysis – Experimental results for DER331-IPD, CPM ref and theoretical calculation for a/e=1, 1.35 and 1.5***

| | *% theo (a/e=1)* | *% theo (a/e=1.35)* | *% theo (a/e=1.5)* | DER331+IPD, a/e=1 | CPM ref |
|---|---|---|---|---|---|
| C | *73.59* | *73.4* | *73.33* | 71.76 | 71.39 |
| H | *8.15* | *8.45* | *8.56* | 8.38 | 8.54 |
| N | *3.07* | *3.89* | *4.21* | 3.55 | 4.06 |
| O | *15.18* | *14.26* | *13.89* | 16.39 | 14.78 |

***Composition by Near–Infrared***

Near-infrared spectroscopy was performed on CPMs. Typical bands for epoxy-amine were identified: primary, secondary amine, epoxy groups and hydroxyl groups (Table 10 - Table 11).

*Table 10: NIR assignments for DGEBA [86]*

| Absorption band ($cm^{-1}$) | DGEBA assignments |
|---|---|
| 7099 | O-H overtone |
| 6072 | First overtone of terminal $-CH_2$ stretching mode |
| 4623 | Overtone of C-H stretching of the aromatic ring |
| 4530 | Combination band of the second overtone of epoxy ring stretching with the fundamental C-H stretching |

*Table 11: NIR assignments for amines [86]*

| Absorption band ($cm^{-1}$) | Amine assignments |
|---|---|
| 6650-6350 | Symmetric and anti-symmetric first overtone of N-H stretching: primary amine + secondary amine |
| 4920 | Combination of N-H stretching and bending |

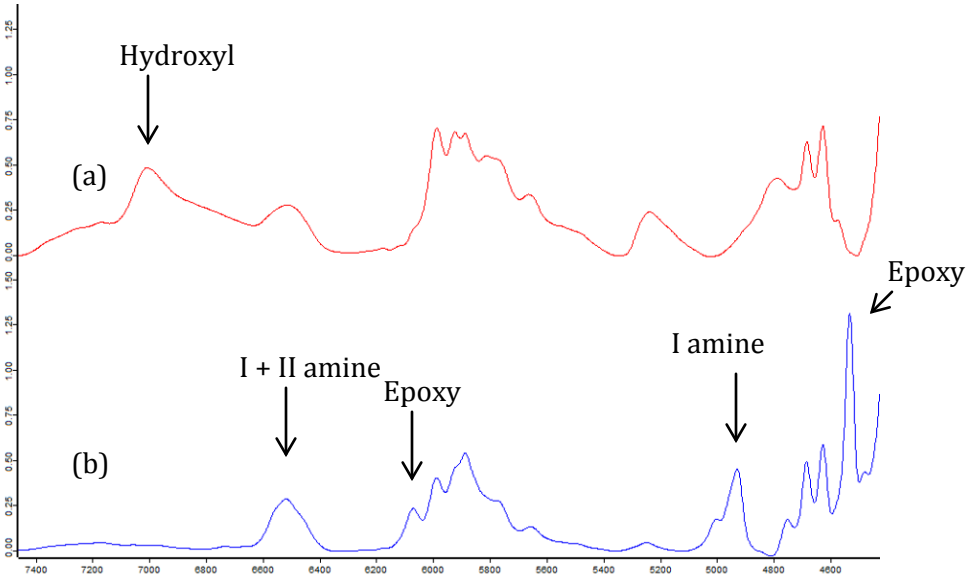


***Figure 48: NIR spectra of CPM ref (a) and DGEBA-IPD $_{t=0}$ before reaction (b), at room temperature, from 7400 to 3800 $cm^{-1}$***

The spectrum of CPM ref is shown in Figure 48 and is compared to that of a DGEBA-IPD network before any reaction. The two characteristic bands of the epoxy groups at 4530 $cm^{-1}$ and 6072 $cm^{-1}$ are not observed in the spectrum. The conversion of epoxy groups in CPM ref was estimated to be approximately 100%. As expected, hydroxyl groups were detected close to 7000 $cm^{-1}$ due to the epoxy-amine reaction and opening of the oxirane ring. Primary amines were not detected on the CPMs at 4920 $cm^{-1}$ but on the contrary, secondary amines were still present. Primary amines from

IPD are very reactive, especially aliphatic ones as they are known to be the most reactive with epoxy groups. The second one is a cycloaliphatic amine and its reactivity is slightly lower. However, as the reaction was performed at high temperatures both primary amines were able to react.

***Reference system - Summary***

By the precipitation polymerization of epoxy-amine system in PPG combined with 10% dodecane, perfectly spherical cross-linked polymer microparticles (CPMs) were easily obtained from a reaction-induced phase separation phenomenon. Schematic representation of the CPM formation during the reaction is given in Figure 49. At 100°C, the cloud point corresponded to 1h47 of reaction, with an epoxy function conversion of 29%. After 24 h of reaction, the epoxy function conversion increased up to 70%. The average particle diameter of the resulting CPMs was about 4.5 µm after 24 h. The glass transition temperature of the CPM particles was close to 112°C.

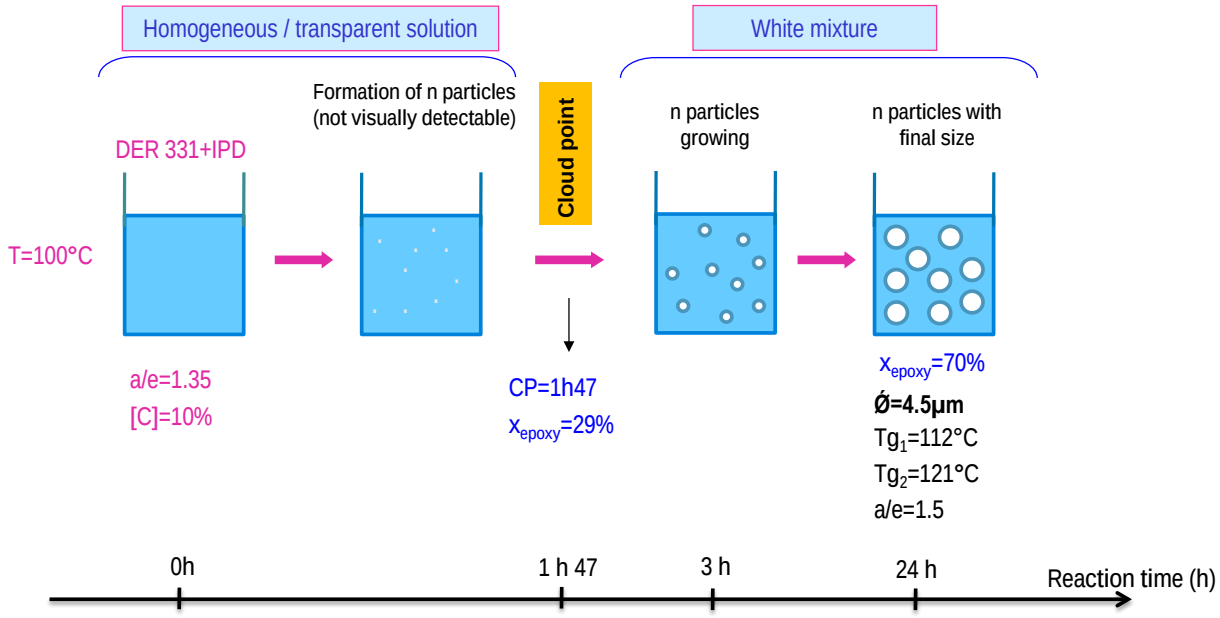


***Figure 49: Reference system – i.e. CPM ref synthesis (a/e = 1.35, 100°C, [monomers] = 10% in PPG: dodecane (90:10), 24 h of polymerization)***

After studying in detail the synthesis process of the reference CPM as well as its morphology, composition and thermal properties, the influence of the stoichiometric ratio and the monomer structure introduced were investigated. The aim was to determine how these parameters influenced the CPM structure. The results are reported in the following paragraphs.

## 3.2 Influence of the stoichiometric ratio

CPMs were synthesized with the protocol used for the CPM ref (section 2.2), except that 3 other stoichiometric ratios were used: a/e = 0.9, 1.05 and 1.5.

These CPMs were characterized with the same techniques:

- Their formation was monitored from the ***cloud point measurement*** in order to investigate the influence of a/e on the time to phase separation.
- The thermal properties were studied by ***DSC*** to measure $Tg_1$ and $Tg_2$ and compare them with an epoxy-amine network with the same stoichiometry as the initial one in the feed, cross-linked in an oven without solvent.
- Morphology was observed by ***SEM*** and their structure analyzed by ***elemental analysis*** to estimate their real stoichiometry.
- Conversion was estimated by Near-Infrared.

All of the data measured are reported in Table 12. The real a/e, $a/e_{calc}$, obtained for the CPMs after reaction, was recalculated from $Tg_2$ and the curve in Figure 47 .

***Table 12: Cloud point (CP), Tg1 & Tg2, Tg theo, $a/e_{calc}$ and Diameters (D) for CPMs synthesized with an a/e from 0.9 to 1.5***

| $a/e_{t=0}$ | 0.9 | 1.05 | 1.35 | 1.5 |
|---|---|---|---|---|
| CP | 2h22' | 2h14' | 1h47' | / |
| $Tg_1$ (°C) | 140 | 134 | 112 | 112 |
| $Tg_2$ (°C) | 143 | 134 | 121 | 118 |
| $Tg_{theo}$ (°C) | 126 | 154 | 134 | 124 |
| $a/e_{calc}$ | 0.97 | 1.35 | 1.55 | 1.59 |
| D (µm) | 3.0 | 4.3 | 4.6 | / |

### *3.2.1 Time to phase separation*

Time to phase separation for the different CPMs gave the following conclusions. As shown in Figure 50, and already observed in a previous study [2], as the a/e ratio increased, the cloud point decreased. Indeed, with an a/e=0.9, the phase separation occurred after 2h22 and with a/e=1.35, the phase separation occurred after only 1h47. The previously discussed possible explanations were as follows:

- With a/e > 1, i.e. an excess of amines, the oligomers formed had a more linear structure compared to those in excess of epoxy. Not all amino groups reacted, leading to a less branched structure. As a consequence, the chemical structure of the network formed was different, which also changed the solubility parameters and provoked a phase separation at a different time.

- Kinetics of the cross-linking reaction has been increased by the increased concentration of amine.

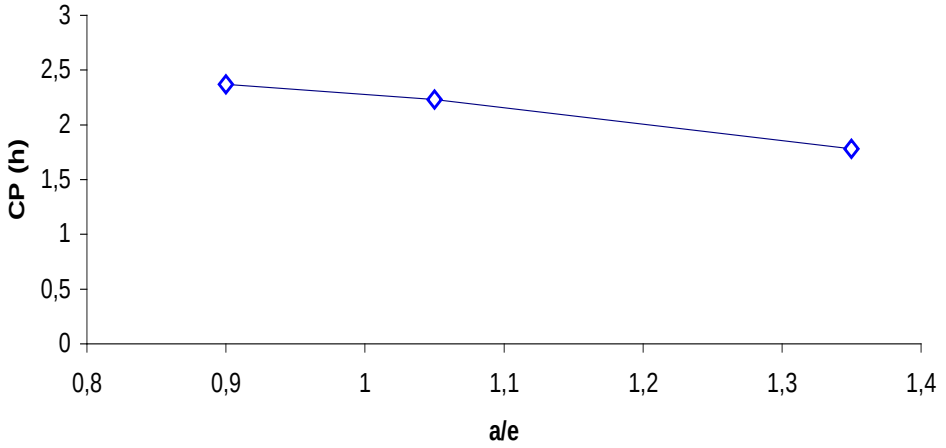


***Figure 50: Cloud points as a function of the initial stoichiometric ratio of the CPMs synthesized at 100°C, in PPG:dodecane (90:10),[monomers] = 10wt%, 24h polymerization***

### *3.2.2 Thermal properties*

In Figure 51, the $Tg_1$ and $Tg_2$ for the four types of CPMs synthesized with a/e from 0.9 to 1.5 are plotted. In most cases, $Tg_2$ was observed to be slightly higher than $Tg_1$ (a few degrees of difference), as observed for the reference CPMs. As shown in Figure 47, for a fully cross-linked epoxy-amine network, the maximum Tg was obtained for a/e=1. In the case of the CPMs, the highest $Tg_{2s}$ were also measured for the stoichiometric ratios close to a/e=1. Then, by increasing the a/e ratio, the Tg decreased. A significant difference was noted comparing the expected value of Tg calculated for the corresponding a/e with the measured $Tg_2$. The explanation is that CPMs have a higher stoichiometric ratio than that introduced in the solvent at t=0. This shift of a/e observed to higher values for all the CPMs has been plotted in Figure 52. The deflection between the initial a/e and the final one was calculated between 0.07 and 0.30. There is an increase in the amount of amino groups in the CPM structure in comparison to the proportion in the initial solution, which can be of great interest for many applications.

An additional observation is that it seems to be more difficult to obtain CPMs with an epoxy functionality because even when an excess of DGEBA was used in the initial solution, the resultant CPMs have a stoichiometry very close to 1.

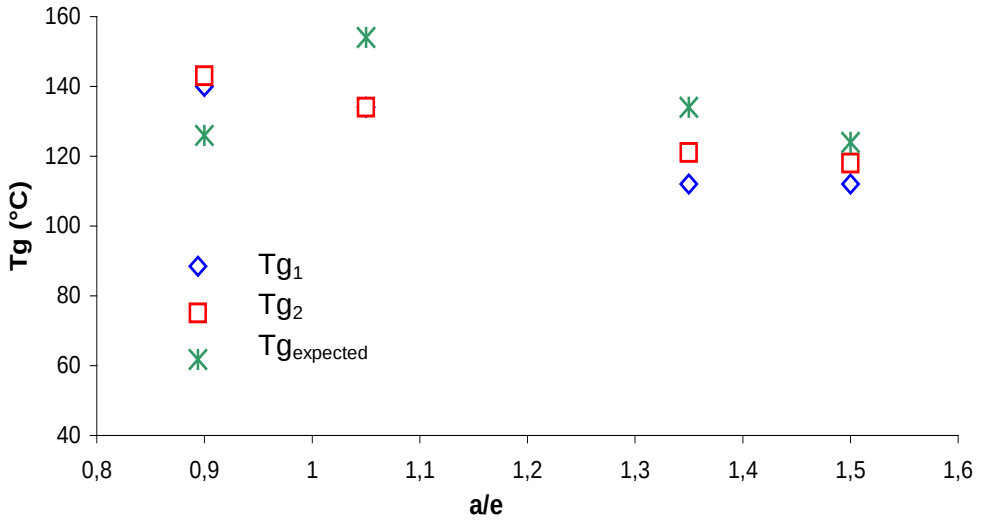


***Figure 51: Influence of the stoichiometric ratio a/e on $Tg_1$ & $Tg_2$ of the CPMs synthesized at 100°C, in PPG:dodecane (90:10),[monomers] = 10wt%, 24h polymerization***

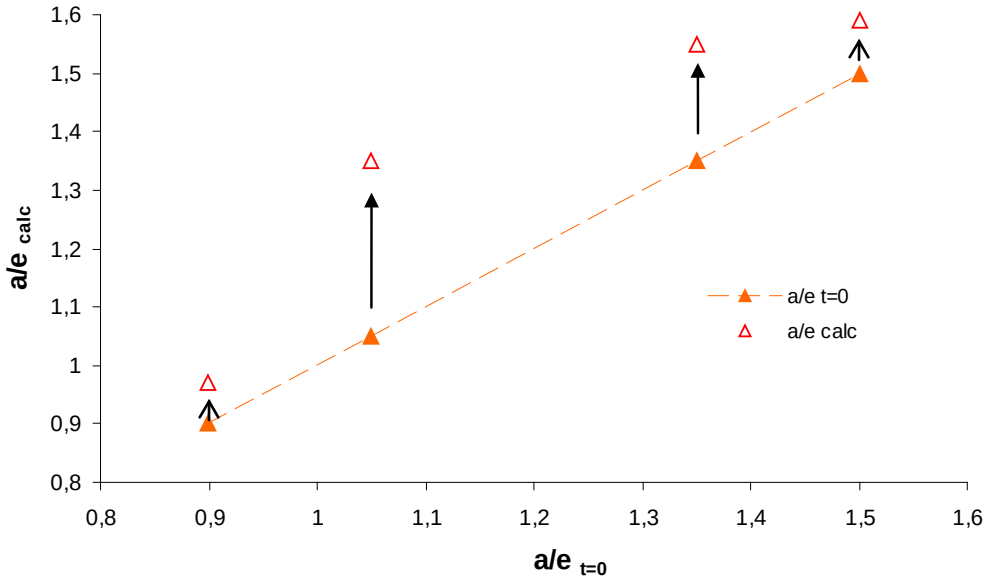


***Figure 52: Deflection between initial a/e of the CPMs and final calculated a/e ratio from Tg measured by DSC***

### *3.2.3 Composition of the CPMs by elemental analysis*

***Elemental analysis*** was used to determine the C, H, N and O content in the CPMs to estimate their real stoichiometric ratio. The evolution of the percentage of each element was in agreement with the theory. Indeed, as a/e was increased, C and O contents decreased, while H and N contents increased. However, although the values were in the same range as the theoretical ones, it was not possible to establish the real a/e of the CPMs using this technique due to the difficult correspondence with the 4 different elements. The results are reported in appendix.

### 3.2.4 Composition by NIR spectroscopy

CPMs with different ratios were analyzed by NIR.

As shown in Figure 53, epoxy groups were never detected by NIR spectroscopy, even for CPMs synthesized in an initial excess of epoxy groups (CPM a/e=$0.9_{t=0}$). This is in agreement with the Tg measured by DSC, which indicated a higher a/e than expected, close to a/e=1. Conversion of epoxy groups included in the CPM structure is about 100%.

Concerning the primary amines, they were also not detected due to their very fast reaction with epoxy groups. Secondary amines were clearly detected for the 3 stoichiometries. The magnitude of the band close to 6500 $cm^{-1}$ logically increased with an increase of the stoichiometric ratio.

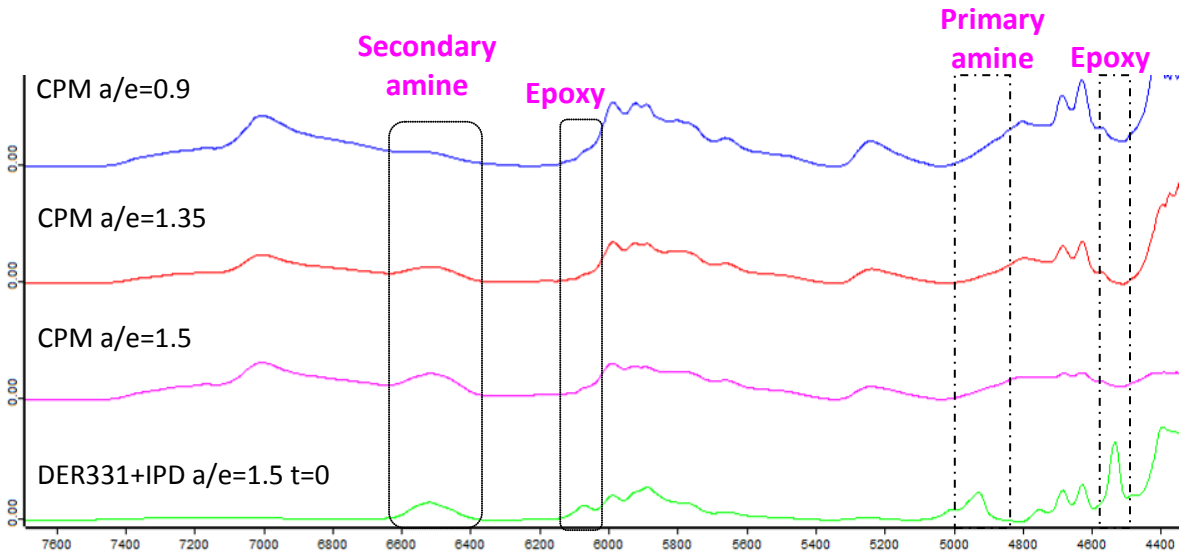


***Figure 53: NIR spectra of CPMs a/e=0.9; 1.35; 1.5 and DER331-IPD mix a/e=1.5 before reaction, measured at room temperature***

### 3.2.5 Morphology

***SEM*** was performed on the CPMs to investigate the influence of the stoichiometric ratio on morphology. Particles were always spherical. Diameters of the resulting CPMs are reported in Table 13. It appears that the average diameter of the CPMs increases with the stoichiometric ratio from 3.0 µm at a/e=0.9 to 4.6 µm at a/e=1.35. This was potentially due to the fact that phase separation occurred earlier (as shown in Figure 50) due the increase in the kinetics, giving them more time to grow.

*Table 13: SEM images of CPM a/e=0.9, 1.05, 1.35 and measured diameters (D) –scale bar: 20 µm*

| a/e = 0.9 | a/e = 1.05 | a/e = 1.35 |
|---|---|---|
| 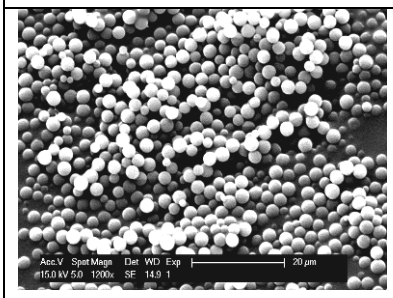 | 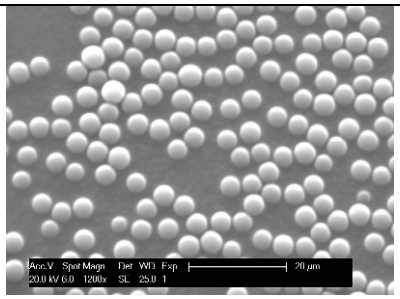 | 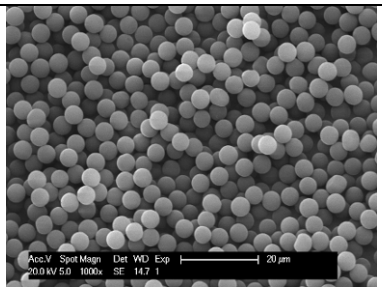 |
| D = 3.0 µm | D = 4.3 µm | D = 4.6 µm |

### *3.2.6 Conclusion*

To conclude on the influence of the stoichiometric ratio on CPMs, the phase separation occurred earlier with an increase in the stoichiometric ratio. It was explained by the changing structure of the CPM network and therefore the modification of the solubility parameter of the oligomers formed, as well as a faster reaction rate. Tg of the CPMs was compared with the theoretical value corresponding to the pure network without solvent with the same composition but cross-linked in oven for 2 h at 80°C followed by 2 h at 180°C. Tgs obtained always corresponded to a higher stoichiometric ratio. This observation was difficult to confirm by elemental analysis where the stoichiometry is a combination of percentages of 4 different elements C, H, N and O. With NIR spectroscopy, the increase in the a/e ratio was confirmed for the CPM a/e=0.9 (no epoxy was detected). Due to the fact that epoxy groups were never detected whatever the a/e, we concluded that the conversion of the epoxy included in the CPMs was close to 100%.

Concerning the morphology, an increase in diameter size was observed with the increased stoichiometric ratio. This is potentially due to the fact that phase separation occurred earlier, which allowed more time for the particle to grow, or created fewer particles which could then grow more efficiently.

## 3.3 Influence of the reaction time

The CPM synthesis was stopped after 3 h of polymerization. This time was chosen to allow for the phase separation phenomenon which occurs after 1h47 of reaction for CPM ref. Thermal properties and morphology of the resulting CPMs are reported in this paragraph. Figure 54 shows the DSC thermogram of the CPM a/e=1.35, 3 h polymerization. Due to evaporation of the residual solvent and post-curing of the CPMs during the first heating scan, it was not possible to measure the Tg ($Tg_1$) of the CPMs. However, $Tg_2$ was measured and the value (120°C) was very close to the $Tg_2$ of

the CPM a/e=1.35, 24h of polymerization, confirming the maximum Tg possible with this ratio. This also shows that the real ratio of the network of the CPM does not change from 3 h to 24 h of polymerization.

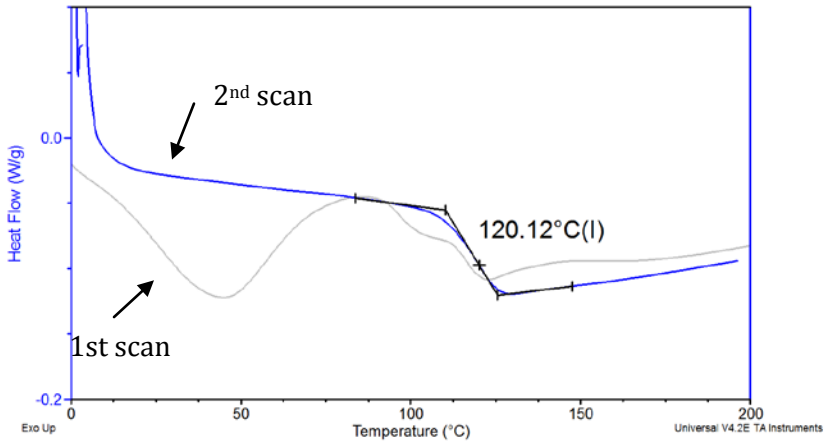


***Figure 54: DSC thermogram of CPM a/e=1.35, 3h of polymerization, 1st and 2nd heating scan – 10°C.min-1***

The morphology of the CPM a/e=1.35, 3h polymerization was observed by SEM. Figure 55 shows the state of the CPMs after drying, washing and grinding.

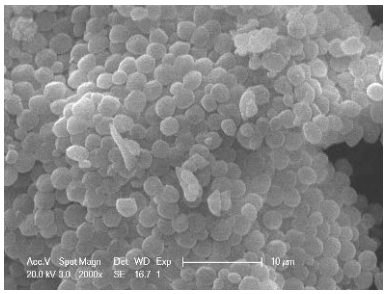

***Figure 55: SEM image of CPM a/e=1.35, 3h polymerization after drying, washing and grinding – scale bar: 10 µm***

The CPMs did not have a spherical shape anymore. They were deformed by the process. Due to their numerous unreacted groups, these CPMs did not have a high cross-linked density, which leads to soft and deformable particles. Their original diameter seemed to be between 2.5 and 3 µm.
Reducing the polymerization time of the CPMs leads to lower Tgs and more unreacted groups, but the same a/e ratio as the CPMs.

## 3.4 Influence of the monomer structure

The following paragraph deals with the influence of the monomer structure. Indeed, all CPMs previously presented were synthesized with an epoxy pre-polymer: DER 331 (DGEBA, n=0.12) and a cycloaliphatic amine: IPD as hardener. Their glass transition temperature ranged from 112°C to

140°C depending on their stoichiometric ratio. In the context of this study on the effect of CPMs on the buildup and properties of epoxy networks, it appeared to be interesting to have CPMs with a lower Tg while keeping similar stoichiometric ratio. Thus, the influence of using a higher molar mass DGEBA and an aliphatic amine was investigated. The protocol of the synthesis was very similar to the one described previously for IPD-based CPMs. Solvent was PPG:dodecane, (90:10), reaction was done during 24 h at 100°C, the stoichiometric ratio a/e was 1.5, but the monomer concentration was increased to 20 wt% (instead of 10 wt%). Consequently, a higher quantity of CPMs was produced. The properties of the CPMs obtained are reported in the next paragraph.

### *3.4.1 Use of an aliphatic amine*

IPD was replaced by an aliphatic polyetheramine, denoted as Jeffamine D230 which has a molar mass of about 230 g.mol-1. The linear structure of this hardener should give more mobility to the resulting network compared to the cycloaliphatic IPD. Both structures are shown in Table 5. As reported in Table 14, the Tg of D230 based CPMs is significantly lower than the Tg measured for the IPD based CPMs. Indeed, using IPD, the $Tg_1$ of the CPMs was about 112°C whereas using D230, $Tg_1$ was about 60°C. This was due to the difference in the structure of the hardener, which has a longer chain and no cycle, which creates longer and more flexible chains between cross-links. Therefore Tg decreased. Once again, CPMs were perfectly spherical (Figure 56 (b)). The diameter of the CPMs was increased to 6.5 µm with the use of D230 but for a monomer concentration of 20 wt% compared to 4.2 µm with IPD, which was synthesized with a monomer concentration of 10 wt%.

***Table 14: $Tg_1$ and diameter size for IPD based and D230 based CPMs, a/e=1.5***

| Hardener | IPD | D230 |
|---|---|---|
| $Tg_1$ (°C) | 105 | 60 |
| D (µm) | 4.2 | 6.5 |

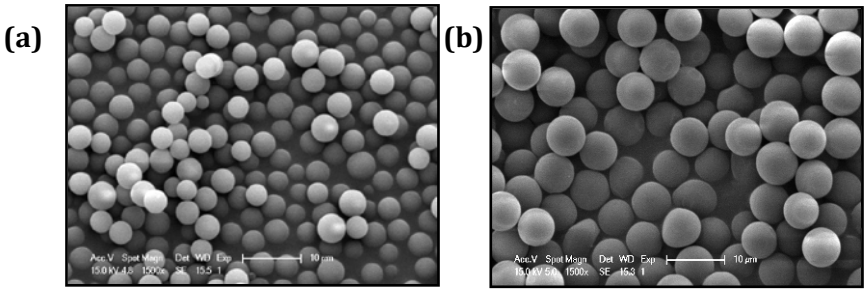


***Figure 56: SEM images of IPD based (a) and D230 based (b) CPMs, a/e=1.5 – scale bar: 10 µm***

The NIR spectrum of D230 based CPMs is reported in Figure 57 and compared to spectrum of the DER 331–D230 mixture before reaction. In agreement with our previous conclusions on IPD-based CPMs, no epoxy as well as primary amino groups was observed. Only hydroxyl and secondary amino groups were detected.

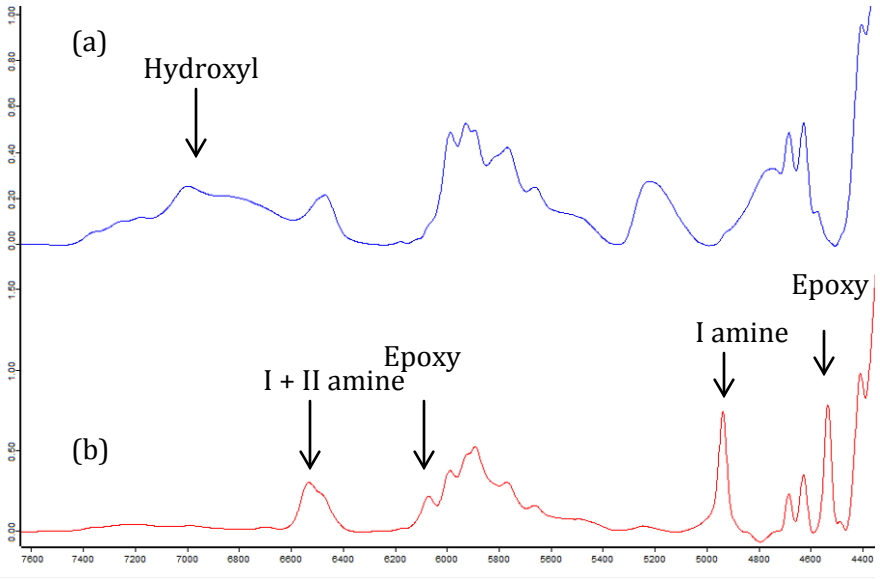


***Figure 57: NIR spectra of D230 based CPM a/e=1.5 (a) and DER331-D230 a/e=1.5 mixture before reaction (b)***

### *3.4.2 Use of a higher molar mass DGEBA*

DER 331 (n ~ 0.12) was substituted by DER 662E (n ~ 3.1), which has an epoxy equivalent weight of 610 g. $mol^{-1}$ compared to DER 331, which has an epoxy equivalent weight of about 187 $g.mol^{-1}$. DER 662E is a solid epoxy resin with a glass transition temperature equal to 45°C. The hardener used was D230. The structure of the DGEBA is shown in Table 5.

The solution of DER 662E with D230 and solvents was not homogeneous at the beginning of the reaction as it is supposed to be for the precipitation polymerization system. A higher molar mass DGEBA probably has different solubility parameters, which induced the heterogeneity of the solution from the beginning of the reaction here. However, after the reaction, two different morphologies were retrieved in the solution: a bulk network and CPMs. The properties of the CPMs are given in Table 15. It was shown (Figure 58) that the particles obtained with the higher molar mass DGEBA (DER 662E) have a very broad size distribution. Indeed, their diameter was between 4 and 16 µm compared to the other CPMs which had an average diameter close to 6.5 µm. Their Tg was measured about 80°C. This value that is superior to that of the DER331-based CPMs (80>60), which was not initially expected due to the fact that higher molar mass DGEBA should extend the chains between the cross-links and give more mobility to the network, thereby decreasing the Tg.

$Tg_0$ of the epoxy pre-polymer was plotted as a function of the epoxy equivalent weight (EEW) (Figure 59) which explained the phenomenon observed. Indeed, $Tg_0$ of the DGEBA quickly increases limiting the possibility of obtaining very low Tg network with an identical hardener. Moreover, the $Tg_2$ values of the obtained CPMs were very close to that measured for a network of the same composition which was 59°C and 81°C for DER331-D230 and DER662-D230, respectively.

***Table 15: Characteristics of CPMs synthesized from DER 662E and D230***

| Epoxy | DER 331 | DER 662E |
|---|---|---|
| EEW (g.mol-1) | 187 | 610 |
| $Tg_1$ (°C) | 60 | 80 |
| $Tg_2$ (°C) | 67 | 90 |
| D (µm) | 6.5 | 4-16 |

**(a)** **(b)**

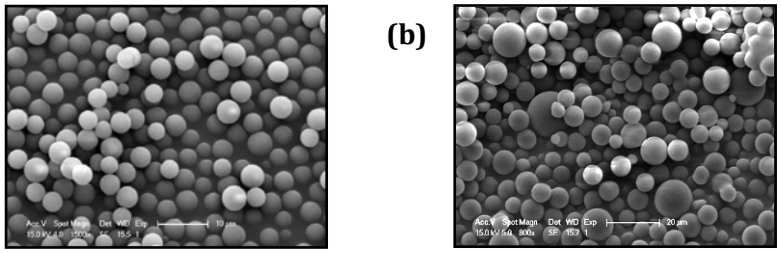

***Figure 58: SEM images of CPM synthesized with DER 331 (a) and DER 662E (b) with D230, a/e=1.5, 24h polymerization in PPG:dodecane (90:10), scale bar: 10 and 20 µm, respectively.***

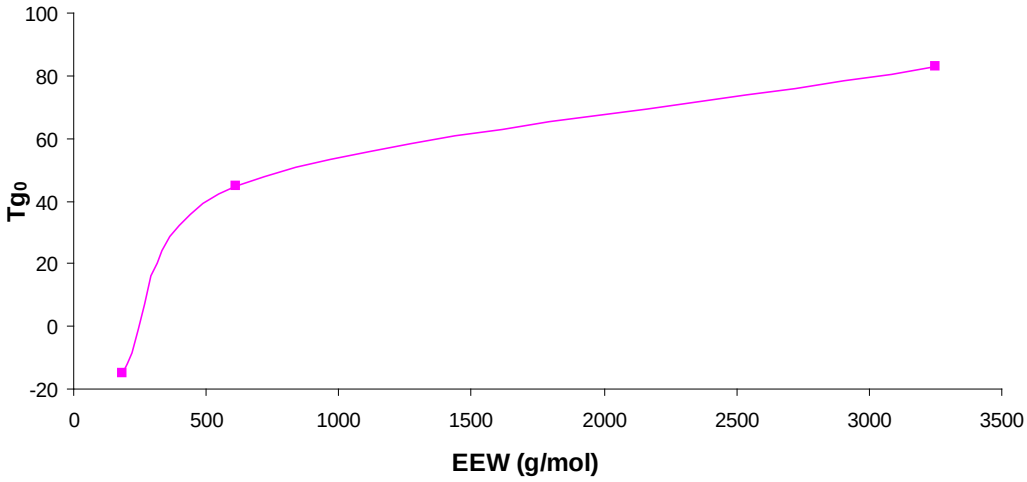


***Figure 59: Initial glass transition temperature ($Tg_0$) of pure DGEBA pre-polymers as a function of the epoxy equivalent weight (EEW) of the pre-polymers***

### *3.4.3 Conclusion*

The final properties of the CPMs depend directly on the structure of the monomers, as it is for a standard epoxy amine network. Monomers giving more mobility to the structure will lower Tgs, as it is the case with the use of D230 instead of IPD. However, solubility parameters always need to be taken into account to ensure that monomers are soluble in the solvent and to apply the principle of precipitation polymerization.

## 4 Conclusions

In this chapter, it was shown that cross-linked polymer microparticles were successfully synthesized by precipitation polymerization via a reaction-induced phase separation phenomenon using DGEBA and an amine cross-linker. It is important to note that it is a very easy process, which does not use any surfactant, and which allows for the formation of perfectly spherical microparticles with a very narrow size distribution.

A wide range of Tgs can be obtained by varying the monomer structure; also, a wide range of amine functionality can be obtained by playing with the stoichiometric a/e ratio.

As a consequence, CPMs can be classified according to their glass transition temperature, Tg. DGEBA-IPD-based CPMs had Tg above 110°C and so can be called high Tg CPMs, or CPM H. On the contrary, DGEBA-D230 CPMs have lower Tgs and are called medium Tg CPM, or CPM M.

| CPMs | Monomers |
|---|---|
| H1 a/e=0.9 | DER331-IPD |
| H2 a/e=1.35 | DER331-IPD |
| H3 a/e=1.5 | DER331-IPD |
| M1 a/e=1.5 | DER662E-D230 |
| M2 a/e=1.5 | DER331-D230 |

***Table 16: CPM nomenclature***

According to the IR spectra and with its limit of sensitivity, it was shown that particles are fully cross-linked after 24 h of polymerization at 100°C (no residual epoxy groups were detected).

This technology easily allows the synthesis of reactive organic microparticles bearing hydroxyl and amino groups, which could be used for different graftings and many applications. This functionality of the CPMs, and above all the amine functionality, is of great interest. The next chapter is dedicated to its titration and understanding under which conditions they can react with epoxy groups from epoxy-amine formulations.

# III CPMS AS REACTIVE FILLERS: QUANTIFICATION OF THE AMINE FUNCTIONNALITY

## 1 Introduction

The identification of chemical functions on the surface of a sample is of great interest for a variety of applications such as self-assembled monolayers, surface wetting, protein adsorption, biosensors, interface filler/matrix characterization, etc.

With the idea of dispersing microparticles in a polymer network, it would be interesting to generate covalent bonds between the particle surface and the network. Indeed, it would give a strong interface/interphase, i.e., a good wettability of the particles, and ensure a good stress transfer, which would confer better mechanical properties to the final materials. Consequently, as the epoxy-amine chemistry for the CPM synthesis was considered, the presence of the remaining reactive amino groups on the surface would enable the reaction with other reactive epoxy groups from the surrounding matrix. For this reason, CPMs were mainly synthesized in an excess of amine to keep residual amino groups in their structure.

Thus, the quantitative titration of reactive and accessible amino groups on CPM surface was investigated in this project using several methods, as detailed in the following sections. However, the concept of surface for polymeric particles which bear reactive groups even in their core is not so easy to define. One cannot have exactly the same approach as that for solid supports. The concept of accessible depth of the surface of the CPM needs to be taken into account.

Moreover, the accessibility of reactive functionalities probably also depends on the method chosen, the size or the nature of the probe and therefore the media used for titration. Indeed, a titration technique developed with a solvent having poor interactions with CPMs will probably produce different results than another or the same technique done using a different solvent. Only a very thin surface thickness of the CPMs will be available. On the contrary, with a solvent having good interactions with epoxy networks, swelling of the CPMs and diffusion of the probe will be helped. More amino groups should be accessible to the titration. Consequently, several methods were tested and are presented in the following paragraphs.

A preliminary study of the different techniques found in the literature to highlight and quantify functionalities on surfaces was carried out and is reported. The theoretical amount of unreacted amino groups was also calculated as a function of the accessible depth. This calculation led to a better approach towards setting up the titration method knowing the range of residual reactive groups. Then, qualitative tests were performed before investigating the quantitative titration of

amino groups and comparing the results with theoretical calculations. Finally, the last step was to investigate the reactivity of the amino groups of the CPMs towards epoxy systems.

## 2 Literature review on titration techniques

As mentioned above, the residual reactive groups on the surface of particles should be qualitatively and quantitatively controlled. Several methods to titrate the amine surface of various samples were used by different teams and are presented in the following paragraphs.

Traditional surface characterization techniques include X-ray photoelectron spectroscopy (XPS), IR, ultraviolet-visible spectroscopy (UV-Vis), time-of-flight secondary ion mass spectrometry (TOF-SIMS), electron spin resonance (ESR), and fluorescence spectroscopy. All of these methods are not specific to amino groups and are not always able to differentiate primary and secondary amines from tertiary amines (like XPS for instance), which is of great interest for this project to differentiate the reactive from the unreactive amines. One more limiting defect of some of these techniques was the sample thickness analyzed, which does not correspond to the accessible layer by other chemical groups. Chemical labeling involves links between labeling molecules and functional groups. Usually, a labeling molecule is chosen to selectively bond to one kind of functional group. The characterization technique has to be sensitive to the new molecule attached. This type of characterization is among the most sensitive surface techniques. Some examples of using chemical labeling are given below. Moreover, other kinds of titration techniques were presented. They were not specific to surface titration but the way in which the authors employed them on solid surfaces was discussed.

### 2.1 Amine titration by fluorescent labeling

The fluorescent dyes were used to label specific chemical groups. This type of labeling gave the visibility, by fluorescence microscopy or spectroscopy, of the wanted chemical group on a surface. To obtain a useful response, the dye has to be chosen to be specific towards the desired chemical groups which are the primary and the secondary amines for our project, rather than the hydroxyl group. Consequently, once the labeling molecule was attached, the emitted fluorescence signal after excitation at the right wavelength was directly proportional to the quantity of the functional groups. If this intensity is monitored and calibrated, a quantitative titration of the dye (and also the functional groups) is possible.

For example, Jung and coworkers [87] used the fluorescent labeling of functional groups on the surface of organically-modified silica particles. The selective labeling of amino functions by fluorescamine and of the mercapto functions by Rhodamine B isothiocyanate on the surface of the

particles indicated the position of the different functional groups. A scheme of their selective dye tagging is given in Figure 1.

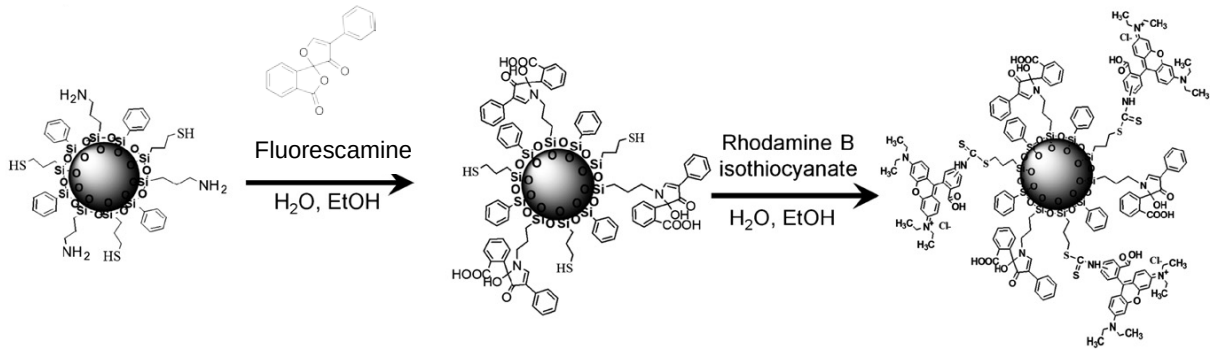


***Figure 60: Selective tagging of two different functional groups on the surface of silica particles [87]***

In this example, only one type of amines, primary amines, was present on the silica particle surface. As a consequence, the authors chose fluorescamine as the fluorescent dye, which reacts specifically with primary amines. Confocal fluorescent microscopy images of dual labeling were carried out to investigate the distribution of functional groups. However, no quantitative analysis of the labeling was reported.

Another example of fluorescence labeling on a solid surface was the specific labeling of various functional groups on a polyethylene surface treated by low pressure plasma and chromic acid [88]. Carbonyl, Carboxyl, hydroxyl and amino groups were present on the surfaces and were specifically labeled. Primary amino groups were again coupled with fluorescamine. In this study, using fluorescence spectrometry, the authors plotted the fluorescent intensity as a function of the $H_2/N_2$ ratio in the plasma gas used to treat the polyethylene surface (Figure 61).

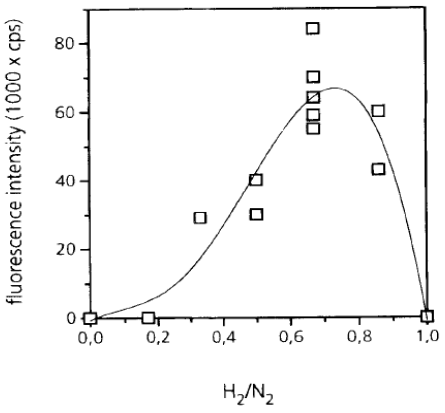


***Figure 61: Fluorescent intensity of fluorescamine coupled to amino groups on the surface of polyethylene treated with a varying gas composition of nitrogen/hydrogen plasma (λ=472nm) [88]***

Another possibility that is often used to label primary amino group on proteins with a fluorescent dye is to employ fluorescein-5'-isothiocyanate (FITC). As an example, it was used by Jang [89] to

check the presence of primary amino groups on the surface of modified magnetic nanoparticles. Fluorescence microscopy showed a green emission that is specific to the FITC grafting. A schematic grafting of the fluorescent probe FITC onto nanoparticles is given in Figure 62.

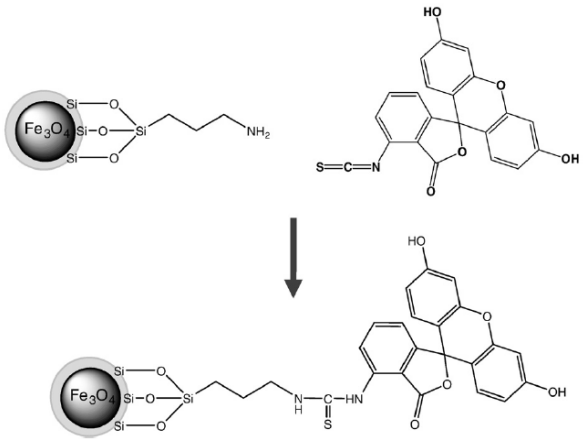


***Figure 62: Schematic grafting of FITC on amine modified magnetic nanoparticle surface***

Moreover, another interesting study was carried out by Elmas and coworkers [90] with the same fluorophore FITC, grafted on polymer microparticles. Poly(glycidyl methacrylate) (poly(GMA)) particles were aminated and then labeled with FITC for characterization by confocal laser scanning microscopy. Looking at the optical section positioned in the mid-plane of the particles, they observed the fluorescence of only the shell of the particles. They concluded that the concentration of primary amine was lower in the core compared to that on the surface. The intensity profile of fluorescence was plotted for three selected particles (Figure 63).

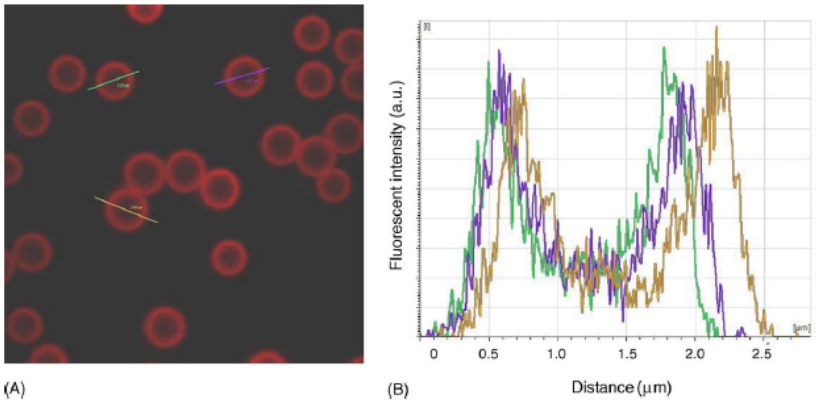


***Figure 63: The optical section (A) and the fluorescent intensity profile (B) of the aminated poly(GMA) particles labeled with FITC [90]***

Fluorescence microcopy is a useful tool for the localization of chemical functions. However, it does not give absolute concentrations of the functional groups. Indeed, it is difficult to establish a

calibration method which has to be performed on a solid sample with a known amount of amino groups.

Quantitative analysis can be performed via fluorescence spectroscopy in solution. Three different methods are reported:

- direct measurement of the fluorescent intensity of the grafted particles
- removal of the grafted fluorescent dye and subsequent measurement of the fluorescent intensity
- measurement of the decrease of the fluorescent intensity of a dye solution due to the reaction of the dye with the surface

Furthermore, only primary amines were labeled using the techniques presented; no labeling of secondary amines and observation by fluorescence confocal microscopy or fluorescence spectroscopy has been reported in the literature to the best of our knowledge.

### 2.2 Acid / Base titration

According to the basic character of amine, they can capture a proton. As a consequence, acid/base titration can be carried out. Several teams reported their results for amine titration by hydrochloric acid (HCl) on monolithic-type solid supports. Mori and coworkers [91] investigated the titration of solid support containing primary amines which were reacted with an aqueous HCl solution for 24 h with stirring. The supports were filtered and washed. The washing solutions were combined with the recovered HCl solution, which was titrated with a standard 0.1 N sodium hydroxide, NaOH, aqueous solution with phenolphthalein as an indicator. This titration was a back titration of the unreacted HCl by NaOH. The same protocol was applied for the determination of the content of amino groups on carbon black [92] and a very similar protocol was also applied on silica particles with primary amines on their surface [93]. Furthermore, another method to monitor the back titration was used by Ganachaud and coworkers [94]: conductometric titration. In that case, an NaOH solution was added to a latex and then the back conductometric titration with HCl was carried out instead of utilizing phenolphthalein as a color indicator.

### 2.3 Amine titration with SPDP

Several studies have focused on the surface properties of copolymer latex particles [94], [95], [96], or on amino-silane microship [97] utilizing N-succinimidyl 3-(2–pyridylthio) propionate (SPDP) to quantify the surface amino and amidino groups. Here, once again, only primary amines were titrated, but this technique should also work with secondary amines. Moreover, this method required a second step which involved a reduction reaction in the presence of dithiothreitol (DDT)

that released pyridine-2-thione, and was finally titrated by measuring the optical density at a wavelength of 343 nm. A scheme of the reaction steps is given in Figure 64.

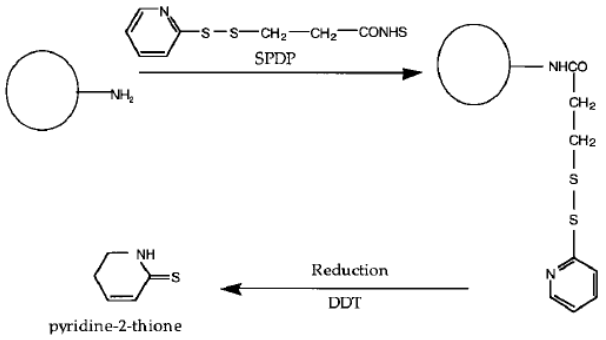


***Figure 64: Reaction scheme of primary amine with SPDP with release of Pyridine 2-thione in presence of DDT [96]***

## 2.4 Amine titration with sulpho-SHPP

As described by Ghasemi [98] in her thesis, Kakabakos and coworkers [99] showed how they set up a method for the quantitative determination of solid-supported (polyethylene, polypropylene etc.) primary and/or secondary amino groups. To titrate both kinds of amino groups, the first step was to activate them with sulpho-succinimidyl-3-(4-hydroxyphenyl)propionate (sulpho-SHPP). In the second step, the hydroxyphenyl groups introduced on the solid surface were titrated through the color formed by incubating the activated supports with bicinchoninic acid (BCA) protein assay reagent containing $CuSO_4$. Indeed, sulpho-SHPP, once grafted onto solid supports, had the ability to reduce $Cu^{2+}$ to $Cu^{+}$ by forming a chelate complex with BCA which was titrated measuring the absorbance of the solution at 562 nm. A scheme of the successive steps of this method applied to the polyethylene supports treated by a $NH_3$ plasma was given by Ghasemi and is represented in Figure 65. As previously explained, the quantity of grafted sulpho-SHPP was indirectly titrated since it quantitatively reduced $Cu^{2+}$ to $Cu^{+}$. The latter formed the chelate complex with BCA, which was finally titrated. Values of the amino group content measured by Kakabakos on several solid supports are reported in Table 17.

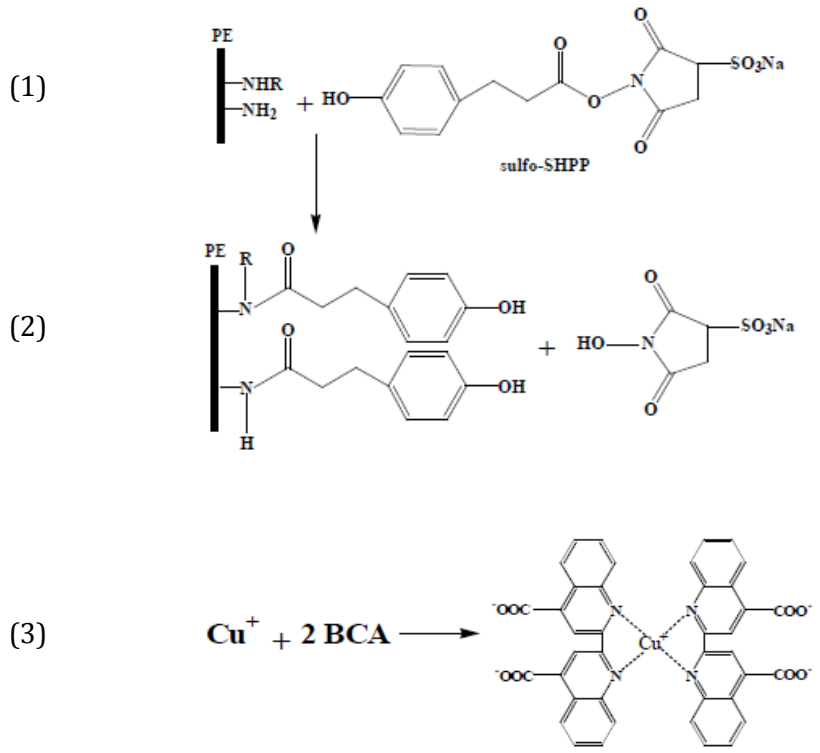


***Figure 65: Principle of the titration of primary and secondary amine with the sulpho-SHPP on a modified polyethylene surface in 3 successive steps [98]***

***Table 17: Data of the determination of the reactive amino group content of several solid supports [99]***

| Solid support | Method used | | | Units |
|---|---|---|---|---|
| | ITL / BCA | ITL / DTNB | sulpho – SHPP / BCA | |
| Polyethylene | 0.0 | 0.0 | 0.0 | nmol/bead |
| Polypropylene | 0.0 | 0.0 | 0.0 | nmol/bead |
| Dylark | 0.0 | 0.0 | 0.0 | nmol/bead |
| AminoDylark | 2.1 ± 0.2* | 2.1 ± 0.1 | 2.2 ± 0.1 | nmol/bead |
| Polystyrene | 0.0 | 0.0 | 0.0 | nmol/bead |
| APIᵗ | 1.7 ± 0.1 | 1.6 ± 0.1 | 1.8 ± 0.1 | nmol/bead |
| APII | 3.3 ± 0.2 | 3.4 ± 0.1 | 3.4 ± 0.2 | nmol/bead |
| APIII | 5.4 ± 0.2 | 5.5 ± 0.3 | 5.7 ± 0.2 | nmol/bead |
| Sepharose 4B | 0.0 | 0.0 | 0.0 | µmol/ml gel |
| AH–Sepharose 4Bᵗ | 7.4 ± 0.3 | 6.7 ± 0.3 | 12.7 ± 0.4 | µmol/ml gel |
| CH–Sepharose 4B | 0.0 | 0.0 | 4.7 ± 0.2 | µmol/ml gel |
| Diaminodipropylamineᵗ | 6.8 ± 0.4 | 6.4 ± 0.3 | 17.3 ± 0.6 | µmol/ml gel |
| MaxiSorp wells | 0.0 | 0.0 | 0.0 | nmol/well |
| CovaLink NH wells | 0.0 | 0.0 | 0.6 ± 0.05 | nmol/well |

## 2.5 Amine titration with ninhydrin

Ninhydrin (2,2-dihydroxyindane-1,3-dione) is a chemical that is used to detect ammonia, and primary and secondary amines [100], [101], [102], [103]. Its chemical structure is given in Figure 66.

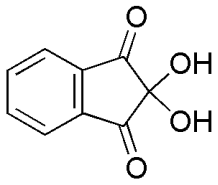

***Figure 66 : Chemical structure of the ninhydrin***

In order to generate the ninhydrin chromophore, the amine was condensed with a molecule of ninhydrin to give a Schiff base. Thus, only ammonia and primary amines can proceed by this step, which produces a deep blue or purple color known as Ruhemann's purple. A scheme of the ninhydrin reaction with an amino acid (which is the most common type of molecule titrated with ninhydrin) and a primary amine is reported in Figure 67.

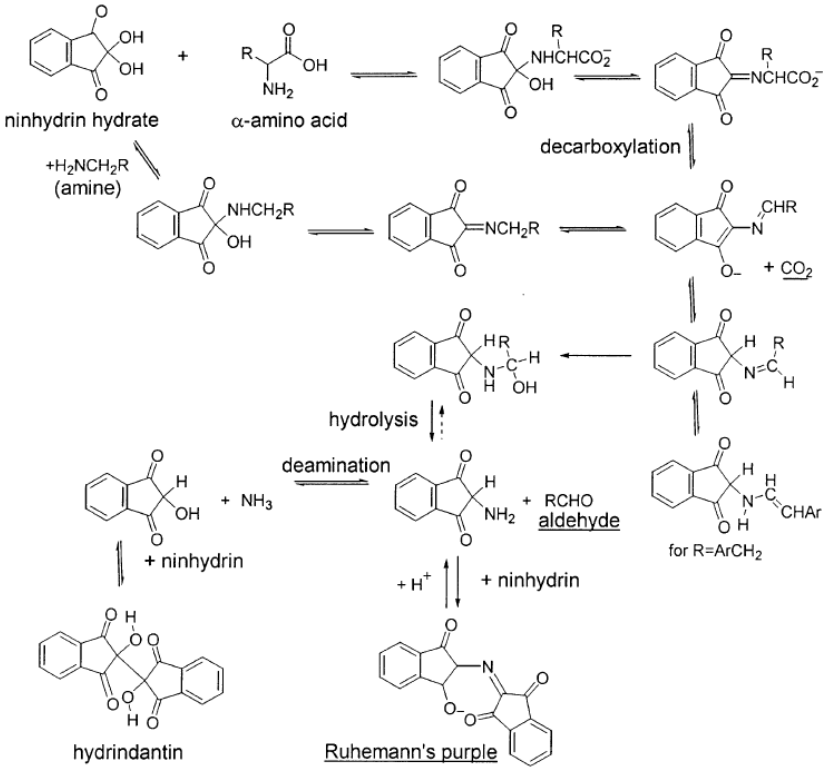


***Figure 67 : Schematic mechanism of the ninhydrin reaction with primary amines [104]***

The reaction of ninhydrin with a secondary amine gives an iminium salt, which is also colored, generally yellow or orange [105]. An example of reaction between the ninhydrin and a secondary amine is given in Figure 68.

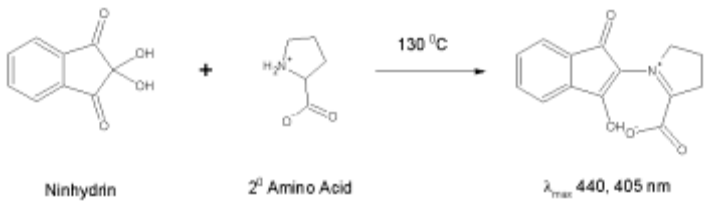


***Figure 68: Example of the reaction of the ninhydrin with a secondary amine [105]***

Thus, as shown in the literature, the ninhydrin reacts twice with primary amine and once with secondary amine, exactly as the epoxy group in an epoxy-amine system. Using ninhydrin to quantify the amount of reactive amino groups seems to be of great interest in our project due its similar behavior with epoxy groups. Mori and coworkers [91] already quoted in section 2.2 for their use of acid/base titration towards monolith-type solid supports with surface amino groups, also applied the ninhydrin method to quantify the surface primary amines. In their work, they spectroscopically determined the amount of Ruhemann's purple formed by the reaction between ninhydrin and the primary amine at a wavelength of 570 nm. Scruggs and coworkers [106] also developed a similar route to characterize the supported amine catalyst with ninhydrin. It was reacted on grafted silica. Absorbance of the colored solution was also measured by a UV-visible spectrophotometer at 565 nm. The schematic ninhydrin reaction with the grafted surface is given in Figure 69.

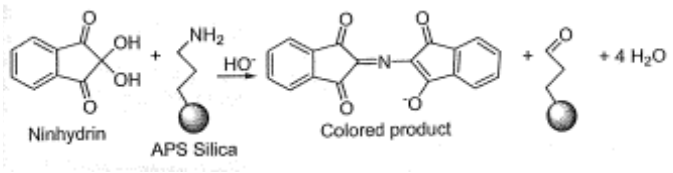


***Figure 69: Schematic ninhydrin reaction with the grafted amine functionalized silica [106]***

Several methods to titrate amino groups on surfaces were presented, but few of them described the quantitative titration of both primary and secondary amines at the same time on the surface of solid materials. Moreover, most of the time, the titrated solid surfaces are considered non-porous and above all impenetrable. As a consequence, only the extreme surface is titrated. To the best of our knowledge, amine titration on organic cross-linked microparticles was never studied and reported in the literature. This is what is presented in this study in the following paragraphs, where new routes to quantify the functionalization of the surface of cross-linked polymer microparticles were developed. These routes were based on fluorescent labeling, titration via ninhydrin, and on differential scanning calorimetry with protocols adapted to the specificity of our particles.

# 3 Experimental

## 3.1 Grafting of a fluorescent dye

### *3.1.1 Selection of the fluorescent dye and synthesis protocol*

Before using the fluorescent labeling for the determination of surface functional groups, the natural CPM fluorescence needed to be investigated to ensure that it would not interfere with the fluorescence from the dye. No natural fluorescence was observed, confirming the possibility of using this technique. The fluorescent dyes mainly used to detect amino groups are the fluorescamine and the fluorescein isothiocyanate (FITC). The fluorescamine only identifies the primary amines and the FITC has a tendency to aggregate. As a consequence, they are not adapted to our study. Indeed, the cross-linked particles have multiple functional groups, mainly secondary amines and hydroxyl groups, as shown by NIR spectroscopy, and possibly primary amines in particular cases. The dye to be selected must react with the primary and secondary amino groups, but not with the hydroxyl groups.

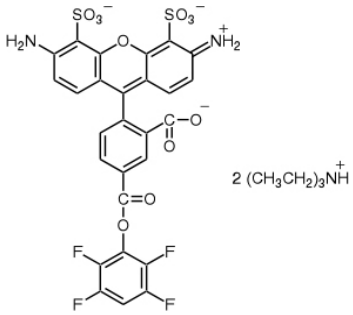


***Figure 70: Alexa Fluor® 488 carboxylic acid, 2,3,5,6-tetrafluorophenyl ester***

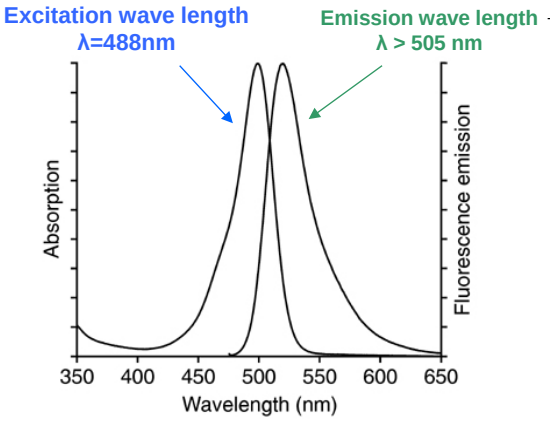


***Figure 71: Absorption and emission spectra of the Alexa Fluor® 488 carboxylic acid, 2,3,5,6-tetrafluorophenyl ester***

Therefore, a fluorescent probe specific toward amines Alexa Fluor® 488 carboxylic acid, 2,3,5,6-tetrafluorophenyl ester (Alexa Fluor® 488 5-TFP, purchased from Life Technologies) was chosen to react with the amines of the CPMs. Its structure is reported in Figure 70. Its absorption and emission spectra are shown in Figure 71. The fluorescent probe must be stored at a temperature under -20°C.

### *3.1.2 Protocol for the grafting of the dye*

The protocol of the grafting was inspired by examples found in the literature [88], [90], [107]. The protocol given by the supplier and usually applied to biological samples (antibodies for example) was adapted to our solid particles.

To perform fluorescent dye grafting, the successive steps were as follows: 1 mg of CPM was dispersed by 1h sonication in 0.5 ml of a basic solution of trisodium phosphate ($Na_3PO_4$), with a pH of 9. One mg of the fluorescent dye was dissolved in 1.5 ml of the trisodium phosphate solution. Then, 0.5 ml of the solution containing the fluorescent dye was added to the CPM dispersion. The reaction medium was stirred for 4 h at room temperature protected from light to ensure a total grafting of the amino groups on the surface of the particles. Finally, the particles were washed five times in water by centrifugation. They were kept in water for easier observation under the microscope, in the dark, between 0°C and 4°C. They could be observed after several weeks but direct exposure to light could seriously degrade the fluorophore. A schematic representation of the fluorescent probe is given in Figure 72.

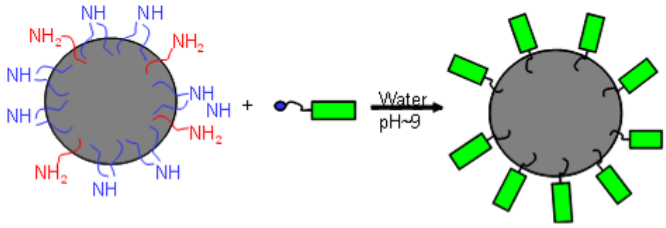


***Figure 72: Grafting of the Alexa Fluor® 488 fluorescent probe on the surface of CPMs***

The fluorescence was observed with a confocal laser scanning microscope (Maximum resolution is 200 nm in X-Y, 500 nm in Z) using an objective of 63x/1.4 OIL and an Argon laser (30 mW), with 4 possible wave lengths (458 nm, 477 nm, 488 nm and 514 nm). All images were recorded with exactly the same parameters. This experimental set up allowed for the comparative study of the fluorescent intensity of CPMs, which was then related to the quantity of amino groups. 3D modeling images of CPMs were acquired by changing the focus in different planes (plane distance ~ 100 nm in z direction).

## 3.2 Amine titration with ninhydrin

### *3.2.1 Protocol for qualitative test*

This test is based on the coloration of the particles after the reaction with ninhydrin. Tests were done in 5 mL vials; 30 mg of CPMs was added to 1 ml of water, before 1 mL of 2% ninhydrin in ethanol was added to the mixture, which was then stirred vigorously. All of samples were heated for 10 minutes at 110°C, and then stirred again, before the immediate observation of the color taken by the particles. CPMs with stoichiometric ratios from 0.9 to 1.35 were analyzed. All particles resulted from a polymerization time of 24 h at 100°C.

One vial was prepared with 3 droplets of IPD as a reference solution to determine the color obtained in presence of primary amino groups only. The same test was done with 3 droplets of a secondary amine, dibutylamine, also to compare the color obtained.

Moreover, the potential reaction of the ninhydrin with the DGEBA and the hydroxyl groups of an epoxy/amine network was investigated. The DGEBA and an epoxy/amine network, fractured to provide accessibility of the core and not only the oxidized parts, with an a/e ratio of 0.7 (to be sure to not have reactive amino groups) was placed in an aqueous solution of ninhydrin until the boiling point of the solution.

### *3.2.2 Protocol for quantitative tests*

This test is based on the back titration of unreacted ninhydrin. A known quantity of ninhydrin was poured into an aqueous solution containing a known amount of particles. Thus, after the reaction between the particle surface and the ninhydrin, the remaining ninhydrin was titrated in the supernatant. In more details, 300 mg of particles was added to 4 ml of water with a few milligrams of ninhydrin (depending on the theoretical value of reactive amino groups left). All of the samples were placed in a preheated oven at 130°C to easily reach the boiling point. They were kept for 1 minute boiling in the oven, before they were removed and then stirred for 15 minutes until they reached room temperature. Before taking a sample from the supernatant for titration of the remaining ninhydrin, samples and their containers were reweighed to determine the water loss during boiling (even if bottles were closed with caps). Samples from the supernatant were filtered and diluted. The CPMs were independently titrated 4 times using the UV absorbance of the supernatant by UV-Vis spectrometry and size exclusion chromatography (SEC) and its UV detector. The same protocol was applied to verify the quantitative detection of secondary amines with ninhydrin. CPMs were replaced by dibutylamine. Comparison between the concentration introduced and that calculated with the back-titration of ninhydrin was done.

***Principle of the back titration of ninhydrin by UV detection***

It is known that, due to its molecular structure which contains unsaturated cycles with the possibility of conjugations, the ninhydrin molecule absorbs in the UV range. The spectrum obtained for a ninhydrin solution ([C] = 2.2 $10^{-3}$ mg/ml) is shown in Figure 73. Following the Beer-Lambert law, which gives a linear response of UV absorbance as a function of the concentration (Equation 17), we can easily obtain the concentration of the solution measuring its absorbance. Two similar methods of titration were set up. The first one used the UV detection of ninhydrin at a given wavelength of a size exclusion chromatography. The second method considered the direct measurement of UV absorbance at a given wavelength with a UV-Visible spectrometer.

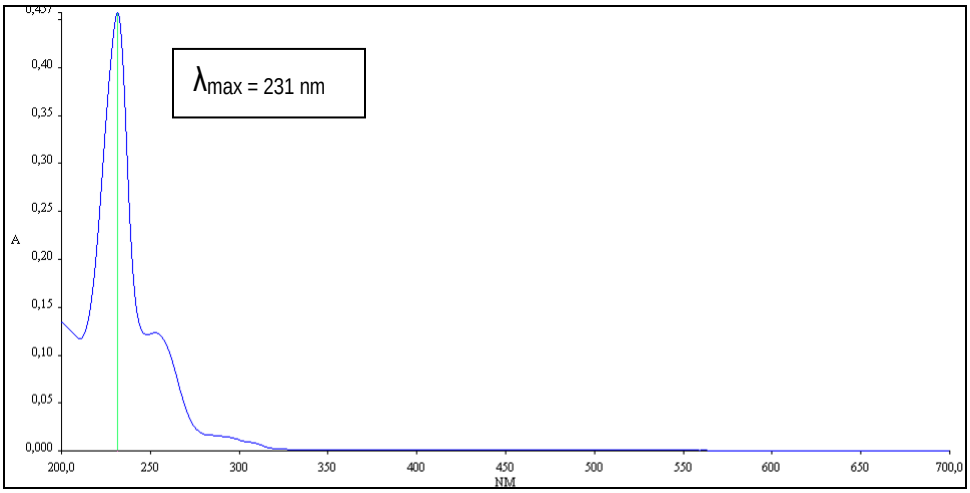


***Figure 73 : UV- Visible absorbance spectrum (from λ = 200 nm to λ = 700 nm) for ninhydrin***

$$A = \log_{10}\frac{I_0}{I} = \varepsilon.l.C \qquad \text{Equation 17}$$

A: Absorbance

ε: Molar absorptivity (L $mol^{-1}$ $cm^{-1}$)

l: Path length of the cuvette (cm)

C: Sample concentration (mol. $L^{-1}$)

***Calibration of the ninhydrin detection by SEC***

The value measured by this technique was the area of the ninhydrin peak detected by size exclusion chromatography in tetrahydrofuran. The value was acquired at a given UV wavelength, chosen in the UV absorbance domain of the molecule (here λ= 254 nm). Thus, the Bert-Lambert law (Equation 17) was applied and the area under the ninhydrin was directly proportional to the concentration. A calibration curve was established with known concentrations; the area under the ninhydrin peak was plotted as a function of the ninhydrin concentration. The curve is given in Figure 74. This curve

was directly used to determine the concentration of ninhydrin in the diluted supernatant solution in tetrahydrofuran, which is directly proportional to the residual ninhydrin in the supernatant.

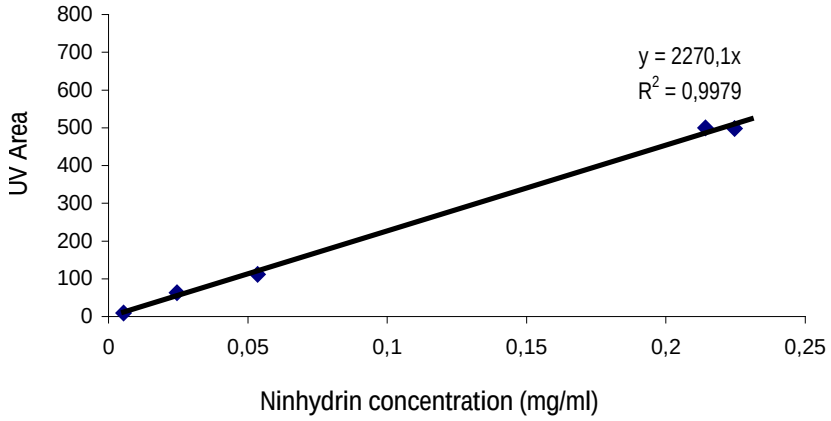


***Figure 74 : Calibration curve - UV response of ninhydrin solutions obtained by SEC (λ=254nm)***

***<u>Calibration of the ninhydrin detection by UV-Visible spectrometry</u>***

This technique measured the UV absorbance which was plotted as a function of the known concentrations of ninhydrin in aqueous solutions, at the maximum absorbance, $\lambda_{max}$. $\lambda_{max}$ was equal to 231 nm. Using this wavelength, errors in the absorbance value were limited. All of the following values were measured at that wavelength.

The calibration curve obtained with four aqueous ninhydrin solutions is given in Figure 75. It is used to calculate the ninhydrin concentration in the supernatant solution into which the ninhydrin reacted at the surface of the particles. The supernatant was diluted to avoid the saturation of the UV response.

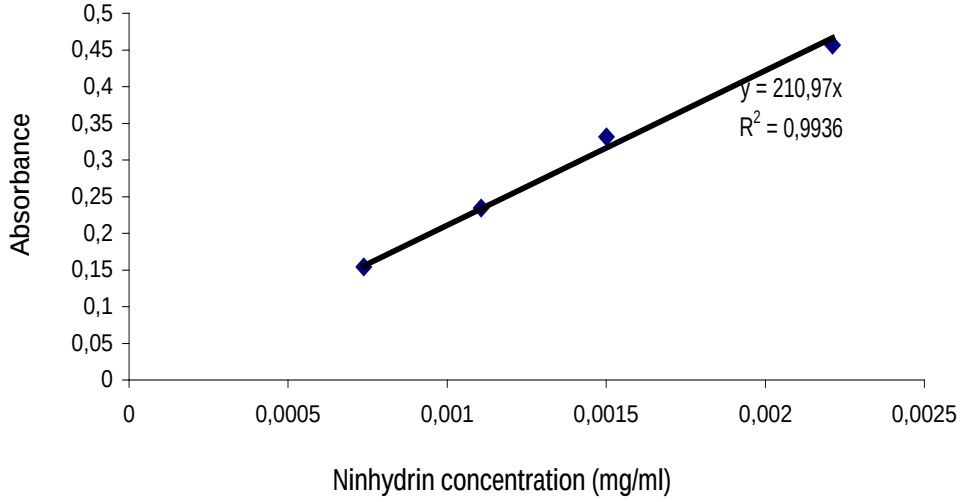


***Figure 75 : Calibration curve: UV response of ninhydrin solutions at λ= 231 nm***

### 3.3 Amine reactivity by differential scanning calorimetry (DSC)

DSC was used in a non-conventional way to determine the quantity of reactive amino groups in the CPMs towards epoxy. Exothermic peaks of the reaction of the dispersion of CPMs in DGEBA (DER 331) and of the neat matrix DER331-IPD were studied by modulated DSC in dynamic mode at 5°C/min from -10°C to 220°C. The values of the temperatures at the start ($T_{start}$), maximum ($T_{max}$) and end ($T_{end}$) of the exothermic peak of reaction, and the enthalpy of reaction ΔH were collected 2 weeks after the dispersion step. Tg was measured at the inflection point of the reversible heat flow signal and the reaction peak was observed from the non-reversible heat flow signal. Measurements were performed with a Q200 and a Q2000 heat flux DSC from TA Instruments. Q2000 was calibrated for temperature using Adamantane (-64.53°C), n-Octadecane (28.24°C) and Indium (156.60°C) at a scan rate of 10°C/min. The heat flow was calibrated using the Indium signal (28.71 J/g). A Tzero calibration using sapphire was performed for the Q2000 instrument.

The recording program was as follows:

4- Equilibrate at -10°C
5- Modulate ± 0.50 every 40 s
6- Isothermal for 5 min
7- Ramp (5°C/min) to 220°C
8- Equilibrate at 10°C
9- Modulate ± 0.50 every 40 s
10- Isothermal for 4 min
11- Ramp (5°C/min) to 200°C.

All of the tests were conducted under nitrogen in Aluminum hermetic pans. The data were analyzed using the TA Universal Analysis software.

### 3.4 Monitoring of CPM reactivity towards DGEBA by Near-Infrared spectroscopy

The NIR spectra, from 4000 to 12000 $cm^{-1}$ were obtained with an FT-NIR spectrometer from Bruker (Billerica, MA), Equinox 55, equipped with a tungsten halogen source, a quartz beam splitter, and an InGaAs detector. All spectra were collected with a resolution of 4 $cm^{-1}$, and 32 scans per spectrum. A heating cell (from room temperature to 120°C) supplied by Bruker and equipped with a sample holder (glass tubes with diameters equal to 5 and 8 mm) was added to the system to monitor kinetics of the reaction at 80°C. This method was used to monitor the potential reaction between residual amino groups on the CPMs and epoxy groups in the DGEBA. Treatment of the signal was done with the software OPUS from Bruker. Typical bands observed for the epoxy-amine reaction were the one corresponding to the disappearance of the oxirane ring at 4530 $cm^{-1}$ or 6071 $cm^{-1}$ or amine disappearance at 6700-6350 $cm^{-1}$.

# 4 Results on surface amine titration

## 4.1 Theoretical calculation of surface amine of CPMs

Before investigating different titration methods to quantify the CPM surface amines, the theoretical calculation of the concentration of the residual amino groups as a function of the stoichiometry, particle diameter, and the depth of penetration of the probe (fluorescent dye or ninhydrin) considered is carried out. Indeed, the CPMs *a priori* have a similar structure in the core and at the surface. Consequently, residual amino groups are present everywhere in the structure. Therefore, the surface amine is related to the accessible thickness, which depends on how deep the probe can diffuse into the CPMs. This depth is called the shell thickness. The calculation is then done for the different shells considered (See the illustration in Figure 76). It was based on the composition of the system; the input data needed are the monomer molar mass of the monomers, $M_{IPD}$ = 170 g.mol$^{-1}$ and $M_{DGEBA}$ = 374 g.mol$^{-1}$, as well as the stoichiometric ratio r = a/e. Their epoxy equivalent weight (EEW) and amine hydrogen equivalent weight (AHEW) were preferably used.

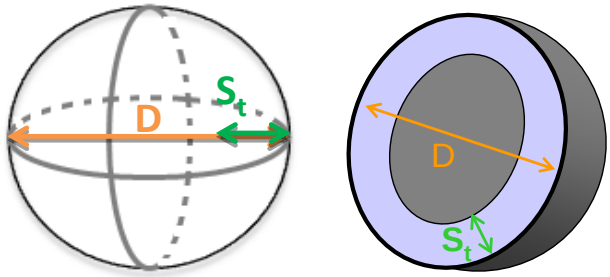


***Figure 76: Illustration of CPMs for the theoretical calculation of residual amino groups***

Several hypotheses were made for the calculation, it was assumed that:

- Particles were homogeneous (homogeneous distribution of reactive groups)
- Networks synthesized reached the fully cured state
- Only the epoxy/amine reaction occurred

DGEBA is a diepoxy and IPD is a diamine, so each mole of IPD gave two moles of primary amine and each amine had a functionality of 2 (they could react twice with epoxy groups). This double reactivity of the primary amine was taken into account in this calculation.

The different calculation steps are reported below.

1. *The first step consists of determining the initial concentration of the amino hydrogen –NH introduced for an epoxy-amine network, which is expressed by [$NH_{tot}$] in mmol.g$^{-1}$:*

$$[NH_{tot}] = \frac{r.AHEW}{r.AHEW + EEW} \times \frac{1}{HEW}$$

2. *The second step is determination of the concentration of unreacted –NH groups assuming that all epoxy groups have reacted. This corresponds to the excess of amine introduced in the synthesis, which are the residual –NH groups, noted: [$NH_{res}$] in mmol.g$^{-1}$of CPM.*

$$[NH_{res}] = \frac{r-1}{r} \times [NH_{tot}]$$

3. *The last step is the determination of unreacted –NH groups calculated for a particle of diameter D, and only considering an external accessible shell, with a thickness $S_t$ (*Figure 76*). It is noted: [$NH_{res\text{-}shell}$] in mmol.g$^{-1}$ of CPM.*

$$[NH_{res\ shell}] = \frac{S_v}{V_{CPM}} \times [NH_{res}]$$

$$[NH_{res\ shell}] = \frac{\frac{4}{3}\pi\left(\frac{D}{2}\right)^3 - \frac{4}{3}\pi\left[\left(\frac{D}{2}\right) - S_t\right]^3}{\frac{4}{3}\pi\left(\frac{D}{2}\right)^3} \times \frac{r-1}{r} \times \frac{r.AHEW}{r.AHEW + EEW} \times \frac{1}{AHEW}$$

With $S_v$: the volume of the shell

$V_{CPM}$: volume of the CPM

An example of the calculation is given in Table 18 for a shell thickness of 0.1 µm and a particle diameter equal to 4 µm. The concentration of residual reactive amino groups at CPM surface [$NH_{res\text{-}shell}$] is plotted in Figure 77 for an a/e ratio of 1.35 and 1.5 as a function of the shell thickness, as we do not know the thickness of the accessible external layer of the CPMs. The calculation was done for an accessible thickness increased up to 2 µm, which corresponds to the entire CPM (D = 4 µm).

The theoretical value of the remaining reactive amino groups on CPM surface was then plotted for five variable shell thicknesses (0.15, 0.2, 0.5, 1 and 2 µm) for all of the stoichiometric a/e ratios from 1 to 1.5. The comparison with the experimental values obtained will give the accessible surface thickness of the CPMs which can participate in the buildup of covalent bonds once dispersed in a matrix. From these curves it appears that the maximum concentration of residual amino groups is close to 2 mmol per gram of CPMs for the CPMs with a/e = 1.5, and close to 1.43

mmol per gram of CPMs for a/e = 1.35. In other words, CPMs with a/e = 1.5 have theoretically 1.4 more unreacted amino groups as compared to CPMs with a/e =1.35.

***Table 18: Example of calculation - Total amino, residual and surface amino groups for a CPM a/e=1.5 and a shell thickness of 0.1µm***

| Diameter of CPM (cm) | Volume of one CPM ($cm^3$) | Density of CPM (g. $cm^{-3}$) | Shell thickness (cm) | Shell volume ($cm^{-3}$) | Shell weight (g) | shell volume / CPM volume |
|---|---|---|---|---|---|---|
| D | $V_{CPM}$ | d | $S_t$ | $S_v$ | $S_w$ | $S_v$ / $V_{CPM}$ |
| D | $(4/3).\pi.(D/2)^3$ | d | $S_t$ | $V_{CPM}$ - $(4/3.\pi.((D/2)-S_t)^3)$ | $S_v$. d | $S_v$ / $V_{CPM}$ |
| 0.0004 | 3.35E-11 | 1.2 | 0.00001 | 4.78E-12 | 5.74E-12 | 1.43E-01 |

| a/e | EEW DGEBA (g.mol-1) | AHEW Hardener (g.mol-1) | 1: Concentration of initial -NH (mmol.g-1 of CPM) | 2: Concentration of residual -NH (mmol.g-1 of CPM) | 3: Concentration of residual -NH in the shell (mmol.g-1 of CPM) |
|---|---|---|---|---|---|
| a/e | EEW | AHEW | $[NH_{tot}]$ | $[NH_{res}]$ | $[NH_{res\text{-}shell}]$ |
| a/e | EEW | AHEW | [r. AHEW / (r.AHEW+EEW)] / HEW | $(r-1)/(r).[NH_{tot}]$ | $[NH_{res}]$. $S_v$ / $V_{CPM}$ |
| 1.5 | 187 | 42.5 | 5.982 | 1.99 | 0.28 |

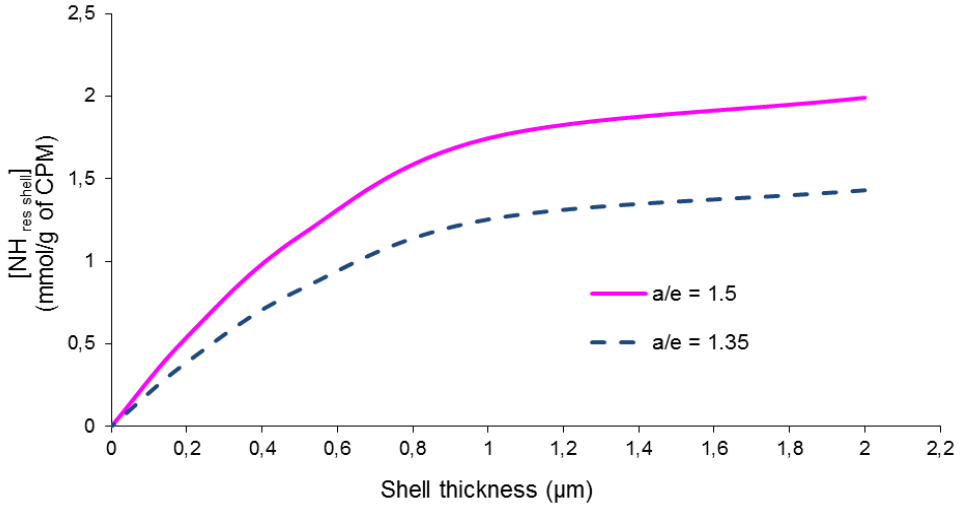


***Figure 77: Concentration of residual reactive amino groups at CPM surface [$NH_{res\text{-}shell}$] as a function of the shell thickness for a/e=1.35 and 1.5. D = 4µm***

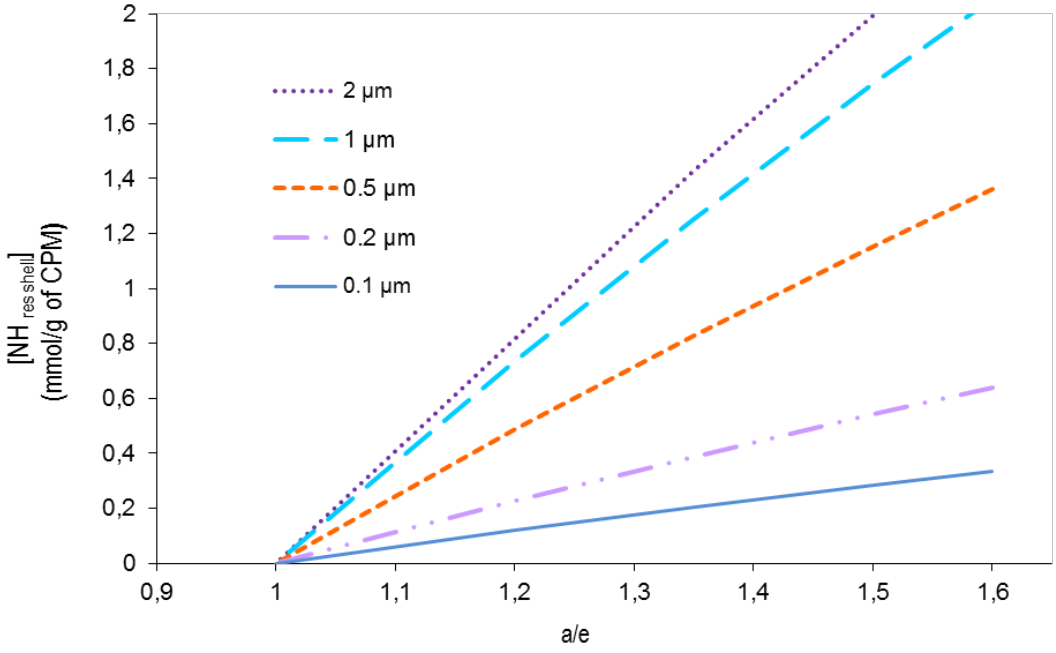


***Figure 78: Theoretical values of the concentration of reactive amino groups [$NH_{res\text{-}shell}$] in the CPM shell for different accessible thicknesses (from 0.1 µm to 2 µm) with various a/e ratios from 1 to 1.6. D = 4µm***

## 4.2 Qualitative titration test

This technique was carried out as a preliminary qualitative test to check the presence of primary and secondary amines on the particle surface, and evaluate the possibility of obtaining a quantitative titration with the same reactant.

This method using ninhydrin as a titrant was chosen due to its speed and its facility to conclude on the presence of primary amine by visual observation of a blue coloration.

A preliminary study of the possible reaction of ninhydrin with DGEBA or hydroxyl groups from the epoxy-amine network was conducted. No coloration of the DGEBA and the network was observed in presence of ninhydrin. Thus, if a coloration is observed, we can be sure of the presence of amine on the particle surface and not to other groups from the network. We do not have to worry about side reactions.

The tests were done in small vials, where the CPMs were in the presence of a ninhydrin solution. After heating of the media for 10 minutes at 110°C, the coloration was observed and gave the results summarized in Table 19. The reference coloration was given in the last vial containing IPD to determine the coloration in the presence of a primary amine.

The colorations of the particles in a ninhydrin solution are shown in Figure 79 and are summarized in the table below as a function of their stoichiometric ratio.

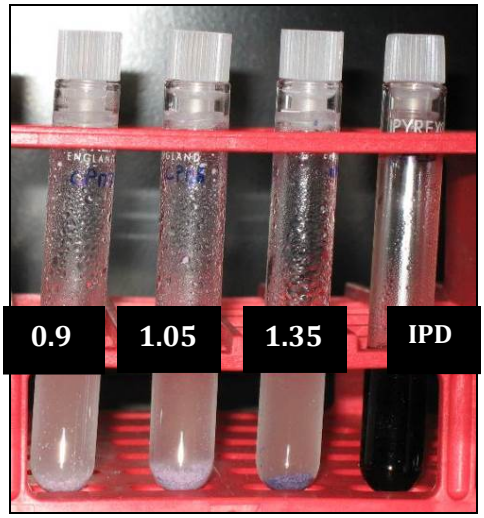


***Figure 79: Picture of CPMs after reaction with ninhydrin – the numbers on the vials are the stoichiometric ratios of the CPMs: a/e from 0.9 to 1.35***

***Table 19: Coloration observation of CPMs in the presence of ninhydrin***

| a/e=0.9 | a/e=1.05 | a/e=1.35 | IPD<br>Ref solution |
|---|---|---|---|
| Very light purple | Light purple | Purple/Dark blue | Dark blue |

A dark blue/purple color was observed for the reference solution containing IPD (molecule with 2 primary amines). The same color but less intense was also obtained on the surface of CPMs a/e=1.35. A light purple color was observed on the surface of the CPMs a/e=1.05. A very light coloration was observed for CPMs a/e=0.9. It is possible that very few primary amino groups were present on the particle surface, which gave this very light coloration.
The same test was done with a secondary amine in the presence of ninhydrin and a yellow solution was obtained. However, no yellow color was observed on CPMs.

To conclude, this ninhydrin test revealed the presence of primary amino groups on the surface of CPMs a/e=1.35 and 1.05 with a decrease in the color intensity. Concerning the CPM a/e=0.9, and particles with a ratio close to one, it was shown that they still owned a few accessible amino groups on their surface which gave the very light blue coloration observed.

The results from the ninhydrin tests appear to be contradictory to the results of IR spectroscopy reported in chapter 2. It was previously concluded that no primary amine was present in the CPMs, in the limit of sensitivity of the IR method. The ninhydrin test seems to be much more sensitive towards primary amines than IR. Only a few primary amino groups give the blue coloration and

probably overlap the yellow coloration given by secondary amines, which are undoubtedly present as shown by IR spectroscopy.

This qualitative test has shown the presence of reactive amino groups on the surface of all types of particles tested, meaning that quantitative measurements could then be investigated to obtain the quantity of reactive groups potentially contributing to the build-up of covalent bonds with an epoxy co-monomer from the matrix.

## 4.3 Quantitative measurements of amino groups on CPM surface

### *4.3.1 Titration of primary and secondary amine with a fluorescent probe: semi-quantification*

The method relies on the intensity of the chosen fluorescent probe, grafted on the amino groups of CPMs, and observed with a confocal microscope after excitation by a laser.

***Check of side reactions and adsorption of the probe***

Firstly, CPM with a/e=0.9 were used. They have very few amino groups but a significant number of hydroxyl groups, which should be present on the surface due to opening of the epoxy cycle. No fluorescence was observed for this type of CPM after the grafting step. The probe did not react with hydroxyl groups and was not adsorbed at the particle surface. The absence of reaction with other chemical groups present at the surface of particles (namely-OH groups) and the potential adsorption of the probe on particle surface were verified. Then, 3 types of CPMs were grafted, either with different a/e ratios (1.35 and 1.05) or polymerization times (3 and 24 h). Comparative observations were carried out through visualization of the fluorescent response of the particles. For the same a/e ratio in the feed, a short polymerization time (3 h) should result in more residual amino groups on the surface compared to a long polymerization time (24 h). A higher a/e ratio in the feed (a/e=1.35) should give more residual amino groups on the surface compared to a lower ratio (a/e=1.05).

***Comparison of the fluorescent intensity***

Pictures obtained by fluorescent confocal microscopy are shown in Figure 80. They were all taken under the same conditions (detector, laser,…) to compare the signal intensity. A very high fluorescent signal was observed for a/e=1.35 with a short polymerization time. The particle surface appeared as an intense green crown. The inside of the particles remained dark. This was particularly visible in Figure 81, looking at the 3D reconstitution of particles, which was shown by the absence of a reaction of the fluorescent probe inside the particle. The accessible surface

represented by crowns was thicker because the signal was a function of the intensity. Moreover, the fluorescent signal strongly decreased when the reaction time was increased up to 24 h. Particles appeared with a light green crown and a dark inside.

The signal continued decreasing when the stoichiometric ratio of the particles was lower: 1.05 (compared to 1.35), and with a longer reaction time. However, the green crown was still visible.

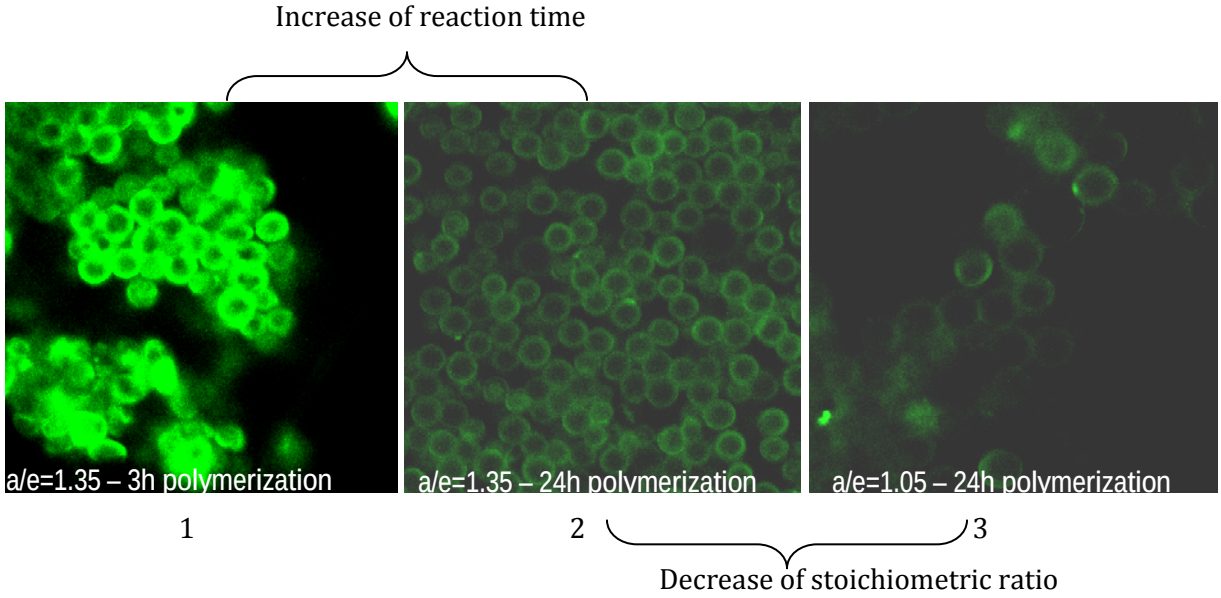


***Figure 80: Photographs of CPMs with fluorescence confocal microscope (1: a/e=1.35 – 3 h of polymerization, 2: a/e=1.35 – 24 h of polymerization, 3: a/e=1.05 – 24 h of polymerization) Stoichiometric ratios are the initial one in the feed***

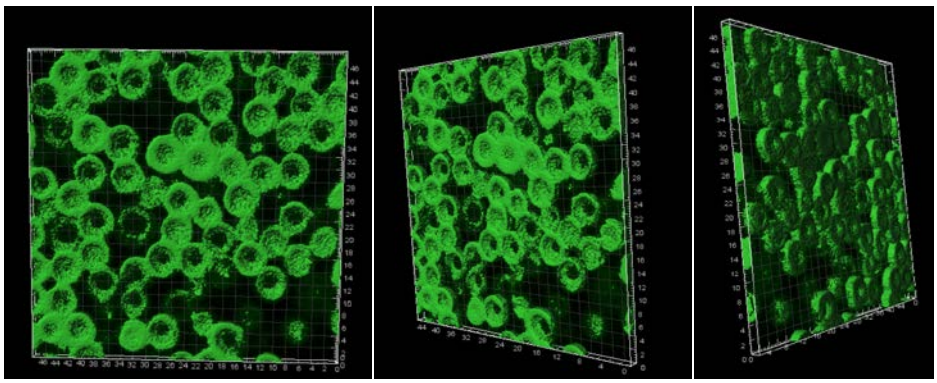

***Figure 81: 3D modeling layer of CPM a/e=1.35 – 3h polymerization***

The fluorescence labeling using the Alexa Fluor 488 probe gave excellent comparative results. Thus, the magnitude of the fluorescent signal related to the quantity of the surface amines was measured. The signal across a particle has been collected for each type of particle and is given in Figure 82. Each signal of the particle presented was chosen to be representative of the sample studied. The

fluorescent crown was even more visible here, with a significant decrease in intensity in the core of the particles. The particles did not have the same size because of their different reaction times. Indeed, in case 1, a smaller fluorescent diameter was measured, close to 4.5 µm compared to 5.5 µm for the 2 other CPMs, which was due to the short polymerization time of 3 h. It was also shown that these CPMs had the highest fluorescent intensity due to their short reaction time and highest stoichiometric ratio. Moreover, the decrease of fluorescent intensity was also observed with a long reaction time and a decreasing a/e ratio.

The intensity of the signal was plotted as grey values. The most intense is the fluorescence, the highest is the grey value. Thus, the results for (1) a/e=1.35, 3 h of polymerization, showed an intensity (about 250 grey value) five times higher than for (2) a/e=1.35, 24 h of polymerization (about 50 grey value) and about ten times higher than for (3) a/e=1.0, 24 h of polymerization (25 grey value). These measures directly corresponded to the quantity of reactive amino groups present at the surface of the particles. Values for the CPMs polymerized during 24 h are not in the same ratio as those calculated in section 4.1. Indeed $[NH_{res\text{-}shell}]$ is theoretically close to seven times higher for the ratio 1.35 than for the ratio 1.05, differing from what is observed with fluorescent intensity. Nevertheless, as the signal was weak for these two CPMs, the sensitivity was low.

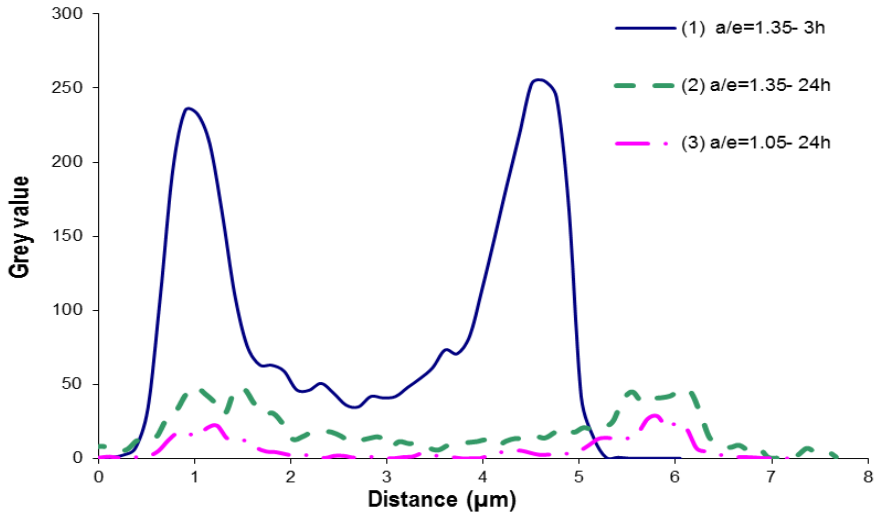


***Figure 82: Fluorescent intensity signal across the CPMs grafted. Grey value versus the distance through the CPM structure***

The thickness of the accessible layer to the probe was also measured and is visible in Figure 82. The thickness of the fluorescent crown was about 1 µm for the 3 types of particles tested with this method, which corresponded to the accessible depth inside the particle. This was true at least for molecules as big as the probe and grafted in an aqueous media. Nevertheless, this thickness was

possibly amplified by the strong response of the fluorescent molecule or by the computer treatment.

### *4.3.2 Titration of primary and secondary amine with ninhydrin*

***Check of the quantitative titration of secondary amines by ninhydrin***

Due to the fact that ninhydrin has been widely used in the literature to highlight primary amines but not secondary amines, a preliminary study regarding the quantitative detection of secondary amines by ninhydrin was investigated. Dibutylamine was identified as a simple molecule bearing a secondary amine. A comparison was made between the known value of dibutylamine introduced and the quantity of ninhydrin reacting; the results are summarized in Table 20. The discrepancy between the value expected and the one measured was calculated; it was between 2 and 12% which is in the same range as that reported in the literature by Scruggs [106] for the titration of primary amines. This method showed that a quantitative titration of secondary amines with ninhydrin was possible. However, due to the accuracy of this method, the results need to be discussed carefully.

***Table 20: Dibutylamine test – quantitative titration of secondary amines by ninhydrin***

| | Test 1 | Test 2 | Test 3 |
|---|---|---|---|
| Dibutylamine introduced (mol) | 4,42E-05 | 4,57E-05 | 6,98E-05 |
| Ninhydrin which has reacted (mol) *titrated by SEC* | 4,34E-05 | 4,12E-05 | 6,120E-05 |
| discrepancy % | 1,9 | 9,9 | 12,3 |

***Determination of the amount of reactive amino groups on CPM surface***

Measurements were repeated four times on three types of particles with an increased a/e ratio from 0.9 to 1.5 and a polymerization time of 24h. The average value was calculated, as was the standard deviation for the two detection techniques. The global mean for the three types of particles titrated is given in Table 21, along with the corresponding standard deviation. Each sample was titrated twice: once by SEC detection and once by UV-Vis detection. The results of the titrations by SEC and UV-Vis, as well as the average of all values obtained, are plotted for the three types of CPMs in Figure 83.

Firstly, both protocols used gave similar results. This was expected because the analysis was done on the same supernatants and was based on the same technology: the UV absorbance of the ninhydrin. A very good linear relationship was obtained between the concentration of unreacted amino groups and the stoichiometry of the particles. The results in Figure 83 show that even the CPMs with an a/e ratio of 0.9, which in theory corresponded to particles without excess of amino groups, owned a few reactive and accessible amino groups on their surface, about 0.008 mmol/g of CPMs. This confirmed our first observation made by the qualitative ninhydrin test: a very light blue coloration of the particle surface demonstrated the presence of primary amino groups.

Secondly, looking at the CPMs with a higher stoichiometric ratio of a/e=1.35, their concentration of unreacted amino groups was 21 times higher compared to the one at a/e=0.9. They bore an average of 0.172 mmol of amino groups per gram of CPMs. The same observation was made at a higher stoichiometric ratio of 1.5: those CPMs had an amine concentration which was multiplied by 29 compared to the less functionalized CPMs titrated here. Comparing these last two a/e ratios, the system with a ratio a/e = 1.5 had 1.35 more unreacted amino groups than for a ratio a/e = 1.35. This is in the same range as the maximum expected value, obtained from our theoretical calculation (which was about 1.4 times more for a/e =1.5 than that for the CPMs with a ratio of 1.35).

***Table 21: Titration of reactive amino groups on CPM surface: SEC and UV-Vis spectrometry***

| a/e | 0.9 | 1.35 | 1.5 |
|---|---|---|---|
| **SEC** (mmol/g) | 0.005 | 0.169 | 0.236 |
| *Standard deviation* | 0.004 | 0.043 | 0.060 |
| **UV-Vis** (mmol/g) | 0.010 | 0.176 | 0.212 |
| *Standard deviation* | 0.006 | 0.035 | 0.068 |
| **Average** (mmol/g) | 0.008 | 0.172 | 0.232 |
| *Standard deviation* | 0.005 | 0.037 | 0.043 |

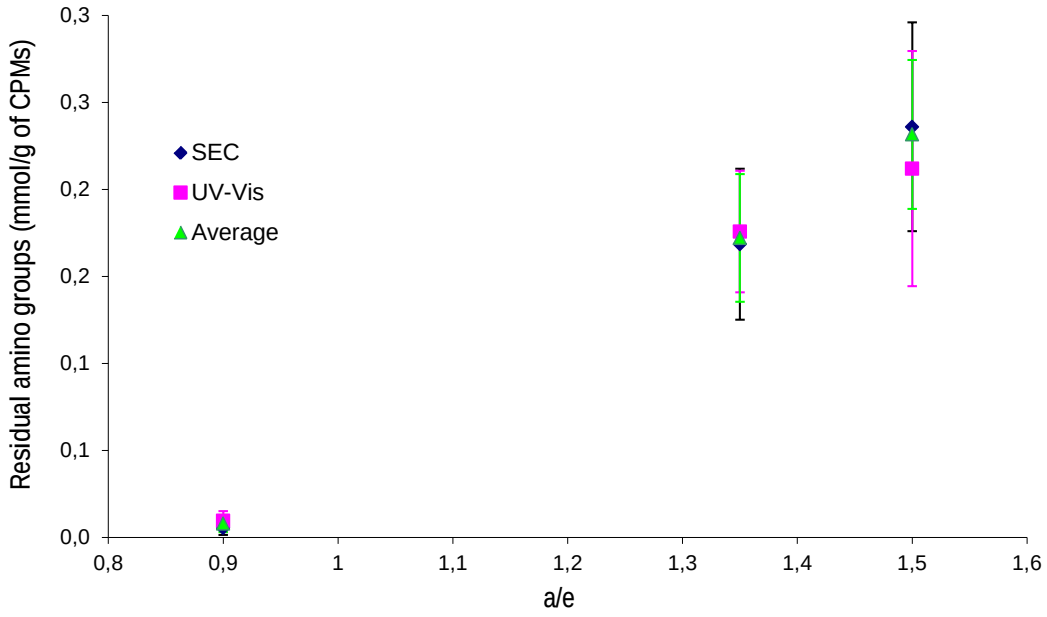


***Figure 83: Values of reactive amino groups obtained by the ninhydrin titration method (by SEC & UV-Vis) for three types of particles: a/e=0.9, 1.35 and 1.5***

As comparison, the titration of primary amines was realized on grafted amine-functionalized silica and gave the following values reported in the literature from 0.26 to 0.9 mmol.g$^{-1}$ which were in agreement with the values expected by the authors [106].

Figure 84 shows the comparison between the experimental values measured of residual amino groups and the calculated shell thickness accessible corresponding to these values, with the same assumptions as those presented in section 4.1. The experimental amount of reactive amine titrated corresponded on average to a theoretical titrated depth close to 0.08 µm. However, the standard deviation obtained for both techniques was not negligible; this is why we will use this result cautiously and above all keep in mind that the results depend on the probe and the reaction conditions.

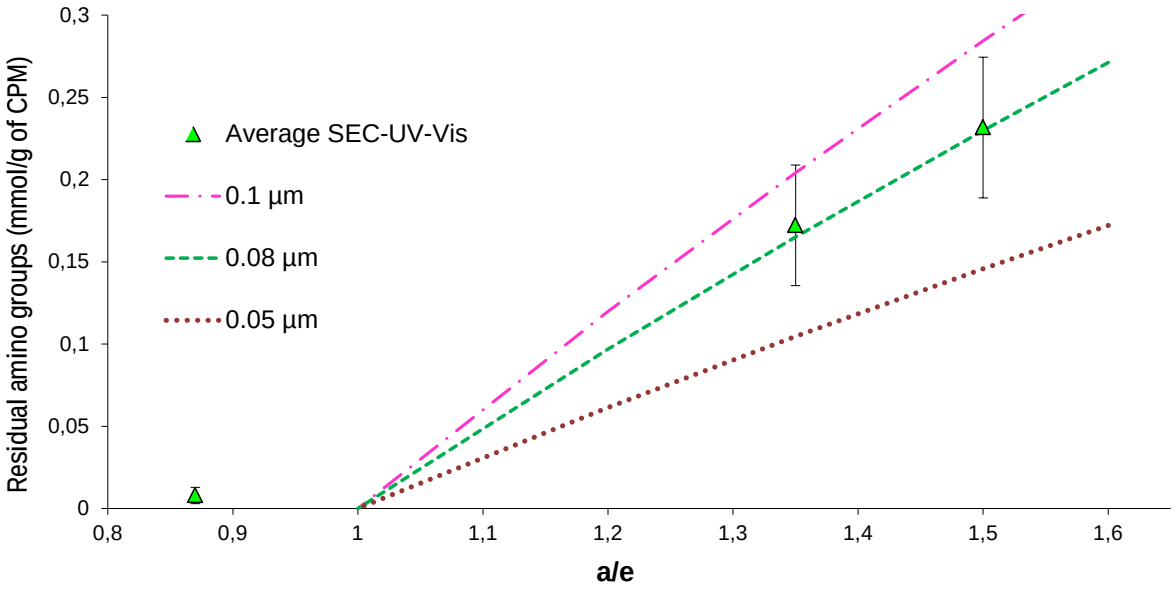


***Figure 84: Average value of reactive amino groups obtained by the ninhydrin titration method for three different types of particles: a/e=0.9, 1.35 & 1.5 – Comparison with the theoretical calculation of [NH $_{res\ shell}$] as a function of the shell thickness between 0.05 and 0.1 µm***

## 4.4 Conclusions

Two different methods were used to characterize the surface amino groups created by the excess of diamine hardener used for the synthesis of CPMs: a semi-quantification method, fluorescent confocal microscopy (FCM), and a quantitative one, titration by ninhydrin. Thus, new methods were developed to titrate both primary and secondary amines on the surface of cross-linked polymer microparticles, which have not been previously reported in the literature to our knowledge.

- The fluorescent method is based on the selective reaction of a fluorescent dye (Alexa Fluor 488 5-TFP) with primary and secondary amino groups of CPMs. It is not a conventional dye grafted on solid or polymer surfaces, but more usually on biologic samples. The observation of the grafted CPM by FCM clearly shows a green crown whose color intensity increases with the stoichiometric ratio, or decreases with the reaction time.
- In the second method, ninhydrin was used to react with primary and secondary amino groups. A back-titration of the unreacted ninhydrin was carried out. The quantification was achieved by measuring the UV absorbance of the solution and using a calibration curve. This titration method allows one to assess the direct amounts of available amino groups to ninhydrin, found between 0.008 and 0.23 mmol/g of CPM for CPM stoichiometric ratios between 0.9 and 1.5, respectively.

In addition a theoretical calculation of the concentration of residual amino groups was done: it was based on the initial stoichiometric ratio introduced to synthesize the particles and on the molar masses of the monomers. The experimental values were compared to theoretical values. The experimental values are in a range that lets us suppose that the amino groups were accessible in a shell with a thickness of around 0.08 µm. However the real value of a/e of the CPMs was always calculated to be higher than the initial one, as shown in chapter 3. Therefore, the accessible shell thickness estimated here was probably slightly overestimated.

Moreover, this thickness may increase or decrease depending on the medium in which the CPM dispersion is made. Indeed, water was the dispersion medium used in our two surface characterization methods, which does not swell epoxy networks easily as compared to some organic solvents. Temperature may also have an influence because it provides more mobility to the network and helps with the diffusion of reactants. These remarks are specific to our type of particles, and are not relevant to inorganic particles (silica, metal oxide) or post-functionalized particles where the reactive groups are found only on the surface and not in the bulk.

# 5 Amine reactivity of CPMs towards epoxy systems

The presence of residual amino groups in the CPM structure was highlighted previously by different methods. Then, their possible reactivity towards epoxy groups is now investigated. Indeed, amino groups born by CPMs are part of the glassy structure. This may have an influence on the mobility and the reactivity of the amino groups. As a consequence, the potential reaction between the amino groups of CPMs and the epoxy pre-polymer was investigated. The CPMs were dispersed in DER 331 to monitor the possible reaction by DSC and Near-Infrared spectroscopy. The aim was to quantify the reactive amino groups potentially participating in the reaction with epoxy groups. The only source of amino groups was in the structure of the CPM; the signal given of a reaction was proportional to the number of reactive amino groups. An illustration of the dispersion of CPMs in DER 331 is shown in Figure 85.

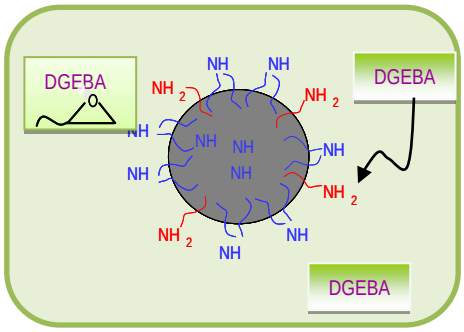


***Figure 85: Illustration of the dispersion of CPMs in DGEBA (DER 331)***

## 5.1 Amine reactivity of CPMs towards DER 331 by DSC

DSC (differential scanning calorimetry) measurements were performed on the dispersion of 23.5 wt% CPMs in DER 331 (23.5 wt% of CPMs correspond to a target percentage of 20 wt% of CPMs in a DGEBA-IPD system at the stoichiometry). The goal was to evaluate the heat released by the reaction between the amino groups from the CPMs and the epoxy groups from the matrix in the DSC pan. This value directly corresponded to the quantity of amino groups reacting. The CPMs used were firstly the CPMs with a high Tg (H1: a/e=0.9, H2: a/e=1.35, H3: a/e=1.5) based on DER 331 and IPD. Then, the comparison was also made with medium Tg CPM (M2) synthesized with DER 331 and D230 with a/e=1.5. A preliminary study of the stability of the dispersions was carried out.

***Stability of the dispersion of CPMs in DGEBA***

As a preliminary test, the stability of the dispersion at room temperature was evaluated. The initial Tg of the CPM was compared to its Tg in the DGEBA, two weeks after the dispersion. The results are

given in Table 22. Similar values were obtained for the Tg of the CPMs before and after the dispersion in DGEBA. It means that DGEBA did not diffuse into CPMs and, as a consequence, did not plasticize the CPM network. Indeed, a decrease in Tg would have been observed in the case of DGEBA diffusion into the CPM core due to the low Tg of the DGEBA ($Tg_{DGEBA}$ = -23°C).

***Table 22: Glass transitions of the CPMs, before and two weeks after dispersion***

| CPM- a/e | Tg $_{CPM}$ (t=0) | Tg $_{CPM}$ in the dispersion |
|---|---|---|
| H1 a/e=0.9 | 138 | Not seen |
| H2 a/e=1.35 | 117 | 117 |
| H3 a/e=1.5 | 112 | 111 |
| M2 a/e=1.5 | 60 | 53 |

***Study of the dispersions in dynamic heating by DSC***

This study was performed with a dynamic heating ramp applied from -10°C to 220°C at a heating rate of 5°C/min. For comparison and calibration, the exothermic peaks of reaction of CPMs with DER 331 were overlaid with those of the neat epoxy-amine matrix created by DER 331 and IPD.

The collected data were the temperatures at the start, $T_{start}$, maximum, $T_{max}$, and end, $T_{end}$, of the exothermic peak of reaction, as well as the enthalpy of reaction, ΔH (Figure 86).

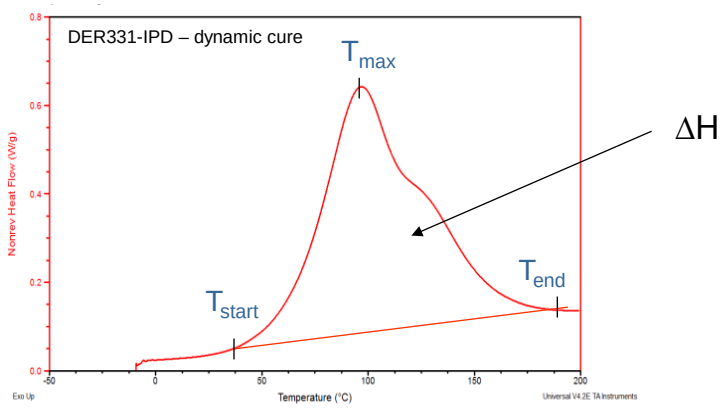


***Figure 86: Measures of ΔH, $T_{start}$, $T_{max}$ and $T_{end}$***

ΔH for DER 331-IPD was equal to 460±9 J/g. It is useful to express this value per epoxy equivalent (EE), or amino hydrogen equivalent (AHE): ΔH=106 kJ/EE or kJ/AHE.

In all our DSC experiments, we considered that the average error on the enthalpy was about 2%, a value which was discussed with individuals from TA Instruments.

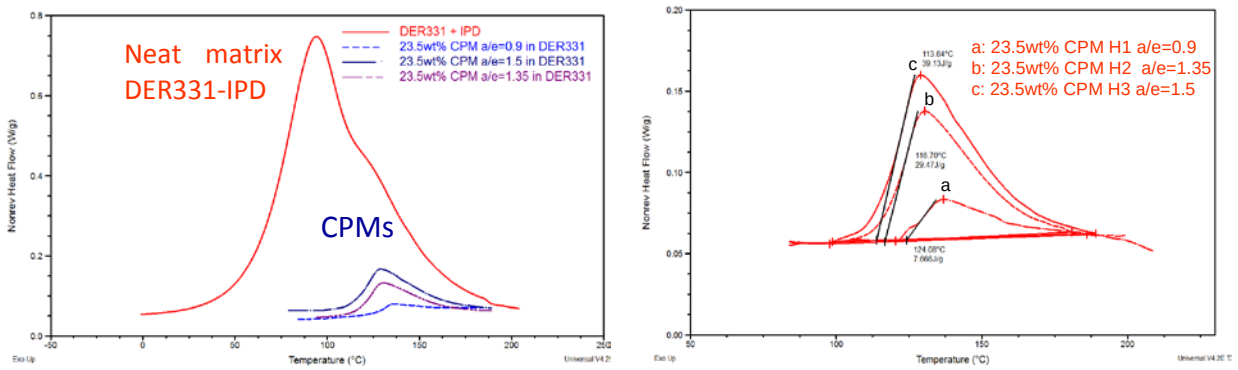


(a) (b)

***Figure 87 : Thermograms of the neat matrix and high Tg CPMs dispersed in DER331 (a) - zoom on the enthalpy peak for the dispersion of CPMs in DER 331 – heating ramp: 5°C/min***

As shown in Figure 87, a reaction peak was observed for the 3 types of high Tg CPMs (H1,H2,H3) dispersed in DER 331, even for the one synthesized in excess of epoxy (H1 a/e=0.9). This peak was due to the reaction of epoxy groups from DER 331 with the amino groups from the CPMs during the dynamic curing in the DSC. We admitted that epoxy groups come from the DGEBA, as infrared analyses in chapter 2 reported that there were no detectable epoxy groups in the CPMs. Temperatures of the beginning, the maximum, and the end of the enthalpy peak are reported in Table 23, in which the values of Tg of the CPMs are also listed. It is observed that the reaction takes place at high temperatures above 90°C, contrary to the reaction in the neat matrix which started close to 30°C. The temperature at the peak maximum was also shifted to higher temperatures.

To conclude, amino groups from CPMs are less reactive than those from the matrix or are reactive but at higher temperatures. One possible explanation is that these groups have a low mobility at room temperature compared to the same ones in the liquid IPD, which limit the reactions with epoxy groups. The Tg of the CPMs explained the reduced mobility at room temperature for all segments of the CPM structure; they were all measured to be above 110°C. Therefore, at low temperatures, the epoxy-amine reaction did not proceed, at least in a short reaction time (a few minutes), as was the case during the DSC experiment.

*Table 23 : Enthalpy ΔH and temperatures of the reaction for 3 types of CPMs (a/e=0.9, 1.35, 1.5) dispersed in DER331.*: 2nd scan = $Tg_2$*

| CPMs | Tg (°C) | ΔH (J/g) | $\Delta H_{CPM}$ (J/g of CPMs) | T peak $T_{start}$-$T_{max}$-$T_{end}$ (°C) |
|---|---|---|---|---|
| H1 a/e=0.9 | 138 (144)* | 8 | 34 | 120-138-175 |
| H2 a/e=1.35 | 117 (123)* | 29 ±1 | 123 ±4 | 97-128-185 |
| H3 a/e=1.5 | 112 (118)* | 39 ±1 | 166 ±4 | 98-125-190 |

The enthalpy of the reaction was measured per gram of dispersion (23.5 wt% of CPMs in DER331) and then re-calculated per gram of CPM. It was observed that the enthalpy of the reaction increased with the stoichiometric ratio of the CPMs, i.e. with the amount of residual amino groups. The value of the enthalpy obtained for the CPM dispersion, $\Delta H_{CPM}$, and the value obtained for the neat matrix were used to estimate the amount of amino groups from the CPMs which reacted with epoxy groups from DER 331. Then, this experimental value was compared to the theoretical one (see section 4.1).

*Table 24: Results obtained for the concentration of reactive -NH groups in CPMs compared to the theoretical value in the whole CPM structure*

| CPMs | Tg (°C) | Theoretical [-NH] (mmol.g$^{-1}$ of CPMs) | Experimental [-NH] (mmol.g$^{-1}$ of CPMs) |
|---|---|---|---|
| H1 a/e=0.9 | 138 | 0 | 0.32 |
| H2 a/e=1.35 | 117 | 1.43 | 1.16 |
| H3 a/e=1.5 | 112 | 1.99 | 1.57 |

From the results in Table 24, it can be concluded that most of the residual amino groups from the CPMs reacted with DGEBA. This means that amino groups from the bulk were involved in the reaction, and not only amino groups from the surface. It also means that DGEBA had time to diffuse into the particle during heating in the DSC pan: from 0°C to 100°C at a rate of 5°C/min, it takes 20 min.

As a comparison, medium Tg CPM M2 with a/e=1.5 were also dispersed in DER 331 and analyzed by DSC. These CPMs had different amino groups in their structure due to the use of the Jeffamine D230 for their synthesis. However, thanks to the close molar mass of IPD and D230, $Mw_{IPD}$ = 170

g.mol$^{-1}$ and $Mw_{D230}$ = 230 g.mol$^{-1}$ respectively, the two types of CPMs had a similar theoretical content of amino groups. Their main difference was therefore their structure, which directly impacts the value of Tg.

The heat released during the reaction with DER 331 in the DSC pan was overlaid to the heat released by a neat matrix a/e=1 of DER331-D230. With these CPMs, ΔH was broad but started at lower temperatures (80°C) compared to the High Tg CPMs (H1, H2, H3) whose $T_{start}$ was close to 100°C.

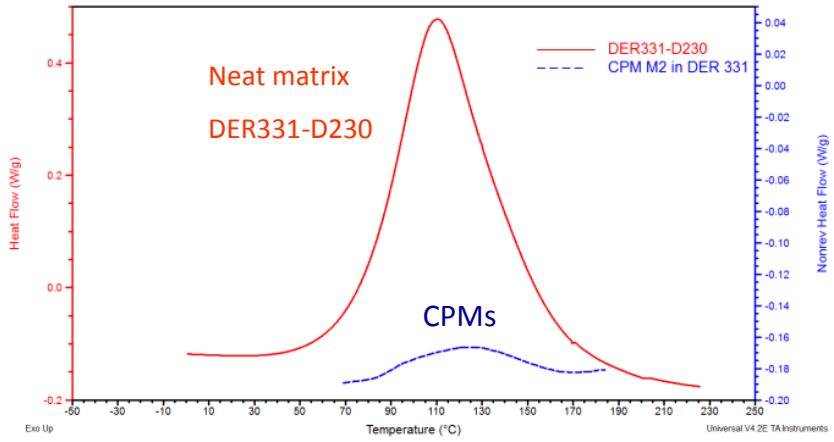


***Figure 88: Thermogram of the neat matrix DER331-D230 and medium Tg CPMs (M2 a/e=1.5) dispersed in DER331 – heating ramp 5°C/min***

The DSC analyses obtained for the CPM M2 and H3 dispersed in DER 331 are reported in Table 25. ΔH measured for the dispersion with the CPM M2 was higher than the dispersion with H3, which was not expected due to the fact that CPM M2 and CPM H3 theoretically bear a similar amount of amino groups. This value is in the same range as the theoretical one; all of the amino groups from the entire CPM (surface + core) reacted with epoxy groups.

***Table 25: Enthalpy ΔH and temperatures of the reaction for the CPM M2 and H3 dispersed in DER331.*: 2nd scan = $Tg_2$***

| **CPMs** | **Tg** (°C) | **ΔH** (J/g) | **$\Delta H_{CPM}$** (J/g of CPMs) | **T peak** $T_{start}$-$T_{max}$-$T_{end}$ (°C) | **Theoretical [-NH]** (mmol.g$^{-1}$ of CPMs) | **Experimental [-NH]** (mmol.g$^{-1}$ of CPMs) |
|---|---|---|---|---|---|---|
| M2 a/e=1.5 | 60 (68)* | 48 ±1 | 204 ±4 | 80-120-170 | 1.83 | 1.95 |
| H3 a/e=1.5 | 112 (118)* | 39 ±1 | 166 ±4 | 98-125-190 | 1.99 | 1.57 |

## 5.2 Amine reactivity of CPMs towards DER 331 by NIR

NIR (Near Infrared) was used in isothermal mode at 80°C to evaluate the kinetics of the reaction between amino groups from the CPMs toward the epoxy from the DER 331. This temperature corresponds to a standard DER 331-IPD first step of curing. The potential decrease of epoxy and amine band, as well as the increase of the corresponding band to hydroxyl groups, was investigated for high Tg CPM H3 and medium Tg CPM M2. They both had an a/e=1.5 and a similar amount of amino groups. The dispersion was placed into the NIR heating cell and left without stirring for 2h. Spectra collected every 30 seconds are reported in Figure 89 and Figure 90.

No significant decrease of epoxy groups was observed for both CPMs (a) and (b), which is not surprising due to the high concentration of DGEBA. No significant decrease in the amount of amino groups and increase in hydroxyl groups were detected for the dispersion of the high Tg CPM H3 (c). On the contrary, in spectrum (d), the band corresponding to the amines decreased in intensity as the band of the hydroxyl groups was increasing. The medium Tg CPM (M2) seemed to be able to react with DER331 at 80°C. Even if the two types of CPMs have a similar amount of amines already included in epoxy-amine network, they do not react exactly at the same temperature. At 80°C, only the CPMs synthesized with Jeffamine D230 whose Tg was about 60°C were able to react when the dispersion was heated for 2h. Only CPMs with a Tg lower than the temperature of the reaction can react.

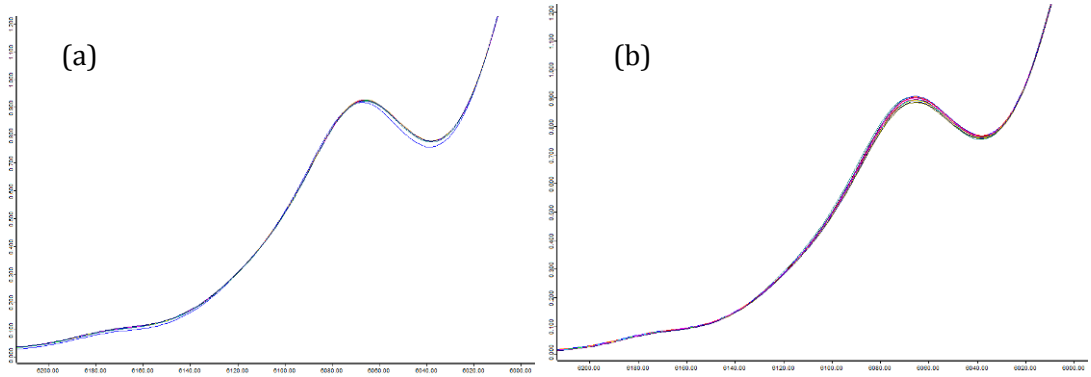


***Figure 89: NIR spectra for the dispersion of H3 (a) and M2 (b) in DER 331 heated at 80°C during 2h. Focus on epoxy band at 6071 $cm^{-1}$ – Spectra collected every 30 seconds.***

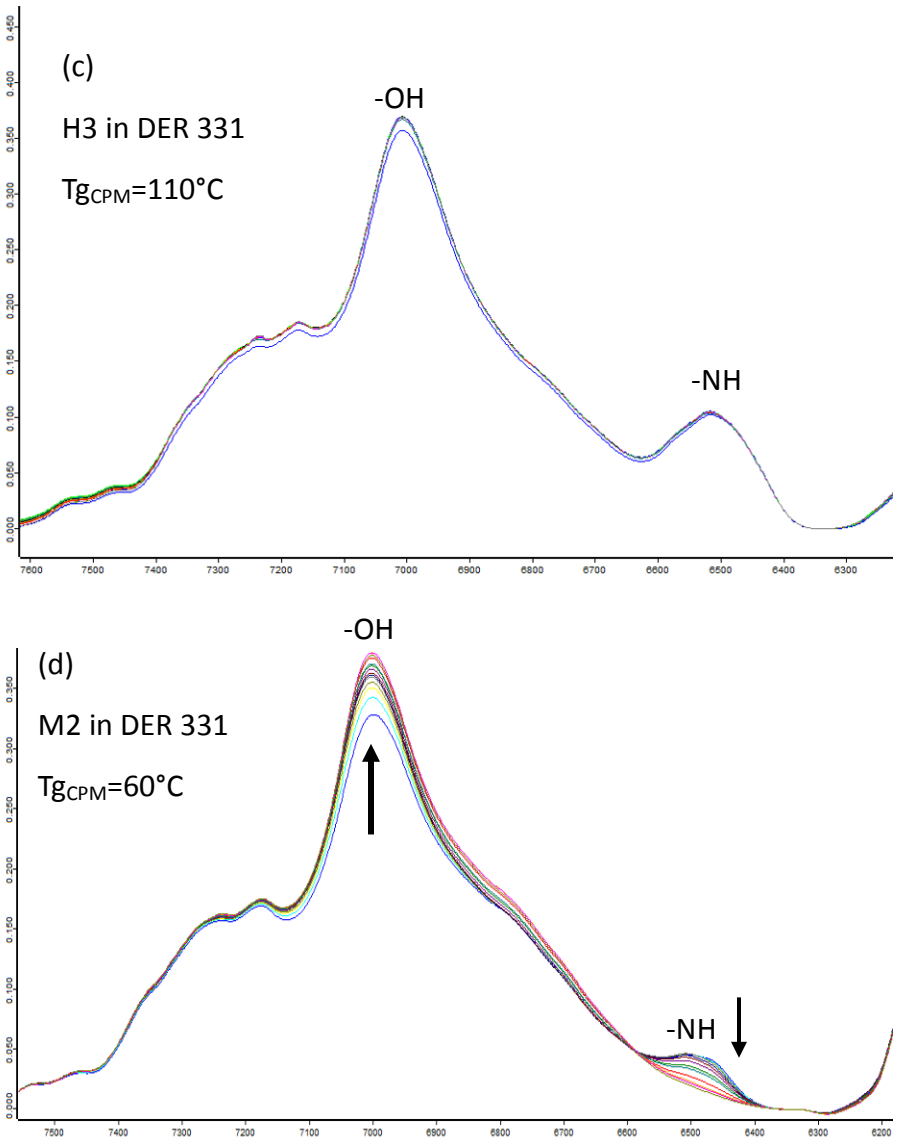


***Figure 90: NIR spectra for the dispersion of H3 (c) and M2 (d) in DER 331 heated at 80 °C during 2h. Focus on hydroxyl band 7000 cm$^{-1}$ and amine band at 6500 cm$^{-1}$ – Spectra collected every 30s.***

To summarize, it was demonstrated by DSC experiments that amino groups from high Tg and medium Tg were able to react with DER 331 when the dispersion was heated to 220°C. However, a reaction peak was observed from 80°C for the medium Tg CPM (M2) and from 100°C for the high Tg CPMs (H3). NIR experiments confirmed that no reaction between amino groups from the CPM and DER 331 occurred at 80°C for H3 and that only the amino groups born by M2 could react at that temperature.

## 6 Conclusion

Several methods were developed to highlight the presence of amino groups on the surface, but also in the CPM core. Ninhydrin assay and fluorescence confocal microscopy showed the presence and accessibility of these amino groups, whereas DSC and NIR were used to investigate in which conditions these amino groups could react with epoxy groups.

For the ninhydrin titration methods, quantitative and qualitative measurements were in agreement. A small quantity of reactive amino groups were titrated on the surface of CPMs even for an a/e ratio close to one. The measurements carried out for the CPMs with a higher a/e ratio of 1.35 and 1.5 gave relevant results corresponding to those calculated for an accessible thickness of 0.08 µm. This ninhydrin titration method gave quantitative results about the surface reactivity of the CPMs, even though these results are thought to depend on the following reaction conditions: size of probe, solvent used and temperature of the reaction. Indeed, another solvent which would better swell the CPMs should give the accessibility to a deeper layer in the CPM core.

However, by confocal fluorescence microscopy, it seems that the accessible shell thickness for the fluorophore was about 1 µm, which is thicker than the result given by the ninhydrin test (0.08 µm). This difference can be explained by the fact that it is known that the fluorescence signal is probably overestimated by the computer treatment or the strong fluorescent response. Moreover, to make the theoretical calculation, we assumed that the CPMs had a homogeneous distribution of reactive amine, which was maybe not exactly the case.

With the DSC and the NIR Infrared analyses on the dispersions of CPMs in DER 331, it has been observed that not only could the amino groups from the CPM surface react with epoxy groups but also the one into the CPM core by diffusion of DER 331. Dynamic mode in DSC and isothermal heating mode in IR showed in which conditions the reaction of amino groups could occur. CPMs need to have a lower Tg than the temperature of the reaction to be able to react with epoxy.

With all of this information, we can imagine the right conditions to have covalent bonds between the CPM and an epoxy-amine matrix for CPM filled epoxy networks. However, this study was done only in the presence of the epoxy pre-polymer without any hardener. We do not know how it could interfere with the epoxy diffusion in the CPM and/or with the reaction between the CPMs and the epoxy pre-polymer.

# IV CONTRIBUTION OF CPMS IN AN EPOXY-AMINE NETWORK – INFLUENCE OF THE PROCESS

## 1 Introduction

Once CPMs synthesis had been studied as well as their amine accessibility and reactivity, their influence as reactive fillers on the buildup of epoxy-amine networks was investigated. Indeed, there is no general rule that can be applied to predict how particular fillers may affect the kinetics of a curing system. Three different processes were used to disperse the CPMs in the epoxy-amine blend. The first process consisted of dispersing the CPMs in DGEBA before adding the amine cross-linker. The second process was the dispersion of CPMs in DGEBA with the assistance of a solvent, i.e. THF. The last process studied involved dispersing the CPMs in IPD and then adding DGEBA to synthesize the material. The influences of the three different processes were investigated on the buildup of the final thermoset network and on its properties (kinetics, morphology, thermomechanical properties).

## 2 Experimental

### 2.1 Materials

For this part of the work, higher amounts of CPM were needed in order to prepare large samples of CPM-filled networks. Therefore, a new series of CPM was synthesized. The protocol was basically similar to the one described in Chapter 2, except that the concentration of monomers was increased to 20 wt% and the volume of the dispersion was increased as well. This modified protocol allowed us to retrieve about 130 g of particles per synthesis batch. The characteristics of the synthesized particles are given in Table 26, as well as the nomenclature that will be used throughout this chapter. CPMs were named according to their glass transition temperature: the high Tg CPMs (designated H), the medium Tg CPMs (designated M) and the low Tg CPMs (designated L) which were obtained by reducing the reaction time to 3h.

This scale-up protocol gave particles with a larger diameter, but Tg remained in the same range as before. By varying the structure of the monomers, the stoichiometric ratio and the reaction time, we were able to obtain a set of particles with Tg ranging from 34°C to 138°C and different amounts of reactive amino groups; theoretically, from 0 mmol/g to greater than 1.99 mmol/g of CPM.

*Table 26: Characteristics of the synthesized CMPs*

| type of CPM | Monomers | a/e* | Tg (°C)¤ | Diameter (µm) | >NH (mmol/g) |
|---|---|---|---|---|---|
| H1 | DER331-IPD | 0.9 | 138 | 6.5 | 0 |
| H2 | DER331-IPD | 1.35 | 117 | 6.7 | 1.43 |
| H3 | DER331-IPD | 1.5 | 112 | 7 | 1.99 |
| M1 | DER662-D230 | 1.5 | 80 | 4-16 | 0.72 |
| M2 | DER331-D230 | 1.5 | 60 | 6.5 | 1.83 |
| L1[#] | DER331-IPD | 1.5 | 68 | / | >1.99 |
| L2# | DER331-D230 | 1.5 | 34 | / | >1.83 |

*: in the feed, ¤: measured 5 days after the end of synthesis (time needed to wash and dry the particles), [#]: reaction time = 3 h, #: reaction time = 3 h 30 min

CPMs were used after washing and drying, as explained in the chapter 2. However, due to these last steps, CPMs were collected as aggregates. They needed to be deagglomerated, to facilitate the dispersion. As a consequence, they were ground by hand with a pestle in a mortar before being added to the formulation.

The CPM-filled epoxy networks were prepared by the crosslinking of DGEBA, DER 331, with the isophorone diamine, IPD, in presence of CPMs. The DGEBA and IPD structures were previously presented for the synthesis of CPMs, and are shown in Table 27.

*Table 27: Epoxy and amine monomers used as the matrix for the CPM-filled epoxy networks*

| EPOXY | AMINE |
|---|---|
| DER 331 | IPD |
| 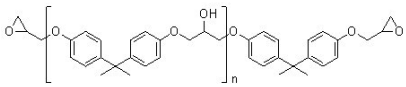 | 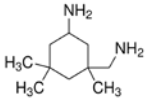 |
| Mw = 374 g.mol$^{-1}$ | Mw = 170 g.mol$^{-1}$ |

## 2.2 Processes in the manufacture of CPM-filled epoxy networks

### *2.2.1 CPM epoxy networks from the dispersion of CPMs in DGEBA*

The CPMs were dispersed in DGEBA with a high speed mechanical disperser (Rayneri 33) for 5 h from 70 to 3000 rpm. Sonication was then applied to the blend for 30 minutes. No aggregates were visible by a naked-eye examination and the dispersion was controlled by optical microscopy. A standard dispersion was typically made to obtain final epoxy-amine networks with 20 wt% CPMs. For a network at the stoichiometry a/e=1, this corresponds to a dispersion of 23.5 wt% CPMs in

DGEBA. IPD was then added to the blend to obtain the complete formulation. When the aim was to make solid samples, the blend was stirred and degassed at room temperature in a reactor for 30 min. This step could not be prolonged due to the increase in the viscosity of the blend because of the DGEBA-IPD reaction starting at room temperature. The blend was poured into a thin silicon mold and crosslinked in an oven. To monitor the buildup of the network (by chemorheology or near-infrared spectroscopy), the blend was used immediately after the addition of IPD and a very short step involving mixing and degassing by sonication. The curing cycle 2 h at 80°C followed by 2 h at 180°C allowed complete conversion [108]. Isothermal curing 2 h at 50°C, 2 h at 80°C, 2 h at 120°C and 2 h at 150°C were also performed to study partially cured samples.

### *2.2.2 CPM epoxy networks from the solvent-assisted dispersion of CPMs in tetrahydrofuran and DGEBA*

This second route was solvent-assisted. CPMs were dispersed in THF in an ultrasound bath for 1 h. DGEBA was added to the CPM/THF dispersion. The obtained mixture was stirred mechanically with a Rayneri 33 disperser, from 70 rpm to 1300 rpm for 30 min. Then, THF was removed under vacuum and continuous mechanical stirring for 3 h. IPD was then added to the epoxy dispersion. The formulation was stirred and degassed under vacuum at room temperature for 30 min as mentioned for the previous process without the solvent. Curing was done as described in section 2.2.1.

### *2.2.3 CPM epoxy networks from the dispersion of CPMs in IPD*

The CPMs were dispersed in IPD with a high speed disperser (Rayneri 33) for a few minutes. In this case, with the classic target of 20 wt% CPMs in the final material and for a matrix at stoichiometry, the CPM dispersion in IPD contained 57.5 wt% CPMs. This high level led to a very viscous or even sandy dispersion which was not easy to mix. Sonication was also applied on this dispersion for a few minutes. To make the final material, DGEBA was added as described for the previous processes, and the blend was mixed and degassed before being used. Curing was done as described in section 2.2.1.

## 2.3 Protocol for the investigation of the diffusion of monomers into the CPM core

### *2.3.1 Diffusion of a fluorescent probe into the CPM core in the presence of tetrahydrofurane*

A fluorescent dye the Alexa Fluor® 555 Hydrazide supplied by Life Technologies was chosen to label DGEBA and investigate its ability to diffuse into the CPM core in the presence of THF as the solvent. This dye bears a hydrazide group terminated with a primary amine and has a molecular weight of about 850 $g.mol^{-1}$. Its exact structure was not given by the supplier (Life Technologies)' but a similar structure is presented in Figure 91.

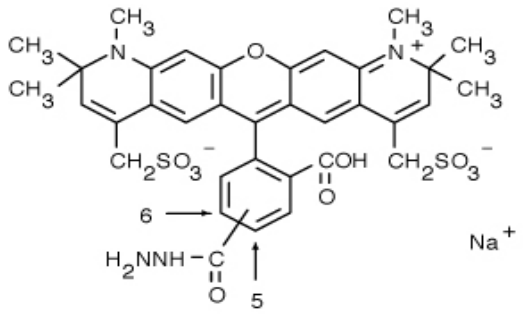


***Figure 91: Chemical structure of the one of a dye similar to Alexa Fluor® 555 Hydrazide (from Life Technologies)***

This protocol was divided into two parts. The first step consisted of the grafting of DGEBA and the second was the diffusion step (Figure 92). For the first step (a), 5 mg of the fluorescent probe was dissolved in THF and $H_20$ (90:10) and added to 30 mg of DGEBA. The solution was stirred at room temperature for 6 h to allow for the grafting of the DGEBA by the reaction between the primary amine of the probe and the epoxy group of the DGEBA. Then, for the second step (b), the solution containing the grafted DGEBA was added to 7 mg of CPM H2 at a/e=1.35. The dispersion was stirred for 30 minutes. The CPMs were then separated from the solution and washed by centrifugation five times in water. They were observed with a fluorescence confocal microscope at a wavelength of 543 nm to determine whether a fluorescent signal was detected in the CPM core, indicative of the diffusion of the grafted DGEBA.

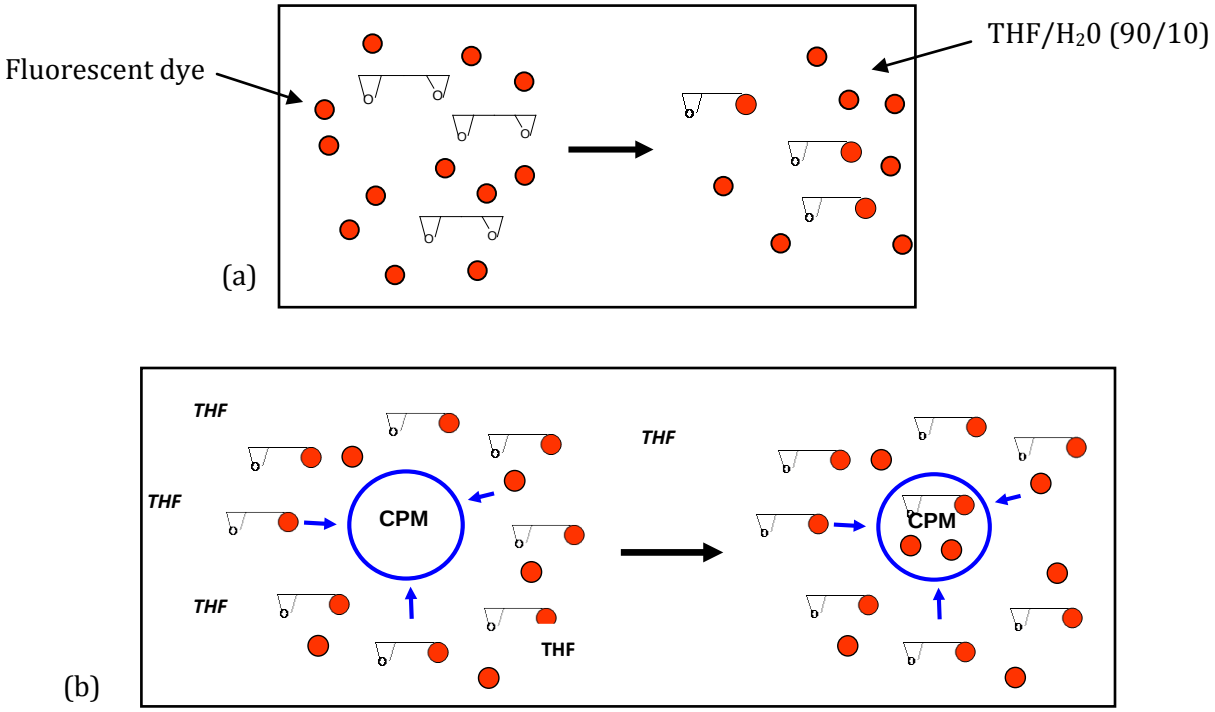


*Figure 92: Grafting of DGEBA with Alexa Fluor® 555 Hydrazide (a) and diffusion of the grafted DGEBA (b)*

### 2.3.2 CPM-filled epoxy-amine network with the use of a brominated epoxy prepolymer

DER 542, a brominated epoxy prepolymer from Dow Chemical, was used to replace DER 331. Its chemical structure is given in Figure 93. This epoxy prepolymer is solid at room temperature, and needed to be previously dissolved in THF. Same process as that described in 2.2.2 was used to disperse the CPMs, evaporate the THF and obtain the complete formulation which was then cured in an oven for 2 h at 80°C followed by 2 h at 180°C. A thin slice of the solid network was cut on a microtome to be observed by transmission electron microscopy (TEM) with X-ray microanalysis. The presence of bromine atoms in the matrix and in the particle core was compared.

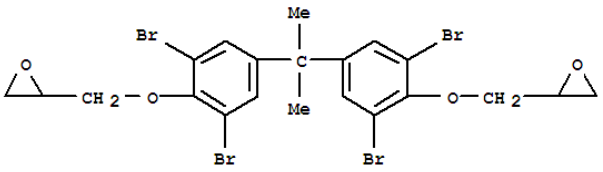


*Figure 93: Chemical structure of the brominated epoxy prepolymer DER 542*

## 2.4 Characterization techniques

### *2.4.1 DSC*

DSC was used to determine the enthalpy of the reaction during crosslinking of the CPM-filled epoxy formulations in situ cured at 80°C, and in dynamic mode. The results were compared to those obtained for the DGEBA-IPD neat network.

*Modulated DSC* was carried out in *dynamic mode* at 5°C/min from -10°C to 220°C to collect the values of the temperatures at the start ($T_{start}$), maximum ($T_{max}$) and end ($T_{end}$) of the exothermic peak of reaction, and the enthalpy of reaction, $\Delta H$. Tg was measured at the inflection point of the reversible heat flow signal, and the reaction peak was observed from the non-reversible heat flow signal. Measurements were performed with a Q200 and a Q2000 heat flux DSC from TA Instruments. Q2000 was calibrated for temperature using adamantane (-64.53°C), n-octadecane (28.24°C) and indium (156.60°C) at a scan rate of 10 °C/min. The heat flow was calibrated using the indium signal (28.71 J/g). A Tzero calibration using sapphire was done for the Q2000 instrument. Hermetically sealed low mass Tzero pans from TA Instruments were employed throughout.

The recording program was as follows:

1- Equilibrate at -10°C
2- Modulate ± 0.50 every 40 s
3- Isothermal for 5 min
4- Ramp (5 °C/min) to 220°C
5- Equilibrate at 10°C
6- Modulate ± 0.50 every 40 s
7- Isothermal for 4 min
8- Ramp (5 °C/min) to 200°C.

The first scan (step 1 to 4) allowed for curing of the sample, while the second scan (step 5 to 8) allowed for measuring the glass transition temperature ($Tg_2$). The data were analyzed using TA Universal Analysis software.

*Isothermal curing* at 80°C was carried out on a Perkin Elmer Pyris Diamond power compensation DSC with the same calibrations as described above. A very fast heating ramp was used to limit the loss of recorded enthalpy of reaction. The recording program was as follows:

1- Hold for 8 min (-10°C)
2- Heat from -10°C to 80°C at 500°C/min
3- Hold for 55 min at 80°C

After isothermal curing, a second and third scan were carried out in order to measure the glass transition temperature, $Tg_2$ (heating rate: 3°C/min) and $Tg_3$ (heating rate: 5°C/min), of the material obtained after the first and second heating step, respectively.

### *2.4.2 Chemorheology experiments*

Gelation and vitrification of the neat network (DGEBA-IPD) and CPM-filled epoxy-amine networks were monitored by rheology on an ARES rheometer at INSA from TA Instruments. It was equipped with parallel plates of 8 mm in diameter. A series of experiments were also done at Dow, on an Anton Paar rheometer (MCR 301) equipped with parallel plates with a diameter of 25mm. Results are reported in appendix. The gap between the parallel plates during the experiment was about 0.5-1 mm. The reactive blends were poured quickly on the preheated plate and a multifrequency sweep test began once target temperature was reached. Test was done at the frequency of 2, 10, and 20 rad/ s with the strain of 5%, 2% and 2% respectively. The gel time was determined according to the Winter-Chambon [109] criteria commented in the chapter 1 which highlight the independence of the damping factor ($\tan \delta = G''/G'$) to the frequency. Consequently, gel times were measured at the crossover of the tan δ, and vitrification which is frequency-dependent was taken at the max of tan δ. When it was not possible due to difficulties in measurements, the maximum of the loss modulus G'' was utilized.

### *2.4.3 Near-infrared (NIR) spectroscopy*

The NIR spectra, in the range of 4000–12000 $cm^{-1}$, were obtained in transmission mode with an FT-NIR spectrometer Bruker (Billerica, MA) Equinox 55, equipped with a tungsten halogen source, a quartz beam splitter, and an InGaAs detector. All spectra were collected with a resolution of 4 $cm^{-1}$, 32 scans per spectrum. NIR was used for monitoring the kinetics of the reaction on CPMs dispersed into DGEBA-IPD reactive formulations for isothermal measurements at 60°C and 80°C. The dispersion was poured in a glass tube (diameter =5 and 8 mm), placed in a heating cell supplied by Bruker. Measurements were also done at room temperature on solid samples, previously cured in oven. Integration under the absorption band for the epoxy conversion was given by the software OPUS from Bruker. Typical bands observed for the epoxy-amine reaction was the ones corresponding to the disappearance of the oxirane ring at 4530 $cm^{-1}$ and 6071 cm-1. A reference band corresponding to the overtone of the C-H stretching of the aromatic ring at 4623 $cm^{-1}$ was used to normalize the signal, to compare samples of different thickness and limit the impact of the changes in temperature [110].

Calculation of the epoxy conversion was done as follows [111, 112]:

$$x_{epoxy,t} = 1 - \frac{(A_{epoxy-4530})_t / (A_{ref-4623})_t}{(A_{epoxy-4530})_{t=0} / (A_{ref-4623})_{t=0}} \qquad \textit{Equation 18}$$

Equation 18 can be utilized only if the Lambert-Beer law is verified for the DGEBA i.e. the DGEBA absorbance is proportional to its concentration according to:

$$A = \log_{10}\left(\frac{I_0}{I_t}\right) = \varepsilon.b.c \qquad \textit{Equation 19}$$

Where,

A: Absorbance

$I_{0:}$ Intensity of the incident radiation

$I_{t:}$ Intensity of transmitted radiation

ε: Molar extinction coefficient ($L.mol^{-1}.cm^{-1}$)

b: Path length of radiation through the sample

c: Molar concentration ($mol.\ L^{-1}$)

Several authors already validated the Lambert-Beer law for the epoxy band at 4530 $cm^{-1}$, either using different concentration of DGEBA [Figure 94] or using DGEBAs with higher molecular weights (Figure 95). The linear response of the absorbance as a function of the DGEBA concentration for the epoxy band as well as for the reference band were shown by Poisson [113] (Figure 94).

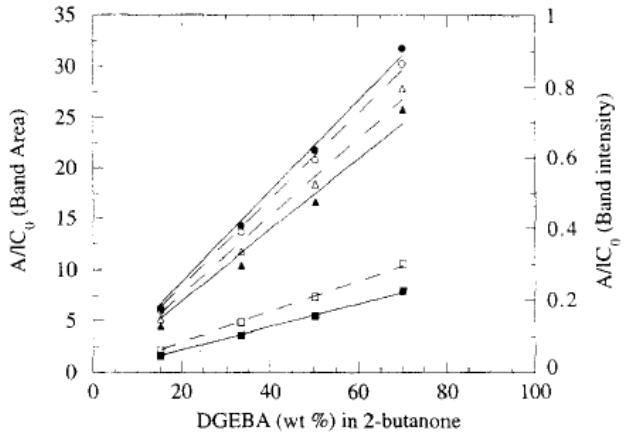


***Figure 94: Band area (–) and band intensity (---) of phenyl groups (4623 cm-1 (■, □, and 4065 cm-1 ( ● ○ and epoxy groups (4530 cm-1 ▲ △) versus weight percent of DGEBA (n=0.15) diluted in 2-butanone [113]***

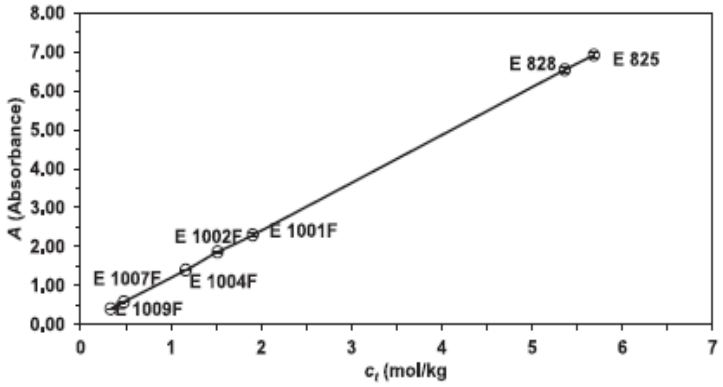


***Figure 95: NIR absorbance versus concentration of DGEBAs of different molecular weights [114]***

In some cases the signal obtained was saturated because the concentration of epoxy groups in the sample holder (glass tube) was too high. We were obliged to reduce the sample thickness by using a different sample holder (glass slides) which did not fit into the heating cell designed for glass tubes only. Therefore the spectra of some unreacted dispersions (t=0) were acquired at room temperature. The value of the absorbance was still normalized with the reference band. To be sure that this will not affect the results, the influence of the temperature on the value of the epoxy absorbance normalized with the reference band was investigated. Pure DGEBA was heated from 5°C to 80°C and the ratio $A_{epoxy}/ A_{ref}$ was plotted as a function of the temperature in Figure 96. It was measured only a deviation of 2% with an increase of the temperature from 50°C to 80°C. This deviation was considered negligible as already mentioned by Poisson [113].

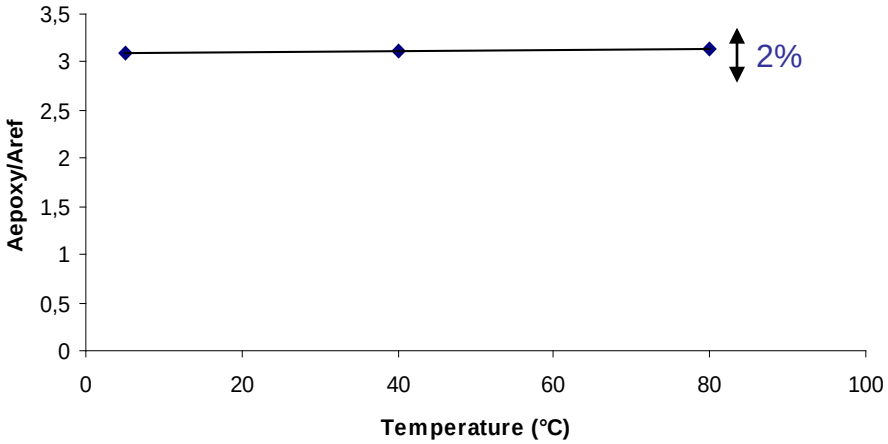


***Figure 96: Variation of the ratio: $A_{epoxy}/ A_{ref}$ for the DGEBA heated from 5°C to 80°C***

### *2.4.4 Scanning electron microscopy (SEM)*

CPM-filled epoxy networks were imaged by scanning electron microscopy. In particular the cross-sections made by freeze-fracture were observed. Freeze-fractures were made by shortly dipping free-standing epoxy films in liquid nitrogen and fracturing them manually. They were observed with a Philips XL20 once stuck on a metal stub and gold coated by sputtering. Micrographs were collected at several magnifications by typically applying a voltage of 15-20 kV. Open source software, Image J, was employed to extract the average particle diameter.

### *2.4.5 Dynamical mechanical analysis (DMA)*

The fully crosslinked filled epoxy networks were characterized by DMA. The measurements were done using either a RSA II instrument (Rheometrics) or on an ARES instrument from TA instruments. RSA was operating in tensile mode with the following experimental conditions: frequency of 1 Hz; strain of 0.01%; sample dimension about 8 to 10 mm in width, 22 to 32 mm in length and 0.3 to 1.5 mm in depth; heating rate 3°C/min, from 30 to 200°C. Storage modulus E', loss modulus E'' and loss factor tan δ were recorded during the experiment. ARES was operated in torsion mode: frequency of 1 Hz, strain of 1%, heating rate 3°C/min, from 30°C to 200°C. G', G'' and tan δ were recorded.

# 3 Results and discussion

The results are reported in the following sections according to the CPM dispersion process: in DGEBA, in THF and in IPD.

## 3.1 CPM epoxy networks from the dispersion of CPMs in DGEBA

Comments on the dispersion are given in the following paragraphs to better understand the data from the curing of complete formulations.

### *3.1.1 Stability of the CPM-DGEBA dispersion*

The stability of all CPM-DGEBA dispersions at room temperature was checked. The CPM glass transition temperature was measured after 2 weeks of storage and compared to the initial one, measured before the dispersion process in DGEBA. The results are reported in Table 28.

***Table 28: Initial Tg of CPMs and two weeks after the dispersion DGEBA***

| type of CPM | Tg (°C) of CPM | Tg (°C) of CPM dispersed in DGEBA, 2 weeks at RT |
|---|---|---|
| H1 | 138 | Not seen |
| H2 | 117 | 117 |
| H3 | 112 | 111 |
| M1 | 80 | 84 |
| M2 | 60 | 53 |
| L1# | 68 | 77 |
| L2# | 34 | 50 |

#: CPMs synthesized in 3 h -# CPMs synthesized in 3 h 30 min

Concerning the high Tg CPMs in Table 28, it is important to note that the Tg of the CPMs was not affected once they were dispersed in DGEBA. This was checked for at least a period of two weeks. This means that there was no plasticization of the CPMs by DGEBA and no diffusion of the DGEBA into the CPM core during storage at room temperature.

For the medium Tg CPMs, no influence was observed for CMP M1 and a slightly decrease in the Tg of 7°C was measured for CPM M2 once it was added to DGEBA. The network of this CPM had more mobility and could be partly plasticized. Nevertheless, this cannot be considered a significant effect.

Low Tg CPMs were synthesized by reducing the time of polymerization to 3 h and 3 h 30 min for CPM L1 and L2, respectively. In that particular case, an increase of 9°C was observed for CPM L1 and 16°C for CPM L2 between the day we collected the dry CPMs (t=5 days) and 11 days later (t=16 days), once dispersed in DER 331. These CPMs stored at room temperature were not stable due their short reaction time and the numerous residual reactive groups. They went on reacting by themselves or during the dispersion step. Thus, it is difficult to know their actual exact structure. It is possible that not only the remaining epoxy groups of the CPMs reacted with the remaining amino groups of the CPMs, but also free the epoxy groups of DGEBA. Those CPMs are possibly "hairier" than the others due to the potential branching of DGEBA on the surface.

### *3.1.2 DSC investigation*

The influence of the addition of CPMs on the dynamic and isothermal curing of DER331-IPD networks was investigated by DSC. Only the high Tg CPMs H1, H2 and H3 were used for this part of the work. 20 wt% CPMs were dispersed in the reactive epoxy-amine formulations. The DSC results obtained on CPM-filled epoxy-amine formulations are discussed. Different scenarios are presented.

**Dynamic curing of CPM-filled epoxy-amine formulations using high Tg CPMs**

The results from the dynamic scans from 0°C to 200°C on neat and CPM-filled epoxy-amine networks are given in Figure 97 and Table 29. The temperatures of reaction of all formulations are in the same range as the measurement at the maximum of the peak close to 95°C, but a decrease in the total heat released, $\Delta H_T$, was observed with the filled formulations. $\Delta H_T$ decreased as the a/e of the CPMs decreased. $\Delta H_T$ is composed of two contributions: the one from the matrix, $\Delta H_M$, and one from the CPMs, $\Delta H_{CPMs}$:

$$\Delta H_T = \Delta H_M + \Delta H_{CPMs}$$

The maximum potential contribution of the CPMs to the global heat released is reported in Table 29. It was calculated according to the results given in chapter 3 from the heat released when CPMs were dispersed in DGEBA. Also, Tgs after the dynamic curing were measured ($Tg_2$=second scan). When two separate values were measured, they were attributed to the CPMs for the lower value (this signal was very weak) and to the matrix for the highest value.

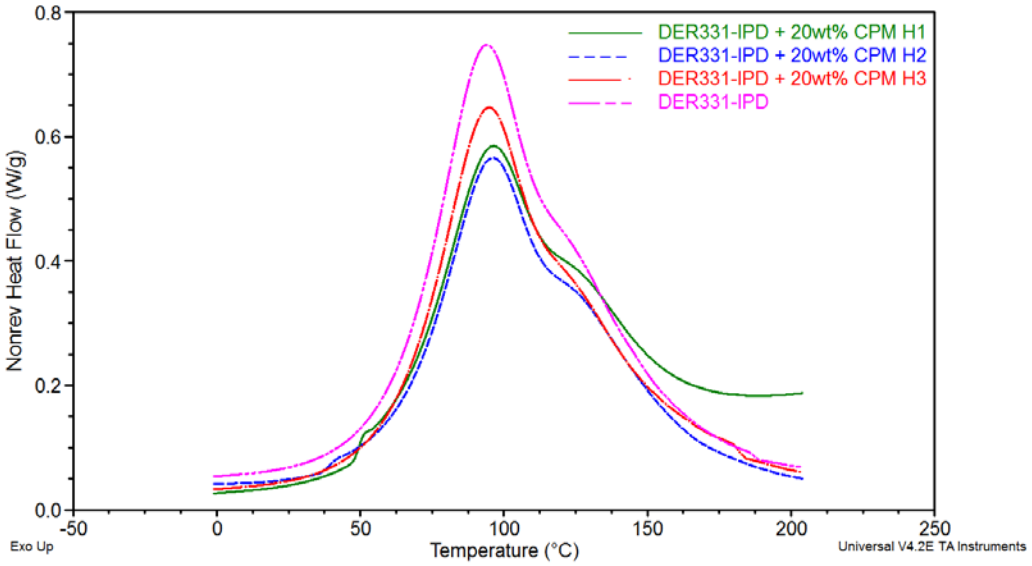


***Figure 97: Dynamic curing of filled and neat DER331-IPD networks***

***Table 29: Enthalpy of reaction in CPM-filled epoxy systems – dynamic curing - Tgs *: second scan***

| | DER331-IPD | 20 wt% CPM H1 a/e=0.9 in DER331-IPD | 20 wt% CPM H2 a/e=1.35 in DER331-IPD | 20 wt% CPM H3 a/e=1.5 in DER331-IPD |
|---|---|---|---|---|
| $\Delta H_T$ (J/g) | 460 ± 9 | 330 ± 7 | 363± 7 | 403 ± 8 |
| $\Delta H_{CPM}$ (J/g) *(max. contribution of CPMs in formulation)* | / | 7 | 25 ± 1 | 33 ± 1 |
| Tg (CPMs) | | 138 | 117 | 112 |
| $Tg_2$*(°C) | 145 | ND | 136 | 118+148 |

Two scenarios can be discussed: the first one considers what should happen if CPMs behave as inert fillers and the second one concerns the case where DGEBA diffuses into the CPMs and reactions between DGEBA and the CPMs occur.

*a) <u>The CPMs do not react and behave as inert fillers during dynamic heating in the DSC</u>*

For 20 wt% CPM-filled networks, only the matrix (80 wt% of the formulation) contributes to the reaction:

$$\Delta H_{M} = 0.8 * \Delta H_{DGEBA\text{-}IPD} = (0.8 * 460) = 368 \text{ J/g}$$

$$\Delta H_{CPM} = 0$$

$\Delta H_T = 368$ J/g

With this hypothesis, we should find a constant value close to 368 J/g for all filled formulations. This was not the case:

- For the network filled with CPM H1, $\Delta H_T = 330$ J/g was lower than the expected value. This low value could be linked to a higher concentration of CPMs than 20 wt% in the DSC pan due to the low amount of the formulation added. Indeed, a CPM content close to 28 wt% would give a $\Delta H_T$ close to 330 J/g.
- For the network filled with CPM H2, $\Delta H_T$ was close to the expected value of 80% of $\Delta H_{DGEBA/IPD.}$
- For the network filled with CPM H3, $\Delta H_T$ was higher than the expected value.

In the two first cases (H1 and H2), it appears that no significant influence of the CPMs on the enthalpy was observed. In the last case, CPM H3 certainly contributed to the reaction. In addition, if the CPMs had no effect at all, then the $Tg_2$ of the filled networks should be equal to the Tg of the neat matrix, cured under the same conditions, 145°C. However, different values were found.

*b) DER331 diffuses into the CPM core during dynamic heating in the DSC and reacts with the amino groups of the CPMs*

The diffusion of DGEBA as well as the presence of reactive amino groups into CPMs was evidenced in Chapter 3 by DSC experiments through the non-negligible enthalpy of reaction released by the CPM-DGEBA dispersion. Such diffusion may lead to the two following phenomena:

- on one hand, an epoxy defect in the matrix, i.e. an increase in a/e which becomes higher than 1. This phenomenon should not contribute to $\Delta H$ because $\Delta H$ does not vary significantly with a small increase of a/e when a/e>1 [115];

- on the other hand, the reaction of epoxy with the amino groups from the CPMs. This will contribute to $\Delta H_T$ and $\Delta H_{CPM}$; the maximum contribution was reported in Table 29.

Another point to consider is that in a ternary blend, DGEBA+IPD+CPM, the diffusion of DGEBA in the CPM is now in competition with the reaction with IPD which starts at room temperature.

Let us examine the effect of each type of CPM:

- **CPM H1** does not theoretically bear amino groups because it was synthesized with an excess of DGEBA in the feed (a/e = 0.9).

However no epoxy groups were detected by NIR spectroscopy and the titration with ninhydrin and DSC highlighted the presence of a low quantity of amino groups. The real stoichiometry of CPM H1 is slightly above 1, but these CPMs are the least reactive of the series. Here, it appears that the diffusion of DGEBA cannot be proven and, regardless, it did not impact the overall behavior.

- For **CPM H2**, the maximum contribution of the CPM to $\Delta H_T$ is 25 J/g. So, the contribution of the matrix should be:

$$\Delta H_M = \Delta H_T - \Delta H_{CPM\ H2} = 363 - 25 = 338\ J/g$$

Therefore, the minimum contribution of the matrix $\Delta H_M$ is about 73% (338/460) as compared to a neat system. This value is a bit low. Some amino groups on the CPMs may take part in the reaction, but less than in the dispersion of CPMs in DGEBA without IPD. This means that the contribution of CPMs to $\Delta H_T$ has been overestimated, i.e. it should be lower than 25 J/g.

- For **CPM H3**, the maximum contribution of the CPMs to $\Delta H_T$ is about 33 J/g. So. the contribution of the matrix should be:

$$\Delta H_M = \Delta H_T - \Delta H_{CPM\ H3} = 403 - 33 = 370\ J/g$$

The value is equal to 80 % of $\Delta H_{DGEBA\text{-}IPD}$ (370/460). This value seems to be in agreement with this scenario.

Therefore, given the value of enthalpy measured, the most realistic scenario for CPM H3 dispersed into a DGEBA/IPD system is that it participates in the reaction during heating in the DSC pan. It means that DGEBA was able to diffuse into the particle core (scenario 2). It is more difficult to conclude in the case of CPM H2; it seems that it did not participate to the reaction (scenario 1). It could be also that the diffusion of DGEBA into the particle core is more difficult because the crosslink density is higher.

**Isothermal curing**

Same formulations with 20 wt% CPMs (H1, H2 and H3) were cured in isothermal mode at 80°C. Values of the heat released at 80°C ($\Delta H_{80°C}$) and its comparison to the neat network are reported in Table 30. This isothermal curing was followed by a temperature ramp in order to obtain $Tg_2$ and to post-cure the material. Then this scan was followed by another scan to obtain the Tg of the post-cured networks ($Tg_3$).

- The enthalpy of reaction obtained with the neat network, 390 J/g, can be used to calculate the conversion, x, reached by the network after isothermal curing at 80°C, $x = 1 - \Delta H_{80} / \Delta H_{dyn} = 85\ \%$ ($\Delta H_{dyn} = 460$ J/g, ).
- Values of ΔH for the filled systems were found to be significantly lower than the value for the neat system. ΔH of the formulations containing CPMs H2 and H3 were identical and slightly higher than the one measured with CPM H1 (as for the dynamic scan). If the reactions in the filled network occurred as in the neat network, and if the CPMs do not participate to the reaction (scenario 1), then we should have obtained the same enthalpy for all filled networks, equal to 80% of $\Delta H_{DER331/IPD\text{-}80°C}$, so 0.8 * 390 = 312 J/g. This is clearly not the case. So, there is an influence of the CPMs on the enthalpy of the reaction since lower values were obtained.
- Additional information came from the values of $Tg_2$ and $Tg_3$. The values of $Tg_2$ on the filled networks (91-98°C), which correspond to the Tg of the system after 1 h at 80°C in the DSC pan, were in the same range as the neat network ($Tg_2$=98°C) cured under the same conditions. The values of $Tg_3$ for the filled systems were always lower than $Tg_3$ of the neat system. In the case of CPM H3, two separated Tgs were observed: at a lower temperature, the Tg of the CPMs and at a higher temperature, the Tg of the matrix (as in the previous dynamic experiment).

***Table 30: Enthalpy of the reaction $\Delta H_{80}$ measured by DSC (isotherm at 80°C) for neat and filled DER331-IPD networks – $Tg_2$: measured at 3°C/min – $Tg_3$: measured at 5°C/min.***

| | $\Delta H_{80}$ (J/g) | $\Delta H_{filled\ system\text{-}80} / \Delta H_{DER331/IPD\text{-}80} * 100$ | $Tg_2$ (°C) (second scan) | $Tg_3$(°C) (third scan) |
|---|---|---|---|---|
| DER331/IPD | 390 | 100 | 98 | 157 |
| 20wt% CPM H1 a/e=0.9 in DER331-IPD | 230 | 59 | 91 | 147 |
| 20wt% CPM H2 a/e=1.35 in DER331-IPD | 254 | 65 | 98 | 136 |
| 20wt% CPM H3 a/e=1.5 in DER331-IPD | 252 | 65 | 97 | 120+152 |

The isothermal DSC experiments, followed by dynamic scans, are difficult to interpret without ambiguity, but some trends can be deduced.

One possible explanation for the low values of ΔH in the filled networks is that the reaction did not proceed as in the neat system, and reached a lower conversion ($59 < x < 74$ %, Table 30), as if the

CPMs hindered the reaction. This explanation seems unrealistic and is not coherent with the fact that the glass transition temperatures of these partially cured filled networks, $Tg_2$, are close to that of the neat network. If the conversion was significantly lower, then $Tg_2$ should be lower too. However care must be taken with the interpretation of these values: in some cases (H2 and H3), the Tg of the CPMs are close to the expected Tg of the partially cured matrix (~98°C) and the signal may result from two contributions, the one of the CPMs and the one from the matrix.

Another explanation is that some monomers diffuse into the CPM during heating the reactive formulation at 80°C. The matrix becomes off-stoichiometric, but this should not decrease the value of $\Delta H$ [115]. So, the low values of $\Delta H_{80}$ remain unexplained. The CPMs do not react with the infused monomer (DGEBA) under these curing conditions, at T=80°C, because they are below their Tg and amino groups have no mobility.

Finally, the eventual diffusion of DGEBA into the CPMs should have an effect on the Tg of the fully cured filled networks. Indeed, as shown in Table 30, it appears that there is a trend toward a lower Tg for the filled networks as compared to the neat matrix (Tg = 157°C). The transitions were broad because the transitions of the CPMs and of the matrix are may be close or overlaid.

In the ternary blend (DGEBA + IPD + CPM), as soon as the temperature was increased, two phenomena occurred: the main one was the reaction of DGEBA with IPD, while the other was the diffusion of DGEBA into the particle. Then, if the temperature was high enough, i.e. higher than the glass transition temperature of the CPMs (T > 100°C in the case considered here), the amino groups from the CPMs reacted with the epoxy groups in DGEBA. The consequence of DGEBA diffusion is an increase in the stoichiometric ratio of the matrix which becomes higher than 1, and a decrease in the stoichiometric ratio of the CPM as compared to its initial value.

CPMs added to a reactive formulation of DER331-IPD contributed to the global epoxy-amine reaction during dynamic curing of the CPMs with the highest a/e of 1.5 (CPM H3). The right conditions for DGEBA diffusion and the reaction were met. However, with an intermediate a/e of 1.35 (H2), the values indicated that either the CPMs did not participate in the reaction or did to such a minor extent that it was in the range of error of the experiment.

Concerning isothermal curing at 80°C, CPMs did not contribute to the epoxy-amine reaction based on the measured $\Delta H_{80}$ and also on the temperature of the reaction between amino groups of the CPMs and epoxy groups (T > 100°C for the dispersion of CPMs in DER331; see chapter 3).

Therefore, CPMs cannot be considered to be inert fillers, even if they do not react with the epoxy. They become active fillers when the right conditions are met. These conclusions, related to DGEBA diffusion, came from indirect measurements made via DSC. The real proof of DGEBA diffusion could be made by developing specific, direct measurements. The difficulty in this study is that the same monomers are involved in the matrix and in the CPMs. We needed to provide contrast between the matrix and the CPMs, in order to observe the diffusion of DGEBA into the CPMs, for example, by DGEBA labeling. This task is described in paragraph 3.2.3 of this chapter.

### *3.1.3 Chemorheology*

The purpose of this study was to explore the ability of the CPMs to modify the gel and vitrification time of DGEBA-IPD networks. Chemorheology was used to monitor the storage modulus G' and the loss modulus G'' of the CPM-filled epoxy formulation cured isothermally at 80°C. The damping factor tan δ = G''/ G' was plotted as function of the reaction time for the multifrequency tests to determine gel and vitrification time. An example of an obtained curve is given in Figure 98.

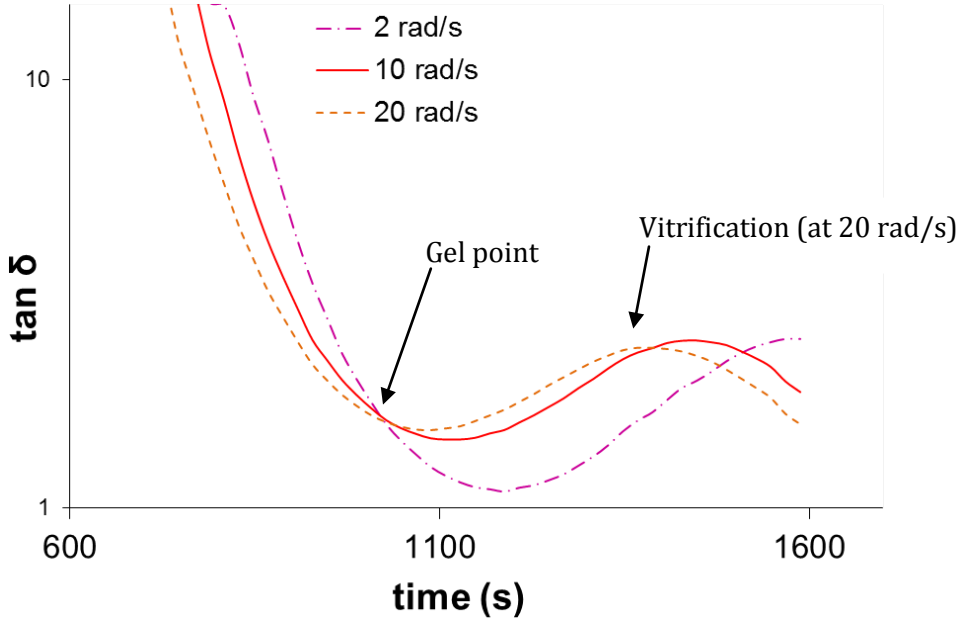


***Figure 98: Tan δ as a function of the time for DGEBA-IPD network crosslinked at 80°C and at 2, 10 and 20 rad/s***

***Neat matrix***

A preliminary study of the influence of the stoichiometric ratio of a neat DGEBA-IPD network on the gel time was carried out. Gel times were plotted as a function of the stoichiometric ratio of DGEBA-IPD blends (Figure 99). As it was reported in the literature and commented on in chapter 1 [116], a decrease in gel time was observed with an increase in the stoichiometric ratio. It is this behavior that was exploited here with the addition of CPMs bearing amino groups to investigate the possible changes in the gelation phenomenon.

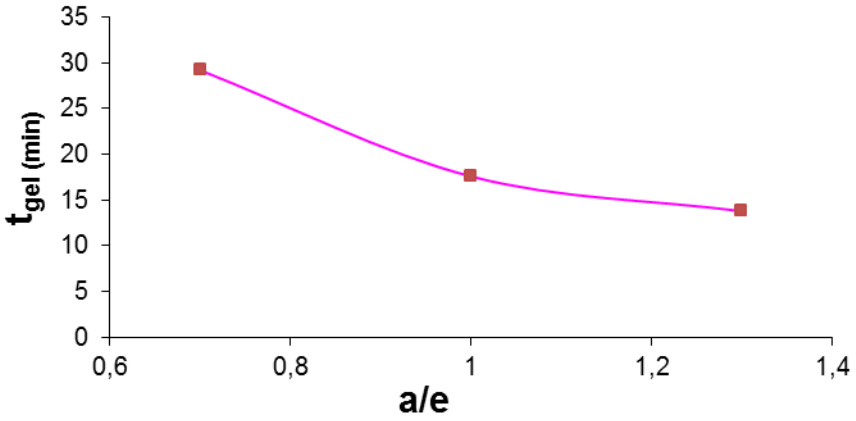


***Figure 99: Experimental values of gel times at 80°C for DGEBA-IPD network as a function of the stoichiometric ratio a/e***

***Influence of the Tg of the CPMs***

A pertinent question is whether the Winter-Chambon criterion for gelation [14] would be applicable for the epoxy formulations in the presence of added fillers. Previous studies in the laboratory on silica-filled epoxy networks or sepiolite-filled epoxy networks showed that this criterion can be applied [117, 118]. As a consequence, the influence of the different types of CPM (H, M or L) on gelation and vitrification times was investigated by chemorheology. The results are given in Table 31.

For each set of experiments, the neat matrix was tested again because the experiments were not done at the same time of year. This is the reason why slightly different gel times are reported for the neat matrix. This difference may be linked to small differences in the oven temperature. In all cases the differences were, at maximum of 1 minute. The high Tg CPMs (H1 and H2) led to a very slight increase of gel time. The results for the experiments done with the medium Tg CPMs (M1 and M2) are also given. This time, a very slight decrease in gel time was observed. This was probably

due to the higher mobility of the CPM structure which allowed amino groups to react with the epoxy groups of the matrix. It was shown in the chapter 3 that with these CPMs, diffusion and reaction of DGEBA into the CPM core was possible at 80°C, and this is what happened in this case. However, there was also a competition between the IPD not yet incorporated into a dense network or into the CPMs. It is easier for DGEBA to react with free IPD rather than with the amino groups on the CPMs. Concerning the last CPMs synthesized, the low Tg CPMs, it was shown that they were not stable during storage and the dispersion step, and consequently did not remain as low Tg CPMs but became medium Tg CPMs. Moreover, due to their unknown exact structure, it is difficult to explain their influence on network buildup. CPM L1 seemed to shorten the gel and vitrification times whereas CPM L2 seemed to delay them, which would be in agreement with the formation of "hairy CPMs" without remaining amino groups but with remaining epoxy groups, as discussed in section 3.1.2.

***Table 31: Gel/vitrification times, 80°C – Addition of High Tg CPMs***

| | **Neat matrix DER331-IPD** | **CPM-filled network (20 wt% H2, H3)** |
|---|---|---|
| Gel time (min) | 16.2 | 17-17.5 |
| Vitrification time max G''-20 rad/s (min) | 18.7 | 19.2-19.4 |
| | | **(20wt% M1, M2)** |
| Gel time (min) | 17.6 +/-0.7 | 16.5-16.8 |
| | | **( 20 wt% L1, L2)** |
| Gel time (min) | 17.6 +/- 0.7 | 16.2-18.2 |
| Vitrification max tan δ 20 rad/s (min) | 23.5 | 21.7-25.3 |

### 3.1.4 Kinetics by NIR spectroscopy

The influence of the addition of CPMs on the buildup of the epoxy networks was investigated by monitoring the epoxy conversion of the CPM-filled epoxy networks by NIR spectroscopy. The crosslinking of the filled formulations with 20 wt% H3 and M2 was done at 80°C. No epoxy groups were detected in the CPMs, as reported in chapter 3, and the epoxy conversion measured is that of the matrix. The evolution of the spectrum of the DGEBA-IPD system reacting for 2 h at 80°C from 4400 to 7600 $cm^{-1}$ is given in Figure 100. It shows the formation of hydroxyl groups at 7000 $cm^{-1}$, the disappearance of the epoxy groups (4530 and 6072 $cm^{-1}$), the disappearance of primary amines (4920 $cm^{-1}$), and primary + secondary amines (6515 $cm^{-1}$). The two bands quoted for the epoxy groups can be used for quantitative measurements. However, preliminary tests highlighted the overestimation of the conversion using the band at 6072 $cm^{-1}$. As a consequence, conversion will be calculated from the absorbance of the band at 4530 $cm^{-1}$, called band 1. The focus on the epoxy band 1 (4530 $cm^{-1}$) and the band used as a reference (4623 $cm^{-1}$) is reported in Figure 101.

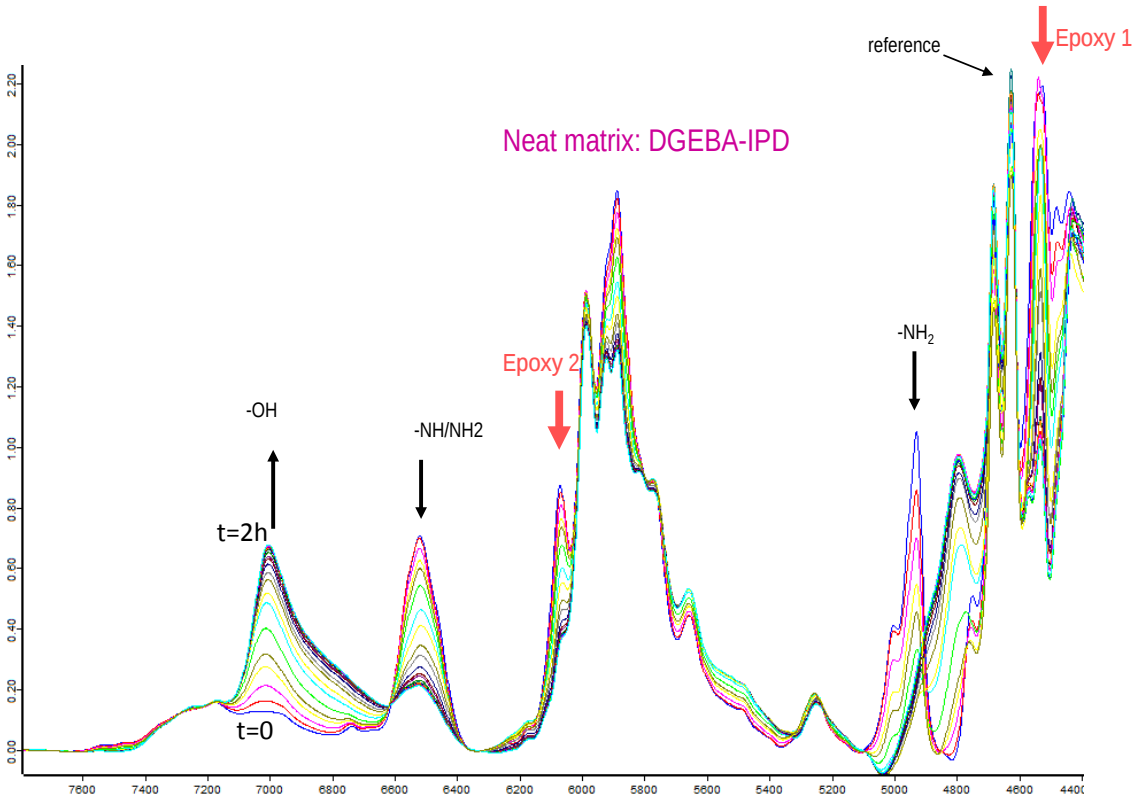


***Figure 100: Main bands observed by NIR for the DGEBA-IPD system***

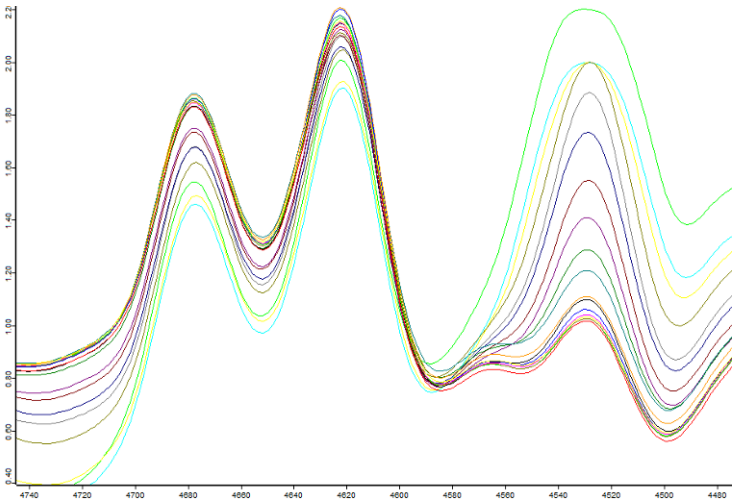

***Figure 101: Focus on the epoxy band at 4530 $cm^{-1}$ and the reference band at 4623 $cm^{-1}$ for the DGEBA-IPD system at 80°C***

The conversion of the epoxy groups from the matrix was plotted for the neat matrix DER331-IPD and the filled systems with 20 wt% CPM M2 and H3 (Figure 102) cured at 80°C for 2 h. The conversion of the neat system was repeated several times and was found to be reproducible. A plateau was reached after about 40 minutes of reaction for the neat system and the one filled with CPM M2 and after 30 minutes for the system filled with H3. This slowing down of the reaction rate was attributed to the vitrification phenomenon. These values are higher than the one measured by chemorheology, which is not surprising due to the use of a different method. The final conversion of the neat matrix was about 85%, which is in agreement with the DSC results in section 3.1.2, giving an enthalpy of the reaction of 390 J/g for the neat matrix cured isothermally at 80°C (Table 30: 390/460 =85%). The Tg value of the sample cured by DSC (Tg = 98°C) is also in agreement with this conversion using the Di Benedetto model for the DER331-IPD system at the stoichiometry. Indeed, the Di Benedetto equation was plotted for the DER331-IPD system from the DSC results and is reported in Figure 103. A Tg of 98°C corresponds to a conversion about 82%, still in agreement with the value obtained by NIR.

For the systems filled with CPM H3 and M2, the final conversion reached was increased by 8% compared to the neat matrix and measured at about 93%. This increase due to the addition of the CPMs was not expected for CPM H3. Indeed, the dispersion of CPM H3 in DER 331 did not show any reaction between the CPMs and the DER 331 when it was heated to 80°C (chapter 3). Here, the same results were obtained with the high Tg CPM H3 and the medium Tg CPM M2 which have a similar quantity of theoretical amino groups, but not the same Tg (112°C and 60°C, respectively) and different behavior once dispersed in DGEBA. The addition of the IPD seemed to change the

behavior of the CPMs during curing, potentially by enhancing diffusion phenomena, decreasing the viscosity, or by plasticizing effects.

Another possible explanation of the increase in epoxy conversion would be a catalytic effect of secondary and tertiary amines from the CPMs. Due to their cross-linked structures, CPMs also bear many tertiary amines, known to catalyze epoxy-amine reactions and to initiate the anionic chain homopolymerization of epoxy [119]. A combination of stepwise and chainwise polymerizations can occur. As a consequence, assumptions made to calculate theoretical conversion at gelation are not required anymore, as conversion at gelation is modified.

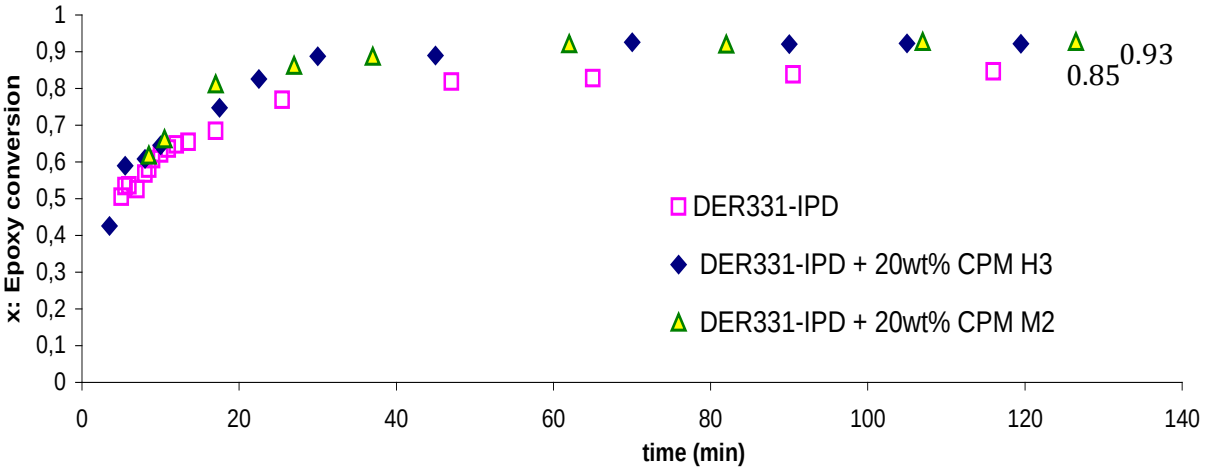


***Figure 102: In situ measurements of epoxy conversion of the matrix of CPM-filled epoxy networks crosslinked at 80°C measured by NIR***

***Table 32: DSC data obtained to plot the Di Benedetto equation, 10°C/min***

| $Tg_0$( °C) | $Tg_\infty$ (°C) | $\Delta Cp_0$ | $\Delta Cp_\infty$ | λ |
|---|---|---|---|---|
| -23 | 155 | 0,56 | 0,28 | 0.50 |

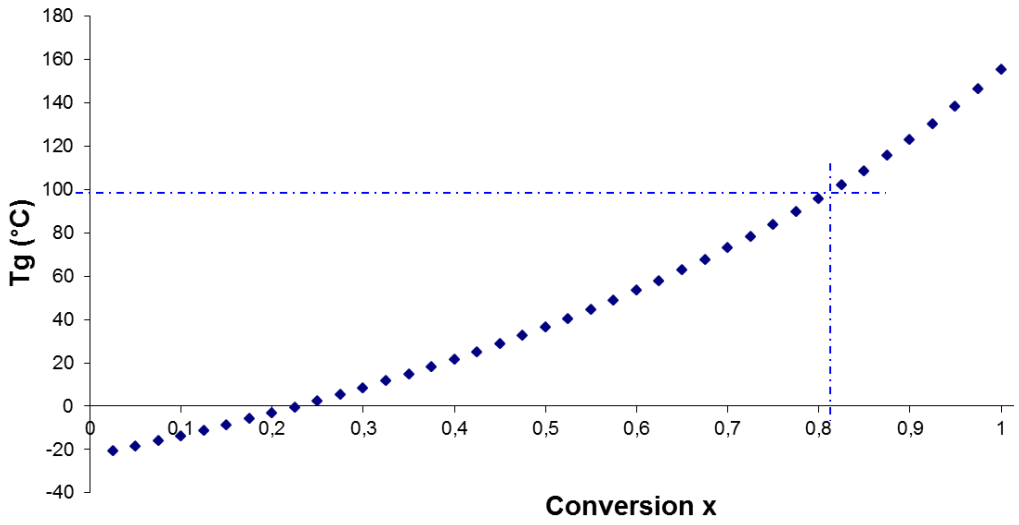


***Figure 103: Di Benedetto equation for the DER 331-IPD system, a/e=1***

The same systems were also monitored by NIR at 60°C. Similar trends were observed at 60°C as at 80°C. An increase in conversion was observed with the addition of the CPMs. Results are reported in the Appendix. The increased conversion values measured with the addition of the CPMs need to be taken into account carefully due to an accuracy of 5%, plus the difficulty in measuring the right absorbance. Indeed, the epoxy band does not have a perfect baseline and a small band overlaps it slightly.

### *3.1.5 Conversion after isothermal curing*

CPM-filled epoxy networks were cured isothermally in an oven at 50, 80, 120, and 150°C for 2 h. The final epoxy conversion was also measured by NIR spectroscopy after 2 h of curing. The results are reported in Figure 104. No significant difference was observed in the epoxy conversion of CPM-filled epoxy networks compared to the neat matrix. As expected a progressive conversion from 77% to 100% was measured when the temperature increased from 50°C to 120°C. At high conversion, this technique is not very sensitive.

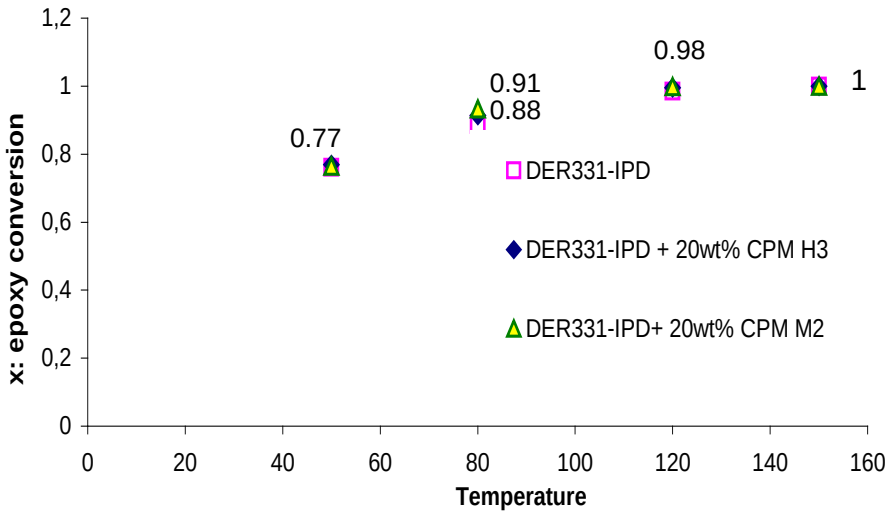


***Figure 104: Epoxy conversion of the matrix of CPM-filled epoxy networks crosslinked for 2 h at 50°C, 80°C, 120°C, 150°C in an oven and measured by NIR at room temperature***

### *3.1.6 Morphology*

The influence of the addition of CPMs was investigated on the morphology of the networks. As a consequence, cross-sections of networks made from the dispersion of 20 wt% high Tg CPMs and medium Tg CPMs were observed by SEM.

First, *the influence of the stoichiometry of high Tg CPMs* was explored by the addition of H1, H2 and H3 (see Table 33). The first observation was that the CPMs were well-dispersed and well-embedded in the epoxy-amine matrix. The fracture occurred across the CPMs which meant that there was a strong CPM/matrix interface. Covalent bonds between CPMs and the matrix occurred for the three different stoichiometric ratios, even for the CPM synthesized with an excess of epoxy. Also, the diffusion of DGEBA and IPD may have helped with the embedding of the CPMs in the matrix. No significant influence of the stoichiometry of the high Tg CPMs was observed on the morphology of the CPM-filled epoxy-amine networks.

***Table 33: SEM images of cross-section by cold fracture of CPM H3 (20 wt%) filled epoxy-amine networks – a/e $_{matrix}$ = 1 – Curing step: 2 h 80°C + 2 h 180°C***

| H1<br>a/e= 0.9 | H2<br>a/e= 1.35 | H3<br>a/e= 1.5 |
|---|---|---|
| 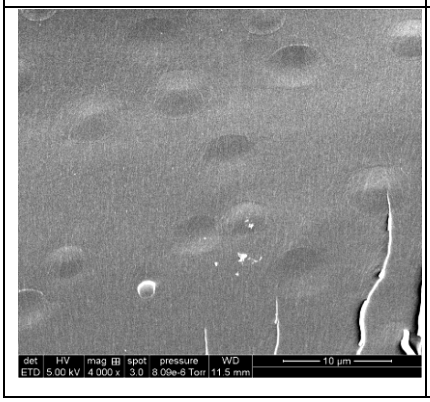 | 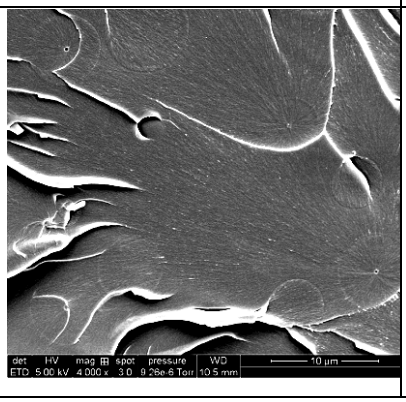 | 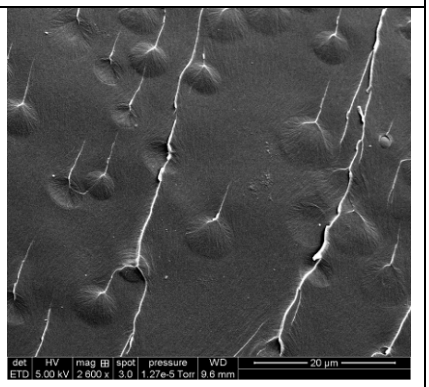 |

Also, *the influence of the Tg of the CPMs* and of *the curing temperature* on the CPM-filled epoxy-amine network morphology was explored. For that, fracture surface of networks made with the addition of H3 and M1 and M2 and cured in isothermal conditions for 2 h at 50, 80, 120 and 150°C were observed. The impact of the curing cycle on the morphology was observed by SEM; the data are summarized in Table 34. Similar behavior was observed for the three types of CPMs dispersed: H3, M1 and M2. Indeed they were all synthesized with an a/e=1.5, which conferred high amount of amino groups able to make covalent bonds at the interphase. For the networks crosslinked for 2 h at 50°C, numerous debondings of the CPMs were observed after fracture. By increasing the temperature, progressively improved embedding of the CPMs in the matrix was observed, leading to a difficult distinction from the matrix at 120°C and 150°C.

Concerning the morphology, there was no influence of the Tg of the CPMs. Fully cured networks always showed embedded CPMs. This was observed for direct crosslinking at 150°C and also with the two-step curing process combining 2 h at 80°C and 2 h at 180°C for CPM H3.

***Table 34: SEM images of cross-sections by cold fracture of CPM-filled epoxy networks – Influence of the use of 20 wt% H3, M1 and M2 in a matrix a/e= 1 – Influence of the curing temperature***

| | 2 h @ 50°C | 2 h @ 80°C | 2 h @ 120°C | 2 h @ 150°C | 2 h @ 80°C + 2h 180°C |
|---|---|---|---|---|---|
| H3 | 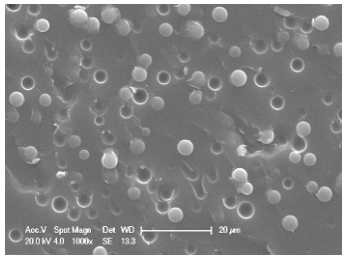 | 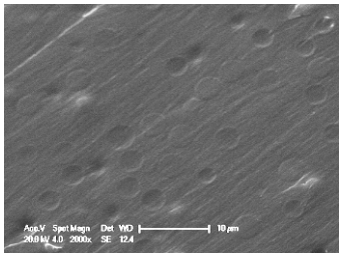 | 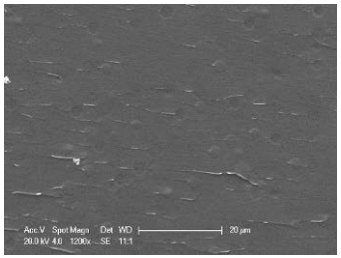 | / | 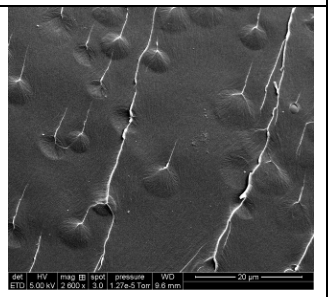 |
| M1 | 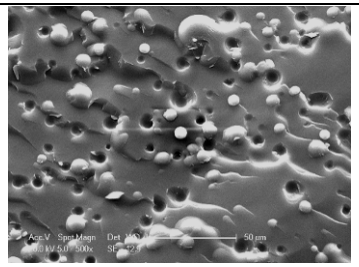 | 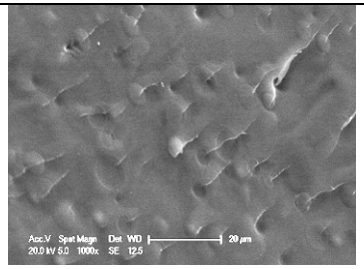 | 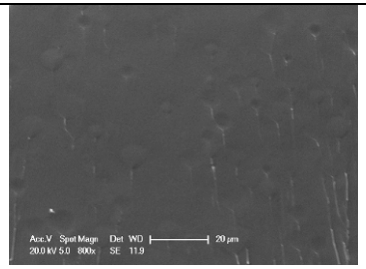 | 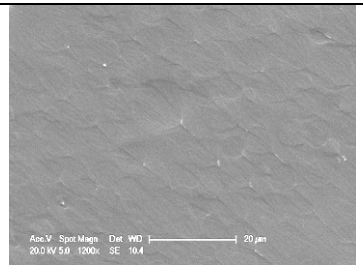 | / |
| M2 |  | 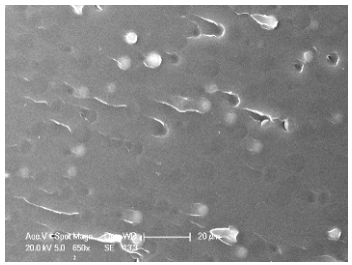 | 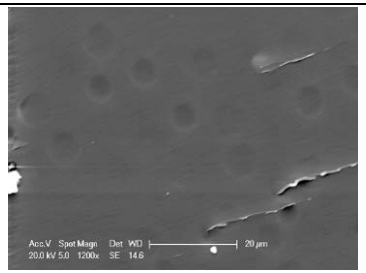 | 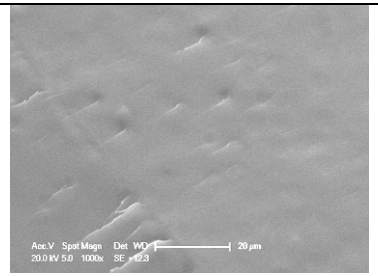 | / |

### *3.1.7 Dynamic solid state properties: DMA*

Networks were synthesized at two different stoichiometric ratios of the matrix: a/e = 1 and a/e = 0.7. Synthesizing DGEBA-IPD networks with a/e=1 allows for obtaining the maximum Tg of the network. A ratio of 0.7 corresponds to an excess of epoxy groups: Tg is decreased, which allows the separation of the α transition of the high Tg CPMs and that of the matrix. The networks synthesized with the two ratios were analyzed by dynamic mechanical analysis recording the loss and storage modulus. The results are reported in the following paragraphs.

***Epoxy-amine matrix with a stoichiometric ratio of 1***

*The influence of the stoichiometry of the CPMs.*

20 wt% high Tg CPMs were dispersed in a DGEBA-IPD mix with an a/e = 1. Networks were obtained after a curing at 80°C (2 h) followed by 180°C (2 h). As shown in Figure 105, the damping factor tan δ was plotted for all networks. The main α relaxation temperature (Tα) was observed close to 150°C, which corresponds to the Tα of the matrix. For the CPM-filled networks, the relaxation of the CPMs was visible with a low intensity and at low temperatures, from 100°C.

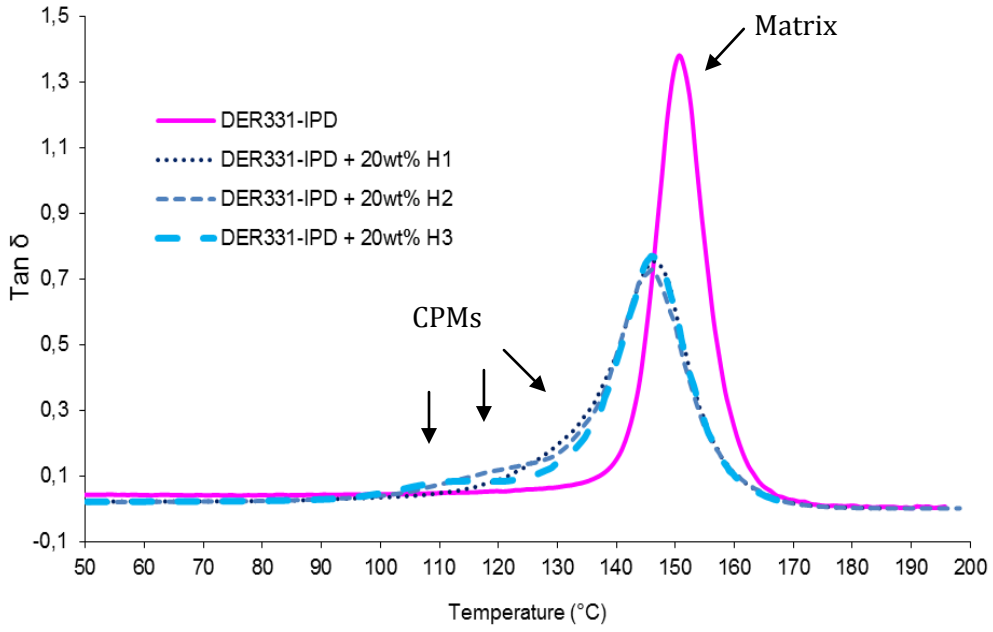


Figure 105: Tan δ as a function of the temperature for DER331-IPD (RSA rheometer) and DER331-IPD with 20 wt% H1, H2 and H3 (ARES rheometer)- $a/e_{matrix} = 1$

The addition of 20 wt% CPMs slightly decreased the Tα of the matrix of the filled networks of 5°C (from 151°C to 146°C). All filled networks had the same Tα of the matrix. Its amplitude decreased

compared to the neat matrix due to the diminished quantity of matrix and became broader with the addition of CPMs. The width of the relaxation peak at mid-height, ΔTα, increased with the addition of CPMs (Table 35). ΔTα of the neat network was about 10°C, whereas with 20 wt% CPMs, it increased to 15°C. No influence of stoechiometry and therefore the Tg of the CPMs was observed.

***Table 35: Tα and ΔTα for DER31-IPD and DER331-IPD + 20wt% H1, or H2 or H3***

| | Tα (°C) | ΔTα (°C) |
|---|---|---|
| DER331-IPD | 151 | 10 |
| DER331-IPD + 20wt% H1 | 146 | 15 |
| DER331-IPD + 20wt% H2 | 145 | 15 |
| DER331-IPD + 20wt% H3 | 146 | 13 |

*The influence of the Tg of CPMs (a/e=1.5) added in epoxy networks* was investigated on the solid state properties after different steps of isothermal curing of the networks. Curing was done for 2 h at 80°C, 120°C and 150°C. DMA obtained for the networks made with the addition of 20 wt% CPM H3 and M2 are reported in Figure 106. The first graph on left corresponds to the networks cured at 80°C and shows very broad Tα. The transition started as the network reached its curing temperature of 80°C and post-curing consequently occurred at the same time as the analysis. Therefore, it is difficult to make conclusions on the properties of the networks. After 2 h at 120°C, the Tα of the CPMs was visible and separated from that of the matrix. $T\alpha_{matrix}$ increased with the addition of the CPM M2 (which had a lower Tg) to 137°C compared to 131°C for the neat matrix. The Tα of the CPM M2 was observed at 90°C, whereas its Tg measured by DSC was at about 60°C. Probably, the DGEBA diffused into the CPMs to react with the remaining amino groups and increased their crosslink density. After curing at 150°C, the Tα peak of the matrix was narrower with still a very slight increase when CPM M2 was used. The storage modulus G' was also plotted. A slight increase at the rubbery plateau was observed after adding CPM M2 compared to the neat system. With CPM H3, the rubbery modulus was decreased.

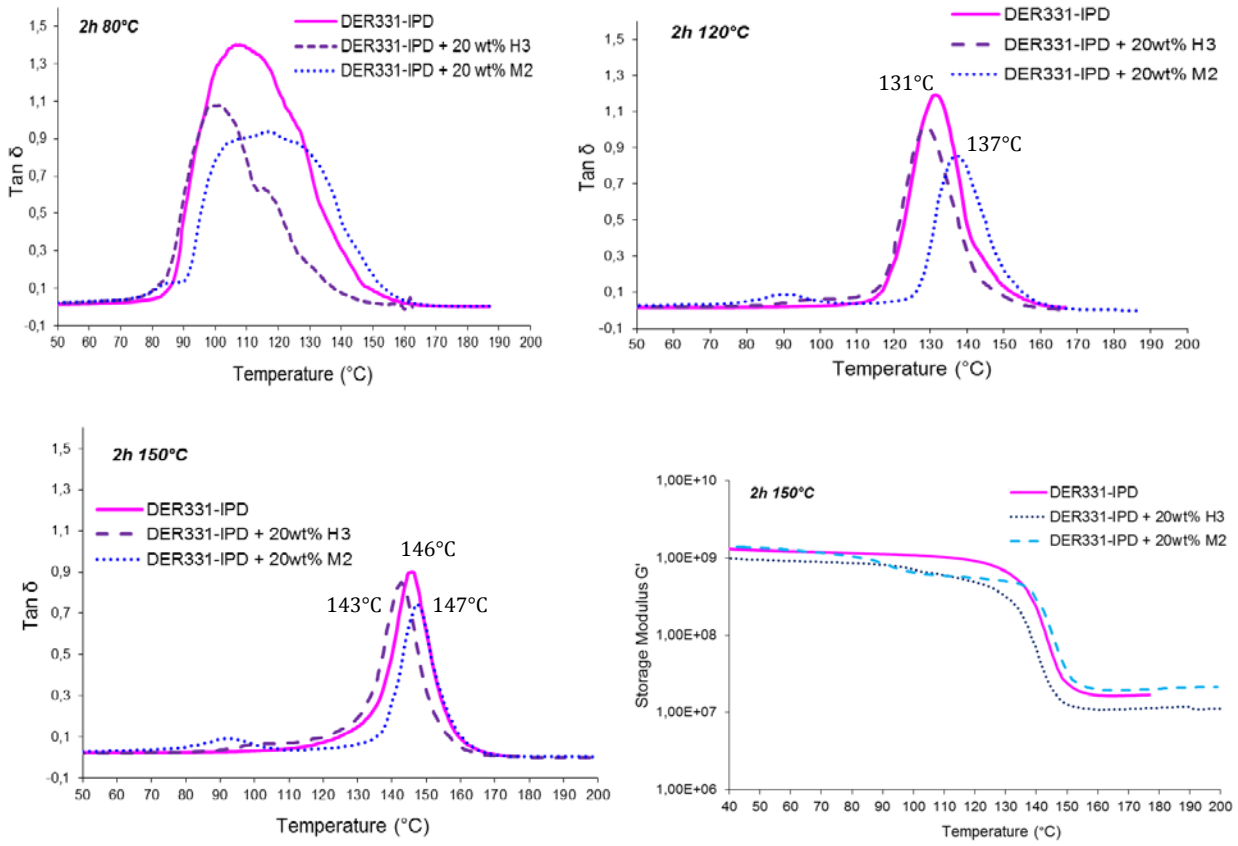


***Figure 106: Tan δ and storage modulus G' as a function of the temperature for DER331-IPD and DER331-IPD with 20 wt% H3 and M2– $a/e_{matrix}$ = 1 – Isothermally cured for 2 h at 80°C, 120°C and 150°C***

## ***Epoxy-amine matrix with a stoichiometric ratio of 0.7***

20 wt% CPM H3 was added to an epoxy-amine matrix with an a/e = 0.7. The DMA of the network obtained and cured for 2 h at 80°C and 2 h at 180°C is reported in Figure 107 and compared to the neat network. With a stoichiometric ratio of a/e = 0.7, the Tα of the matrix was about 96°C. With the addition of 20 wt% CPM H3, the Tα shifted to a higher temperature and broadened. The Tα of the CPMs was observed at about 155°C. This temperature corresponds to the stoichiometric ratio of 1 for the DGEBA-IPD network and not to that of the introduced CPMs (close to 1.5). This means that the networks of the CPMs developed an increased crosslink density by the reaction with the epoxy groups from DGEBA of the matrix. DGEBA diffused into CPM H3 and modified its structure, leading to a CPM network close to stoichiometry. The matrix also lost some DGEBA, which led to an increase in a/e and consequently an increase in Tg.

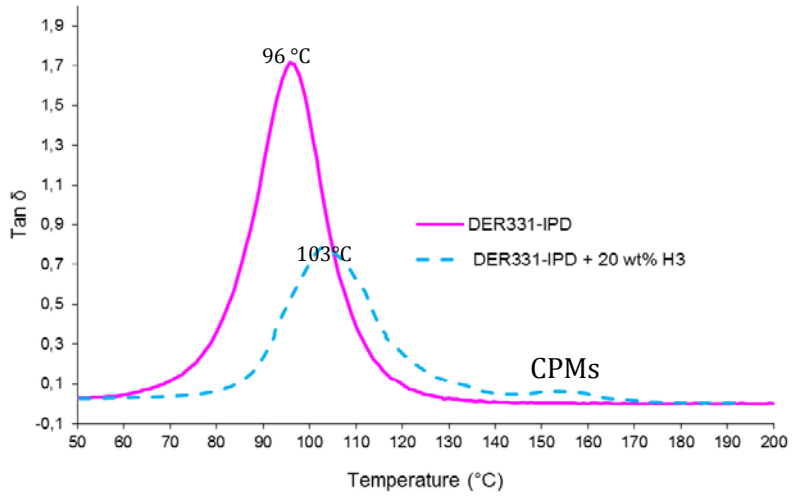


***Figure 107: Tan δ as a function of the temperature for DER331-IPD and DER331-IPD with 20 wt% H3 – $a/e_{matrix}$ = 0.7***

#### *3.1.8 Conclusions*

The influence of the addition of CPMs by a dispersion process in DGEBA without a solvent was investigated based on the buildup of the network, its morphology and its dynamic solid state properties. DSC experiments revealed the influence of CPM H3 with a higher stoichiometric ratio on the global reaction of the network during dynamic heating. With DSC experiments, it was also concluded that the high Tg CPMs were probably not able to react at 80°C due to their lack of mobility. On the contrary, the opposite behavior was observed by NIR, where a higher epoxy conversion was measured for the filled systems cross-linked at 80°C. Also, the DMA experiment highlighted the influence of the use of CPMs, which always modify the glass transition temperature of the matrix for a fully cross-linked network. This is certainly due to the diffusion phenomenon of DGEBA into the CPMs, which changes the stoichiometry of the matrix as well as that of the CPMs.

### 3.2 CPM epoxy networks from the solvent-assisted dispersion of CPMs in tetrahydrofuran and DGEBA

#### *3.2.1 Morphology*

The morphology of the networks obtained from the dispersion of the CPMs in DGEBA assisted by THF was observed by SEM. The matrix, with a stoichiometric ratio of 0.7 and 1, and CPMs of

different stoichiometric ratios were used to make CPM-filled epoxy-amine networks. All the networks were cured for 2 h at 80°C followed by 2 h at 180°C.

***Epoxy-amine matrix with a stoichiometric ratio of 0.7***

For this series of samples, 10 wt% CPMs H1, H2 and H3 were added to an epoxy-amine formulation whose stoichiometric ratio was a/e=0.7, i.e. a matrix with an excess of epoxy. SEM images of the fracture of the networks are shown in Table 36. The surface was rough and particles were well-dispersed in the matrix, independently of their stoichiometric ratio. The fracture did not occur across the particles as was previously observed in filled networks prepared via the dispersion of CPMs into DGEBA (Table 13 and 14); here, the fracture occurred in the matrix. The particles were obstacles to crack propagation, which was deflected. Some holes were also observed due to a debonding process; however, not all the particles were debonded. It can be established from literature that particles can induce shear yielding by facilitating a change in stress state. This may result in the formation of voids and debonding effects at the crack tip [120]. The number of debonded particles did not show any clear trends related to the stoichiometry of the particles, in other words, with the functionality or Tg of the particles, if we looked to a larger number of micrographs.

THF helped with the dispersion and embedding of the CPMs thanks to facilitated diffusion of the monomers, but this also created defects when there were traces of solvent remaining in the network.

***Table 36: 10 wt% high Tg CPM H1, H2, H3 in epoxy-amine formulation a/e $_{matrix}$ = 0.7***

| CPM H1- a/e=0.9 | CPM H2 – a/e = 1.35 | CPM H3 – a/e = 1.5 |
|---|---|---|
| 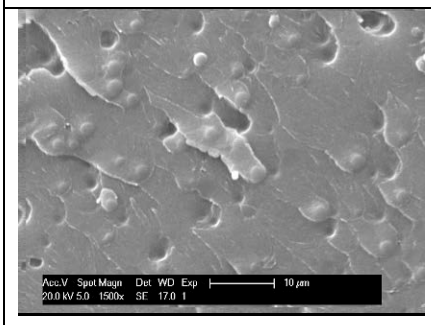 | 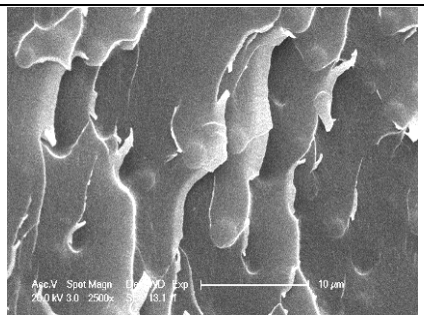 | 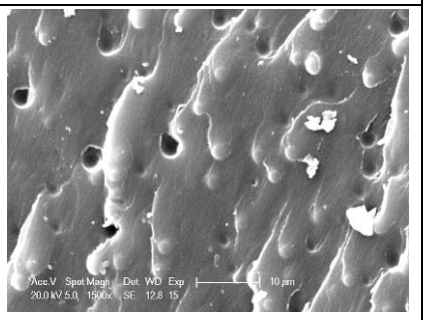 |

***Epoxy-amine matrix with a stoichiometric ratio of 1***

Examples of the morphologies of cross-sections of the filled networks obtained by the dispersion of 10 wt% CPMs in an epoxy-amine matrix at a stoichiometric ratio equal to 1; the data are summarized in Table 37. A very rough surface was observed for the network filled with CPMs having an a/e = 1.05, with stick-slip features. The debonding/embedding of the CPMs in the matrix

was not so obvious in these cases, and perfect embedding of the CPMs was not observed here. The dispersion process with THF did not seem very reproducible and led to different fracture mechanisms.

***Table 37: 10 wt% high Tg CPM in an epoxy-amine formulation with a/e $_{matrix}$ = 1***

| CPM a/e = 1.05 | CPM H2 - a/e = 1.35 |
|---|---|
| 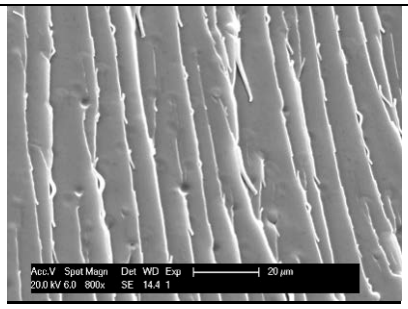 | 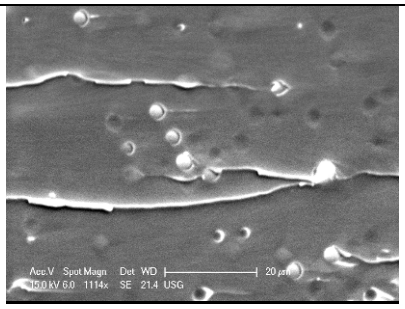 |

### *3.2.2 Solid state properties*

The influence of the addition of high Tg CPMs in two matrices with stoichiometric ratios of 0.7 and 1 was investigated by dynamic mechanical analysis. The results are presented in the following paragraphs.

***<u>Epoxy-amine matrix with a stoichiometric ratio of 1</u>***

The variation of tanδ as a function of temperature for the networks filled with 10 wt% H2 and 20 wt% H3, and for the neat matrix, is reported in Figure 108. The curves show a decrease in the temperature at the maximum of the peak, Tα, of the matrix by adding 10 wt% H2 or 20% H3 in the formulation (Table 38). In addition, the heterogeneity of the material increased with the addition of CPM H3. The glass transition temperature of the CPMs was not detected here and was probably hidden by the peak of the matrix. The decrease in Tα is again explained by an increase in the stoichiometric ratio of the matrix, initially equal to 1, due to the diffusion of DGEBA into the CPMs. The effect was more pronounced if the network was filled with 20 wt% CPMs. The use of THF to disperse CPMs probably modifies the behavior of DGEBA. CPMs were swollen by the solvent, which also decreased the viscosity of the medium, leading to better diffusion of DGEBA into the CPMs.

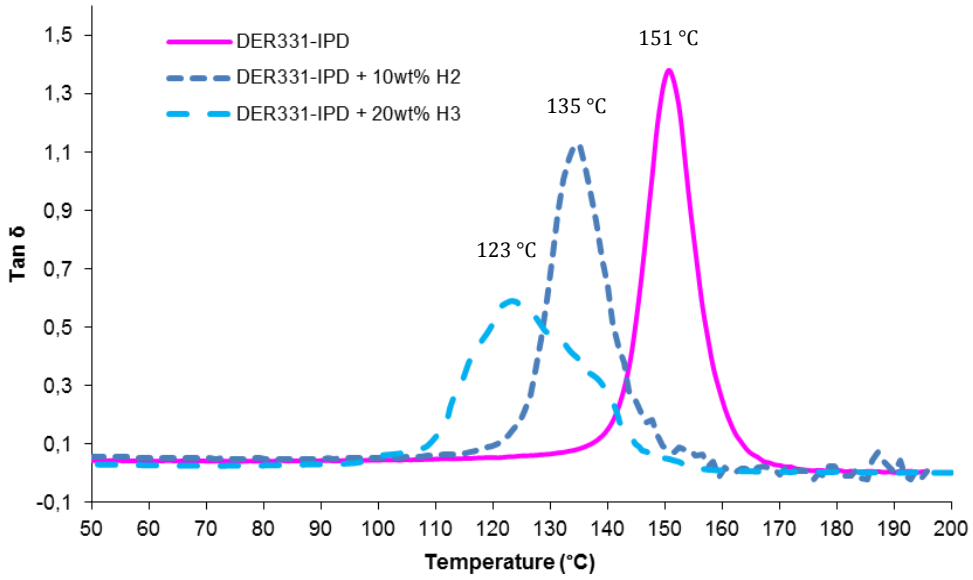


***Figure 108: Tan δ as a function of the temperature for DER331-IPD and DER331-IPD with 10 wt% CPM H2 and 20 wt% H3 – $a/e_{matrix}$ = 1***

***Table 38: Tα and ΔTα for DER331-IPD and DER331-IPD + 10 wt% H2 and 20 wt% H3 - $a/e_{matrix}$ = 1***

| | Tα (°C) | ΔTα (°C) |
|---|---|---|
| DER331-IPD | 151 | 10 |
| DER331-IPD + 10wt% H2 | 135 | 10 |
| DER331-IPD + 20wt% H3 | 123 | 26 |

***Epoxy-amine matrix with a stoichiometric ratio of 0.7***

As already mentioned for the dispersion process without a solvent, using a stoichiometric ratio off-stoichiometry helps to separate the Tα of the CPMs from that of the matrix.

*The influence of the addition of* 10 and 20 wt% *CPM H1* to the DGEBA-IPD network ($a/e_{matrix}$ = 0.7) on the dynamic mechanical properties of the final materials was investigated. The variation of tan δ as a function of temperature is reported in Figure 109. The addition of CPM H1 led to a progressive shift in the Tα of the matrix, from 96°C for the neat matrix, to higher temperatures, i.e. 103°C and 112°C for the 10 wt% and 20 wt% filled networks, respectively. Simultaneously, a progressive decrease in the amplitude of Tα was observed, explained by the increased amount of CPMs added. The Tα of the CPMs was more obvious in the network filled with 20 wt% CPMs at a temperature close to 143°C, which is close to the Tα of the CPMs (cf. chapter 2). CPM H1 (a/e=0.9) bears only a

few amino groups, as shown in Chapter 3. DGEBA probably diffused into the CPMs during the dispersion process, which changed the matrix stoichiometry, i.e. it was higher than 0.7. As a consequence, its Tα increased. Not all epoxy groups from the DGEBA that had diffused can react with the amino groups from CPMs due to their low functionality. Therefore, a kind of plasticization of the CPMs by the unreacted or partially reacted DGEBA may have occurred, which prevented these CPMs from obtaining the maximum Tα, which was observed in Figure 107 at about 155°C.

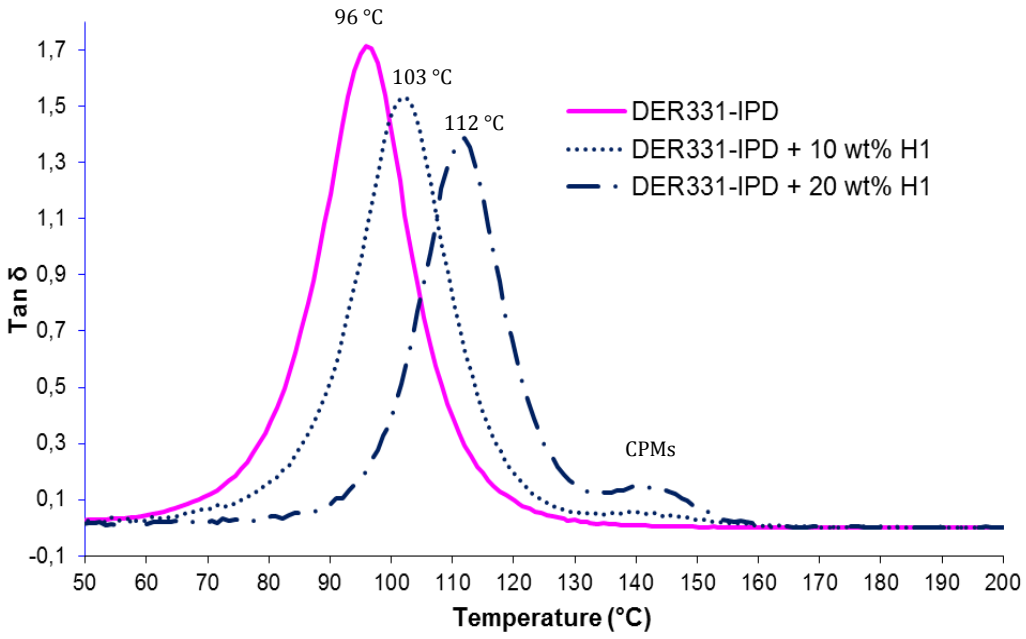


***Figure 109: Tan δ as a function of the temperature for DER331-IPD and DER331-IPD with 10, 20 wt% CPM H1– $a/e_{matrix}$ = 0.7***

The influence of the stoichiometric ratio of the CPMs on the dynamic mechanical properties of networks filled with 10 wt% CPMs was investigated. The results are plotted in Figure 110, 110 and 111. The variation in tan δ (Figure 110) as a function of temperature shows that there was also a shift in the Tα of the matrix. This shift to higher temperatures (Table 39) is emphasized with the increase in the stoichiometric ratio of the CPMs. With the addition of 10 wt% H1 (a/e=0.9), Tα was increased by 7°C compared to the neat system, with 10 wt% H2 (a/e=1.35), Tα was increased by 13°C, and with 10 wt% H3 (a/e=1.5) it was increased by 22°C. The increase in the stoichiometric ratio of the CPMs corresponded to a decrease in Tg, a lower crosslinking density and an increase in the remaining amino groups. Thus, the diffusion of DGEBA was facilitated and more epoxy groups from DGEBA could react, thereby shifting the glass transition of the matrix because its stoichiometric ratio became higher than 0.7.

A zoom of the region of the glass transition of the CPMs is given in Figure 111. It shows that all Tα of the CPMs were between 140°C and 160°C. H2 and H3 had a Tα close 155°C, whereas their original Tg was about 117°C and 112°C, respectively. This means that their stoichiometric ratio changed to reach a stoichiometric ratio close to 1. This is only possible by the diffusion of DGEBA into the CPM core during the process and its reaction with residual amino groups from the CPMs. Because it is visible by DMA, it is not only a phenomenon occuring at the surface of the particles, and it even occurs inside the CPMs. This confirms conclusions drawn in previous chapters. Thus, the diffusion of monomers during the dispersion process using THF was studied to validate this hypothesis. The results are presented in the next section (3.2.3).

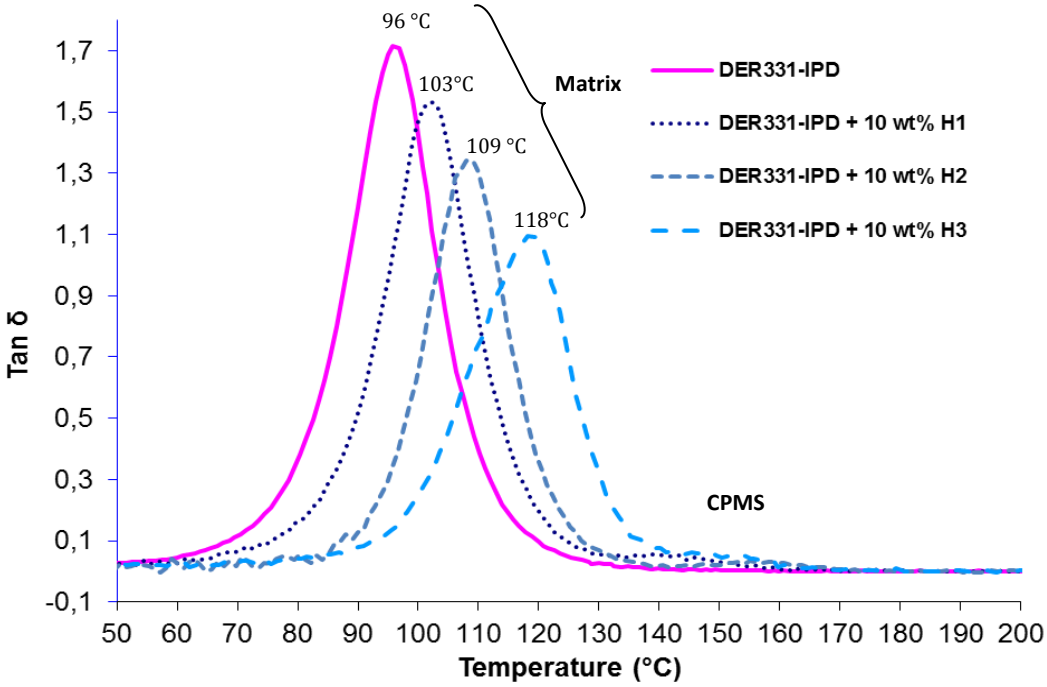


***Figure 110: Tan δ as a function of the temperature for DER331-IPD and DER331-IPD with 10 wt% H1, H2 and H3 – $a/e_{matrix}$ = 0.7***

***Table 39: Tα and ΔTα for DER331-IPD and DER331-IPD + 10 wt% H1, H2, H3***

| | Tα (°C) | ΔTα (°C) | $E_R'$ (MPa) |
|---|---|---|---|
| DER331-IPD | 96 | 25 | $7.2\ 10^6$ |
| DER331-IPD + 10wt% H1 | 103 | 23 | $9.8\ 10^6$ |
| DER331-IPD + 10wt% H2 | 109 | 16 | $1.22\ 10^7$ |
| DER331-IPD + 10wt% H3 | 118 | 19 | $8.8\ 10^6$ |

The storage modulus E' was also plotted to compare the value at the rubbery plateau. A slight increase in the rubbery modulus was observed with the addition of the three types of high Tg CPMs

(Table 39), but without an evident trend related to the stoichiometry or functionality of the particles. Nevertheless, the increase in the rubbery modulus in all filled networks is an indirect indication that CPMs were linked to the surrounding matrix and acted as an additional multifunctional crosslinker.

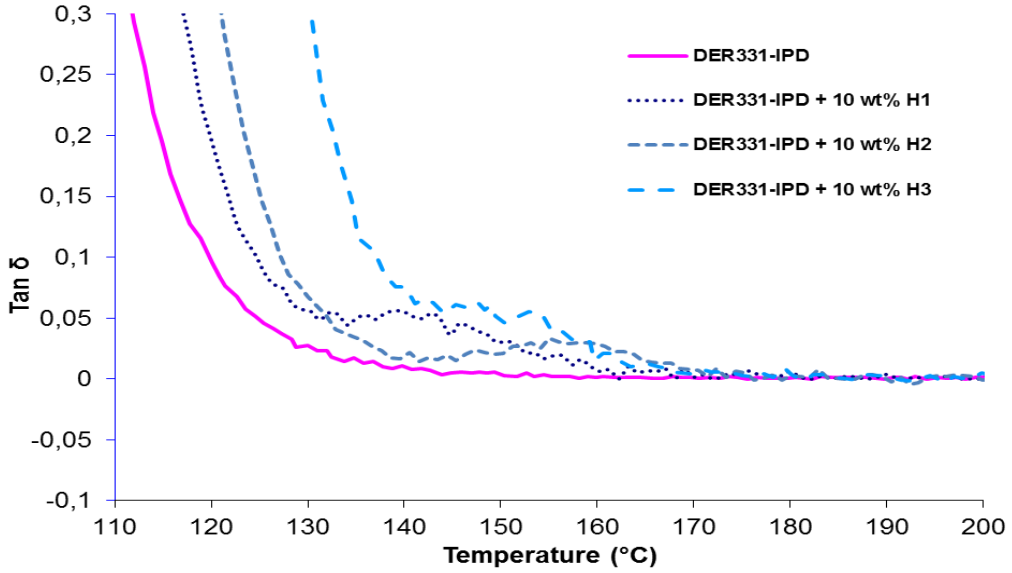


***Figure 111: Zoom of Figure 110 of the Tα of the CPMs***

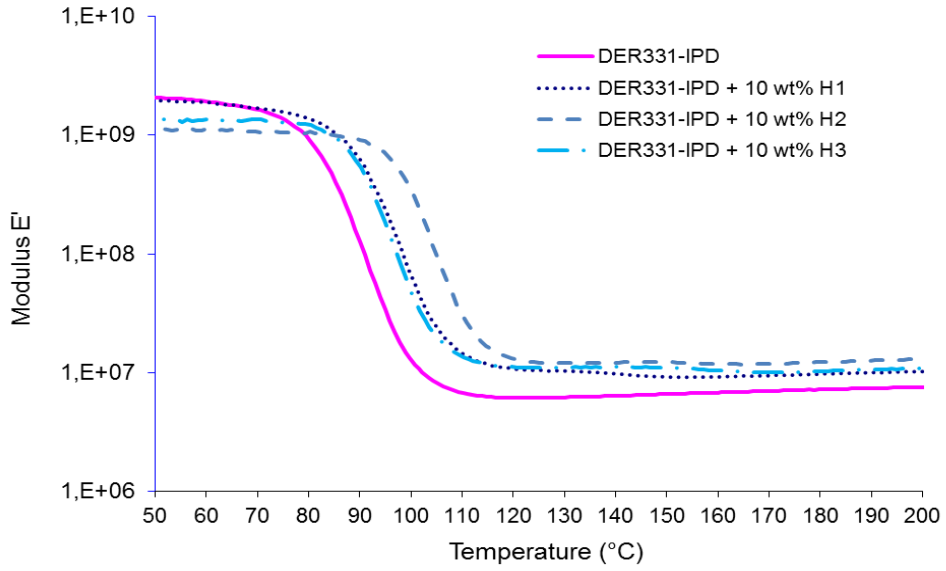


***Figure 112: Storage modulus E' as a function of the temperature for DER331-IPD and DER331-IPD with 10 wt% H1, H2 and H3 – $a/e_{matrix}$ = 0.7***

The influence of the temperature of the post-curing step was also investigated; for that, 10 wt% CPM H1 was dispersed in an epoxy-amine formulation ($a/e_{matrix}$=0.7), then cured for 2 h at 80°C, followed by a different post-curing step (PC) of 2 h at either 120°C, 150°C, or at the standard temperature of 180°C. Tan δ as a function of temperature for the three types of networks is plotted in Figure 113, as well as for the neat matrix. The post-curing step at 120°C and 150°C led to a glass transition temperature inferior to that of the same network post-cured at 180°C. This can be explained by incomplete curing of the two first samples. However, it was interesting to note that the filled network post-cured at 150°C had about the same glass transition temperature, Tα = 93 °C, as the unfilled matrix post-cured at 180 °C, Tα = 96 °C, which was fully cured.

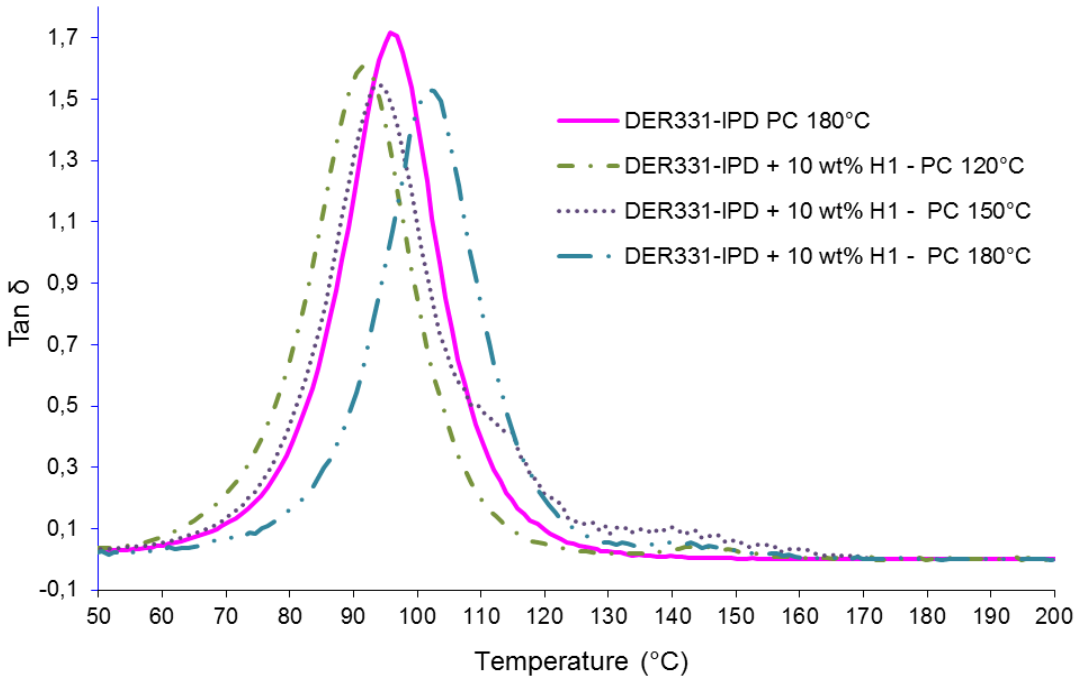


***Figure 113: Tan δ as a function of the temperature for CPM-filled epoxy networks with 10 wt% CPM H1 cured for 2 h at 80°C + post-curing (PC) for 2 h at 120°C, 150°C and 180°C – $a/e_{matrix}$ = 0.7***

### *3.2.3 Study of the diffusion of monomers into CPM during the process*

To validate the assumption of the diffusion phenomenon of the monomers (DGEBA and/or IPD) into the CPM core during the dispersion process assisted by THF, two specific experiments were carried out. The first one consisted of fluorescently labeling DGEBA followed by microscopic observation of the CPM core to verify the presence or absence of fluorescence. The second experiment involved making a CPM-filled epoxy network with brominated DGEBA and then checking for the presence of bromine atoms in the CPM core.

***Validation of the diffusion of DGEBA by fluorescence***

DGEBA was labeled by the reaction of epoxy with a primary amine terminated fluorescent probe, the Alexa Fluor® 555 Hydrazide. Then, the CPMs were dispersed into this modified DGEBA in the presence of THF. The type of CPM chosen was the reference CPM H2 (a/e= 1.35). Fluorescence confocal microscopic observation of the CPMs was performed after they were washed and separated from the DGEBA solution. Examples of images are shown in Figure 114. The spherical CPMs were not exactly in the same focal plane, which is why circles of different sizes are seen. The small diameters correspond to a section in the upper part of the CPMs, while for the maximum diameters, the central part of the CPMs was observed. For all CPMs, red fluorescence was detected everywhere in the particle core and not only at the periphery of the CPMs, meaning that the diffusion of labeled DGEBA occurred in the whole CPM and even in the CPM core. This experiment demonstrated that using THF during the CPM dispersion process leads to the diffusion of DGEBA into the CPM core.

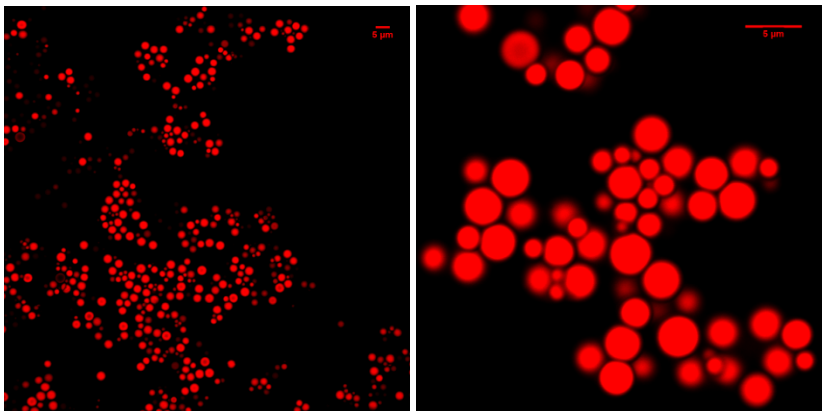

***Figure 114: Fluorescence confocal microscopy images of the CPMs a/e=1.35, 24 h of polymerization, after 30 min of stirring with labeled DGEBA and THF***

***Validation of the diffusion of DGEBA using brominated DGEBA and X-ray microanalysis***

A CPM-filled epoxy network was made from an epoxy prepolymer bearing bromine atoms on the phenyl groups; the reference of this monomer is DER 542 (from the Dow company). The same IPD curing agent and CPM H2 were used. The cured network was cut by a microtome and observed by TEM (Figure 115). The embedded CPMs were distinguished from the matrix. No porosity was observed. X-ray analysis of the matrix and CPM core was carried out and the spectra are reported in Figure 116. The zone of microanalysis is noted and is visible as a darker area.

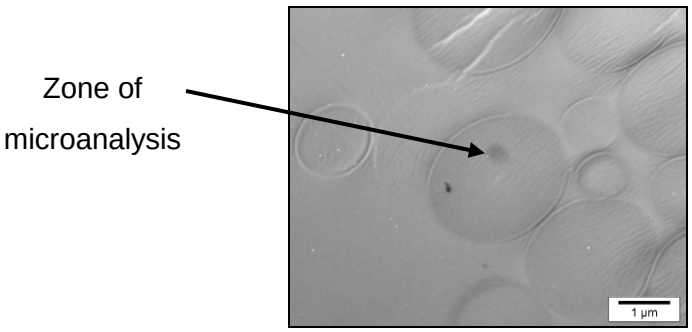


***Figure 115: TEM image of a thin slice of a DER 542-based CPM-filled epoxy network cut by a microtome***

The results of the X-ray analysis are given as qualitative results. As expected, in matrix (a), atoms of carbon, oxygen and bromine were detected in significant quantities. Concerning the CPM core (b), the same atoms were detected as well. Bromine atoms from DER 542 were detected even in the CPM core, meaning that the brominated epoxy prepolymer diffused into it during the dispersion process. Similar behavior probably occurred using DER 331 instead of DER 542 and explains the shift in the Tα of the CPMs to higher temperatures.

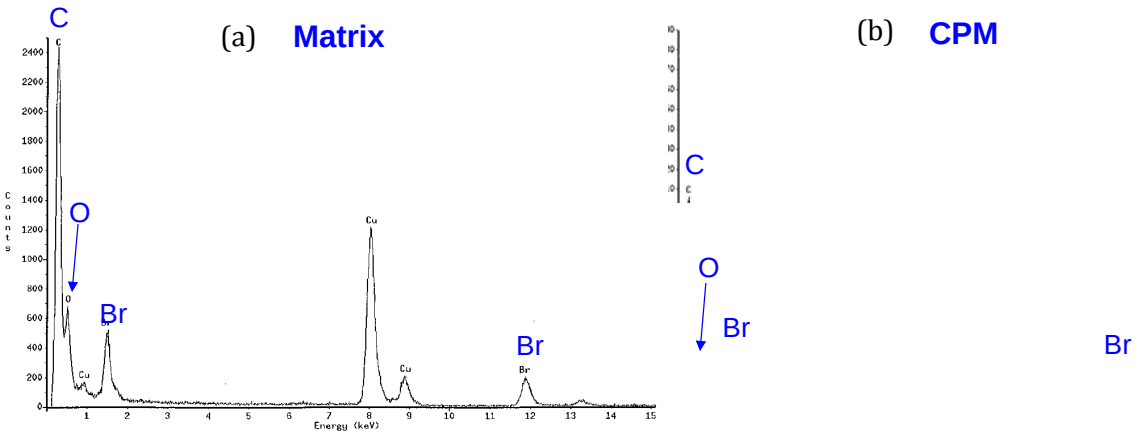


***Figure 116: X-ray microanalysis of the matrix (a) and the CPM core (b) for a DER 542 based CPM-filled epoxy network***

As a conclusion, it was shown by two different experiments that DGEBA is able to diffuse into the CPM core when using THF in the dispersion process.

### *3.2.4 Conclusions*

Using THF is interesting for the preparation of small quantities of filled formulations that could not be processed in bulk, but it was shown in this section that it can also have an impact on the properties of the final networks. Indeed, with the first process presented which was the mechanical dispersion of the CPMs in DGEBA without the use of a solvent, the diffusion of DGEBA during the

process was a possible explanation for the final properties of the materials. The phenomenon of a shift in glass transition of temperature was also observed for this process and was even amplified by the addition of THF in the process. The diffusion of the epoxy monomer into CPMs using this solvent protocol was shown by two different methods. It also suggested the possibility of the same behavior with a low viscosity epoxy prepolymer, as it is the case for DGEBA heated to 80°C. Adding THF in the formulation is useful, but it can also bring more defects in the final material if THF is not totally removed from the CPM; this is a difficult process to control, with results that are not always reproducible.

### 3.3 CPM epoxy networks from the dispersion of CPMs in IPD

A different approach for the process is to disperse the CPMs in the hardener, IPD. The dispersion of CPMs in IPD had different effects depending on the nature of the hardener used to synthesize the CPMs.

High Tg CPMs (H3) synthesized with IPD provided a sandy mixture once dispersed in IPD, whereas medium Tg CPMs (M1 and M2) gave a wetted powder (Figure 117). IPD is able to diffuse inside the CPMs, especially for the medium Tg CPMs that are synthesized from Jeffamine D230. In these CPMs, the molecular chains between crosslinks have a more linear structure and the crosslink density is lower. These two features may explain this easier diffusion of IPD in M1 and M2 as compared to H3.

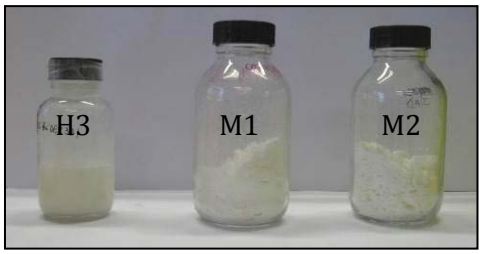


***Figure 117: Photo of the dispersion of the CPM H3, M1 and M2***

MDSC analyses were also carried out on the dispersion of the CPMs in IPD to investigate the Tg. The MDSC thermogram obtained for the dispersion of the CPM H3 is shown in Figure 118. The Tg values for CPM M1 and M2 are reported in Table 40 as well. The Tg of the CPMs in IPD were significantly lower than the values measured before dispersion in IPD. The diffusion of IPD into the CPM core led to the plasticization of the network of CPM H3, M1 and M2.

*Table 40: Tg of CPM H3, M1 and M2 in IPD (57.5 wt% CPMs)*

| CPMs | Tg (CPMs) before dispersion (°C) | Tg (CPMs) in IPD (°C) |
|---|---|---|
| H3 | 112 | 77 |
| M1 | 80 | 59 |
| M2 | 60 | 53 |

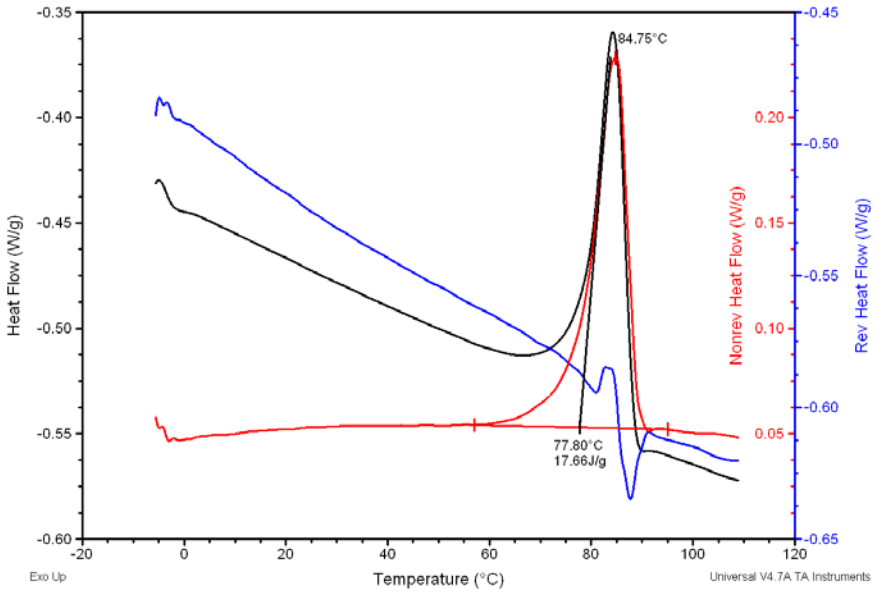


*Figure 118: MDSC thermogram of the dispersion of CPM H3 (57.5 wt%) in IPD – (5°C/min)*

### *3.3.1 Chemorheology*

For this experiment, only high Tg CPM H3 were used. As shown in Table 41, gel and vitrification times were slightly reduced (1 min) by the addition of 20 wt% CPM H3 as compared to the unfilled matrix. This difference in the gel and vitrification times was checked using experiments performed at Dow in Terneuzen (results reported in the Appendix). We remind the reader that the opposite effect was observed when the CPMs H3, H2 or H1 were dispersed in DER 331 (3.1.2), i.e. a small increase in gel and vitrification times was found. The scenario of events up to gelation is difficult to establish because several phenomena occur: first, during the dispersion process, a large part of the IPD diffused into the CPMs and plasticized them, as revealed by visual observations and the DSC results; then, DGEBA was added at room temperature. Simultaneously, at 80°C, DGEBA started to react with available free IPD (not that inside the CPMs) and also diffused inside the plasticized

CPMs and reacted. This reaction may occur with the amino groups from the CPMs or from the IPD inside the CPMs. A certain amount of IPD escaped from the particles (as coming experiments will show) and reacted with DGEBA. At the end, the gel time was slightly decreased because the matrix was off stoichiometry (a/e > 1) and because the functionalized particles were more effective as an additional curing agent with high functionality. In other words, there was greater participation of the amino groups from CPM H3 because of their higher mobility and better ability to react with DGEBA.

***Table 41: Gel and vitrification times for CPM H3-filled epoxy networks at 80°C with pre-dispersion in IPD***

| | Neat matrix DER331-IPD | CPM-filled network (20 wt% H3) |
|---|---|---|
| Gel time (min) | 16 | 15 |
| Vitrification max tan G'' 5 rad/s (min) | 19 | 18 |

### *3.3.2 Morphology*

The morphology of the CPM-filled epoxy-amine networks made from the dispersion of CPMs in IPD was investigated as well for high (H3) and medium Tg CPMs (M1 and M2) using different curing temperatures from 50°C to 180°C, as for the dispersion process in DGEBA.

The first important observation is that CPMs were well-dispersed in all networks. As observed for the networks made from the dispersion in DGEBA, a progressive embedding of CPMs H3, M1 and M2 was noted with an increase in the curing temperature. After 2 h of curing at 50°C, many holes were observed in the micrographs due to the debonding of CPMs. The matrix was undercured and no strong interface could be established at this curing temperature. No significant differences were noted for one-step curing at 120°C or 150°C and two-step curing for 2 h at 80°C followed by 2 h at 180°C.

***Table 42: SEM images of cross-sections by cold fracture of CPM-filled epoxy networks – Influence of the use of 20 wt% H3, M1 and M2 in a matrix a/e = 1 – Influence of the curing temperature***

| | 2 h @ 50°C | 2 h @ 80°C | 2 h @ 120°C | 2 h @ 150°C | 2 h @ 80°C + 2h 180°C |
|---|---|---|---|---|---|
| H3 | 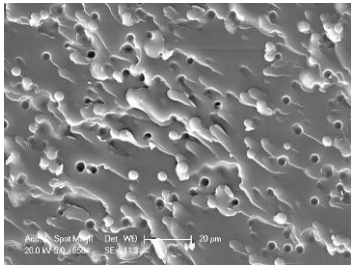 | 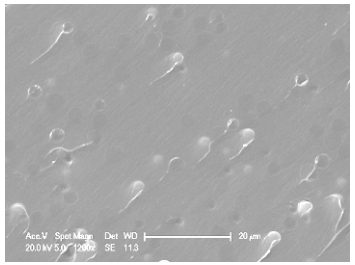 | 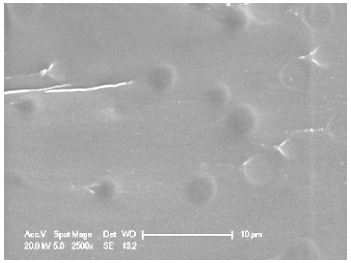 | 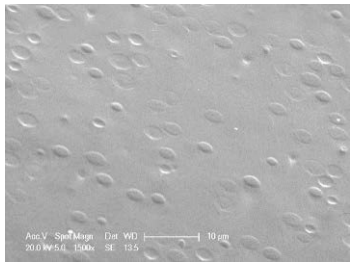 | 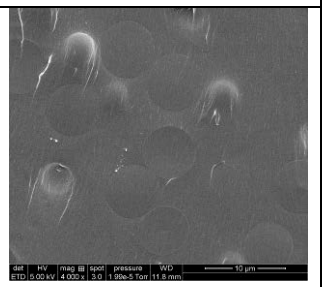 |
| M1 | 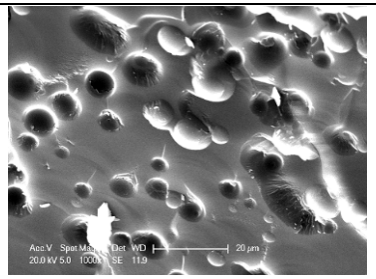 | 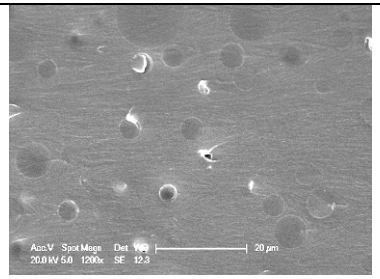 | 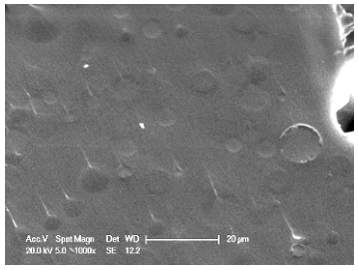 | 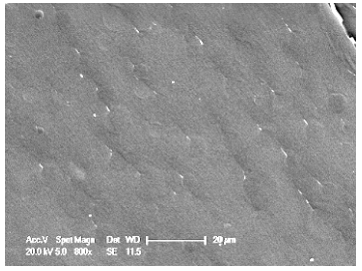 | / |
| M2 | 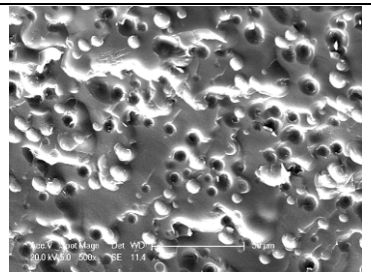 | 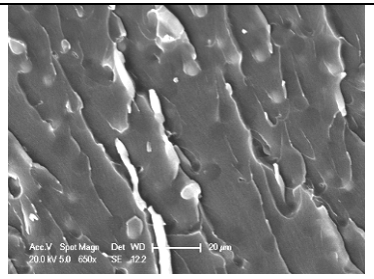 | 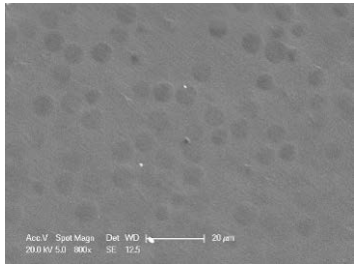 | 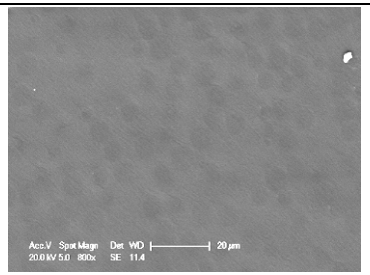 | / |

### 3.3.3 Solid state properties

The dynamic mechanical properties of the networks made from the dispersion of the three types of CPMs in IPD and cured under isothermal conditions were investigated. Variations in tanδ as a function of temperature are reported in Figure 119. The DMA of the networks cross-linked at 80°C showed a very broad tanδ peak due to the post-curing of the samples during the experiments. However, the Tα of CPM M2 was close to 75°C. This α transition was observed at a higher temperature for the network crosslinked at 120°C and 150°C, i.e. close to 85°C. The crosslink density of the CPMs certainly increased due to a facilitated diffusion of DGEBA into the CPMs at higher temperatures. After 2 h of crosslinking at 120°C, all filled networks showed an increased Tα of the matrix as compared to the neat system cured under the same conditions. After 2 h at 150°C, only the addition of CPM M2 led to an increase in Tα. These experiments show that the α transition observed in filled networks is in the same range as in the neat matrix. It means that the stoichiometry in the different networks was similar, and leads to the conclusion that most of the curing agent, IPD, was able to escape from the CPMs and react very rapidly with DGEBA.

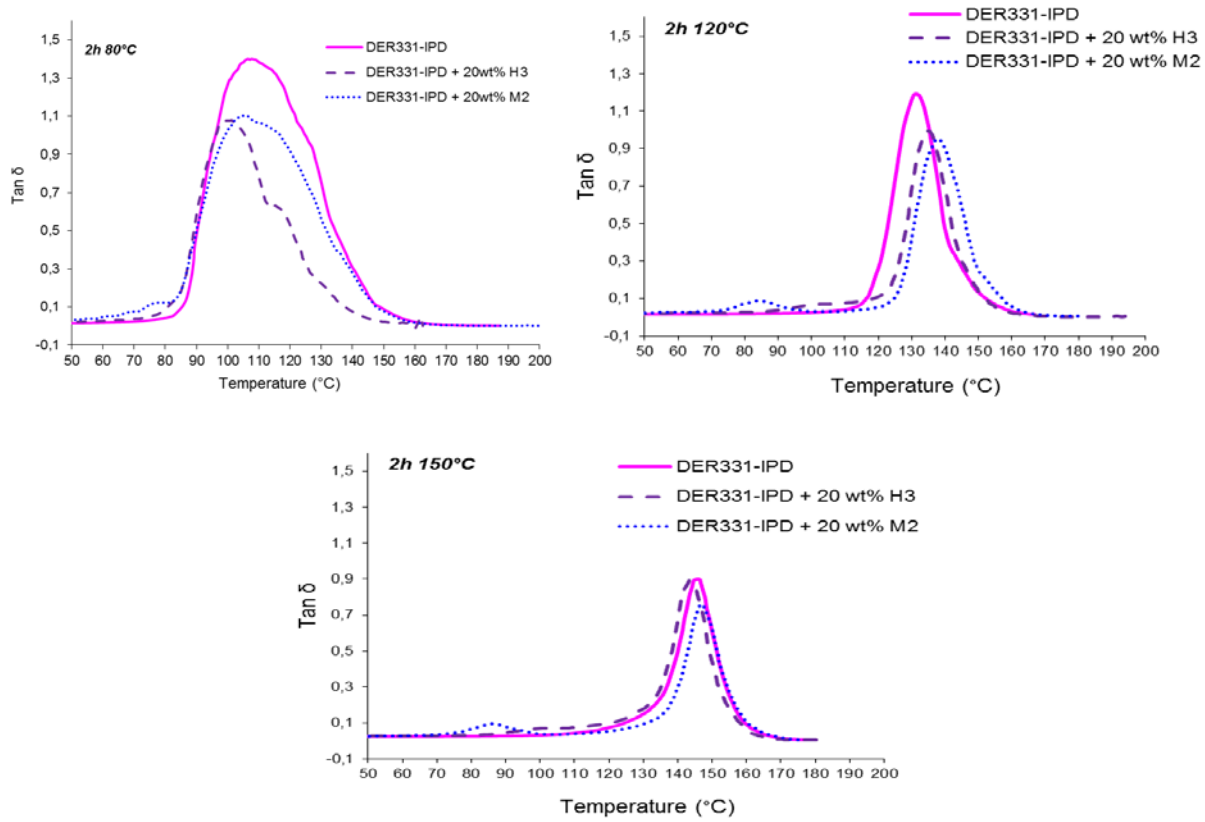


***Figure 119: Tan δ as a function of the temperature for DER331-IPD and DER331-IPD with 20 wt% H3 and M2– $a/e_{matrix}$ = 1 – Isothermal curing for 2 h at 80°C, 120°C and 150°C***

The dynamic mechanical analysis was also done on an H3-filled network cured with a two-step curing cycle, i.e. 2 h at 80°C followed by 2 h at 180°C. The variation in tanδ as function of temperature is plotted in Figure 120. A very broad transition was observed with a maximum at 120°C, and a width at mid-height of $\Delta T\alpha$ = 24°C. This represents a huge decrease in $T\alpha$ as compared to the neat matrix, cured under the same conditions, and to the network cured isothermally at 150°C (close to full curing). This matrix is clearly off stoichiometry; the most realistic explanation is that not enough IPD was able to escape the CPM and the consequence is an excess of DGEBA in the matrix, a/e < 1.

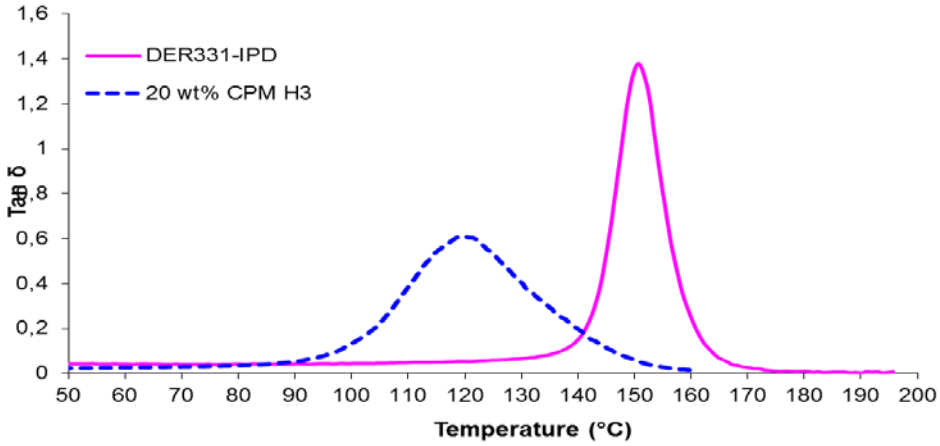


***Figure 120: Tan δ as a function of the temperature for DER331-IPD with 20 wt% CPM H3. $a/e_{matrix}$=1***

### *3.3.4 Conclusions*

The last possibility studied to disperse the CPMs was the dispersion in the amine curing agent. The dispersions appeared sandy or as wetted powders; this was very different from the other two dispersion processes. Dispersing the CPMs in IPD slightly shortened the gel and vitrification times, whereas dispersing the CPMs in DGEBA slightly delayed them. Concerning the morphology and the dynamic solid state properties, they were similar. However, due to the fact that IPD is totally adsorbed into CPMs or diffuses into the CPM core, this process seems poorly reproducible. We already showed that it depends on the crosslink density of the CPM. IPD immediately enters the CPM structure and must escape to react with DGEBA and form the matrix network. The driving force for this phenomenon is not well-understood; it seems unrealistic that IPD always behaves exactly the same, in particular it may depend on the particle size, and IPD may be sometimes captured in the CPM structure. The whole process is very complex. More studies on the diffusion

process should be done to have a clearer understanding, for example by applying a similar methodology as we did for the study of the epoxy diffusion process, i.e. using a labeled curing agent.

## 4 Comparison of the processes

The contribution of CPMs in epoxy-amine networks was investigated with a focus on the network buildup, its kinetics, morphology and dynamic mechanical properties. Three different processes to pre-disperse the CPMs were studied: in the first one, the CPMs were dispersed in the DGEBA monomer, in the second one, the CPMs were dispersed in a solution of DGEBA and the THF solvent and in the third one, the CPMs were dispersed in the isophorone curing agent. In the three processes, a high speed mechanical stirrer was used at room temperature. The visual appearance of the CPM dispersion was not the same: while the two first processes led to a viscous dispersion, the third one led to a wetted or sandy powder.

CPM-filled networks were prepared via isothermal curing or via a two-step curing process that gave either partially cured networks or fully cured networks. Matrices with an excess of the epoxy monomer (a/e = 0.7) or with an equivalent amount of epoxy and amino hydrogen (a/e = 1) were combined with CPMs of different crosslink density and amino functionality. In all cases, the CPMs were very well-dispersed into the epoxy matrices, but depending on the conversion of the matrices, the interface between the particles and the matrix was more or less strong. In the particular case of a low conversion matrix, most of the particles were debonded. Debonding also appeared in networks prepared via the second process (solvent-assisted process).

Our first thought at the beginning of this project was that CPMs with a high cross-link density were not porous and that the reaction with epoxy would occur at the surface of the particles. Diffusion of molecules into them was not envisaged; however, many results oriented the discussion towards the opposite direction, i.e. the diffusion of DGEBA into the CPM core. The use of THF was shown to amplify this phenomenon. The use of a labeled epoxy monomer definitely proved that this diffusion phenomenon occurred during the crosslinking of the network.

There were some consequences to the structure of the resulting networks. It was interesting to compare the results of DMA experiments obtained on filled networks based on the DGEBA + IPD matrix with a/e = 1, filled with 20 wt% CPM H3, and prepared according to the three processes (Figure 121).

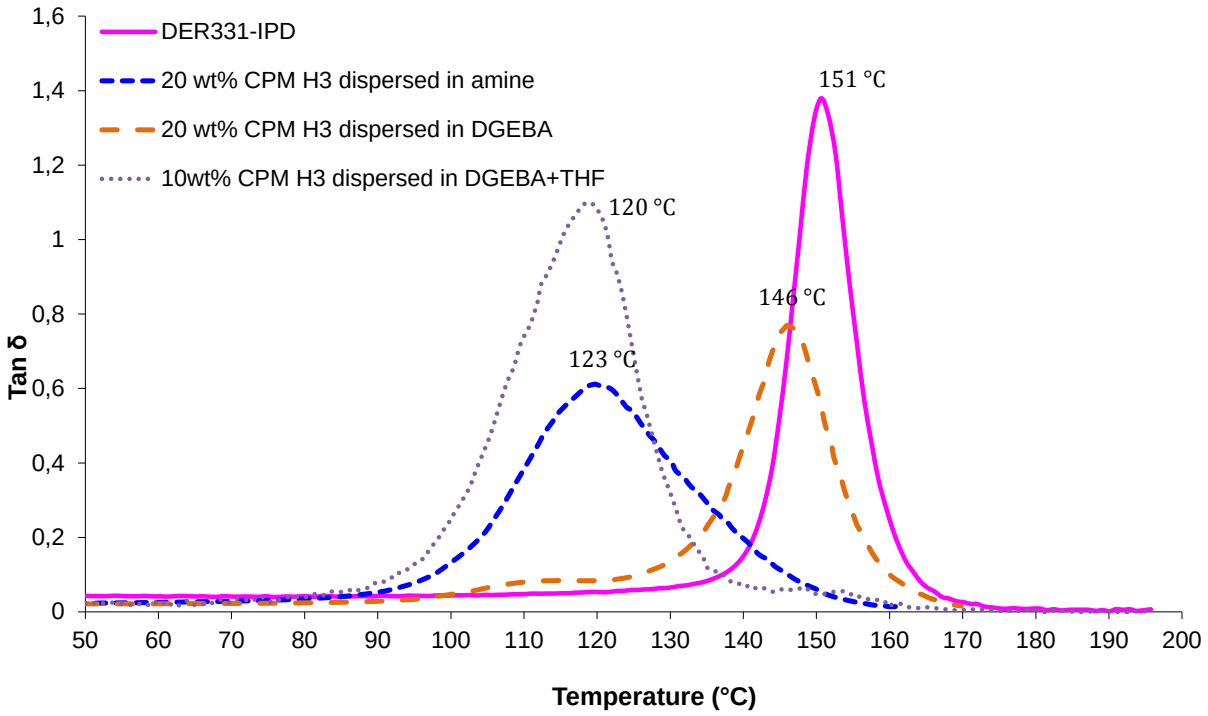


***Figure 121: DER331-IPD with 10 wt% CPM H3 dispersed in DGEBA&THF, 20 wt% CPM H3 dispersed in DGEBA, and, 20 wt% CPM H3 dispersed in IPD- $a/e_{matrix} = 1$***

These three filled networks had exactly the same composition but their behavior was different. Only a small decrease in Tα equal to 5°C was noted for the network prepared via the first process, while a larger decrease close to 30°C was observed for the networks prepared via the two other processes. As already commented on in the previous paragraphs, this decrease was explained by a shift in the stoichiometry of the matrix. It is now clear that the diffusion of DGEBA in the CPM core explains the behavior of the filled network prepared via the second process and that a/e becomes higher than 1, but this is not the same phenomenon that happened during the third process. In this latter case, we think that a part of the IPD remained trapped in the CPM and, as a consequence, the stoichiometric ratio of the matrix become lower than 1.

This comparison illustrates how complex the behavior of CPM-filled networks can be, because it results from the selection of the stoichiometric ratio of the matrix, the stoichiometric ratio of the particles (so their functionality), the dispersion process and the curing cycle. Concerning the reproducibility of the results, it seems more interesting to disperse the CPMs in DGEBA without the assistance of a solvent. With pre-dispersion in DGEBA, it was shown that a perfect dispersion of CPMs in epoxy-amine was obtained, leading to the embedding of the CPMs in the matrix with a higher conversion of the epoxy groups after the curing step at 80°C.

# V CONCLUSIONS AND PERSPECTIVES

Throughout this work, we have studied the influence of the addition of cross-linked epoxy microparticles in epoxy-amine formulation on the kinetics, morphology and thermo-mechanical properties of the final networks.

First, an easy, robust and well-controlled protocol was developed to obtain a large range of CPM size, Tg and amine functionality, which was reported in the second chapter of this thesis. This protocol based on reaction induced phase separation via precipitation polymerization was also applied to different chemistries and water soluble epoxy prepolymer showing the large possible applications of this method. The capacity of obtaining a good compatibility between the CPMs and the matrix was ensure by synthesizing the CPMs in excess of amino groups. Therefore the influence of the stoichiometric ratio of the CPMs was investigated on their kinetics of formation, time to phase separation, which was shorter in excess of amine, on the CPM size also slightly increasing with the amine excess, and on their glass transition temperature always maximum at the stoichiometry a/e=1. The study of the remaining reactive amino groups was of great interest and therefore deeply studied in the Chapter 3. It was then highlighted that even though these cross-linked microparticles were not porous, amino groups are available into the core if DGEBA from the matrix can diffuse to them. As a consequence, depending on the amine titration technique and the medium used, different results of available amino groups were found. The surface amine titration is therefore not of great interest, but the knowledge of how many amino groups can interact with free DGEBA during the network crosslinking give information on the influence of the addition of CPMs in the network.

Whatever the combination of CPM and matrix of different stoichiometric ratio and dispersion process considered, CPMs were always well dispersed in the matrix. One of the key points highlighted in this work was the diffusion phenomenon of monomers, DGEBA or IPD, in the CPM core. The intensity of this phenomenon influences the glass transition temperature of the filled networks.

Indeed, it was shown that the diffusion of monomers into the CPM core occur but differently depending on the dispersion process. Using tetrahydrofuran as solvent to help for the dispersion, increases the diffusion of DGEBA into the CPM core and changes the thermo-mechanical properties of the final network by modifying the stoichiometric ratio of the matrix. Same phenomenon was observed but less amplified when CPMs were mechanically dispersed in DGEBA. Regarding the dispersion of CPMs in IPD, a complete absorption of IPD was observed into D230 based CPMs, leading then to the desorption of IPD to create the network. This last process does not seem reproducible.

Thus, a very complex behavior of CPM was observed in presence of monomers or/and solvent: swelling and diffusion phenomena that are dependent on a number of parameters such as temperature, CPM crosslink density, solubility parameters, etc. The intensity of those phenomena leads to a variety of behaviors when CPMs are added into an epoxy-amine formulation:

- Slight decrease of gel times and increase of conversion
- Modification of glass transition temperature of the matrix

Moreover, amines with similar reactivity were used to form the matrix and synthesize the CPMs. Using different amines would be interesting to investigate. It could enable the labeling of the different amines to better understand the network formation mechanism. The use of a very reactive amine at low temperature to synthesize the CPMs would increase the participation of the CPMs in the network build-up.

Those CPMs were synthesized with the aim to be re-dispersed in epoxy formulation but we can also imagine their application in many fields. Due to their amine and hydroxyl functions, they could be used as reactive fillers with others polymers or be the support for the grafting of other targeted molecules. Core-shell or hairy particles could also be formed from the CPMs.
Depending on the monomer used for their synthesis, the use of the CPMs as tracer could also be considered if the final structure is fluorescent for example.
Of course, the use as toughening agent or modifiers of mechanical properties by playing with the Tg of the CPMs would be an interesting approach as well for microparticles synthesized with a very easy and robust process.

# VI APPENDIX

## 1 Monitoring of the CPM synthesis by microdieletrometry

A second method was also developed to visualize the cloud point. It consisted in microdielectrometric measurements of the solution containing all the reactants. The conductivity and the permittivity were monitored as a function of time. The formation of particles induced changes in the conductivity of the solution which enables the measurements of the cloud point at low frequencies. Conductivity of the CPM solution and of the solvent without monomer was monitored during the formation of CPM ref as shown by the picture in Figure 122. This method was used to check if the time to phase separation could be measured by microdielectrometry.


***Figure 122: Image of microdieletrometry experiment – Monitoring of the CPM formation inside an oven at 100°C.***

A severe decrease of the conductivity (Figure 123) was observed from 150 min especially at very low frequency where the phenomenon is amplified. This value did not exactly correspond to the cloud point measured with light transmittance through the solution which was about 1h47 or 107 min. With microdieletrometry the value was higher and probably corresponds to the time of formation of bigger particles.

What is observed here is the variation of the conductivity with the disappearance of the monomer in the solution and the formation of solid entities growing during the reaction.

As a conclusion, microdieletrometry is one possible way to monitor the formation of particles in the solution but the results cannot be directly compared with the ones from others techniques.

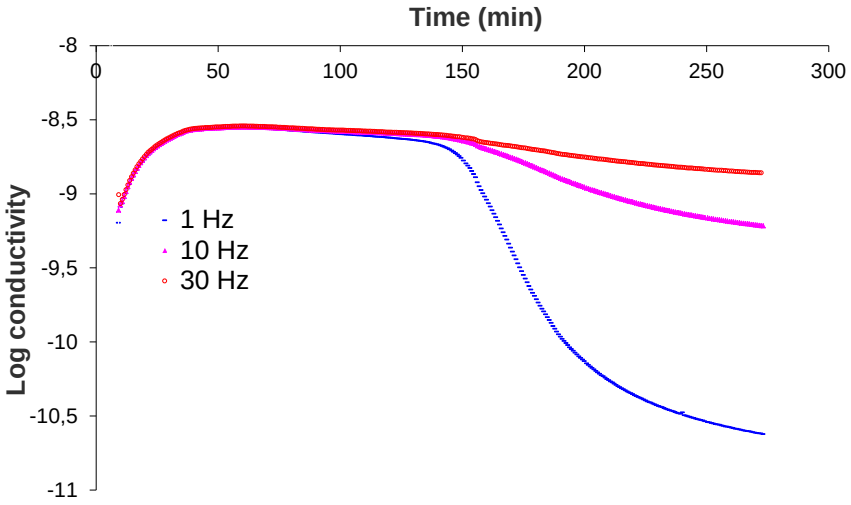


***Figure 123: Logarithm of the conductivity of the CPM ref solution during their formation at 100°C, at 1Hz, 10 Hz, 30 Hz***

## 2 TGA – FTIR on CPM ref

The CPM ref were sent to SCA (CNRS central department of analysis, Lyon, France) to be analyzed by TGA-FTIR.

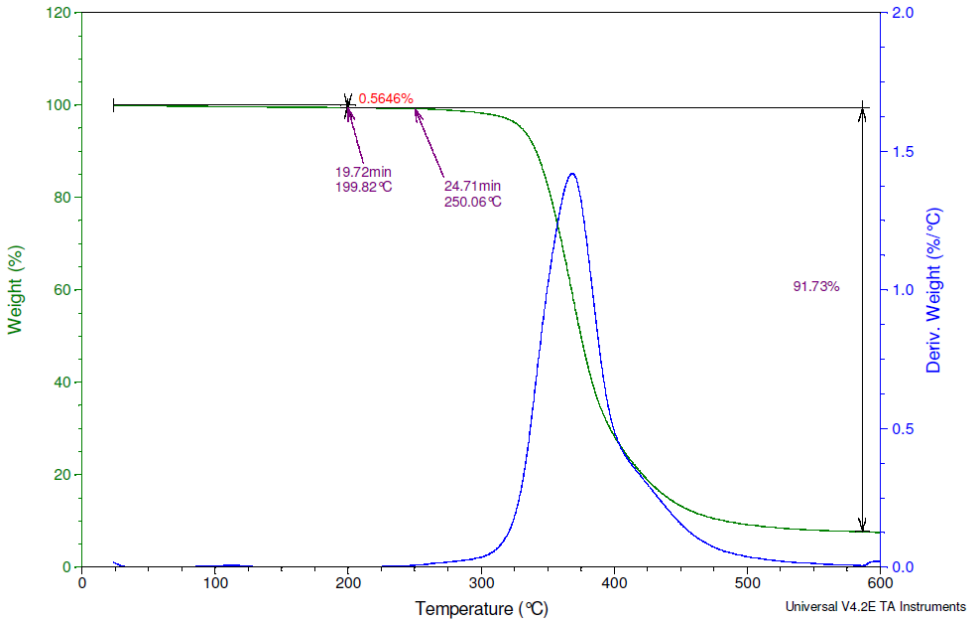


***Figure 124: Thermogram obtained by TGA-FTIR for CPM ref***

The following comments were given by the SCA. The mass loss between room temperature and 250°C is about 0.6%. Water release is observed until 60°C. From 90°C to 135°C, at least two others products are released. The first one is THF and for the second one the signal was too low to be identified but could be related to acetone or dodecane.

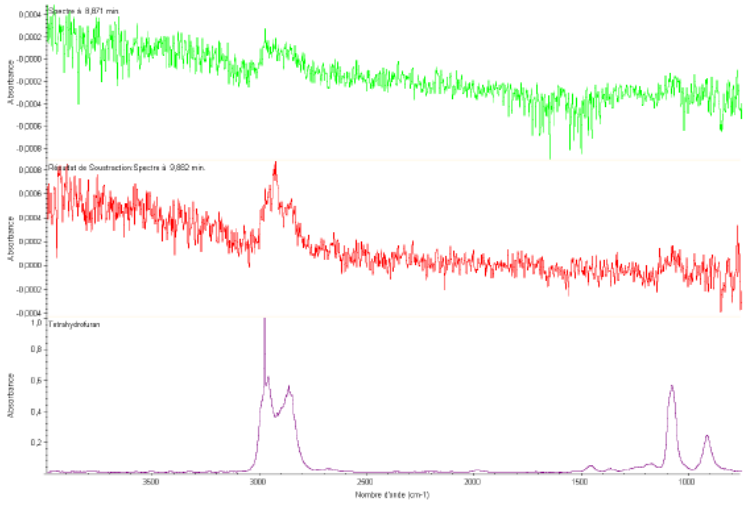

***Figure 125: Spectra from TGA-FTIR of CPM ref – Comparison with THF***

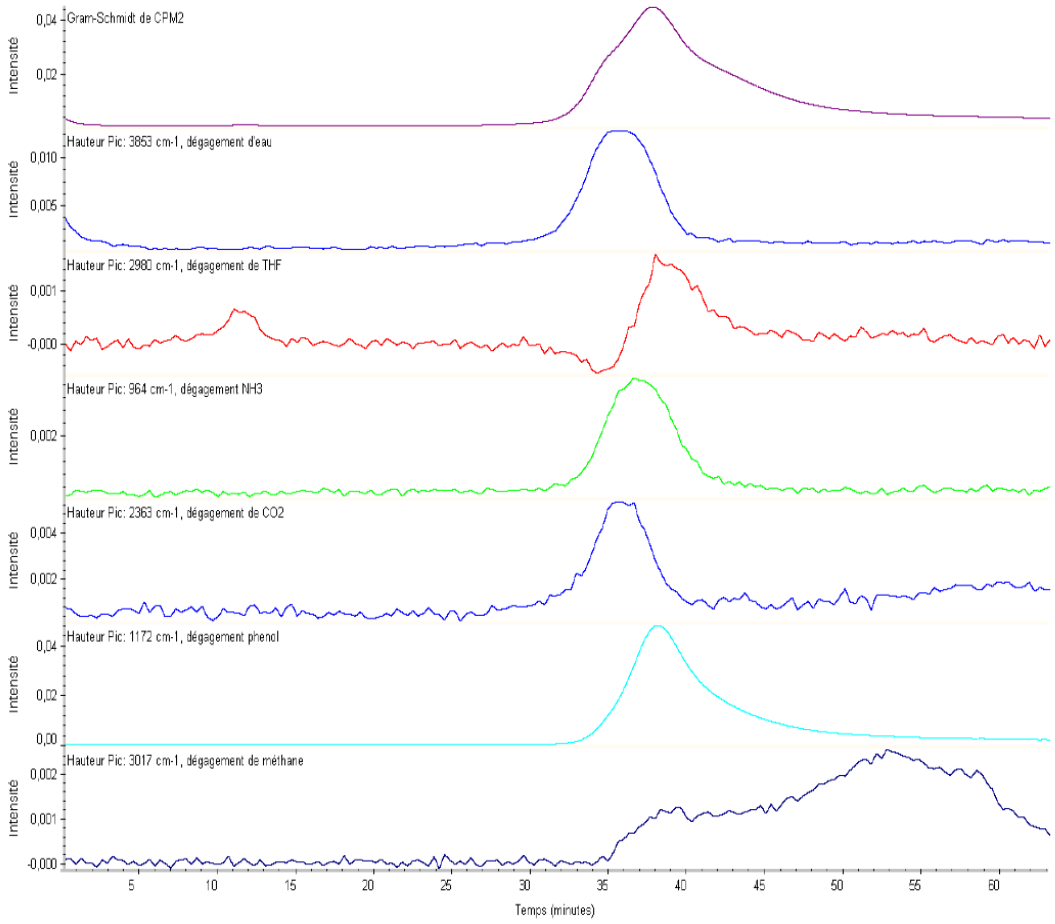


***Figure 126: Gram-Schmidt (IR Chromatogram of heated products) of identified products***

## 3 Composition of the CPMs by elemental analysis

***Elemental analysis*** was used to determine the C, H, N and O content in the CPMs to estimate their real stoechiometric ratio. The evolution of the percentage of each atom was in agreement with the theory. Indeed, as a/e was increased, C and O contents decreased unlike H and N contents increased. However, although values were in the same range as the theoretical one, it was not possible to establish the real a/e of the CPMs by this technique, due to the difficult correspondence with the 4 different elements. It was also important to point out here that a few percentage of residual solvent like THF and dodecane (as shown by the TGA-FTIR), possibly present in the CPM structure, have not been taken into account.

***Table 43: Theoretical (a) and experimental (b) values for elemental analysis of CPMs***

(a)

| | *% theo (a/e=0.9)* | *% theo (a/e=0.97)* | *% theo (a/e=1.05)* | *% theo (a/e=1.35)* | *% theo (a/e=1.5)* | *% theo (a/e=1.6)* |
|---|---|---|---|---|---|---|
| C | *73.65* | *73.61* | *73.57* | *73.4* | *73.33* | *73.29* |
| H | *8.06* | *8.12* | *8.2* | *8.45* | *8.56* | *8.63* |
| N | *2.81* | *2.99* | *3.2* | *3.89* | *4.21* | *4.42* |
| O | *15.47* | *15.27* | *15.04* | *14.26* | *13.89* | *13.66* |

(b)

| | *% exp (a/e $_{t=0}$ =0.9)* | *% exp (a/e $_{t=0}$ =1.05)* | *% exp (a/e $_{t=0}$ =1.35)* | *% exp (a/e $_{t=0}$ =1.5)* |
|---|---|---|---|---|
| C | *72.36* | *72.31* | *71.99* | *72* |
| H | *7.81* | *8.38* | *8.34* | *8.43* |
| N | *3.26* | *3.46* | *3.84* | *4.04* |
| O | *15.57* | *15.18* | *15.15* | *14.81* |

## 4 Epoxy reactivity of CPMs towards IPD by DSC

CPMs were also dispersed in IPD. Same study as for the CPMs dispersed in DER 331 was carried out. The dispersion was heated with a dynamic ramp in the DSC pan. This time the only source of epoxy groups was the CPMs.

Although NIR spectroscopy did not detect any residual epoxy groups from the CPM structure for any types of CPMs, a reaction peak was observed for the dispersions of 57.5 wt % of H2 and H3 with a/e=1.35 and 1.5 respectively (Figure 127). As unexpected, these reaction peaks were very narrow: the heat release was detected between 70 and 90°C. Values of the enthalpy peak measured were summarized in Table 44. Calculation was done to obtain the corresponding value of residual epoxy groups. 0.63 and 0.46 mmol of residual epoxy groups per gram of CPMs were measured for H2 and H3 respectively.

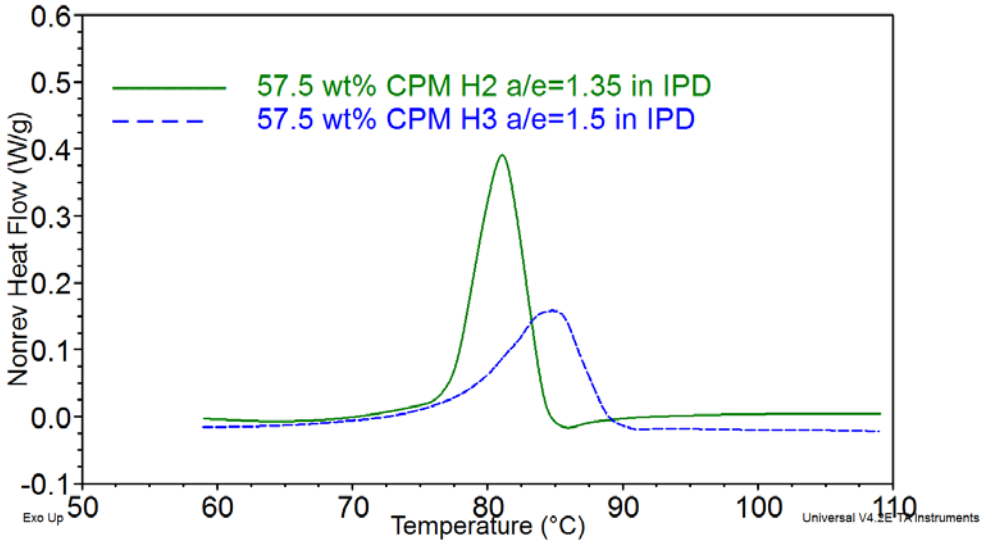


***Figure 127: Thermogram of the dispersion of 57.3 wt % CPM H2 & H3 in IPD***

***Table 44: DSC measurements for the dispersion of H2 and H3 in IPD***

| CPMs | $\Delta H_{disp}$ (J/g) | $\Delta H_{CPM}$ (J/g of CPMs) *(2 weeks after dispersion)* | Residual epoxy groups (mmol.g$^{-1}$ of CPMs) |
|---|---|---|---|
| H2 a/e=1.35 | 22 | 38 ±1 | 0.63 |
| H3 a/e=1.5 | 16 | 28 ±1 | 0.46 |

## 5 Kinetics by NIR spectroscopy of CPM filled epoxy networks

The addition of 20 wt% CPM H3 and H2 in DER331-IPD was investigated on the epoxy conversion of the matrix cross-linked at 60°C. As it was observed at 80°C, epoxy conversion after vitrification was increased by the presence of the CPMs and no significant influence of the kind of CPM was observed. However, the value obtained at the plateau for the neat DER331-IPD system (x=0.61) seemed to be underestimated compared with the theoretical value at the gel point of $x_{gel}$ = 0.58 and the values measured by Mounif at 50°C and 70°C [121], which were about 65% and 73%, respectively.

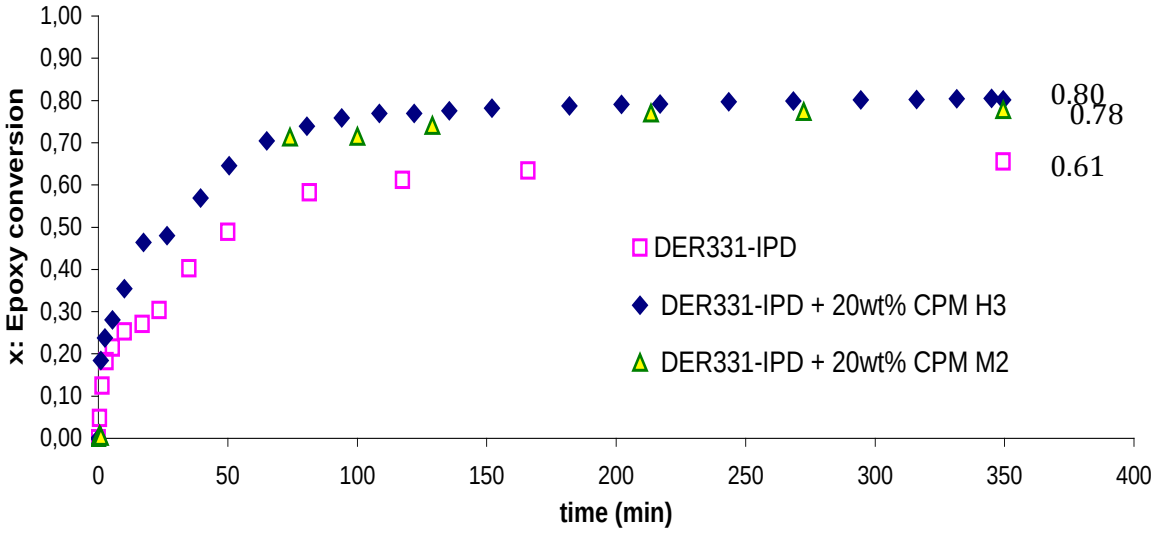


***Figure 128: In situ measurements of epoxy conversion of the matrix of CPM-filled epoxy networks crosslinked at 60°C by NIR***

Table 45 summarizes the in situ measurements of epoxy conversion at 60°C and 80°C.

***Table 45: Maximum epoxy conversion of the matrix of CPM-filled epoxy networks (with 20 wt% H3 and M2) cured at 60°C and 80°C***

| T (°C) | 60°C | 80°C |
|---|---|---|
| Epoxy conversion of neat matrix | 61% | 85% |
| Epoxy conversion of CPM-filled epoxy networks | 78-80% | 93% |

# 6 Chemorheology measurement done at Dow, Terneuzen

***Table 46: Gel and vitrification times of DGEBA-IPD and CPM (20 wt%) filled epoxy networks at 80°C (on Anton Paar rheomether)***

| | DGEBA-IPD | CPM H1, H2, H3 filled epoxy networks |
|---|---|---|
| $t_{gel}$ (min) | 25 | 27 |
| $t_{vit}$ (min) | 31 | 32 |

***Table 47: Gel and vitrification time for CPM H3 filled epoxy network at 80°C with pre-dispersion in IPD (on Anton Paar rheomether)***

| | Neat matrix DER331-IPD | CPM filled network (20 wt% H3) |
|---|---|---|
| Gel time (min) | 24 | 22 |
| Vitrification max tan G'' 5 rad/s (min) | 31 | 29 |

## VII REFERENCES


[1] D. Ratna, Handbook of Thermoset Resins, Smithers, Shawbury UK, 410p, 2009.

[2] M. Traina, J. Galy, J-F. Gérard, T. Dikic, T. Verbrugge, Colloid and Interface Science, 368, 158, 2012.

[3] J-P Pascault, H. Sautereau, J. Verdu, R. Williams, Thermosetting polymers, Marcel Dekker, 477p, 2002.

[4] M. Chrysanthos, Thesis, Novel biobased epoxy networks derived from renewable resources: structure-property relationships, INSA Lyon, 2012.

[5] L. Shen, J. Haufe, M. Patel, Product overview and market projection of emerging biobased plastics, PROBIP, 2009.

[6] A. Apicella, I. Nicolais, M. Iannone, P. Passerini, Journal of Applied Polymer Science, 29, 2083, 1984.

[7] J. Mijovic, A. Wijava, Polymer, 35, 2683, 1994.

[8] E. Mounif, V. Bellenger, P. Mazabraud, F. Nony, A. Tcharkhtchi, Applied polymer science, 116, 969, 2010.

[9 ] P. Flory, American Chemical Society, 63, 3083, 1941.

[10] P. Flory, Principles of Polymer Chemistry, chap IX, Molecular weight distribution in nonlinear polymers and the theory of gelation, Cornell University, 1953.

[11] W. Stockmayer, Journal of chemical physics, 11, 45, 1943

[12] R. Stepto, Polymer networks: Principles of their formation structure and properties, Blackie academic & professional, p36, 1997.

[13] J-P Eloundou, Thesis, Gelification de systèmes epoxy-amines: Etudes cinétiques, rhéologiques et diéléctrique, INSA Lyon, 1996.

[14] H. Winter, F. Chambon, Journal of Rheology, 30, 367, 1986.

[15] H. Winter, Polymer Engineering and Science, 27, 1698, 1987.

[16] L. Matejka, Polymer Bulletin, 26, 109, 1991.

[17] J. Enns, J. Gillham, Journal of Applied Polymer Science, 28, 2567, 1983.

[18] J. Gillham, Polymer Engineering and Science, 26, 1429, 1986.

[19 ] L. Chan, H. Naé, J. Gillham, Journal of Applied Polymer Science, 29, 3307, 1984.

[20] M. Marks, R. Snelgrove, Applied Materials and Interfaces, 1, 921, 2009.

[21] I. Kroutilova, L. Matejka, A. Sikora, K. Soucek, L. Stas, Journal of Applied Polymer Science, 99, 3669, 2006.

[22] H. Lu, G. Lovell, C. Bowman,, 34, 8021, 2001.

[23] J-P Pascault, R. Williams, Polymer Science, Part B: Polymer physics, 28, 85, 1990.

[24] E. Mounif, V. Bellenger, A. Tcharkhtchi, Journal of Applied Polymer Science, 108, 2908, 2008.

[25] L. Nunez, J. Taboada, F. Fraga, M. Nunez, Journal of Applied Polymer Science, 66, 1377, 1997.

[26] E. Karayannidou, D. Achilias, I. Sideridou, European Polymer Journal, , 42, 3311, 2006.

[27] D. Serrano, D. Harran, European Polymer Journal, 24, 667, 1988.

[28] L. Wu, S. Hoa, Minh-Tan, Ton-That, Journal of Applied Polymer Science, 99, 580, 2006.

[29] J. Galy, A. Sabra, J-P Pascault, Polymer Engineering and Science, 26, 1514, 1986.

[30] J. Duchet, J-P Pascault, Polymer Science: Part B: Polymer Physics, 41, 2422, 2003.

[31] K. Dusek, J. Plestil, F. Lednicky, S. Lunak, Polymer, 19, 393, 1978.

[32] J. Racich, J. Koutsky, Journal of Applied Polymer Science, 20, 2111, 1976.

[33] C. Sahagun, S. Morgan, Applied Materials and Interfaces, 4, 564, 2012.

[34] W. Wu, B. Bauer, Polymer, 27, 169, 1985.

[35] J-P Geisler, S Petri, Patent, US5358982, 1994.

[36] M. Hönel, G. Walz, P. Ziegler, U. Kubillus, Patent, US5135970, 1992.

[37] B. Jansen, K. Tamminga, H. Meijer, P. Lemstra, Polymer, 40, 5601, 1998.

[38] M. Imanaka, S. Motohashi, K. Nishi, Y. Nakamura, M. Kimoto, Adhesion and Adhesives, 29, 45, 2009.

[39] L. Valette, J-P Pascault, B. Magny, Macromolecular Materials Engineering, 288, 751, 2003.

[40] C. Carfagna, V. Ambrogi, G. Cicala, A. Pollicino, A. Recca, G. Costa, Applied Polymer Science, 93, 2031, 2004.

[41] M. Frigione, E. Calò , A. Maffezzoli, D. Acierno, C. Carfagna, V. Ambrogi, Journal of Applied Polymer Science, 100, 748, 2006.

[42] V. Ambrogi, S. Cosco, C. Carfagna, G. Cicala, L. Oliveri, A. Recca, Polymer Engineering and Science, 46, 1739, 2006.

[43] K. Tauer, Encyclopedia of polymer science and technology, 6, 410p, 2003.

[44] W. Funke, O. Okay, B. Joss-Muller, Advances in Polymer Science, 136, 139, 1998.

[45] S. Kawaguchi, K. Ito, Advances in Polymer Science, 175, 299, 2005.

[46] R. Arshady, Colloid and Polymer Science, 270, 717, 1992.

[47] Y. Almog, M. Levy, Polymer Science: Polymer Chemistry, 20, 417, 1982.

[48 ] M. Yoshida, T. Yokota, M. Asano, M. Kumakura, Colloid and Polymer Science, 267, 986, 1989.

[49] W. Yang, D. Yang, J. Hu, C. Wang, S. Fu, Polymer Science, Part A: Polymer Chemistry 39, 555, 2001.

[50] S. Klein, V. Manoharan, D. Pine, F. Lange, Colloid and Polymer Science, 282, 7, 2003.

[51] K. Takahashi, S. Miyamori, H. Uyama, S. Kobayashi, Polymer Science, Part A: Polymer Chemistry, 34, 175, 1996.

[52] D. Horak, Polymer Science: Part A: Polymer Chemistry, 37, 3785, 1999.

[53] M. Okubo, M. Shiozaki, M. Tsujihiro, Y. Tsukuda, Colloid and Polymer Science, 269, 222, 1991.

[54] J. Ugelstad, K. H. Kaggerud, F. K. Hansen, A. Berge, Makromolecular Chemie, 180, 737, 1979.

[55] M. Jonsson, Thermally expandable microspheres prepared via suspension polymerization, Thesis, KTH, Stockholm, 2010.

[56] P. Dowding, B. Vincent, Colloids and Surfaces A: Physicochemical and Engineering Aspects, 161, 259, 2000.

[57] F. Hofman, K. Delbruck, German Patent 250 690, 1909.

[58] K. Gottlob, US patent, 1149577, 1915.

[59 ] O. Durham, S. Krishnan, D. Shipp, Macro Letters, 1, 1134, 2012.

[60] C. Chern, Progress in polymer science, 31,443, 2006.

[61] K. Tauer, R. Deckwer, I. Kuhn, C. Schellenberg, Colloid and Polymer Science, 277, 607, 1999.

[62] H. Ni, G. Ma, M. Nagai, S. Omi, Applied Polymer Science, 82, 2692, 2001.

[63] A. Pich, W. Richetering, Advances in Polymer science, 234, 1, 2010.

[64] G. Caneba, Free-Radical-Retrograde-Precipitation Polymerization, Springer, p. 4, 2010.

[65] N. Tsujioka, N. Ishizuka, N. Tanaka, T. Kubo, K. Hosoya, Polymer Science, Part A: Polymer Chemistry, 46, 3272, 2008.

[66] A. Loera, F. Cara, M. Dumon, J-P. Pascault, Macromolecules, 35, 6291, 2002.

[67] J. Kiefer, J. Hedrick, J.Holborn, 147, 161, 1996.

[68] R. Pelton, P. Chibante, Colloids Surfaces, 20, 247, 1986.

[69] R. Pelton, Advances in Colloid and Interface Science 85, 1, 2000.

[70] M. Das, Thesis, Stimulus-Responsive Microgels: Design, Properties and Applications, Toronto, 2008.

[71] A. Loxley, B. Vincent, Colloid and Polymer Science, 275, 1108, 1997.

[72] L. Valette, J-P. Pascault, B. Magny, Macromolecular materials and engineering, 287, 31, 2002.

[73] I. Kaneda, B. Vincent, Colloid and Interface Science, 274, 49, 2004.

[74] S. Rouzeau, F. Méchin, J-P. Pascault, B. Magny, European Polymer Journal, 43, 4398, 2007.

[75] H. Ni, H. Kawaguchi, T. Endo, Macromolecules, 40, 6370, 2007.

[76] J. Downey, G. McIsaac, R. Frank, H. Stöver, Macromolecules, 34, 4534, 2001.

[77] H. Hseih, E. Woo, Journal of Polymer Science, Part B: Polymer Physics, 34, 2591, 1996.

[78] K. Hibino, Y. Kimura, Colloid and Polymer Science, 278, 565, 2000.

[79] X. Yu, C. Zhang, Y. Ni, S. Zheng, Journal of Applied Polymer Science, 128, 2829, 2013.

[80] R. Pelton, P. Chibante, Colloids and Surfaces, 20, 247, 1986.

[81] S. A. Page, R. Mezzenga, L. Boogh, J. C. Berg, J.A.E. Manson, Colloid and Interface Science, 222, 55, 2000.

[82] D. van Krevelen, K. te Nijenhuis, Properties of Polymers, 4th edition, Elsevier, p.189, 2009.

[83] R. Mezzenga, S. Page, J-A. Manson, Colloid and Interface Science, 250, 121–127, 2002.

[84] D. Verchère, H. Sautereau, J. P. Pascault, C. C. Riccardi, S. M. Moschiar, R. J. J. Williams, Macromolecules, 23, 725, 1990.

[85] J. Galy, A. Sabra, J-P. Pascault, Polymer Engineering and Science, 26, 1514, 1986.

[86] M. Ganzales Gonzales, J-C. Cabanelas, J. Baselga, Infrared spectroscopy – Material Science, Engineering and technology, T. Theophanides, p.267, 2012.

[87] C. Jung, J. Kim, H. Kim, J. Ha, Y. Kim, S. Koo, Journal of Colloid and Interface Science, 367, 67, 2012.

[88] V. B. Ivanov, J. Behnisch, A. Hollander, F. Mehdorn, H. Zimmermann, Surface and Interface Analysis, 24, 251, 1996.

[89] J. Jang, H. Lim, Microchemical Journal, 94, 148-158, 2010.

[90] B. Elmas, M. Tuncel, G. Yalçin, S. Senel, A. Tuncel, Colloids and Surfaces A: Physicochemical and Engineering Aspects, 269, 125-134, 2005.

[91] T. Mori, T. Kubo, K. Kaya, K. Hosoya, Colloid and Polymer Science, 287, 513-523, 2009.

[92] N. Tsubokawa, K. Kbayashi, Y. Sone, Polymer Journal, 19, 1147, 1987.

[93] C. Chan, N. Choudhury, P. Majewski, Colloids and Surfaces A: Physicochemical and Engineering Aspects, 377, 20, 2011.

[94] F. Ganachaud, B. Bouali, L. Vrron, P. Lantéri, A. Elaissari, C. Pichot, Colloids and Surfaces A: Physicochemical and Engineering Aspects, 137, 141-154, 1998.

[95] T. Delair, V. Marguet, C. Pichot, and B. Mandrand, Colloid and Polymer Science, 272, 962-970, 1994.

[96] F. Sauzedde, F. Ganachaud, A. Elaissari, C. Pichot, Journal of Applied Polymer Science, 65, 2331-2342, 1997.

[97] T. Nakagawa, T. Tanaka, D. Niwa, T. Osaka, H. Takeyama, T. Matsunaga, Journal of Biotechnology, 116, 105–111, 2005.

[98] M. Ghasemi, Thesis, Immobilisation de la trypsine sur un support de polyéthylène fonctionnalisé par voie plasma, Paris VI, p.64, 2007.

[99] S. Kakabakos, P. Tyllianakis, G. Evangelatos, D. Ithakissios, Biomaterials, 15, 289, 1994

[100] D. McCaldin, Chemical Reviews, 60, 39, 1959.

[101] E. Kaiser, R. Colescott, C. Bossinger, P. Cook, Analytical Biochemistry, 34, 595, 1970.

[102] V. Sarin , S. Kent, J. Tam, R. Merrifield, Analytical Biochemistry, 117, 147, 1981.

[103] W. Troll, R. K. Cannan, Journal of Biological Chemistry, 200, 803, 1953.

[104] M. Friedman, Journal of Agricultural and Food Chemistry, 52, 385, 2004.

[105] Application manual : Amino Acids, Pickering Laboratories, Inc., 2002.

[106] B. Scruggs, S. Kilgore, S. Hruby, B. Shanks, B. Chandler, Catalysis of Organic Reactions, 22ndedition, Taylor and Francis Group, 38, 339, 2009.

[107] M. A. Markowitz, P. E. Schoen, P. Kust, Bruce P. Gaber, Colloids and Surfaces A: Physicochemical and Engineering Aspects, 150, 85, 1999.

[108] Y-G Won, Thesis, Influence de la structure de réseaux époxydes modèles sur les propriétés volumétriques, mécaniques et viscoélastiques, INSA Lyon, 235p, 1989.

[109] H. Winter, F. Chambon. Journal of Rheology, 30, 367, 1986.

[110] C. Sahagun, S. Morgan, Thermal control of nanostructure and molecular network development in epoxy-amine thermosets, Applied Materials and Interfaces, 4, 564, 2012.

[111] E. Mounif, G. Liang, W. Cook, V. Bellenger, A. Tcharkhatchi, Polymer International, 58, 2009.

[112] S. Pandita, R. Mahendran, V. Machavaram, M. Harris, G. Ferando, Thermochimica Acta, 543, 9, 2012.

[113] N. Poisson, G. Lachenal, H. Sautereau, Vibrational Spectroscopy, 12, 237, 1996.

[114] M. Pramanik, S. Mendon, J. Rawlins, Polymer Testing, 31, 716, 2012.

[115] M. Garcia del Cid, M Prolongo, C. Salomi, C. Arribas, M. Sanchez-Cabezudo, R. Masegosa, Journal of Thermal Analysis and Calorimetry, 108, 741, 2012.

[116] L. Wu, S. Hoa, Minh-Tan, Ton-That, Journal of Applied Polymer Science, 99, 580, 2006.

[117] E. Bugnicourt, Thesis, Development of sub-micro structured composites based on an epoxy matrix and pyrogenic silica: mechanical behavior related to the interactions and morphology at multi-scale, INSA Lyon, 2005.

[118] E. Franchini, Thesis, Structuration of nano-objects in epoxy-based polymer systems: nanoparticles & nanoclusters for improved fire retardant properties, INSA Lyon, 2008.

[119] J.-P. Pascault, R. Williams, Epoxy polymers – New materials and innovations, Weinheim Germany, Wiley, p. 5, 2010.

[120] B. Wetzel, P. Rosso, F. Haupert, K. Friedrich, Engineering fracture mechanics, 73, 2375, 2006

[121] E. Mounif, V. Bellenger, P. Mazabraud, F. Nony, A. Tcharktchi, Journal of Applied Polymer Science, 116, 969, 2010.

THESE SOUTENUE DEVANT L'INSTITUT NATIONAL DES SCIENCES APPLIQUEES DE LYON

NOM : MICHON DATE de SOUTENANCE : 14 février 2014

Prénoms : Marie-Laure

TITRE : Heterogeneous epoxy-amine networks from the dispersion of cross-linked polymer microparticles

NATURE : Doctorat Numéro d'ordre : 2014ISAL0018

Ecole doctorale : Matériaux de Lyon

Spécialité : Matériaux Polymères et Composites

RESUME :
Throughout this work, the influence of the addition of cross-linked polymer microparticles (CPMs) in epoxy-amine formulations on the kinetics, morphology and thermo-mechanical properties of the final networks have been investigated. First, an easy, robust and well-controlled protocol was developed to obtain a large range of CPM size, Tg and amine functionality. This protocol based on reaction induced phase separation via precipitation polymerization was also applied to different chemistries and water soluble epoxy pre-polymers showing the large possibilities of this method. The capacity of obtaining a good compatibility between the CPMs and the matrix was ensure by synthesizing the CPMs in excess of amino groups. The study of the remaining reactive amino groups on the CPMS was of great interest and therefore deeply investigated. The titration of the surface amine was performed by developing a new protocol that enabled the quantification of primary and secondary amines on CPMs. It was then highlighted that even though these cross-linked microparticles were not porous, amino groups are available into the core and can react with other molecules that are able to diffuse into the CPM core. It was shown that when CPMs were dispersed into epoxy-amine blends, the diffusion of monomers into the CPM core occurred but differently depending on the dispersion process. Indeed, using tetrahydrofuran as solvent to help for the dispersion increased the diffusion of DGEBA into the CPM core and changed the thermo-mechanical properties of the final network by modifying the stoichiometric ratio of the matrix. Same phenomenon was observed but less amplified when CPMs were mechanically dispersed in DGEBA. Regarding the dispersion of CPMs in the amine cross-linker, IPD, its complete absorption could be observed into the CPMs, leading then to the desorption of IPD to create the network. Thus, a very complex behavior of CPMs was highlighted in presence of monomers or/and solvent: swelling and diffusion phenomena that are dependent on a number of parameters such as temperature, CPM cross-link density, solubility parameters, etc. The intensity of those phenomena leads to a variety of behaviors when CPMs are added into an epoxy-amine formulation: (a) slight decrease of gel times and increase of conversion, (b) modification of glass transition temperature of the matrix.

MOTS-CLES : Epoxy, Thermosetting polymers, cross-linked polymer microparticles, phase separation, precipitation polymerization, surface amine characterization, gelation, vitrification

Laboratoire (s) de recherche : IMP@ INSA

Directeur de thèse:
Dr. Jocelyne Galy (INSA de Lyon)
Prof. Jean-François Gérard (INSA de Lyon)

Président de jury : Dr. Timothy McKenna (CPE Lyon)

Composition du jury :
Dr. M. Duskova , (IMC, Prague, République Tchèque)
Prof. M. Dumon, (ENSCBP Bordeaux)
Dr. J. Galy (INSA de Lyon)
Prof. J-F. Gérard, (INSA de Lyon)
Dr. T. Dikic, (Dow Chemical, Pays-Bas)
T. Verbrugge, (Dow Chemical, Pays-Bas)